Technical Report: NAVTRADEVCEN 1205-3

SIMULATION OF HELICOPTER AND V/STOL AIRCRAFT

VOLUME III, PART I

COMPUTATIONAL METHODS ANALOG

Study, Equations of Motion of Vertical/Short Take-Off and Landing Operational Flight/Weapon System Trainers

R. A. Castle
A. L. Gray
Walter McIntyre

Melpar, Inc.
3000 Arlington Boulevard
Falls Church, Virginia

May 1964

Contract No. N61339-1205

TABLE OF CONTENTS

Section		Page
I	INTRODUCTION	1
II	ASPECTS GOVERNING THE CHOICE OF THE OPTIMUM ANALOG COMPUTER	2
	A. AIRCRAFT DATA CONVERSION FOR USE IN THE COMPUTER .	2
	B. SIMPLICITY OF SIMULATION EQUATIONS	3
	C. COMPUTER FLEXIBILITY	4
	D. COMPUTATIONAL SEQUENCE	4
	E. CHOICE OF CARRIER	5
	1. AMPLIFICATION	9
	2. INTEGRATION	10
	3. MULTIPLICATION	10
	4. TRIGONOMETRIC RESOLUTION	10
	5. FUNCTION GENERATION	10
III	MECHANIZATION OF EQUATIONS OF MOTION	12
	A. GENERAL MECHANIZATION	12
	B. HELICOPTER MECHANIZATION	26
	1. SINGLE ROTOR HELICOPTER	26
	2. TANDEM ROTOR HELICOPTER	54
	C. V/STOL MECHANIZATION	61
	1. SIMILARITY OF V/STOL EQUATIONS	63
	2. TILT-WING MECHANIZATION	65
IV	SUMMARY	
	A. AIRCRAFT DATA CONVERSION FOR USE IN THE COMPUTER .	97
	B. SIMPLICITY OF SIMULATION EQUATIONS	97
	C. COMPUTER FLEXIBILITY	97

TABLE OF CONTENTS

Section		Page
	D. COMPUTATIONAL SEQUENCE	98
	E. CHOICE OF CARRIER	98
	F. CHOICE OF SYSTEM	98
V	BIBLIOGRAPHY	99
VI	NOMENCLATURE AND EQUATIONS	100
	A. HELICOPTER	100
	1. NOMENCLATURE	100
	2. HELICOPTER SIMULATION EQUATIONS	108
	B. V/STOL AIRCRAFT (TILT-WING)	131
	1. NOMENCLATURE USED IN XC-142A EQUATIONS . . .	131
	2. TILT WING AIRCRAFT SIMULATION EQUATION . . .	133

LIST OF TABLES

Table		Page
1.	Comparison of Fixed Wing and Helicopter Maximum Angular Rates and Accelerations	6
2.	Block Terminology	14
3.	Symbols Used in Mechanization	15
4.	Euler Angle Tabulation	19
5.	Wind Resolution Tabulation	23
6.	Aerodynamic Variables Single Rotor Helicopter	30
7.	Tail Rotor Aerodynamics	31
8.	Fuselage Aerodynamics	34
9.	Local Vertical Velocity	34
10.	Tangential Velocity	37
11.	Blade Angle of Attack	40
12.	Blade Element Flapping Moment and Lift	40
13.	Blade Element Drag and Main Rotor Torque	44
14.	Flap Angle Coefficients and Main Rotor Lift	44
15.	Rotor Hub Moments	47
16.	Rotor Forces and Angular Velocity	47
17.	Force Summations	50
18.	Single Rotor Tabulation	53
19.	Single Rotor Summary	54
20.	Single Rotor - Tandem Rotor Comparison	55
21.	Additional Components Tandem Rotor Helicopter	61
22.	Tandem Rotor Summary	62
23.	Tilt-Wing Aerodynamics Tabulation Block (4)	94
24.	Tilt-Wing Tabulation	95
25.	Tilt Wing Summary	96

LIST OF ILLUSTRATIONS

Figure		Page
1.	General Block Diagram	13
2.	Center of Gravity (c.g.) Mass, and Inertia	17
3.	Velocity Integration AC Mechanization	18
4.	Block (10) AC Mechanization	20
5.	Euler Angle AC Mechanization	21
6.	Euler Angles DC Mechanization	22
7.	Velocity Summation and Wind Resolution	24
8.	Velocity Summation and Wind Resolution DC Mechanization	25
9.	Simplified Block Diagram Single Rotor Helicopter	27
10.	Aerodynamic Variables	28
11.	Tail Rotor Aerodynamics	32
12.	Fuselage Aerodynamics AC Mechanization	33
13.	Simplified Block Diagram	35
14.	Local Vertical Velocity	36
15.	Tangential Velocity	38
16.	Blade Angle of Attack	39
17.	Blade Element Flapping Moment, and Lift	41
18.	Blade Element Drag	42
19.	Blade Element Drag and Main Rotor Torque	43
20.	Flap Angle Coefficients	45
21.	Blade Flap Angle AC Mechanization	46
22.	Rotor Hub Moments	48
23.	Rotor Forces and Angular Velocity	49
24.	Force Summations	51
25.	Moment Summation and Angular Rates	52

LIST OF ILLUSTRATIONS

Figure		Page
26.	Swash Plate Angles and S.A.S.	58
27.	Aft Rotor Terms, Tandem Rotor Helicopter AC Mechanization	59
28.	Tandem Rotor Angular Velocities AC Mechanization . .	60
29.	Simplified Block Diagram	66
30.	Aerodynamic Variables AC Mechanization	67
31a.	Propeller Aerodynamics Velocities AC Mechanization	69
31b.	Propeller Aerodynamics Velocities AC Mechanization	70
32.	Propeller Aerodynamics Advance Ratio AC Mechanization	71
33.	Propeller Aerodynamics Coefficients	72
34.	Propeller Aerodynamics Coefficients AC Mechanization	73
35.	Propeller Aerodynamics T_n and Q_n AC Mechanization .	74
36.	Propeller Aerodynamics , M_n, N_n and Y_n AC Mechanization	75
37.	Propeller Aerodynamics **Y and M Components**	76
38.	Propeller Aerodynamics Forces AC Mechanization . .	77
39.	Propeller Aerodynamic Moment - $(\Delta L_a)_p$ AC Mechanization	78
40.	Propeller Aerodynamics Moment - $(\Delta M_a)_p$ AC Mechanization	79
41.	Propeller Aerodynamics Moment - $(\Delta N_a)_p$ AC Mechanization	80
42.	Wing Aerodynamics α_w, β_w, V_w	81
43.	Wing Aerodynamics Coefficients AC Mechanization . .	82
44.	Wing Aerodynamics Coefficients AC Mechanization . .	83
45.	Wing Aerodynamics Forces and Moments AC Mechanization	84
46.	Vertical Stabilizer Aerodynamics Force and Moments AC Mechanization	85

LIST OF ILLUSTRATIONS

Figure		Page
47.	Horizontal Stabilizer	86
48.	Tail Rotor Aerodynamics Force and Moments (Sheet 1) AC Mechanization	87
49.	Fuselage Aerodynamics Forces and Moments AC Mechanization	89
50.	Force Σ Moment Σ AC Mechanization	91
51.	Integration - Velocities (U, V, W) AC Mechanization	92
52.	Integration - Angular Velocities (p, q, r) AC Mechanization	93

SECTION I

INTRODUCTION

The economical production of helicopter simulators is a complex problem in which experience is not as widespread as in the fixed-wing field. The simulation of small perturbation reaction as practiced by helicopter manufacturers may be sufficient for their purposes, but it is impossible to extend this approach to the unrestricted case without gross modifications. As a matter of history, these modifications appeared to be of such magnitude that prior to the design of the first full flight regime helicopter trainer (Device 2F54, H-37A Helicopter) Melpar, Inc. sought a more analytical scheme for the expressions of helicopter flight. The investigation took full advantage of earlier work performed at NACA and various other institutions and agencies. As a result of this effort the Modified Blade Element Approach was developed and was further expanded and improved during the development of the HSS-2 WST, Device 2F64. Further extensions and simplifications of the technique were then applied to the HRB-1 OFT. Device 2F75. The equations utilized by the Modified Blade Element Approach are developed in reference 1.

A variety of sources have, in the past established criteria for the selection of computer components and systems for aircraft simulation. Their diagnosis has been thorough and well-established. Mark E. Connelly in Computers for Aircraft Simulation, Report 7591-R-2, developed under ONR Contracts N5 ori-07895 and N61339-45, produced a remarkable presentation of analog computer component analysis. No attempt will be made here to repeat or improve on that analysis. References will be made to Mr. Connelly's report and in places injections of practical considerations and variations imposed by the chosen method of helicopter simulation will be made which influence choices of computer components. After a review of computer components, the chosen components will be employed in the simulation task.

SECTION II

ASPECTS GOVERNING THE CHOICE OF THE OPTIMUM ANALOG COMPUTER

This volume will present recommendations derived from the study of the simulation equations as set forth in Volumes I and II. The recommendations are intended as a guide to the selection of an optimum analog mechanization for the single rotor helicopter, tandem rotor helicopter, and tilt-wing simulation equations. No attempt will be made here to present an analysis of analog computer characteristics. Sufficient study reports exist that adequately present the details of analog computer techniques, and reference will be made to these reports in support of certain technique selections in the optimization of the mechanizations.

In the selection of a computer type to be used for aircraft simulation purposes there are several factors that must be considered to arrive at an optimum selection. The optimum computer must have, first of all, a means of communication in order to accept input data which describes the simulation problem and defines the aircraft operational characteristics. Secondly, the simulation equations which describe the problem parameters must be able to be simplified to the extent required by the problem accuracy and still be expressed in the machine language. A third consideration is the need for computer flexibility in order to accept the anticipated aircraft manufacturers design changes. The computational sequence, dictated by the optimum use of components and the type of computer, is a fourth point of consideration. The fifth and most important factor is the choice of carrier to be used in the computer.

A. AIRCRAFT DATA CONVERSION FOR USE IN THE COMPUTER

Considering the first point mentioned above, it has been the writer's experience that the aircraft data supplied by the aircraft manufacturers is, of necessity, empirical in nature. For instance, the coefficient of lift versus angle of attack curves for rotor airfoils are plots of wind tunnel empirical data. Since this data is predominantly empirical and presented in the form of smooth curves as functions of one or two variables, the introduction and storage of these functions is particularly suited to analog function generation techniques.

These techniques, as the reader well knows, are manifested in several different forms such as tapped or shaped potentiometers or some form of electronic function generators, such as diode function generators. These techniques usually produce straight line approximations of the desired function. The accuracy of the approximation is determined by the number of break points selected during the design.

The person selecting the method of function generation to use in the computer should take into consideration the required simulation accuracy and flexibility of the chosen method as well as cost considerations. The present state-of-the-art (reference 4) provides the servo potentiometer as the most economical means of generating slowly varying

functions, like the aerodynamic functions required in OF/WST's. The electronic methods provide a more accurate and flexible method but at a higher cost.

The optimum choice of function generation recommended for the V/STOL simulation then is the servo potentiometer, since this is the most economical method and provides sufficient accuracy for the desired simulation. Once the choice has been made to use potentiometers the data conversion aspects do not bear any further on the choice of the computer since potentiometers are equally useful in either an AC or DC carrier computer.

B. SIMPLICITY OF SIMULATION EQUATIONS

The mechanization of unabridged equations of motion for an OFT will produce a needless superfluity of equipment that is completely out of proportion to the amount required to provide adequate training. Consequently it is highly desirable to simplify the equations of simulation to the extent that an optimum balance exists between the information supplied by the equations and the information required for training purposes. For instance, in Volume I (reference 1) equations 5-25a, b, and c give the complete expressions for velocities in the X body axes as

$$U_G = \int\left(\frac{X_a}{M_i} - g \sin\theta + V_G r - W_G q\right) dt$$

$$V_G = \int\left(\frac{Y_a}{M_i} + g \cos\theta \sin\Phi + W_G p - U_G r\right) dt$$

$$W_G = \int\left(\frac{Z_a}{M_i} + g \cos\theta \cos\Phi + U_G q_1 - V_G p\right) dt$$

In order to simplify the expressions and provide a less complex mechanization it was noted that U_G is usually the predominantly large velocity. Consequently the contributions of the V_G and W_G cross-coupling terms may be omitted giving the final expressions

$$U_G = \int\left(\frac{X_a}{M_i} - g \sin\theta\right) dt$$

$$V_G = \int\left(\frac{Y_a}{M_i} + g \cos\theta \sin\Phi - U_G r\right) dt$$

$$W_G = \int\left(\frac{Z_a}{M_i} + g \cos\theta \cos\Phi + U_G q_1\right) dt$$

as given by 5-26 of Volume I.

Although this simplification does alter the validity of the expressions, the errors caused in the final velocities are negligible and not detectable by the student and consequently the same training value is obtained with less hardware than if the simplification had not been made. In this manner, the balance between input and output information is achieved.

The extent of simulation required by the trainer specifications is the limiting factor that controls the extent of simplification of the simulation equations. In general, the hardware reduction bears a direct proportion to the amount of simplification of the simulation equations. Consequently, the simplification of the equations does not influence the choice of the computer but only reduces the complexity of the final mechanisation.

C. COMPUTER FLEXIBILITY

The flexibility of a computer is the ease with which the computer can be reprogrammed to perform a different computation. In the design of OF/WST's the procuring agency usually desires the development of the trainer to be performed concurrently with the development of the aircraft being simulated. This necessitates a close liaison with the aircraft manufacturer in order to keep abreast of design changes required during the aircraft development. Consequently, the design of the OF/WST must include a consideration of the flexibility of the selected computer in order that airframe design changes may be quickly and efficiently incorporated into the OF/WST design.

Fortunately the changes made by the airframe manufacturers are usually slight modifications to the numerical functions describing the aerodynamics, such as the coefficients of lift and drag. In an analog computer these functions are formed by tapped or shaped potentiometers on the various servo shafts. A change in these constants would result in OF/WST modification to the associated potentiometers and amplifier gain adjustments. If as in section II.A the choice is made to use potentiometers as function generators, no flexibility advantage is realized in either an AC or DC carrier computer. Consequently, the flexibility consideration does not affect the choice of analog computer for the OF/WST.

D. COMPUTATIONAL SEQUENCE

The computational sequence formed by the interconnection of the computational elements directly affects the optimum use of components no matter what type of computer is selected for the OF/WST. This is obviously true if one considers the result of forming a computational sequence without regard to optimum component use. For example, the expression for the HSS-2 landing gear pitching moments is given in Volume I as

$$M_{LG} = 4.38(F_{RW} + F_{LW}) - 18.99\ F_{TW} + 5.36\ X_{LG}$$

This could be mechanized by first forming (F_{RW} + F_{LW}) as the output of a summing amplifier and then scaling 4.38 (F_{RW} + F_{LW}) at the input of a second summing amplifier which sums 4.38 (F_{RW} + F_{LW}) with -18.99 F_{TW} + 5.36 X_{LG}. Obviously the optimum sequence that should be used here is to scale 4.38 F_{RW} and 4.38 F_{LW} separately into a single summing amplifier with -18.99 F_{TW} + 5.36 X_{LG} and thus eliminate one summing amplifier. While this is an extremely obvious example it does illustrate the value of sequence considerations for component optimization.

Computational sequence also affects the extent of simulation achievable with a given computer. Since a finite response time is inherent in each individual computational element, the accumulative response time of a complete computational loop must be matched to the response times of the system being simulated if a realistic simulation is to be achieved. For example, the CH46-A tandem-rotor helicopter response is such that a 1.58 inch step input of longitudinal forward stick deflection will produce a maximum pitch acceleration of 24 degrees per second^2, and the time to reach this maximum acceleration is 0.33 seconds after initiation of the stick deflection. If the simulator is to present a realistic simulation of this computational loop the pitch rate servo, q_1, must exhibit at least the response indicated above, if a similar step input to the longitudinal stick is applied to the simulator. This will certainly occur if the computational sequence is arranged to minimize the computational elements and the response times of the q_1 integrator shaft is scaled to produce the required loop response.

Thus, it is evident the computational sequence is an extremely important aspect as far as obtaining a minimum component quantity for an optimum response match. However, it has very little bearing on an optimum choice of computer type, as an AC or DC carrier.

E. CHOICE OF CARRIER

The choice of the carrier to be used for a particular simulation computer design is by far the most important aspect to be considered in the selection of an optimum computer. There are three possible solutions that may be decided upon. They are, namely, an AC carrier, a DC carrier or a hybrid AC-DC combination. One additional decision must be made in the event an AC carrier is to be used, and that is the frequency of the AC carrier.

Let us first consider the AC carrier computer and decide which frequency is best suited for application in V/STOL aircraft simulation. The most stringent requirement of the computer is the response characteristics dictated by the angular rates and accelerations of the aircraft to be simulated. Table 1 is a comparison of maximum rates and accelerations of fixed wing and helicopter type aircraft. The fixed wing aircraft values are taken from the MIT-Whirlwind and the Goodyear-Cyclone program (pages 174-175, reference 4). The helicopter angular

	FIXED WING		HELICOPTER	
	MIT - Whirlwind	Goodyear-Cyclone	Single Rotor HSS-2	Tandem Rotor Vértol HRB-1
p (roll rate)	+ 6.3 to -7.8 rad/sec	± 10 rad/sec	± 2.4 rad/sec	± 2 rad/sec
q (pitch rate)	+ .86 to -1.0 rad/sec	± 1 rad/sec	± 1.44 rad/sec	± 3 rad/sec
r (yaw rate)	+ 1.12 to -.13 rad/sec	± 1.2 rad/sec	± 1.28 rad/sec	± 5 rad/sec
$\dot{p}$ (roll acc.)	+ 36.8 to -20.85 rad/sec^2	± 40 rad/sec^2	± 3.3 rad/sec^2	± 3 rad/sec^2
$\dot{q}$ (pitch acc.)	+ 5.94 to 4.10 rad/sec^2	± 8 to -5 rad/sec^2	+ 1.5 rad/sec^2	± 5 rad/sec^2
$\dot{r}$ (yaw acc.)	+ 4.47 to -2.82 rad/sec^2	± 5 rad/sec^2	± 1.5 rad/sec^2	± 1 rad/sec^2

Table 1. Comparison of Fixed Wing and Helicopter Maximum Angular Rates and Accelerations

rates and accelerations are those used in the HSS-2 flight trainer and those furnished to Melpar by Vertol Division of Boeing Aircraft for the CH46-A flight trainer. It is easily seen that there is a great difference in the maximum response capabilities of the fixed wing aircraft and the helicopters chosen. Likewise there is a variation in the computational speed requirement of flight simulator computers for helicoptar and fixed wing aircraft.

Assuming that the response of a 60 cycle system is marginal in fixed wing applications, it can be seen in Table 1 that a 60 cycle system is better than simply marginal for helicopter simulation since none of the helicopter angular rates and accelerations in Table 1 are as large as the fixed wing rates and accelerations. Note that q_1, $\dot{q}_1$, r and $\dot{r}$ are not too different from helicopter to fixed wing, however there is a marked difference in p and $\dot{p}$. The required computational speed is based on the highest single rate and acceleration, i.e. roll rate and roll acceleration for the fixed wing aircraft.

Chapter II, page 25 of reference 4 gives an analysis of servo systems and concludes that 400 cycle servos should result in a servo response that is three to four times better than is possible with a comparable 60 cycle system. This is quite true, and one may wonder why bother with 60 cycle systems if 400 cycle systems offer such improvement in response as well as accuracy and size. Both large and small computers have successfully utilized 400 cycle systems. For example, operational airborne computers are predominantly 400 cycle systems, also large operational shipboard fire control systems operate from a 400 cycle carrier. If such systems are developed, then why should flight trainer manufacturers be hesitant to discard a 60 cycle carrier system? Unlike the manufacturer of operational tactical systems the flight trainer manufacturer does not develop flight trainers with weight and size reductions as a prime design goal. Neither does the prototype serve simply as a production model. What argument then can induce a simulator manufacturer to discard an operational 60 cycle system to develop 400 cycle systems with little hope of operational improvement? Before discussing this development consider another point before the problem is considered from a broad viewpoint. Suppose the case arises where the carrier system employed introduces reduced fidelity into the system at maximum accelerations, but operates at a sufficiently high response to follow satisfactorily the highest accelerations or rates that one would normally expect--which may be quite different from the maximum. Compared to other aspects of the trainer how important is maximum fidelity in this extreme operating region? These regions are most often reached just before a crash situation occurs. Very little, if any, actual training is accomplished at the extreme operation region of the aircraft. Regardless of the importance of highly accurate simulation in these areas, the decisions concerning the choice of carrier frequency are based on a balance of performance and cost.

Progressing from the earlier assumption that the response of either a 60 or 400 cycle system is sufficient for helicopter simulation, but

that a 400 cycle carrier offers a greater response margin of safety, consider some other factors that affect the choice of carrier frequency. Factors influencing carrier frequency choice are listed on pages 26 and 27 of reference 4. The statements contained in reference 4 are very true but the injection of some practical considerations may lead to a more selective choice of carrier frequency. The seven factors which follow are similar to those listed in reference 4.

1. 60 cycle power is widely available; 400 cycle power must be generated at the OFT in kilowatt quantities and in some cases, with undistorted waveshape and carefully controlled phase.

2. A 400 cps carrier produces a smaller and lighter weight computer. This, of course, is the primary reasoning behind the adoption of a 400 cps carrier for airborne and shipboard equipment, but is seldom highly influential in flight trainer design unless space for some special reason is at a premium.

3. The problem of phase shift (due to stray capacitance and inductance) and pickup is more likely to occur in a 400 cps system than in a 60 cps system. As reference 4 points out, pickup may be eliminated by proper engineering precautions such as the maintenance of low driving impedance levels, shielding, and careful placement of wiring. This sounds easy to accomplish, but the consideration of the practical aspects of the accomplishment may be enlightening. We must remember that OFT prototype development periods are commonly 16 to 18 months, and the present trend is toward fixed-price contracts. Shielding, for example, should be avoided whenever possible for a number of reasons. First, shielded wires produce as many maintenance troubles (which lead to an increase of computer cost with no increase in design) as any other single factor, particularly in the course of prototype debugging, where wiring is constantly being flexed. The ferrules at the end of each shielded wire cut through the insulation shorting the conductor to the shield and consequently to ground. Each time this occurs, the trainer is turned off and check-out halts. Components are also lost, particularly potentiometers where the wiper becomes grounded due to a fault in the shielded cable. Shielded cable is also costly, bulky, stiff and generally very difficult to work with particularly in large quantities. Another point to consider here is the difficulty of simultaneously reducing stray capacitance and using shielded cable. Available shielded cable has a capacitance of approximately 100 $\mu\mu$f per foot. Extremely long cable runs are sometimes necessary especially in two trailer trainers. If these cable runs are shielded then buffer amplifiers must be used to reduce the source impedance sufficiently to minimize phase shift. High impedance wire-wound potentiometers also produce conditions (high source impedance and high inductance) which leads to further phase shift.

4. The fact that most aircraft instruments utilize a 400 cycle carrier is of no consequence since a 400 cycle synchro transmitter may be driven by a servo operating on any desirable carrier. With the present trend of reducing GFE, instruments are generally built to any carrier specified by the contractor.

5. Amplifier design for a 400 cps system will be simpler in that the lower sideband component of any reasonable signal does not approach zero frequency as it may in the case of a 60 cps system. Particularly in the case of transistorized amplifiers, a 400 cycle center frequency is easier and cheaper to obtain than a 60 cycle midfrequency.

6. Tachometers to .03% linearity as discussed in reference 4 are very expensive and greatly exceed the requirements of present-day training devices. Tachometer linearities in the order of 1% with zero speed voltages as low as 9 millivolts are much more common. These may be more cheaply obtained either as 400 or 60 cps units.

7. The seventh factor discussed in reference 4 states the advantages of using magnetic amplifiers to reduce the power and maintenance requirements. The following reductions were realized in a study by Goodyear Aircraft Company: number of tubes--54.5%, power consumption--56.25%, size--46%. Since the advantage may be realized only while employing a 400 cycle carrier, it is implied that this is an advantage that should be credited to a 400 cps carrier. A good deal of these advantages are dependent upon the size and characteristics of the tube type amplifiers. There is also the unanswered question as to whether or not a conversion to transistor circuitry would not have produced equivalent or larger reductions of maintenance and power consumption.

It is recommended then from the above that if an AC computer is selected for the V/STOL mechanization a 60 cycle system should be chosen. While it is true that a 400 cycle system would provide a definite advantage in response and accuracy, it is felt that these advantages are overshadowed by the reduced response requirements of the V/STOL aircraft frequencies. Also the de-emphasis of computer size restrictions in simulators and the maintenance and phase shift problems introduced by 400 cycle carrier further enhance the 60 cycle carrier choice.

Having selected the frequency of the carrier in the event that an AC computer is chosen the choice must now be made between an AC carrier, a DC carrier, or an AC-DC hybrid computer. First, let us make a comparison between AC and DC computers on the basis of the various computational techniques. Reference 4 gives an excellent discussion of the relative merits of AC and DC techniques. A summary of each of the discussions is presented here in support of the choice between AC and DC computers for the V/STOL mechanization.

1. AMPLIFICATION. Amplifiers occur in very large quantities in OF/WST analog computers due to the fact that they are used in so many different applications, such as isolation, summation, servo motor drive, inversion, etc. Consequently, the AC amplifier is afforded a large advantage over the DC amplifier in quantity required for a given mechanization, since the AC amplifier can produce both polarity outputs by virtue of its center-tapped output transformer. The DC computer requires two separate amplifiers whenever both signal polarities are required. Also, DC amplifiers have an inherent drift problem and require a special consideration in the design to insure that adequate regulation is

provided by the power supplies. This is not required during the design of the AC computer. Due also to the drift problem, DC amplifiers are usually more complex, since stabilization circuits are required. The only advantage of the DC amplifier over the AC amplifier is its ability to form various transfer functions by the use of passive network. Consequently, the advantage definitely lies with the AC computer as far as amplification is concerned.

2. INTEGRATION. DC electronic integration techniques have several decided advantages over AC servo integration methods. The DC technique can integrate much higher frequency signals, have a much higher dynamic range, have a smoother output, cost less and require less space and power. One feature, however, prevents them from being suited to OF/WST application. That is their inability to perform long term open loop integrations as is required in the integration of the Euler angle derivatives for instance. This application requires an angular output of unlimited range which can only be obtained with servo integrators. While a DC servo integrator can be used a DC tachometer is required to provide a response better than an AC servo integrator. Unfortunately, this increases starting and running friction. As far as integration techniques are concerned then AC servo integrators are slightly more desirable for the V/STOL mechanization.

3. MULTIPLICATION. No advantage lies with either AC or DC systems in performing multiplication operations, since nothing can compete economically or from the standpoint of versatility with the servo potentiometer.

4. TRIGONOMETRIC RESOLUTION. The use of AC resolvers for coordinate resolution as opposed to sine-cosine potentiometers provides greater accuracy, greater resolution, longer life, and less friction. If the poorer conformance of sine-cosine potentiometers to the trigonometric functions can be tolerated then trigonometric resolution can be accomplished in an AC system more economically using potentiometers rather than resolvers. This can be seen by considering that both the resolver and the potentiometers require two input and two output amplifiers. Even though it's true that the summing of components takes place internally in the resolver, the potentiometer outputs can be summed in the succeeding input amplifiers. The AC techniques definitely have the advantage here.

5. FUNCTION GENERATION. Economically and versatility-wise the servo potentiometer has the advantage here. Consequently, AC or DC systems are equally optimum since potentiometers can be used in either system.

On the basis of the merits of the computing techniques described above it appears that the AC carrier computer would have the advantage over the DC carrier computer in the mechanization of the V/STOL aircraft. In all of the areas discussed, except function generation and multiplication, the AC methods would appear to be the more optimum. In the mechanization of some of the supersonic fixed wing aircraft, where the signal frequencies that would be encountered were expected

to be much higher than one or two cycles, some of the hybrid methods of DC integration followed by an AC position shaft or DC electronic function generation might be more applicable. In general, it has been the experience of the writer that if the requirements of the simulation problem are such that either an AC or DC carrier computer is adequate to perform the simulation, then the only thing that is achieved by combining AC and DC techniques is additional equipment. This additional equipment is required to make up the AC-DC interface.

It is therefore recommended, on the basis of examination of the merits of the various techniques, that the optimum mechanization for the V/STOL aircraft would be a 60 cycle AC computer. Section III will examine the mechanizations in detail from the standpoint of optimum sequence and optimum cost and complexity.

SECTION III

MECHANIZATION OF EQUATIONS OF MOTION

A. GENERAL MECHANIZATION

This section deals with the mechanization of the equations of motion for helicopter and V/STOL aircraft. The mechanizations of these aircraft will reflect the use of 60 cps AC, 400 cps AC, DC and possible AC-DC hybrid carrier frequencies, however the flow charts in this section are developed for an AC mechanization with explanation of additions or deletions to these flow charts that are necessary to form flow charts for DC and AC-DC mechanizations. To aid in this extensive task a general flow chart independent of aircraft type and applicable to either helicopter or V/STOL aircraft is developed. In Figure 1 areas of mechanization are the blocks containing a bracketed number i.e. (1). The second task is then to develop the blocks in Figure 1 that are dependent upon the particular aircraft type. This leads to the helicopter and V/STOL mechanizations. Tabulations of the various components necessary to mechanize the various blocks in Figure 1 will be made as a function of AC or DC mechanization so that conclusions regarding optimum mechanization can be made in Section IV.

Before developing the blocks in Figure 1 that have identical representation for any aircraft in this section, a few ground rules will be established. Inputs to a block are described by arrow heads intersecting the blocks and outputs are defined as lines intersecting a block. Table 2 contains definitions of numbered blocks in Figure 1 and Table 3 establishes the meaning of the symbols in the mechanization flow charts. In the actual mechanization all inputs for a particular flow chart are assumed to be previously generated. Each block in Figure 1 will be considered in the following paragraphs.

Block (1) - Pilot Control. The signal inputs that will be shown for the various aircraft will be due to control stick movements. The particular signal inputs will be observed as inputs to Block (4) for each aircraft described. Inputs to Block (2) are not considered.

Block (2) - Engine Simulation. The signal inputs to Block (4) from the Engine Simulation represent the required performance output parameters. Simulation of engines is not described in this report; only the specific output terms necessary for the simulation of the particular aircraft.

Block (3) Aero Variables. The aerodynamic (Aero) variables are generated by signals that complete the major loop in the computer representing the aircraft equations of motion. Block (8) for the V/STOL aircraft and Block (12h) for the helicopters feedback the velocities U, V and W to Block (3). Block (10) or Block (12) feed back the pressure altitude (h_p) to Block (3).

Block (4) Aero Terms. In this block the aerodynamic equations are formed that will result in the generation of the aerodynamic forces (X_a, Y_a and Z_a) and moments (L_a, M_a and N_a). The mechanization representing

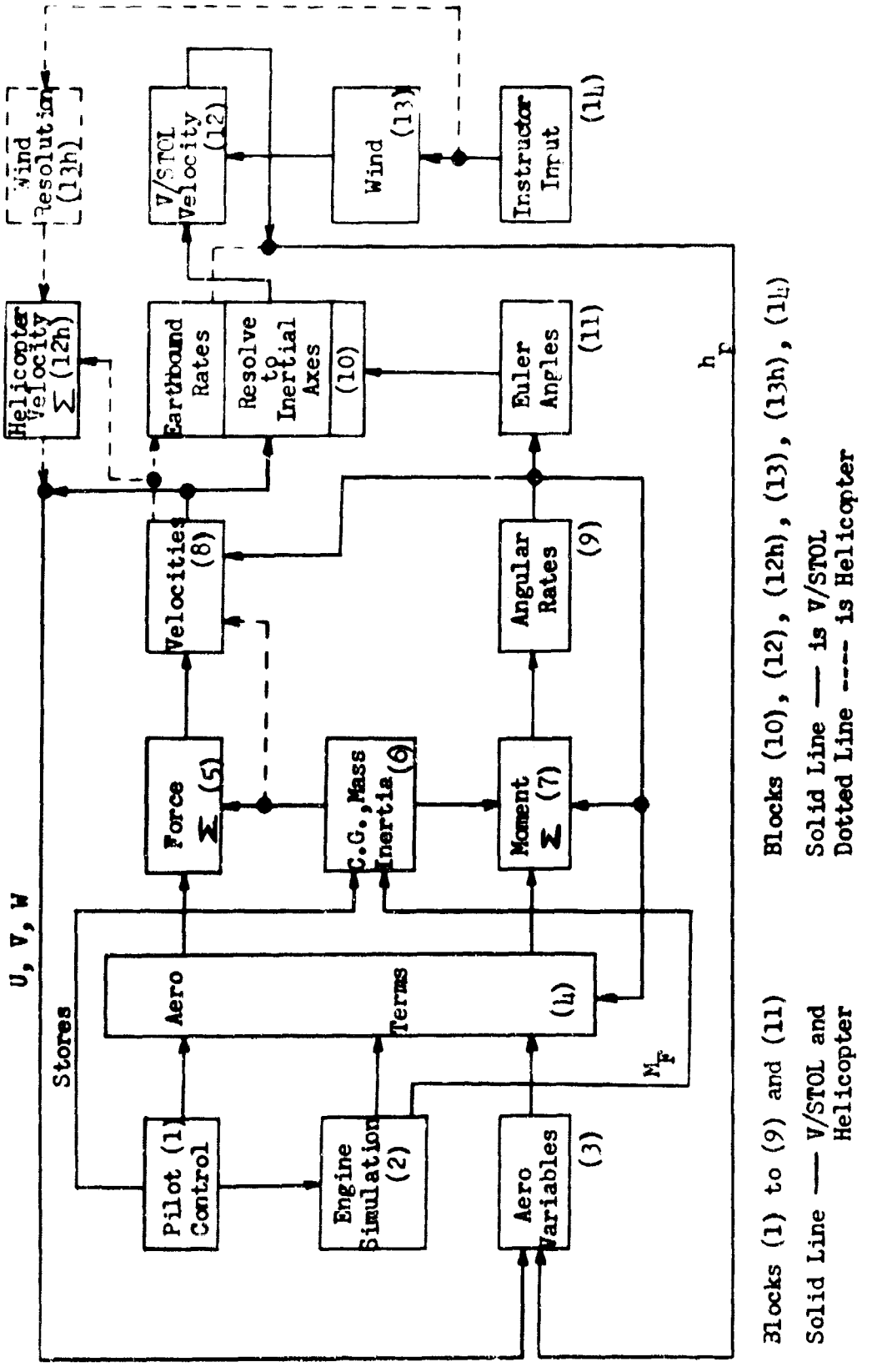

Figure 1. General Block Diagram

BLOCK	HELICOPTER	V/STOL AIRCRAFT
(1)	Pilot Control	Pilot Control
(2)	Engine Simulation	Engine Simulation
(3)	Aerodynamic Variables	Aerodynamic Variables
(4)	Aerodynamic Terms	Aerodynamic Terms
(5)	Force Summations	Force Summations
(6)	Center of Gravity (c.g.) Mass, Inertia	Center of Gravity (c.g.) Mass, Interia
(7)	Moment Summations	Moment Summations
(8)	Linear Velocities	Linear Velocities
(9)	Angular Rates	Angular Rates
(10)	Form Earth Axis Velocities	Resolve Linear Velocities to Inertial Velocities
(11)	Formation of Euler Angles	Formation of Euler Angles
(12)	--	Summation of Wind and Aircraft Inertial Velocities
(12h)	Summation of Wind and Body Axis, True or Ground Velocities	--
(13)	--	Wind Inputs from Instructor
(13h)	Resolution of Wind Inputs to Body Axes	--
(14)	Instructor Input	Instructor Input

Table 2. Block Terminology

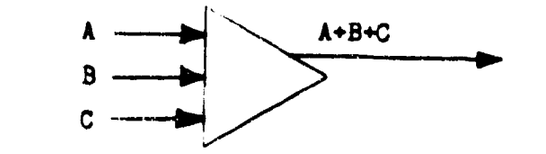

Summing Amplifier

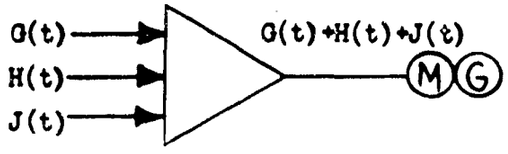

Amplifier and Position Servo

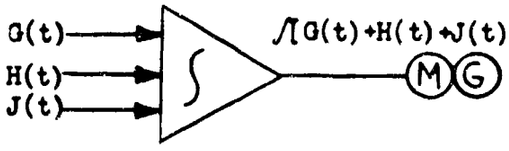

$\int[G(t)+H(t)+J(t)]dt$

Amplifier and Integrating Servo

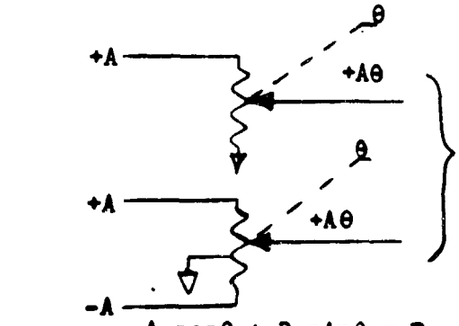

Potentiometer

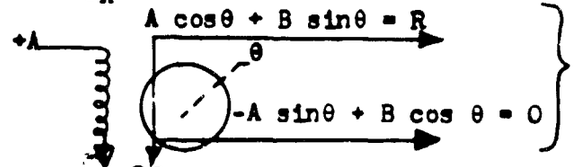

Resolver

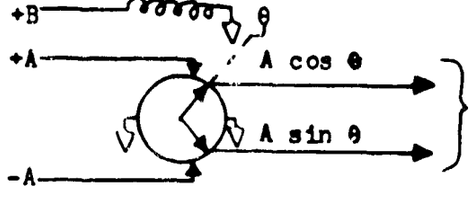

Sine-Cosine Potentiometer
(Various signs of cos θ and sin θ can result depending on initial wiper orientation)

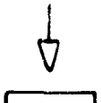

Ground

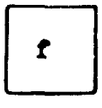

Function

Table 3. Symbols Used in Mechanization

the Aero terms will be shown for each particular aircraft further on in this section.

Block (5) Force. The force summations are basically the same for all aircraft. Each force component (X_a, Y_a and Z_a) has an associated summing amplifier. The inputs from Block (4) are the important portion of the mechanization.

Block (6) Mass, C.G. Mass (M) and center of gravity (c.g.) location are obtained as servo shaft positions. This mechanization involves simple summation. In Figure 2 notice that the feedback potentiometer is connected for division operation for mass mechanization. The shaft position is then an inverse function $(\frac{1}{M})$. This is done to avoid the scaling computations required for potentiometer divisions since M is used as a divisor in its associated equations. Shift in c.g. in Figure 2 is along the x-body axis and is denoted by dx. Usually c.g. shifts along the x-body are the only shifts considered, however if a c.g. shift in the y or z body axis is important for a particular aircraft, it will be mentioned at that time.

Block (7) Moment. The moment summations are basically the same for all aircraft. Each moment component (L_a, M_a, N_a) has an associated summing amplifier. The inputs from Block (4) are the important portion of the mechanization.

Block (8) Velocities. In block (8) the interest is in developing the linear velocities (U, V and W). These are computed by summing the respective force (X, Y or Z) divided by the mass of the aircraft with the appropriate gravity and angular rate effects and then integrating. Figure 3 shows the three integrations to get V_G, U_G and W_G with associated inputs. Servo shaft positions are not required to mechanize these velocities but since Figure 3 is for an AC mechanization, servo shafts are required for the integrators. The integrations could have been done DC just as well and more economically. Choice of AC or DC should not be made at the subsystem level--but for large computation areas. This will be done in the summary.

Block (9) Angular Rates. Having computed the moments in Block (7), the calculation of the respective angular rate (p, q, or r) is accomplished by the integration of the respective moment which has been divided by the proper inertia term. Integrations can be performed by AC servo, DC servo or DC resistive capacitance circuits. Blocks (4) and (7) are the important determinants as to whether to use AC or DC in mechanization. Consequently, the development of Aero Terms as well as the summary mechanization considerations of Section III will have a decisive influence on the way in which the integration is performed.

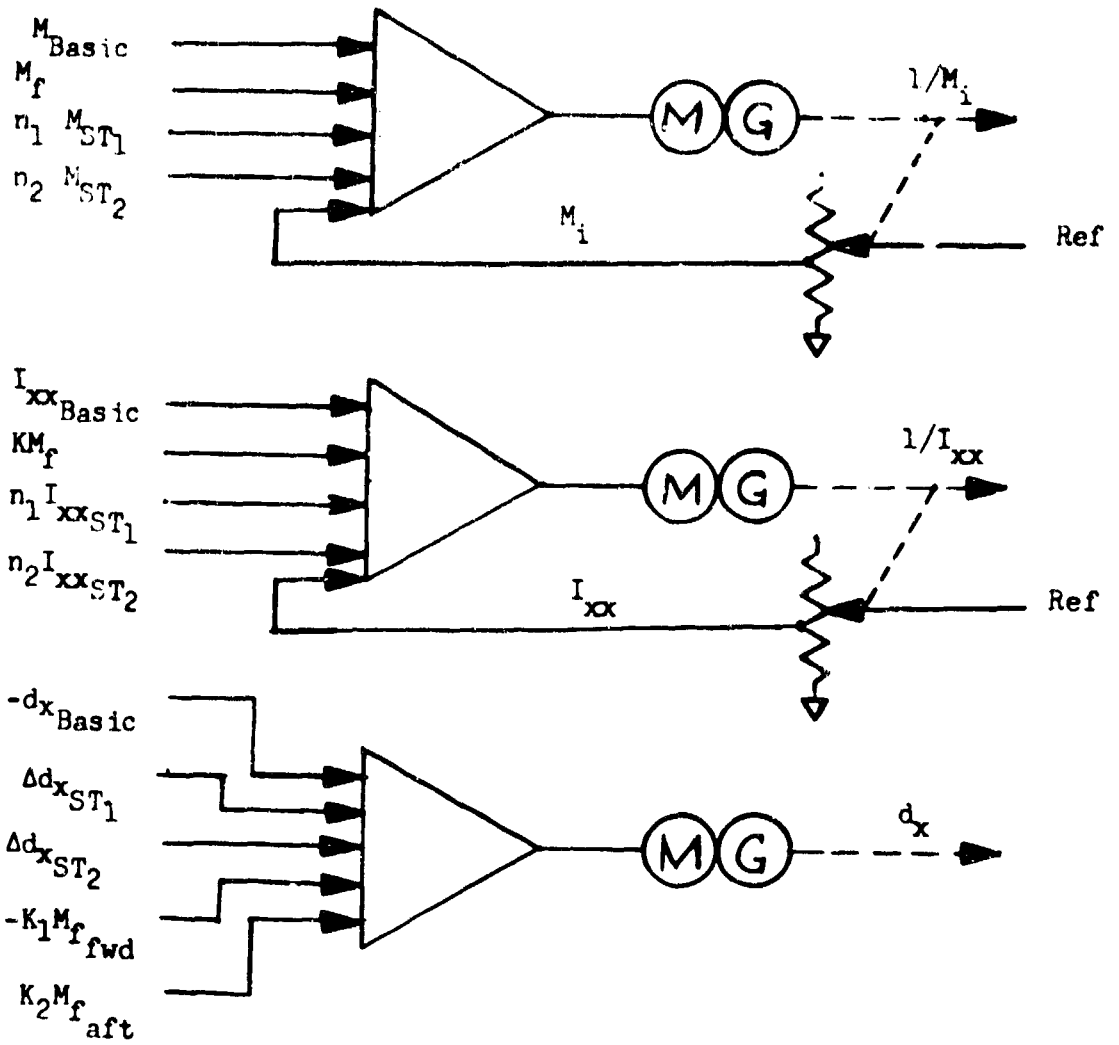

$$M_i = M_{Basic} + M_f + n_1 M_{ST_1} + n_2 M_{ST_2}$$

$$I_{xx} = I_{xx_{Basic}} + K M_f + n_1 I_{xx_{ST_1}} + n_2 I_{xx_{ST_2}}$$

$$d_x = -d_{x_{Basic}} + \Delta d_{x_{ST_1}} + \Delta d_{x_{ST_2}} - K_1 M_{f_{fwd}} + K_2 M_{f_{aft}}$$

$dy = dz = 0$ $\quad I_{yy} = Const.$ $\quad I_{zz} = Const.$

$-K_1 M_{f_{fwd}}$ and $K_2 M_{f_{aft}}$ = Δd_x due to mass of fuel forward and aft, respectively

Where:

K = distance from c.g. to centroid of fuel mass

M = Mass

Subs:

Basic = based on design weight empty

n_1 or n_2 = number of stores of Type 1 or 2

ST_1, ST_2 = stores, Type 1 or 2

Figure 2. Center of Gravity (c.g.) Mass, and Inertia

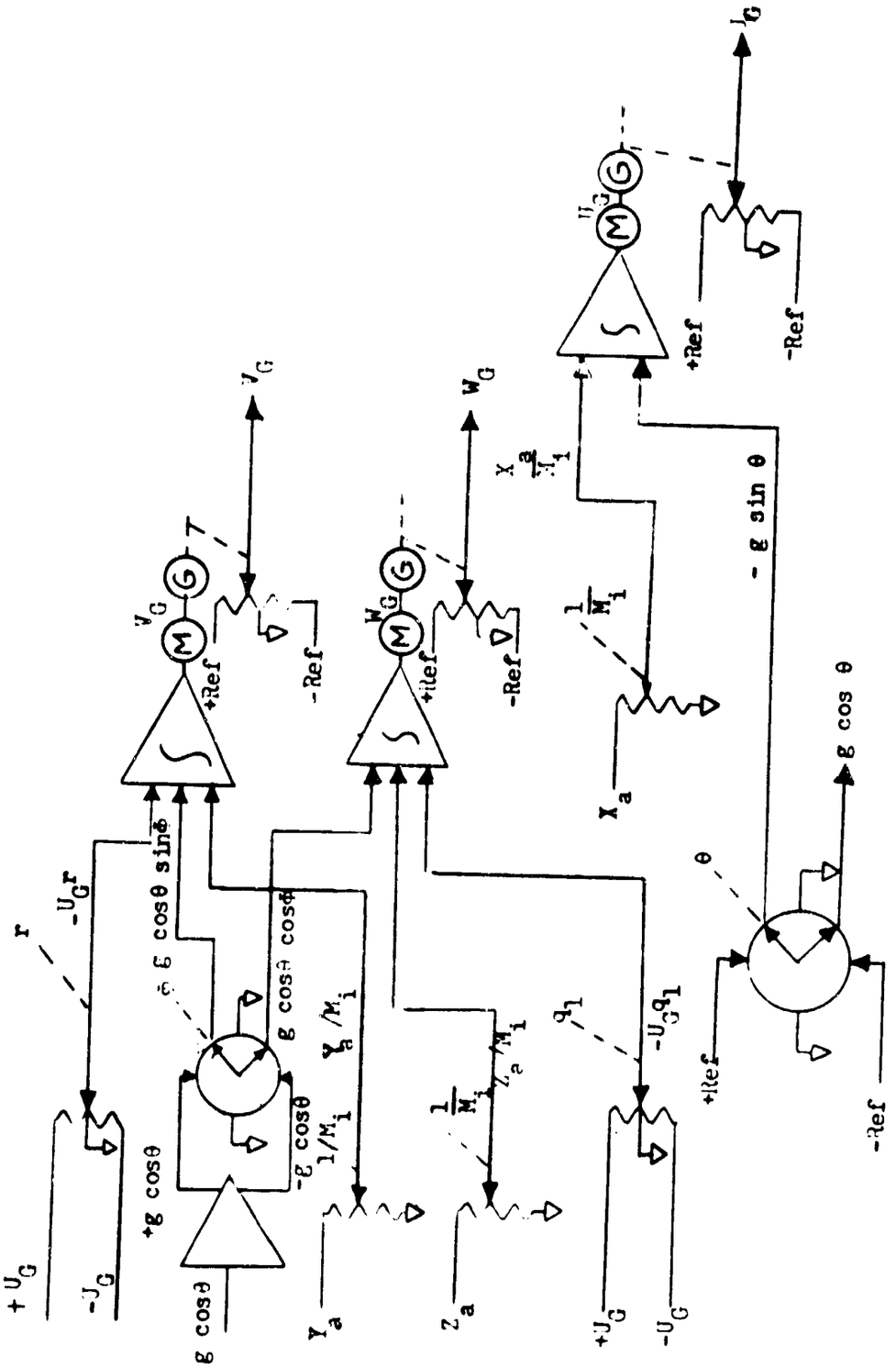

$$U_G = \int [\frac{X_a}{M_i} - g \sin\theta] \, dt$$

$$V_G = \int [\frac{Y_a}{M_i} + g \cos\theta \sin\phi - U_G r] \, dt$$

$$W_G = \int [\frac{Z_a}{M_i} + g \cos\theta \cos\phi - U_G q_1] \, dt$$

Figure 3. Velocity Integration
AC Mechanization

Block (10) Resolve to Inertial. Body axis velocities (U, V, W) for V/STOL aircraft are resolved to the inertial frame through the Euler angles (Φ, θ, ψ) then added to instructor inputs to give the earthbound rates. For the helicopter, ground velocities (U_G, V_G, W_G) are resolved in Block (10) to form earthbound rates. Figure 4 shows an optimum mechanization for this resolution. Resolvers have been chosen to perform the coordinate resolution to the inertial frame since it is necessary to provide the accuracy to insure reliable integration for position. The integrators in Figure 4 must have the capability of long integration times, since these outputs are generally used for plotting boards and altimeters.

Block (11) Euler Angles. The computation of Euler angles is a combination of coordinate resolution and integration. Figure 5 is an AC mechanization using resolvers and AC servos for integration. Figure 6 is a DC mechanization using DC amplifiers, sine-cosine potentiometers and DC electronic integrators followed by DC position servos.

	AC		DC	
Component	No.	Wt.	No.	Wt.
Amplifier	7	7	12	24
Servo	3	21	3	21
S-C Pots	2	1/2	4	1
Resolvers	1	1/2		
Complexity	13	29	19	46

Table 4. Euler Angle Tabulation

The weight factor, (Wt.) of components, in Table 4 are those used by Connelly in references 3 and 4. The weighting of components will be used for later evaluation of mechanizations. The weight factors are as follows: an AC amplifier is one (1), a DC amplifier is two (2), AC and DC servos are seven (7), a potentiometer is one-fourth (1/4), a resolver is one-half (1/2) and function generation is unspecified as to weight, but is specified by number (no.). Any function generation is assumed to be done by potentiometers which would be equal in number in an AC or DC system.

Block (12) V/STOL Velocity. At this point inertial velocities U_I, V_I and rate of climb (R/C) are mixed with instructor wind inputs ($\dot{N}_w$ and $\dot{E}_w$) to yield the earthbound rates ($\dot{N}$, $\dot{E}$, R/C). This is a simple process and consequently requires two summing amplifiers.

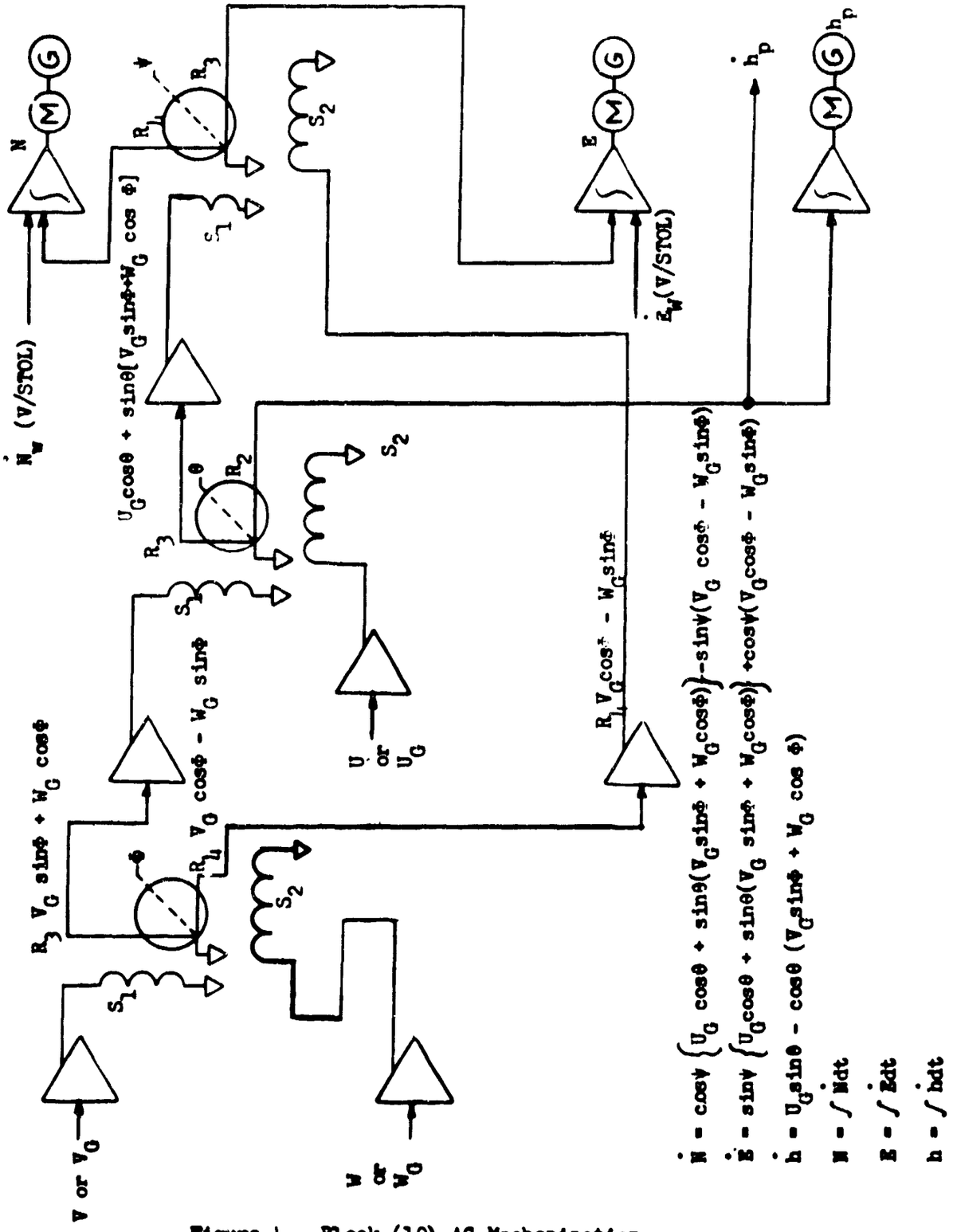

Figure 4. Block (10) AC Mechanisation

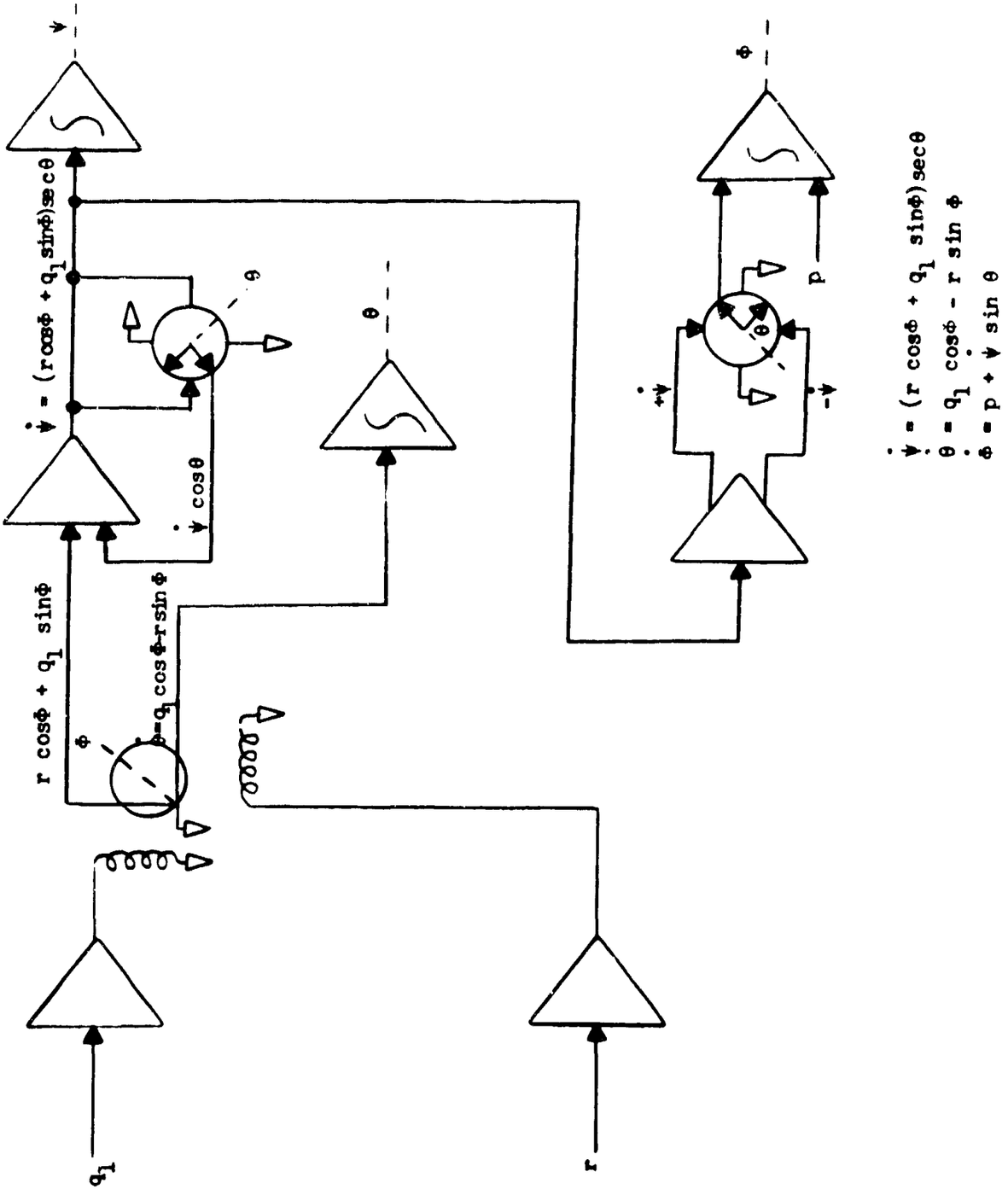

Figure 5. Euler Angle AC Mechanization

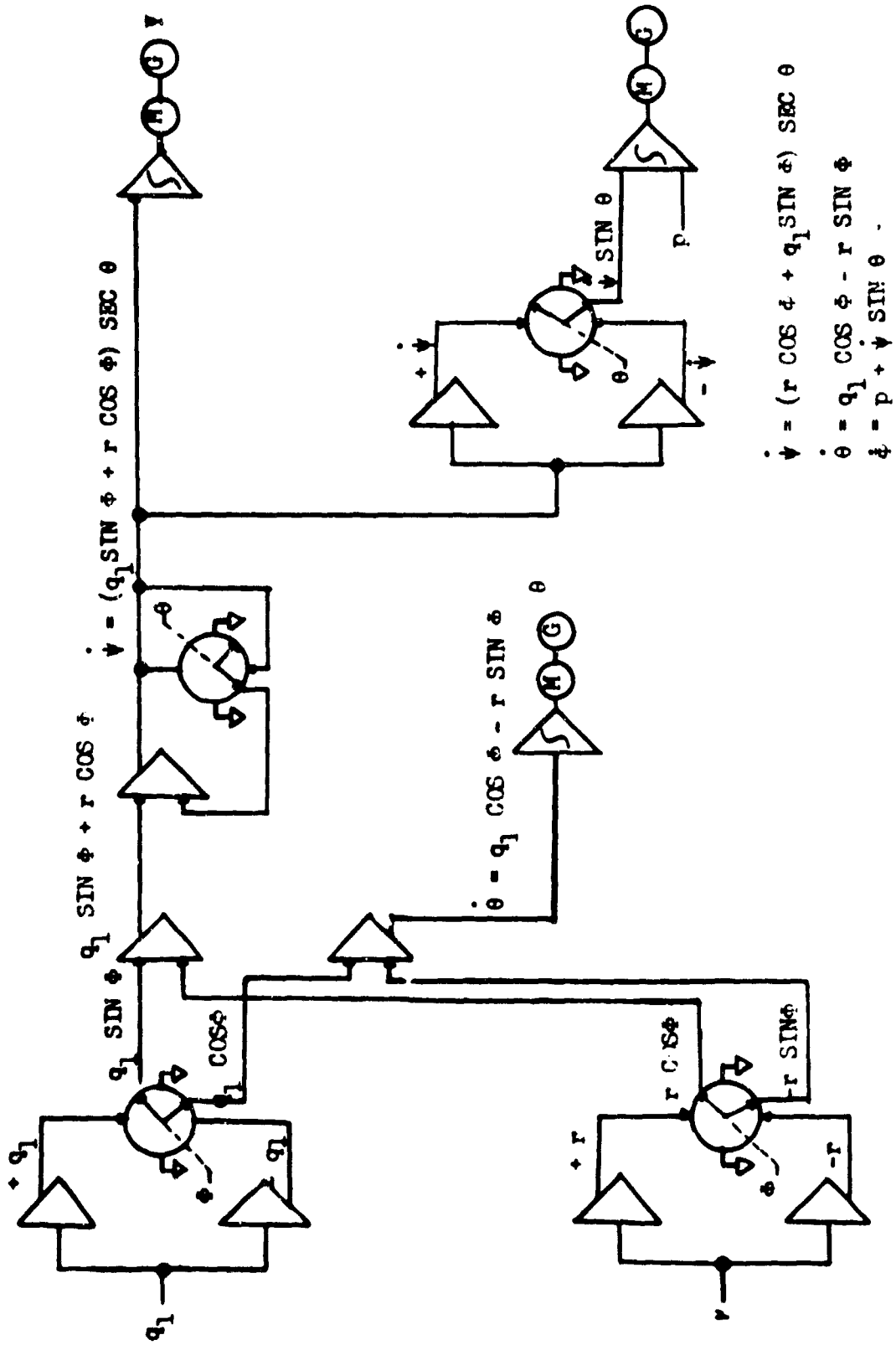

Figure 6. Euler Angles DC Mechanization

Block (12h) Helicopter Velocity. In the helicopter simulation the velocity outputs (U_G, V_G, W_G) from Block (8) are summed with the wind velocities (U_w, W_w, V_w) from the instructor in order to give body axes velocities in the air mass (U, V, W). This operation is a simple summing process and consequently requires three summing amplifiers. This summing is done in Figure 7 by amplifiers (7-2), (7-3), and (7-4). However, if DC computation is used, a servo is indicated for W and both signs are necessary for U and V so that two more amplifiers are needed for generating (+V, -V and +U, -U).

Block (13) Wind. These are simply signal inputs from the instructor so that no equipment is specified.

Block (13h) Wind Resolution. In Block (13h) instructor inputs representing wind direction (ψ_w) and velocity (v_w) are transformed to components U_w, V_w and W_w for the helicopter simulation. In the AC mechanization of Figure 7, v_w is the input to amplifier (7-1). By the use of a sine-cosine (S-C) potentiometer and resolvers, the velocities U_w, V_w and W_w are obtained. Figure 8 is the DC representation of Figure 7.

	AC		DC	
Component	No.	Wt.	No.	Wt.
Amplifier	6	6	14	28
Servo	1	7	1	7
S-C Pots	1	1/4	6	1-1/2
Resolvers	3	1-1/2		
Complexity		14-3/4		36-1/2

Table 5. Wind Resolution Tabulation

Table 5 is a comparison of the AC and DC mechanizations of equations shown in Figures 7 and 8.

Block (14) Instructor's Inputs. These inputs are signals controlled by potentiometers at the instructor's console. There is no associated equipment for this operation. This is the last block to be considered in Figure 1. The next task is to consider mechanization of specific aircraft of which the single rotor helicopter will be the first.

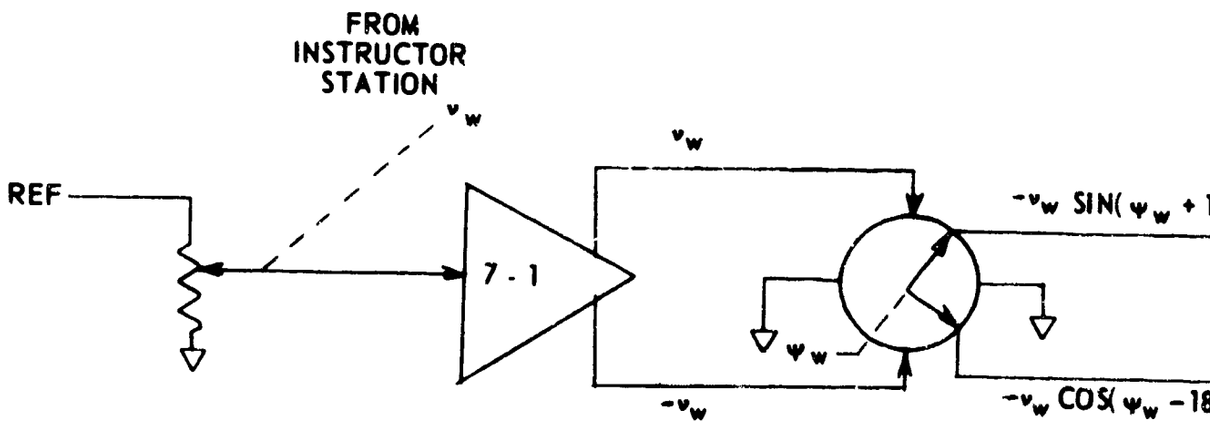
FROM
INSTRUCTOR
STATION
v_w
REF
7 - 1
v_w
$-v_w$ SIN(ψ_w +
ψ_w
$-v_w$ COS(ψ_w -18

A

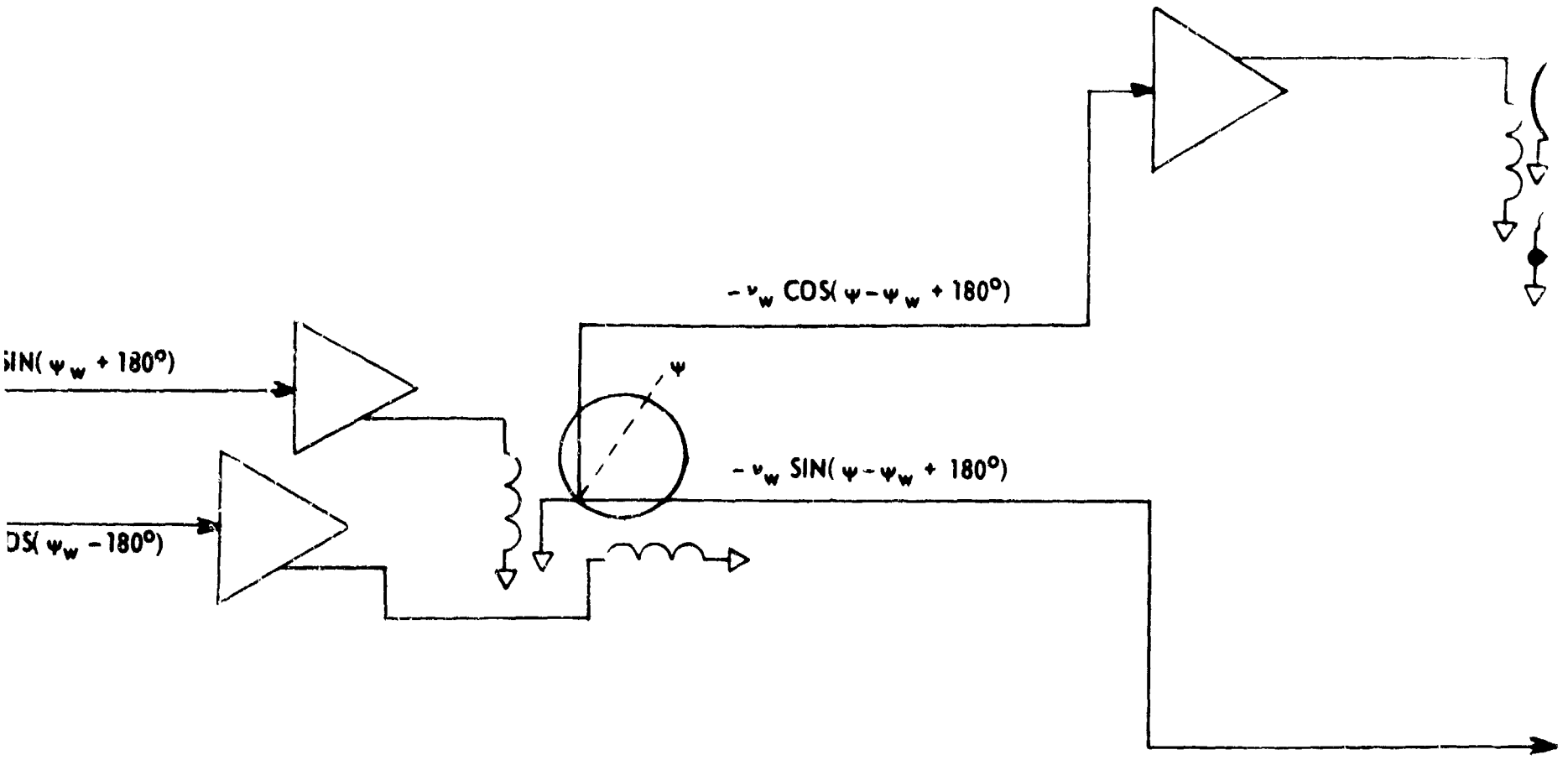
$-v_w \cos(\psi - \psi_w + 180^\circ)$
$\sin(\psi_w + 180^\circ)$
ψ
$-v_w \sin(\psi - \psi_w + 180^\circ)$
$\cos(\psi_w - 180^\circ)$

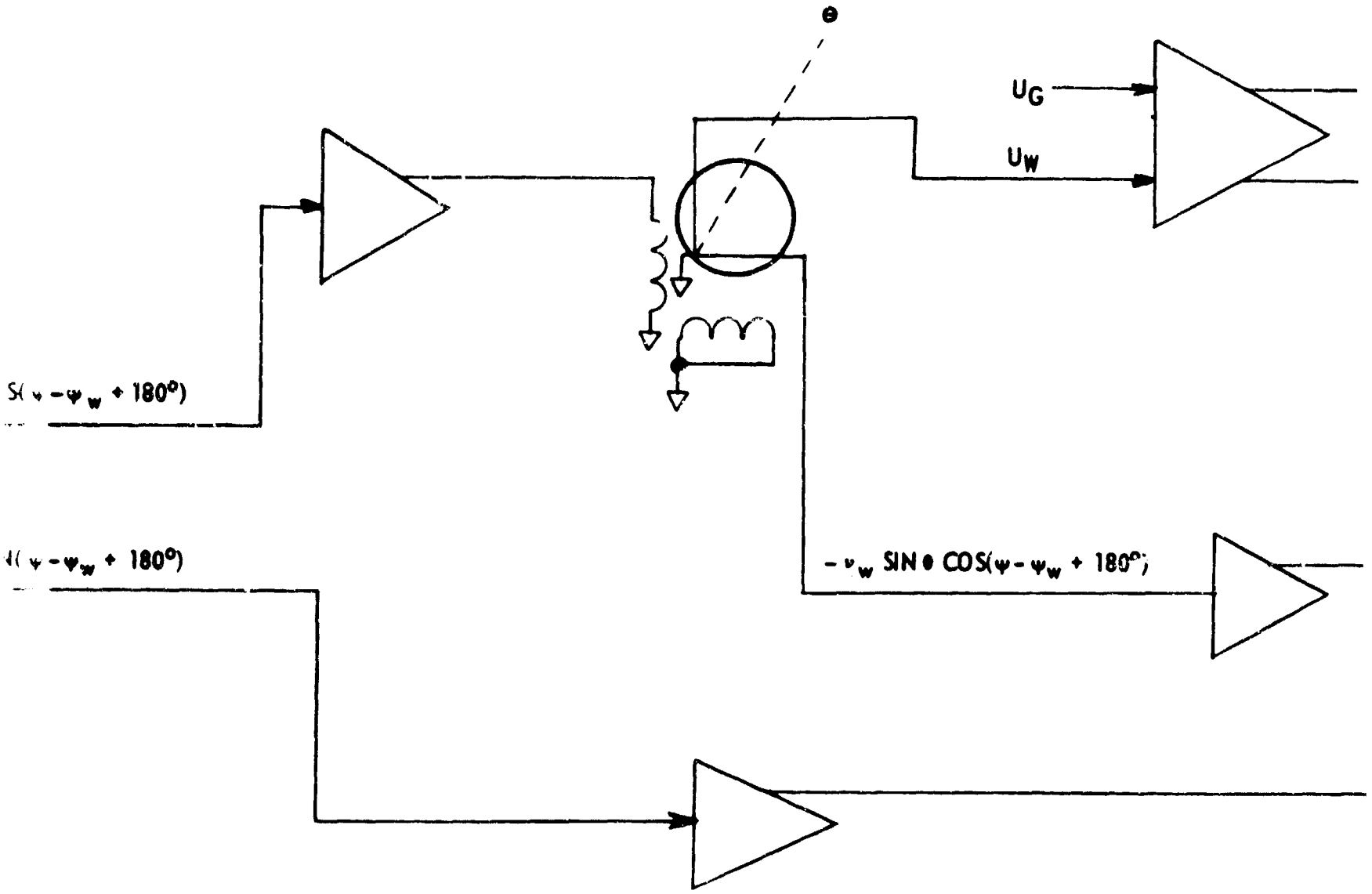

$U = U_G - U_W$
$V = V_G - V_W$
$W = W_G - W_W$

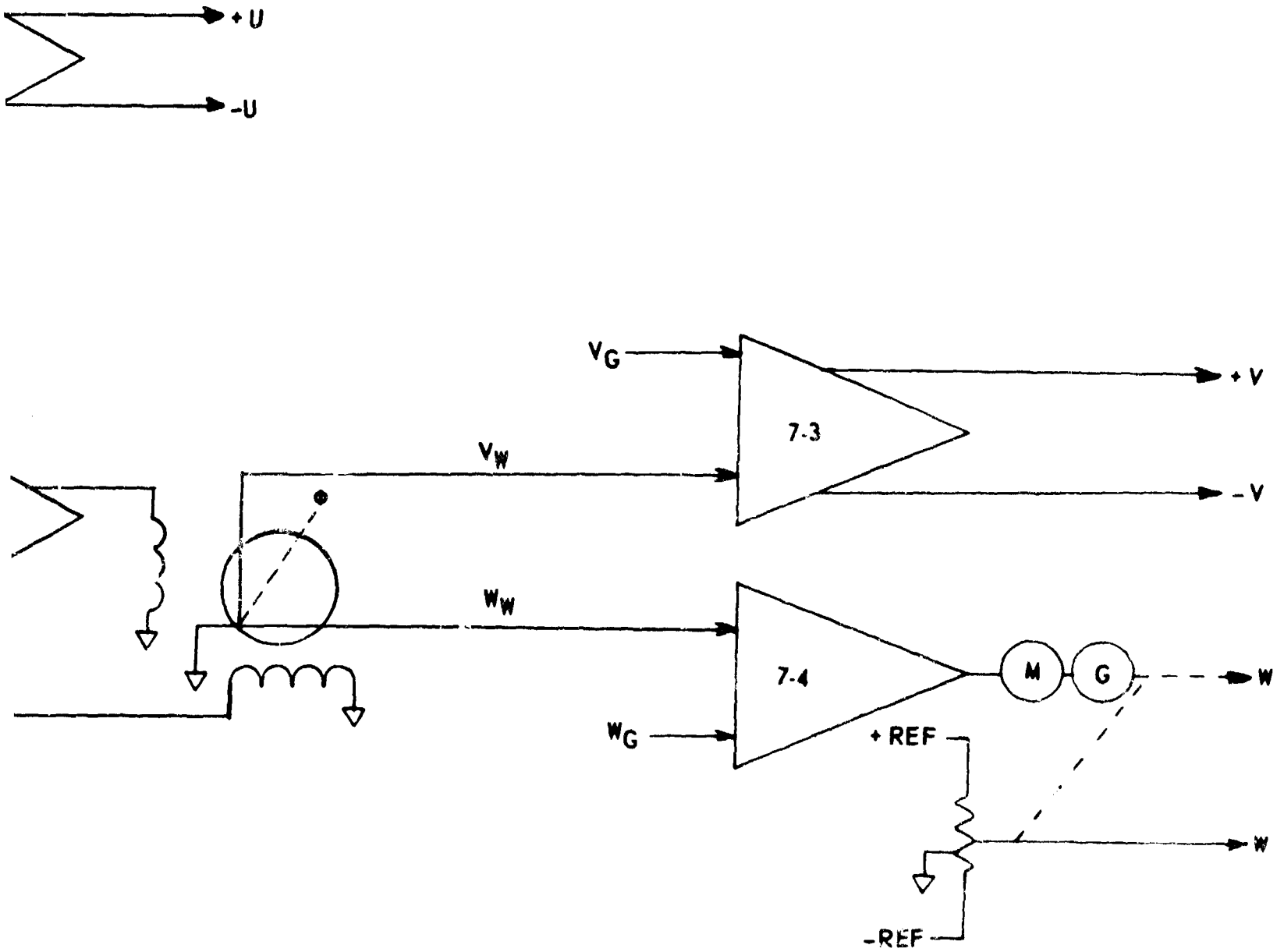

$$-U_W = {}^{v}w \cos \theta \cos (\psi - \psi_w + 180^\circ)$$

$$-V_W = {}^{v}w \left[\sin \theta \sin \theta \cos (\psi - \psi_w + 180^\circ) + \cos \theta \sin (\psi - \psi_w + 180^\circ)\right]$$

$$-W_W = {}^{v}w \left[\sin \theta \cos \theta \cos (\psi - \psi_w + 180^\circ) + \sin \theta \sin (\psi - \psi_w + 180^\circ)\right]$$

B

Figure 7 Velocity Summation and Wind Resolution AC Mechanization

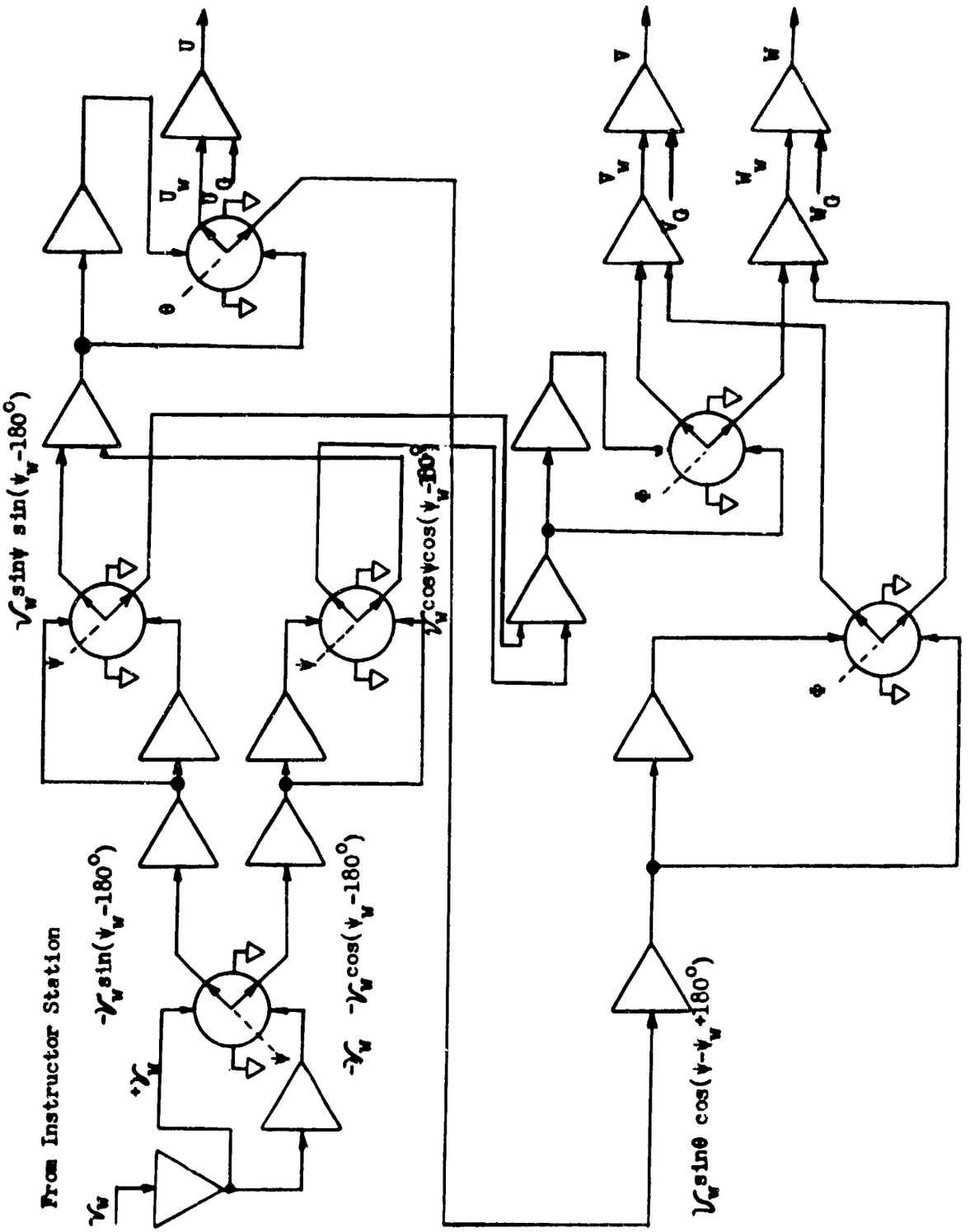

Figure 8. Velocity Summation and Wind Resolution DC Mechanization

Wind blows from Ψ_W heading (true) at v_W ft./sec.

$$U_W = (-)v_W \cos\theta \cos(\Psi - \Psi_W + 180^\circ)$$

$$V_W = (-)v_W \{\sin\theta \sin\Phi \cos(\Psi - \Psi_W + 180^\circ) - \cos\Phi \sin(\Psi - \Psi_W + 180^\circ)\}$$

$$W_W = (-)v_W \{\sin\theta \cos\Phi \cos(\Psi - \Psi_W + 180^\circ) + \sin\Phi \sin(\Psi - \Psi_W + 180^\circ)\}$$

$$U = U_G + U_W$$

$$V = V_G + V_W$$

$$W = W_G + W_W$$

Figure 8. (Cont'd.) Velocity Summation and Wind Resolution DC Mechanization

B. HELICOPTER MECHANIZATION

Mechanisations for two helicopters are considered--the single rotor helicopter represented by the HSS-2 and the tandem rotor helicopter represented by the CH-46A. The major portion of the mechanization discussed is for the single rotor equations of motion. In Volume I of this report (NAVTRADEVCEN 1205-1) it was shown that the tandem rotor could be simulated by considering one rotor as a function of the other rotor—that is to say that a single rotor simulation is sufficient for the tandem rotor simulation.

1. SINGLE ROTOR HELICOPTER. Figure 9 is a block diagram for the HSS-2, Device 2F64, single rotor helicopter which is similar to Figure 1. Again each block in the flow diagram will be considered separately. On each mechanization dr wing are the applicable equations from Section VI. Mechanization drawings are for AC carrier except in a few cases where it was necessary to include DC mechanizations for the sake of clarity. These drawings may be used for 60 or 400 cycle AC as well as DC with slight modification. Each block in Figure 9 will now be considered and the mechanizations discussed with regard to optimization. Definitions of helicopter symbols are outlined in Section VI.A.1.

Block (1) Pilot Control. Block (1) of Figure 9 produces the outputs (A_{os}, A_{1s}, B_{1s}) as a result of control movement. Definitions of these terms are contained in Section VI.

Block (2) Engine Simulation. Block (2) of Figure 9 has as outputs the torques (Q_{EL}, Q_{ER}) of the two engines in the HSS-2. These are considered as available signals since no engine simulation is considered here.

Block (3) Aero Variables. The AC mechanization of Block (3) of Figure 9 is shown in Figure 10. Equations 6.1, 6.2, 6.6 and 6.82 are mechanized to produce the outputs α, β, q, ρ, V_T and $W_{i_{mean}}$. The mechanization of $W_{i_{mean}}$ is included in Figure 10 since it is directly related to the generation of the aerodynamic variables. A literal step-by-step discussion of Figure 10 will now be given. This will not be done for many of the remaining drawings since the methods of mechanizations in Figure 10 are repeated throughout the report, and such a continuous literal discussion when the equations are on each drawing and each line in the drawing is labeled would be laborious, redundant and difficult to read.

In Figure 10 $W_{i_{mean}}$ is formed by dividing main rotor lift over air density ($-L_{MR}/\rho$) by the total velocity of the helicopter (V_T). This signal ($-KL_{MR}/V_T$) is fed into a servo amplifier whereby $W_{i_{mean}}$ is generated by a servo shaft. $W_{i_{mean}}$ is used as position feedback and the rate feedback is $\dot{W}_{i_{mean}}$.

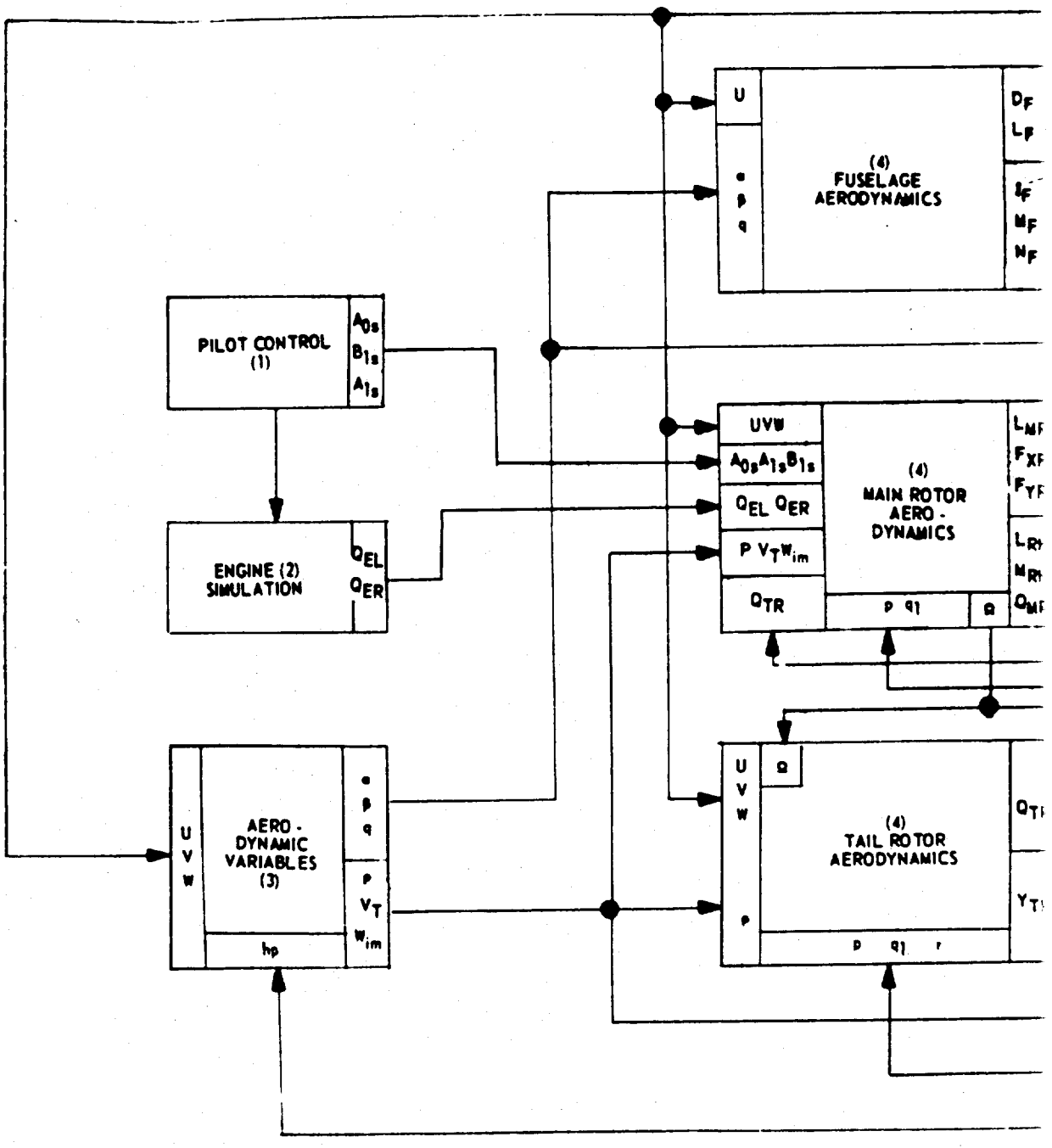
U
α
β
q
(4)
FUSELAGE
AERODYNAMICS
D_F
L_F
Y_F
M_F
N_F
PILOT CONTROL
(1)
A_{0s}
B_{1s}
A_{1s}
UVW
$A_{0s}A_{1s}B_{1s}$
Q_{EL} Q_{ER}
P V_T W_{im}
Q_{TR}
(4)
MAIN ROTOR
AERO -
DYNAMICS
p q1
Ω
ENGINE (2)
SIMULATION
Q_{EL}
Q_{ER}
U
V
W
AERO -
DYNAMIC
VARIABLES
(3)
α
β
q
P
V_T
W_{im}
h_p
U
V
W
Ω
(4)
TAIL ROTOR
AERODYNAMICS
p
p q1 r

A

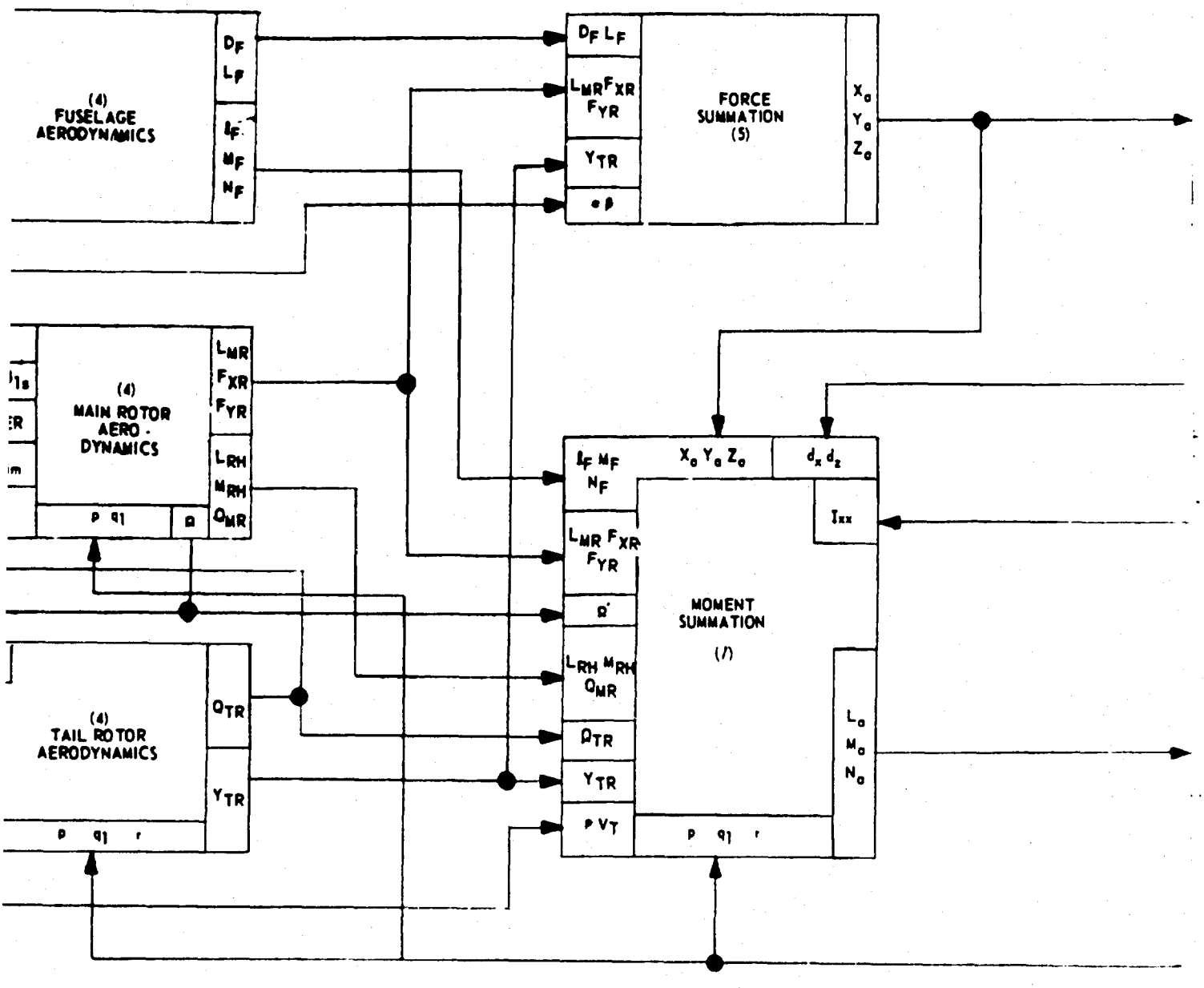
(4)
FUSELAGE
AERODYNAMICS
D_F
L_F
ℓ_F
M_F
N_F
D_F L_F
L_{MR} F_{XR}
F_{YR}
Y_{TR}
α β
FORCE
SUMMATION
(5)
X_a
Y_a
Z_a
(4)
MAIN ROTOR
AERO-
DYNAMICS
L_{MR}
F_{XR}
F_{YR}
L_{RH}
M_{RH}
Q_{MR}
p q1
Ω
ℓ_F M_F
N_F
X_a Y_a Z_a
d_x d_z
I_{xx}
L_{MR} F_{XR}
F_{YR}
Ω̇
L_{RH} M_{RH}
Q_{MR}
Q_{TR}
Y_{TR}
p V_T
MOMENT
SUMMATION
(7)
L_a
M_a
N_a
(4)
TAIL ROTOR
AERODYNAMICS
Q_{TR}
Y_{TR}
p q1 r
p q1 r

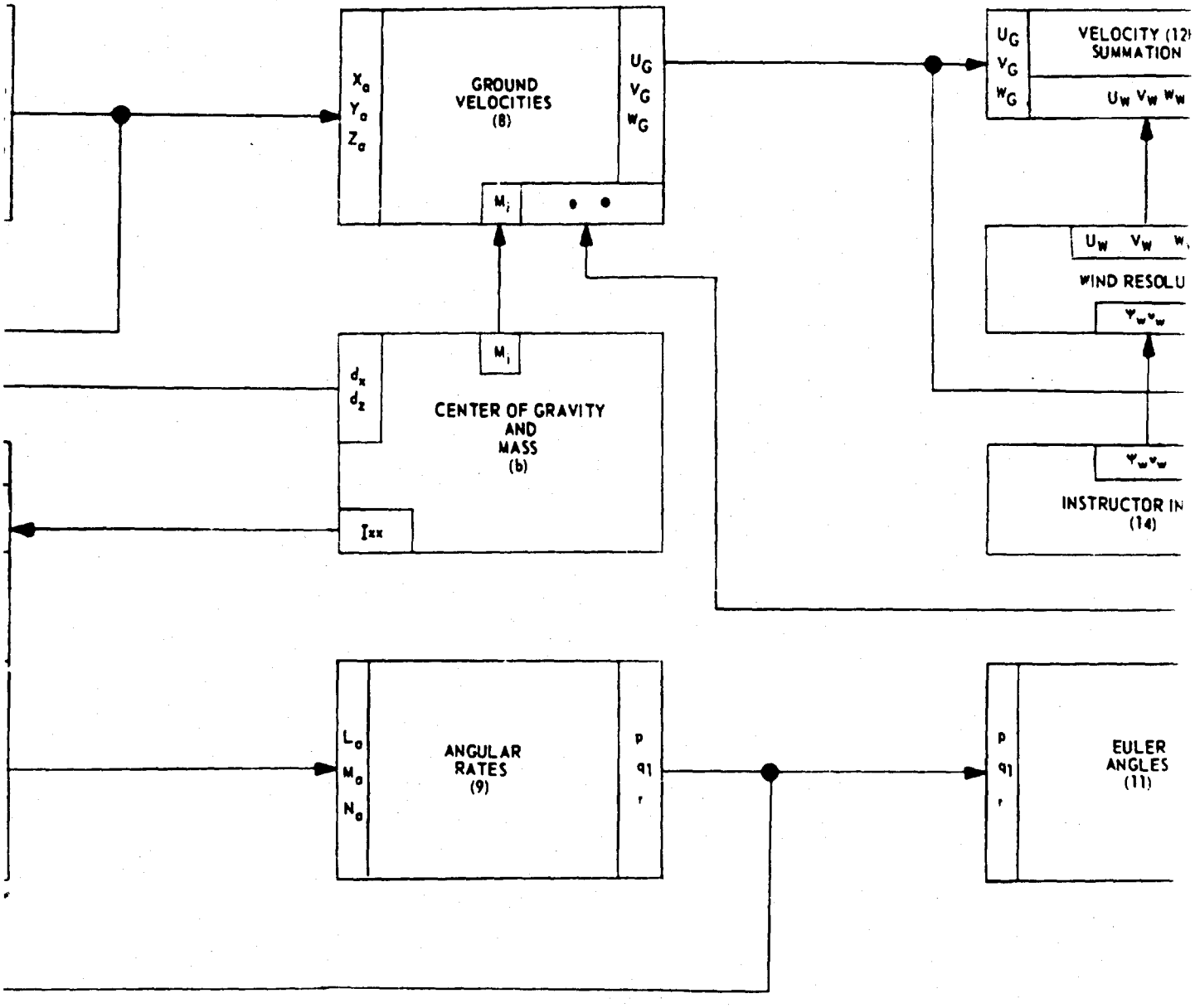
X_a
Y_a
Z_a
GROUND VELOCITIES (8)
U_G
V_G
W_G
M_i
U_G
V_G
W_G
VELOCITY (12)
SUMMATION
U_W V_W W_W
U_W V_W
WIND RESOLU
M_i
d_x
d_z
CENTER OF GRAVITY AND MASS (b)
I_{xx}
INSTRUCTOR IN
(14)
L_a
M_a
N_a
ANGULAR RATES (9)
p
q
r
p
q
r
EULER ANGLES (11)

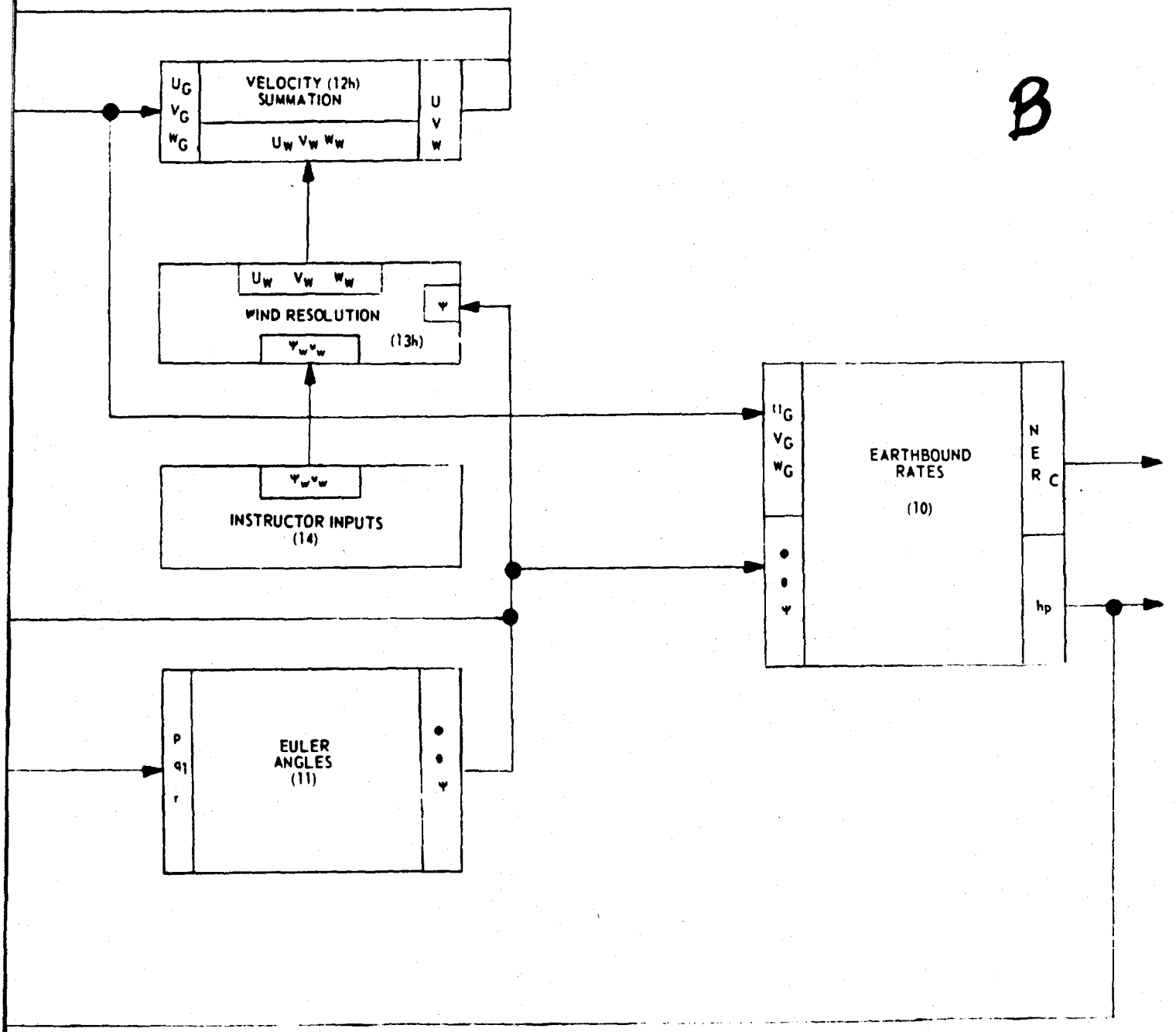

B

Figure 9. Simplified Block Diagram Single Rotor Helicopter


2
FRAMES

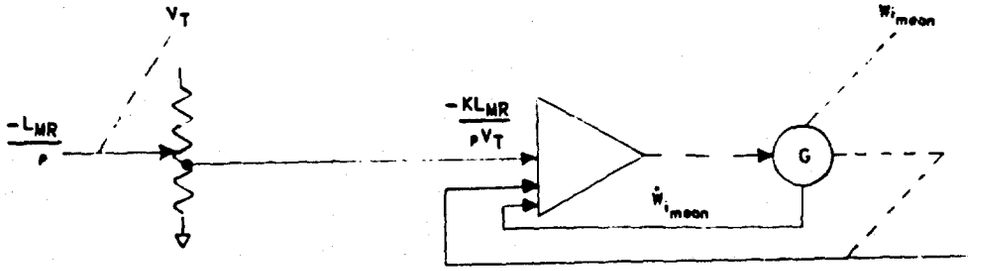
V_T
$-\frac{L_{MR}}{p}$
$-\frac{KL_{MR}}{pV_T}$
$W_{i_{mean}}$
G
$\dot{W}_{i_{mean}}$

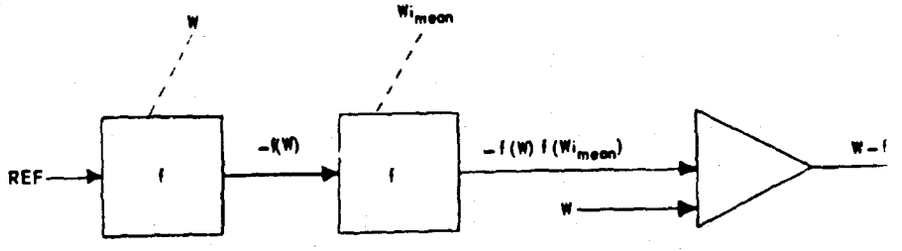
W
$W_{i_{mean}}$
REF
f
$-f(W)$
f
$-f(W)\,f(W_{i_{mean}})$
W
W – f

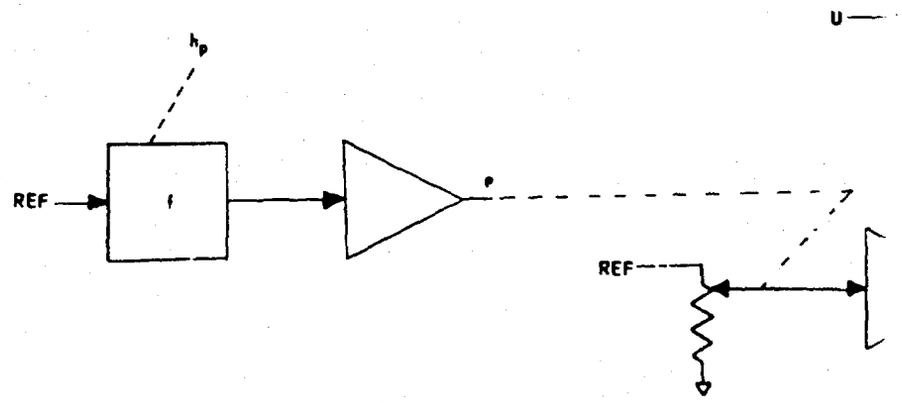
U
h_p
REF
f
p
REF

A

$$5.1 \quad \alpha = 4^\circ + \text{ARC TAN} \frac{W - f(W_{i_{mean}})\, f(W)}{U}$$

$$5.2 \quad \beta = \text{ARC TAN} \frac{V}{\sqrt{U^2 + [W - f(W_{i_{mean}})\, f(W)]^2}}$$

$$5.6 \quad V_T = \sqrt{U^2 + V^2 + [W - f(W_{i_{mean}})\, f(W)]^2}$$

$$5.82 \quad (w_i)_{mean} = \frac{L_{MR}}{2\rho\pi R^2 \sqrt{U^2 + [W - f(W_{i_{mean}})\, f(W)]^2 + V^2}}$$

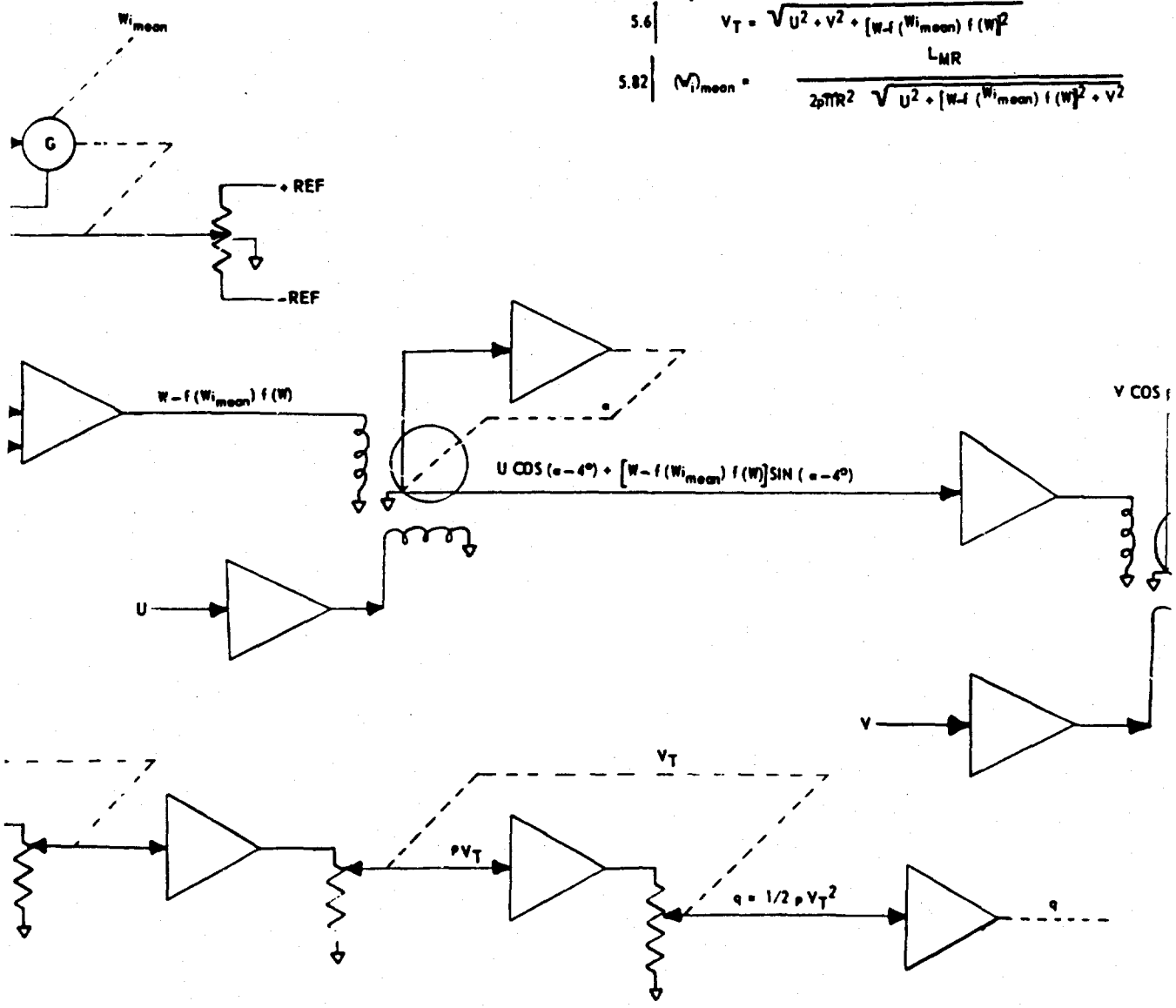

Figure IQ Aero

$$5.1 \quad \alpha = 4^\circ + \text{ARC TAN} \frac{W - f(W_{i_{mean}})\, f(W)}{U}$$

$$5.2 \quad \beta = \text{ARC TAN} \frac{V}{\sqrt{U^2 + [W - f(W_{i_{mean}})\, f(W)]^2}}$$

$$5.6 \quad V_T = \sqrt{U^2 + V^2 + [W - f(W_{i_{mean}})\, f(W)]^2}$$

$$5.82 \quad (V_i)_{mean} = \frac{L_{MR}}{2\pi R^2 \sqrt{U^2 + [W - f(W_{i_{mean}})\, f(W)]^2 + V^2}}$$

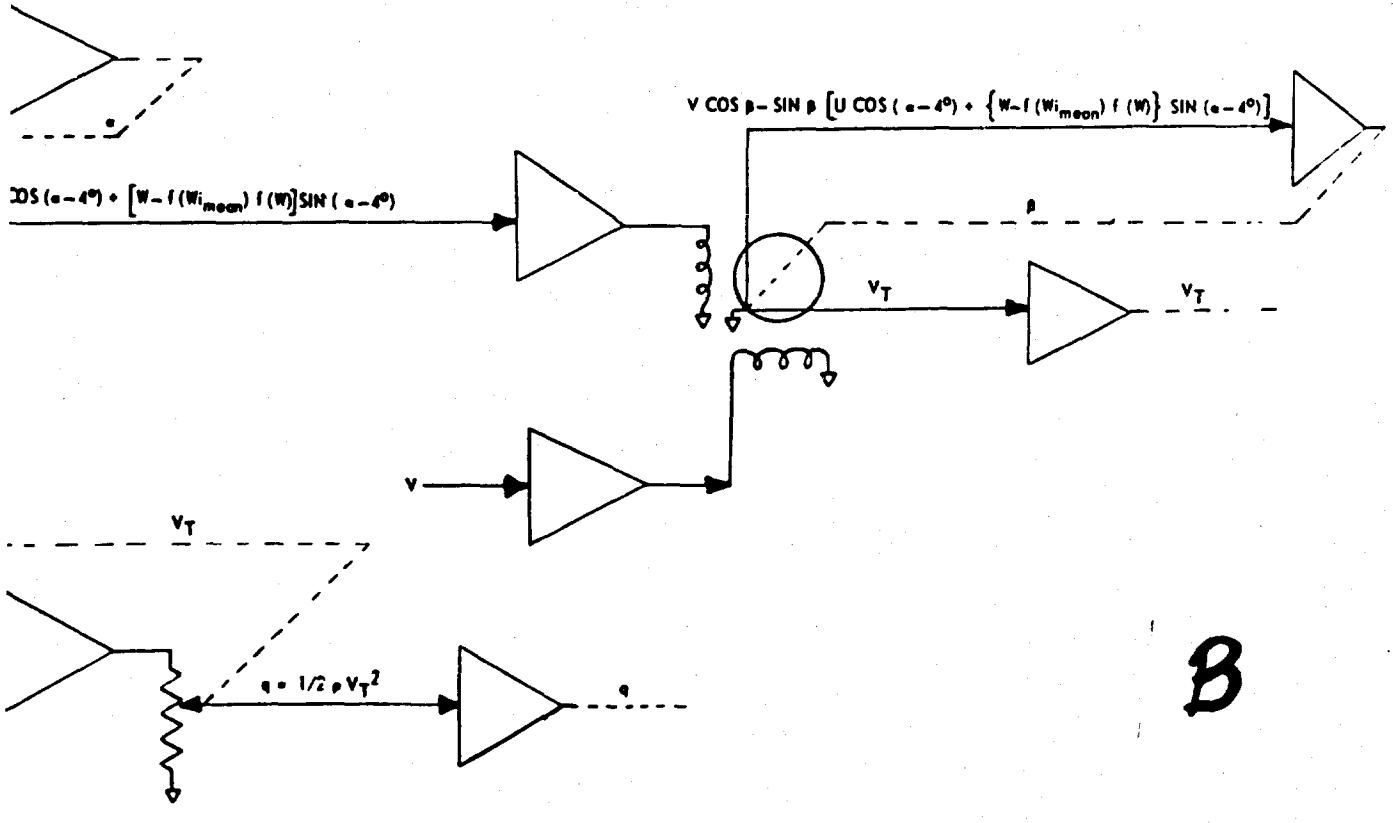

Figure 10. Aerodynamic Variables AC Mechanization

V_T is formed next in Figure 10. A function of vertical velocity, $-f(W)$, is developed first. This is then multiplied by a function of $W_{i_{mean}}$ to give $-f(W)f(W_{i_{mean}})$. The functions are generated by shaped potentiometers, f_1 and f_2. Next, $-f(W)f(W_{i_{mean}})$ is added to vertical velocity, W, in a summing amplifier to form the output $[W - f(W)f(W_{i_{mean}})]$ which is then fed into the stator winding of a resolver on the α servo shaft. The other stator winding of the resolver is driven by the helicopter forward velocity, U, through a resolver drive amplifier. The output of one rotor forms the function $[W - f(W)f(W_{i_{mean}})] \cos \alpha - U \sin \alpha$ which is fed to motor amplifier of the α servo shaft. Now, since output of the resolver is the driving source of the servo shaft, the servo shaft will continue to drive the resolver until the resolver output is zero. When this occurs, then

$$[W - f(W)f(W_{i_{mean}})] \cos \alpha - U \sin \alpha = 0$$

and $$\frac{\sin \alpha}{\cos \alpha} = \tan \alpha = \frac{[W - f(W)f(W_{i_{mean}})]}{U} .$$

If the resolver is zeroed such that $(\alpha - 4^\circ) = 0$ when $\alpha = 4^\circ$ then equation 5.1 will have been mechanized, $[W - f(W)f(W_{i_{mean}})] \cos (\alpha - 4^\circ) - U \sin (\alpha - 4^\circ)$ will be identically equal to zero and the servo shaft will form the function α. Since the shaft of the resolver is now positioned automatically to α and the resolver is zeroed so that its shaft positions to $(\alpha - 4^\circ)$ the remaining rotor winding forms the function $U \cos (\alpha - 4^\circ) + [W - f(W)f(W_{i_{mean}})] \sin (\alpha - 4^\circ)$, which is easily seen to identically equal $\sqrt{U^2 + [W - f(W)f(W_{i_{mean}})]^2}$ if one considers U and the W function as legs of a right triangle and the hypotenuse as the sum of the projections of the legs as shown in the sketch below.

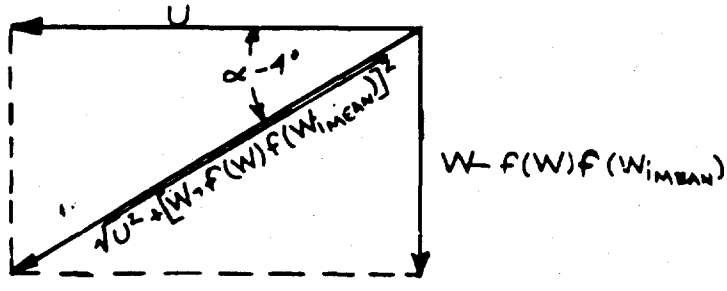

In a manner similar to the above the helicopter sideward velocity, V, and $U^2 + [W - f(W)f(W_{i_{mean}})]^2$ are used to drive a resolver on the β servo shaft. The relation $V \cos\beta - \sin\beta \left[U \cos(\alpha - 4^\circ) + \left\{W - f(W)f(W_{i_{mean}})\right\} \sin(\alpha - 4^\circ)\right]$ is used to drive the servo shaft so that the shaft positions to the angle equal to β and equation 6.2 is mechanised. The remaining rotor output is conveniently found to be the helicopter total velocity, V_T, since it forms the square root of the sum of the squares of the resolver inputs in the same manner as the α resolver. The output, V_T, is fed to a motor amplifier to drive the V_T servo shaft.

The last mechanization in Figure 10 is that of dynamic pressure (q). Initially, functions of pressure altitude (h_p) are fed into an amplifier as air density (ρ) to form a ρ servo. A ρ servo shaft potentiometer wiper output is fed into a buffer amplifier whose output drives a potentiometer located on a V_T servo shaft. The wiper output of this potentiometer is ρV_T which is fed into a buffer amplifier whose output is $1/2\ \rho V_T$ and drives a potentiometer located on a V_T servo shaft. The wiper output of this potentiometer is $1/2\ \rho V_T^2$ which is equal to q. In turn, q is fed into an amplifier which drives the q position servo.

DC mechanization of Figure 10 involves sine-cosine potentiometers and additional amplifiers for buffer and sign inversion purposes to replace resolvers. If resolvers are used with DC, modulators and demodulators would be necessary. This component complexity is due to the interfacing of AC and DC equipment. Table 6 is a comparison of AC and DC components.

	AC		DC	
Component	No.	Wt.	No.	Wt.
Amplifier	12	12	18	36
Servo	6	42	6	42
Pots	5	1 1/4	5	1 1/4
S-C Pots			4	1
Resolvers	2	1		
Complexity		56 1/4		80 1/4

Table 6. Aerodynamic Variables Single Rotor Helicopter

For each resolver in the AC mechanization two sine-cosine potentiometers and three additional amplifiers are necessary for a DC mechanization.

Block (4) Aero Terms. The AC mechanization of Block (4), Figure 9 is divided into three parts--Tail Rotor Aerodynamics, Fuselage Aerodynamics and Main Rotor Aerodynamics.

a. Tail Rotor Aerodynamics. In Figure 11 is shown the AC mechanization of the tail rotor equations (6.7 through 6.17 and 6.26). The component tabulation is in Table 7. A literal discussion would be similar to that of Block (3) Aero Variables, Figure 10.

	AC		DC	
Component	No.	Wt.	No.	Wt.
Amplifier	19	19	25	50
Servo	7	49	7	49
Pots	8	2	8	2
S-C Pots			4	1
Resolvers	2	1		
Function (f) Generation	10	-	10	
Complexity		71		102

Table 7. Tail Rotor Aerodynamics

The function generators (f) are composed of potentiometers either in AC or DC mechanization. It is conceivable that more buffer and sign inversion amplifiers may be necessary to achieve function generation for the DC mechanization.

b. Fuselage Aerodynamics. The mechanization of fuselage aerodynamics is simply a summing operation of function generator outputs. Figure 12 is the recommended AC mechanization. The DC mechanization would be dependent on the relationship of the components with the remainder of the mechanization, however DC mechanization should be the same as that shown in Figure 12. Table 8 is a list of components showing the similarity between a DC mechanization and the AC mechanization of Figure 12.

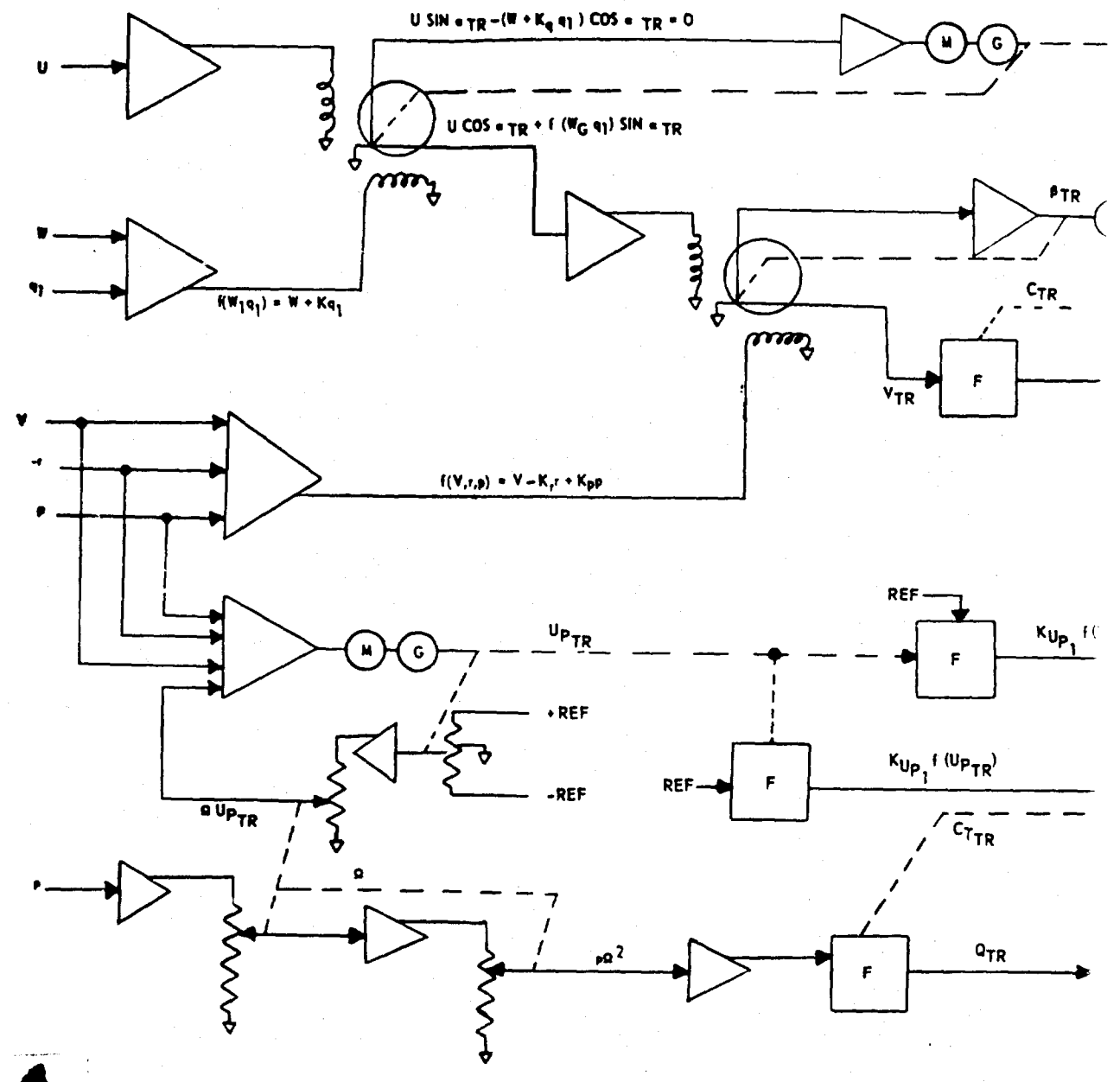
U SIN α TR − (W + Kq q1) COS α TR = 0
U
M
G
U COS α TR + f (WG q1) SIN α TR
W
q1
f(W1q1) = W + Kq1
βTR
CTR
VTR
F
V
r
p
f(V,r,p) = V − Kr r + Kpp
REF
UPTR
KUP1 f(
+REF
-REF
Ω UPTR
KUP1 f (UPTR)
Ω
pΩ2
CTTR
QTR

A

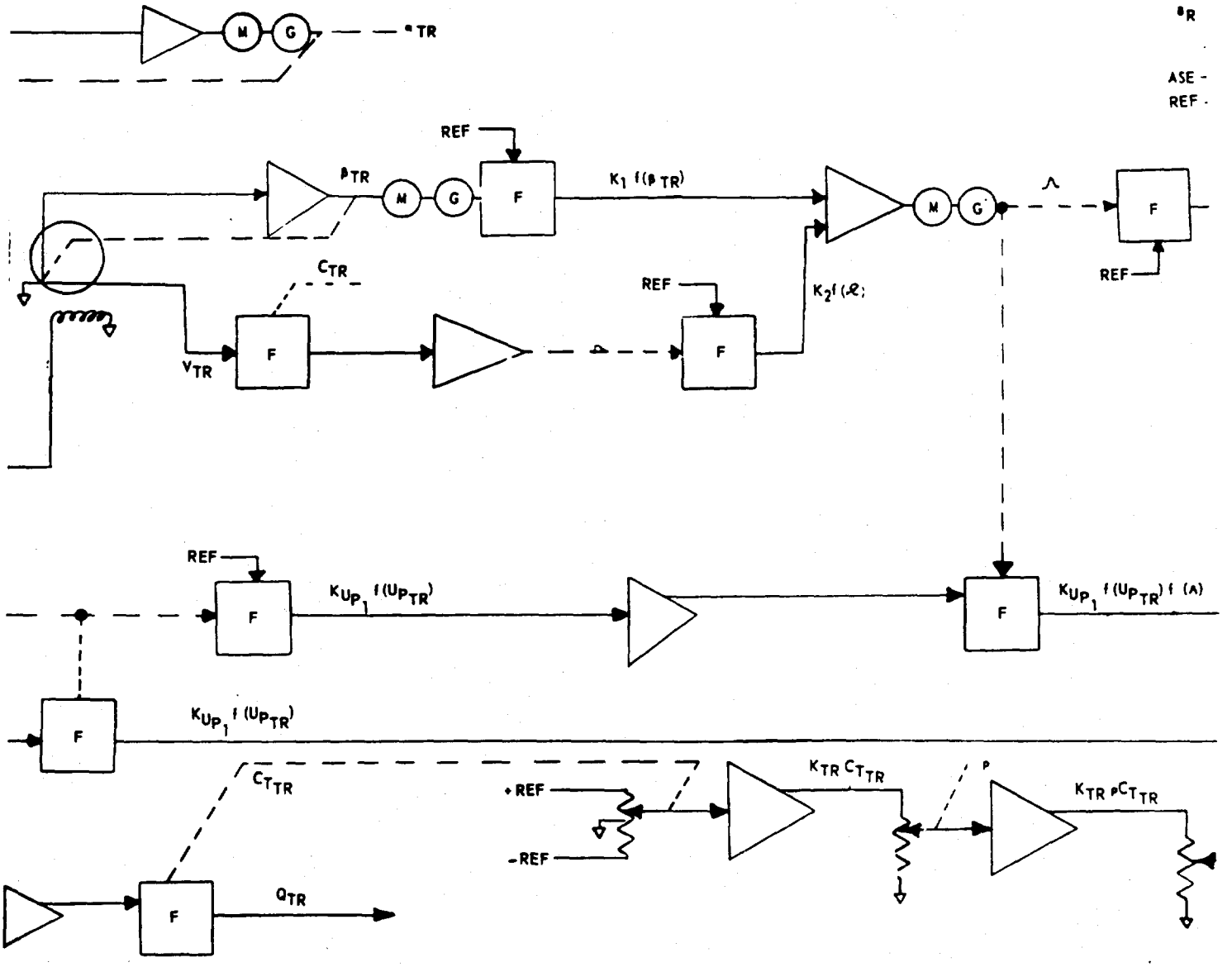
M
G
REF
F
REF
F
REF
F
REF
F
F
F
F
F
+REF
-REF
P

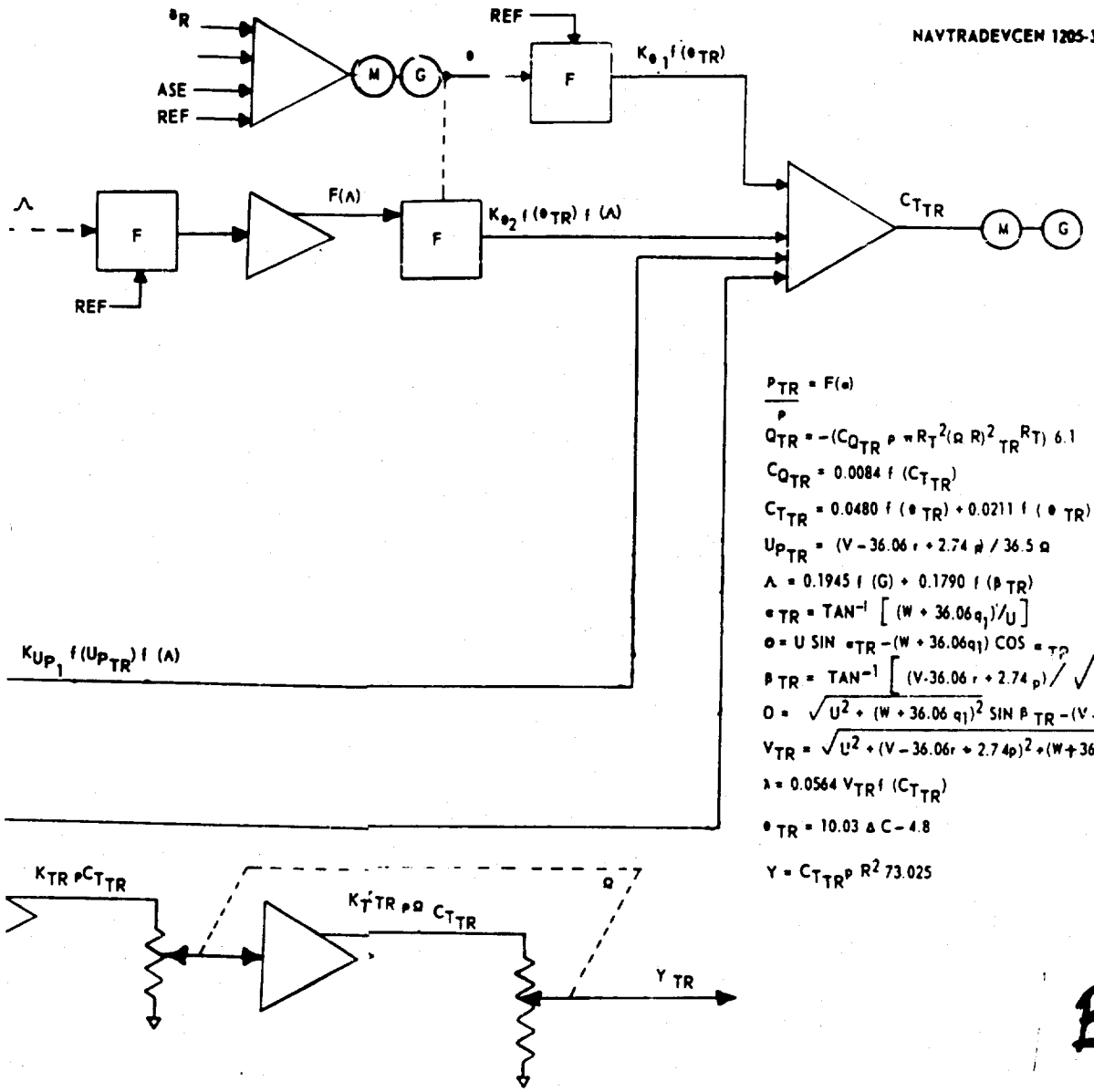

$\frac{P_{TR}}{\rho} = F(\sigma)$

$Q_{TR} = -(C_{Q_{TR}} \rho \pi R_T^2 (\Omega R)^2 {}_{TR} R_T)$ 6.1

$C_{Q_{TR}} = 0.0084 f(C_{T_{TR}})$

$C_{T_{TR}} = 0.0480 f(\theta_{TR}) + 0.0211 f(\theta_{TR}) f(\Lambda) + B_{32}$

$UP_{TR} = (V - 36.06 r + 2.74 p) / 36.5 \Omega$

$\Lambda = 0.1945 f(G) + 0.1790 f(\beta_{TR})$

$\alpha_{TR} = TAN^{-1} \left[(W + 36.06 q_1) / U \right]$

$\sigma = U \sin \alpha_{TR} - (W + 36.06 q_1) \cos \alpha_{TR}$

$\beta_{TR} = TAN^{-1} \left[(V - 36.06 r + 2.74 p) / \sqrt{U^2 + (W + 36.06 q_1)^2} \right]$

$O = \sqrt{U^2 + (W + 36.06 q_1)^2} \sin \beta_{TR} - (V - 36.06 r + 2.74 p) \cos \beta_{TR}$

$V_{TR} = \sqrt{U^2 + (V - 36.06 r + 2.74 p)^2 + (W + 36.06 q_1)^2}$

$\lambda = 0.0564 V_{TR} f(C_{T_{TR}})$

$\theta_{TR} = 10.03 \Delta C - 4.8$

$Y = C_{T_{TR}} \rho R^2 73.025$

B

Figure 11. Tail Rotor Aerodynamics AC Mechanization

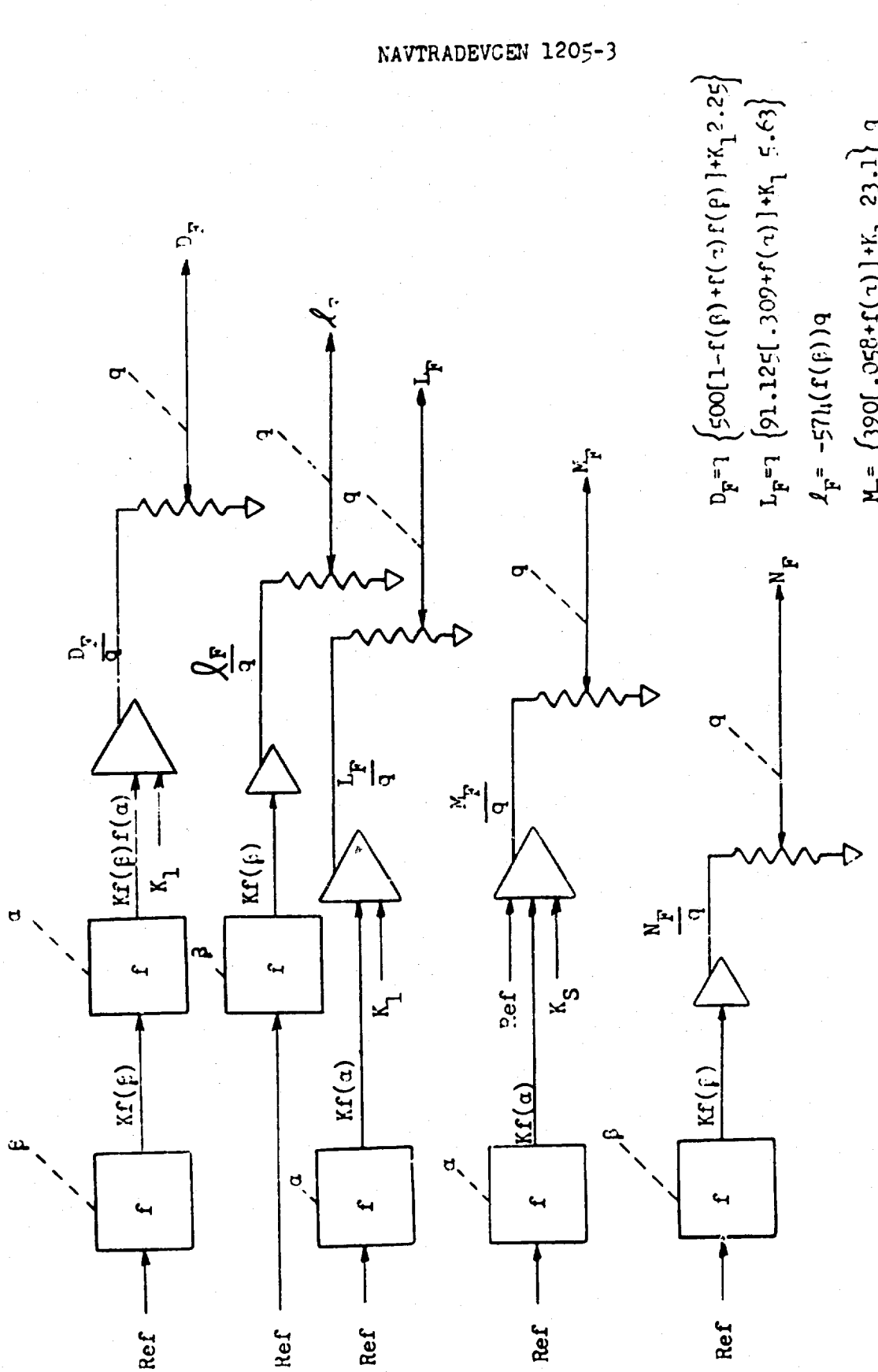

Figure 12. Fuselage Aerodynamics
AC Mechanization

	AC		DC	
Component	No.	Wt.	No.	Wt.
Amplifier	5	5	5	5
Pots	5	1 1/4	5	1 1/4
Complexity		6 1/4		6 1/4

Table 8. Fuselage Aerodynamics

c. Main Rotor Aerodynamics. The main rotor aerodynamics mechanization of the blade element equations involves more computing equipment than that required to generate all other functions in the mechanization of the equations of motion. For this reason the main rotor aerodynamic mechanization is divided into several smaller mechanizations to facilitate discussion and insertion in the report.

Figure 13 is a simplified block diagram showing the interconnection and function flow between these subsections.

(1) Block (1) Local Vertical Velocity. Consider first the mechanization of the local vertical velocity, $U_{P_{\psi-y}}$, in Block (1) of Figure 14. Eighteen $U_{P_{\psi-y}}$ functions of both polarities must be developed from external inputs U, V, W, $W_{i_{mean}}$, Ω, p and q_1 and internally generated feedback inputs a_{1s}, b_{1s} and $\beta\psi$. This involves the basic operations of potentiometer multiplying and amplifier summing. Since these are such simple operations the optimization decision is entirely decided on the economics and complexity aspects. The DC mechanization differs from the AC only in the number of amplifiers required for the positive and negative functions. The DC mechanization required 36 amplifiers instead of 18. From the standpoint of economy the AC mechanization with less amplifiers seems optimum. The complexity of the equipment is certainly in proportion to the number of components. Consult Table 9 for tabulation of components.

	AC		DC	
Component	No.	Wt.	No.	Wt.
Amplifier	18	18	36	36
Pots	17	3 3/4	17	3 3/4
Complexity		21 3/4		39 3/4

Table 9. Local Vertical Velocity

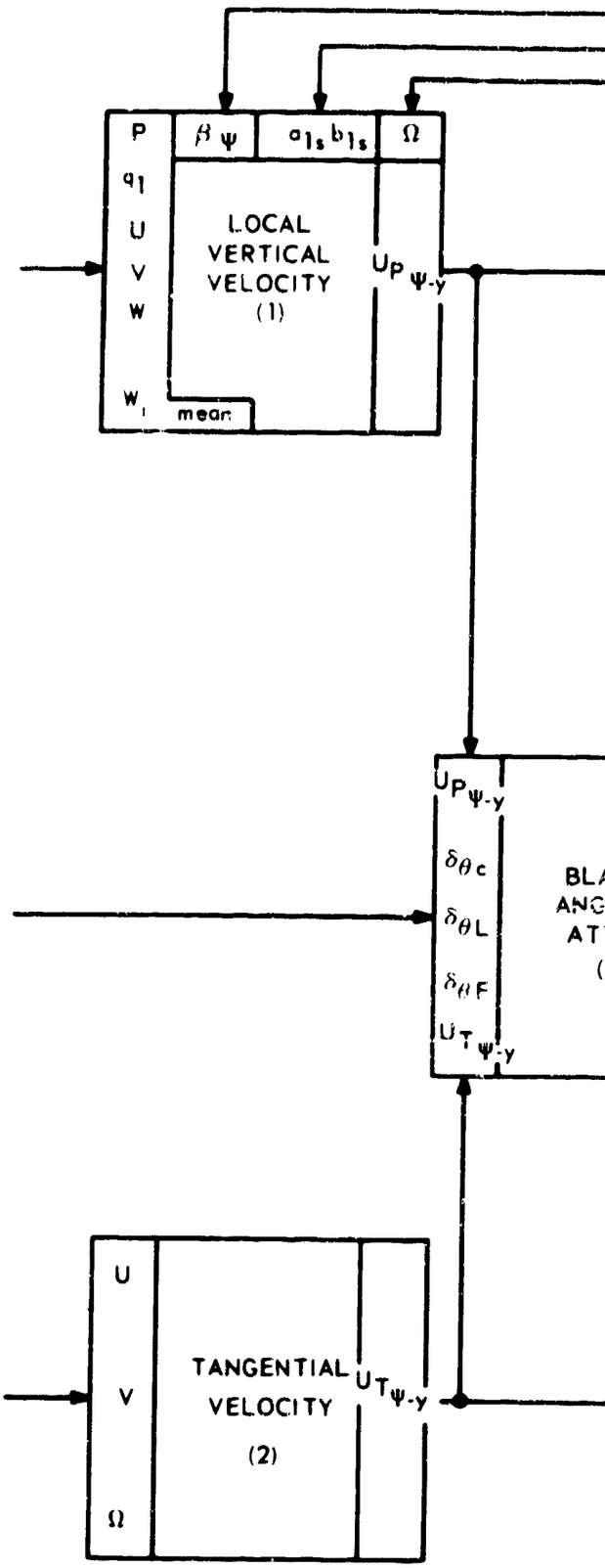
P
β_ψ
a_{1s} b_{1s}
Ω
q_1
U
V
W
W_1
mean
LOCAL VERTICAL VELOCITY (1)
$U_{P_{\psi-y}}$
$U_{P_{\psi-y}}$
$\delta_{\theta c}$
$\delta_{\theta L}$
$\delta_{\theta F}$
$U_{T_{\psi-y}}$
BLA
ANG
AT
U
V
Ω
TANGENTIAL VELOCITY (2)
$U_{T_{\psi-y}}$

A

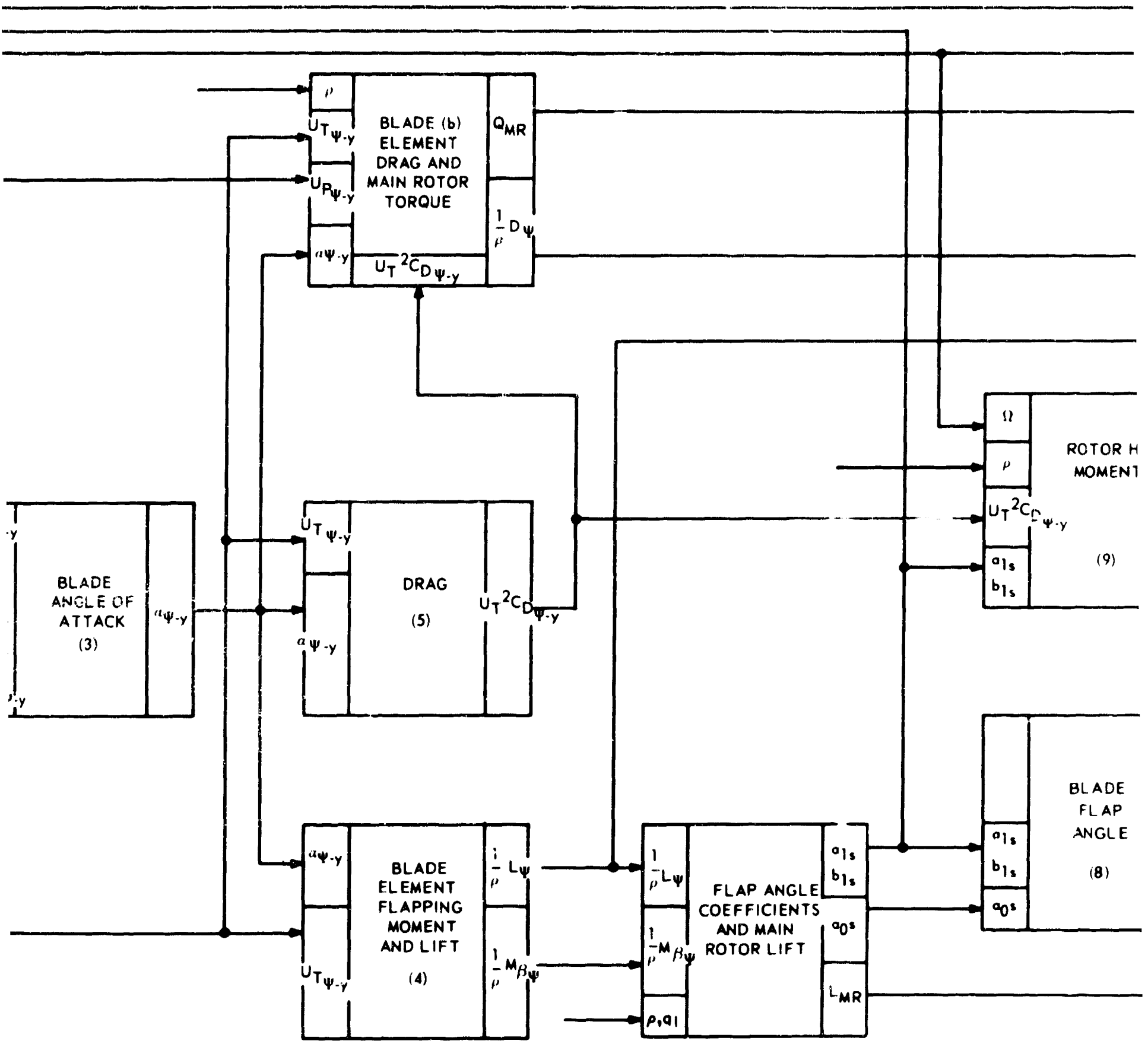

Figure 13 SIMPLIF

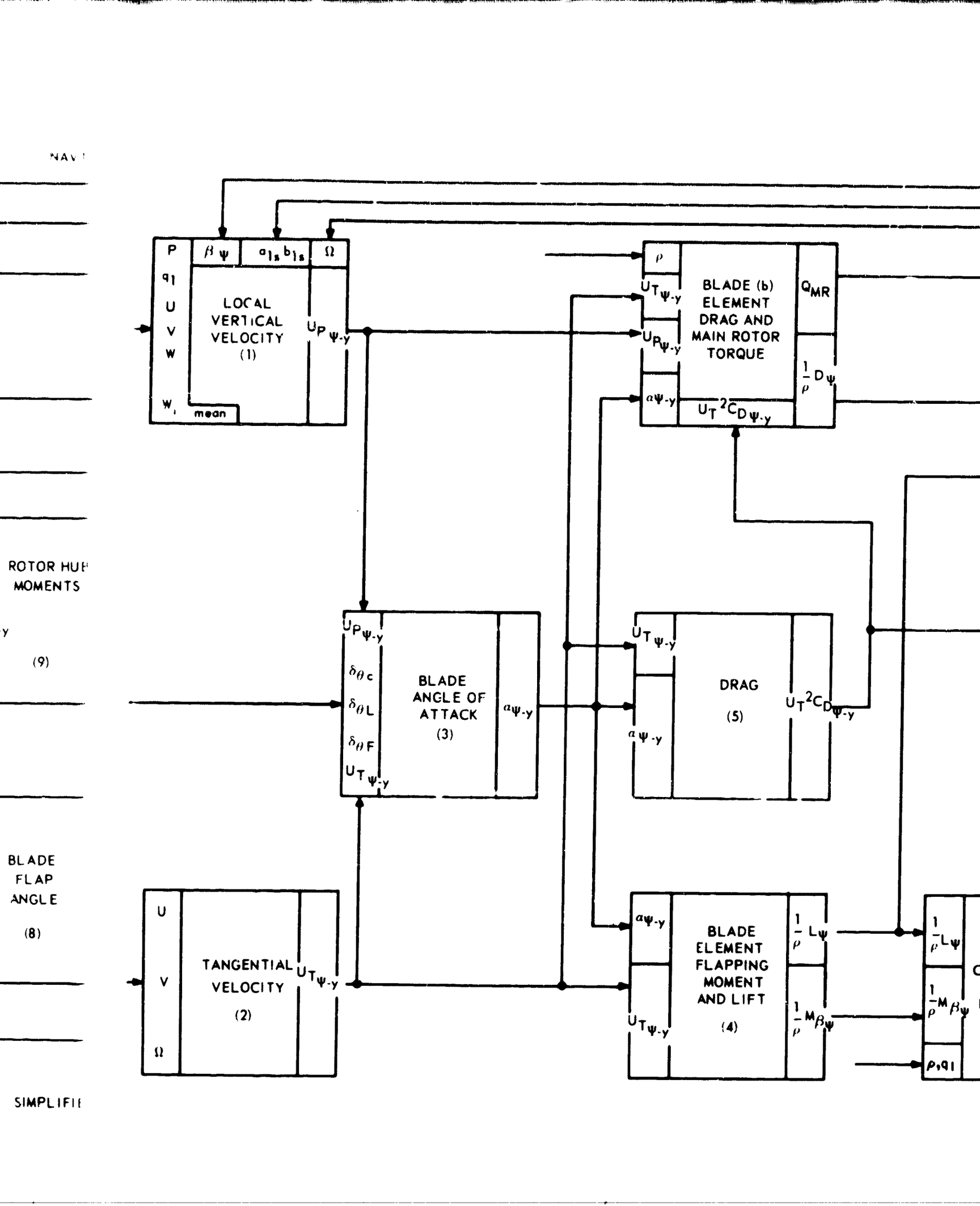
P
q
U
V
W
W_i
mean
β_ψ
a_{1s} b_{1s}
Ω
LOCAL VERTICAL VELOCITY (1)
$U_{P_{\psi-y}}$
ρ
$U_{T_{\psi-y}}$
$U_{P_{\psi-y}}$
$\alpha_{\psi-y}$
BLADE (b) ELEMENT DRAG AND MAIN ROTOR TORQUE
$U_T{}^2 C_{D_{\psi-y}}$
Q_{MR}
$\frac{1}{\rho} D_\psi$
$U_{P_{\psi-y}}$
$\delta_{\theta c}$
$\delta_{\theta L}$
$\delta_{\theta F}$
$U_{T_{\psi-y}}$
BLADE ANGLE OF ATTACK (3)
$\alpha_{\psi-y}$
$U_{T_{\psi-y}}$
$\alpha_{\psi-y}$
DRAG (5)
$U_T{}^2 C_{D_{\psi-y}}$
U
V
Ω
TANGENTIAL VELOCITY (2)
$U_{T_{\psi-y}}$
$\alpha_{\psi-y}$
$U_{T_{\psi-y}}$
BLADE ELEMENT FLAPPING MOMENT AND LIFT (4)
$\frac{1}{\rho} L_\psi$
$\frac{1}{\rho} M_{\beta_\psi}$
$\frac{1}{\rho} L_\psi$
$\frac{1}{\rho} M_{\beta_\psi}$
ρ, q_1

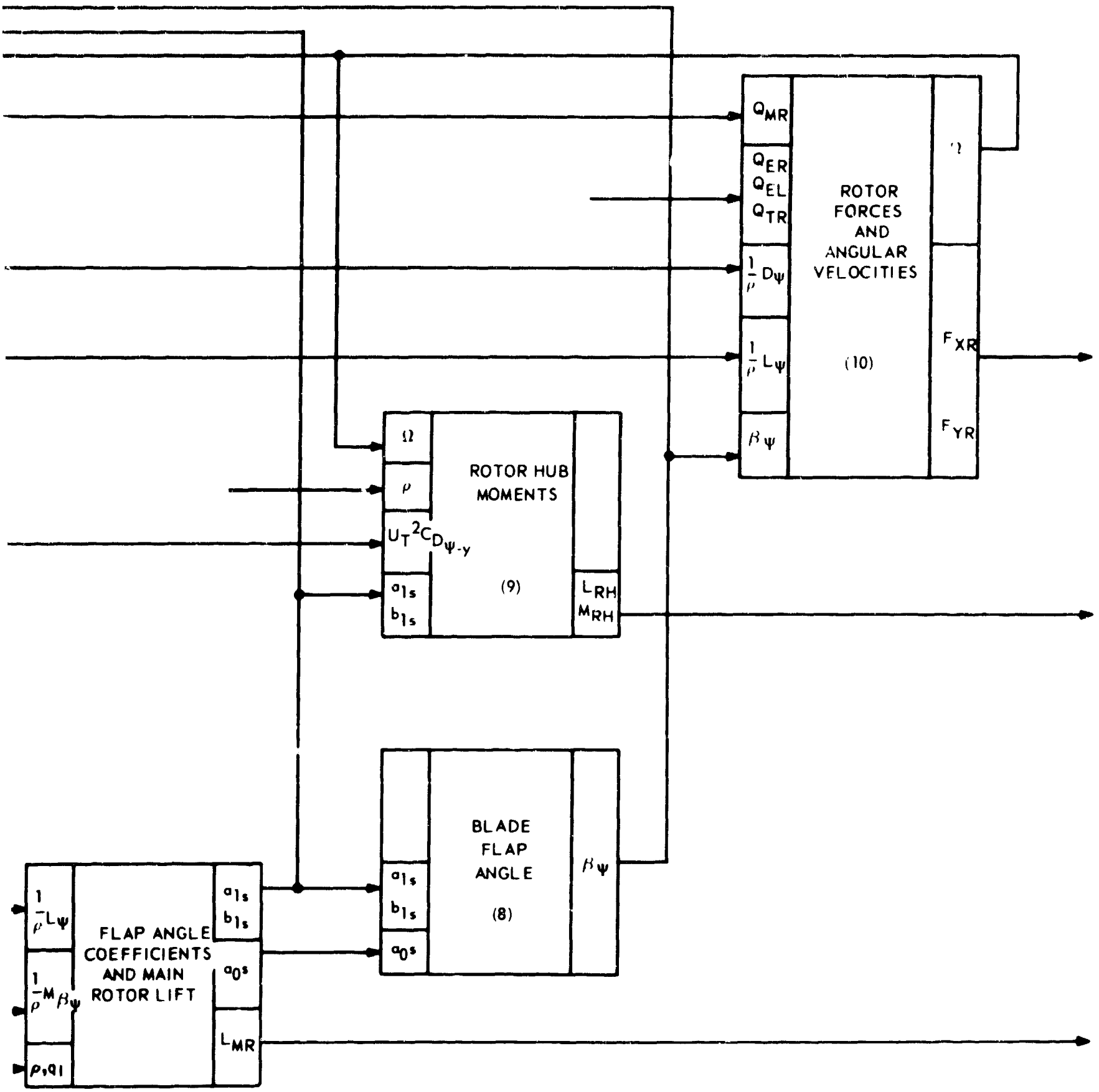

Figure 13 SIMPLIFIED BLOCK DIAGRAM ROTOR AERODYNAMICS

B

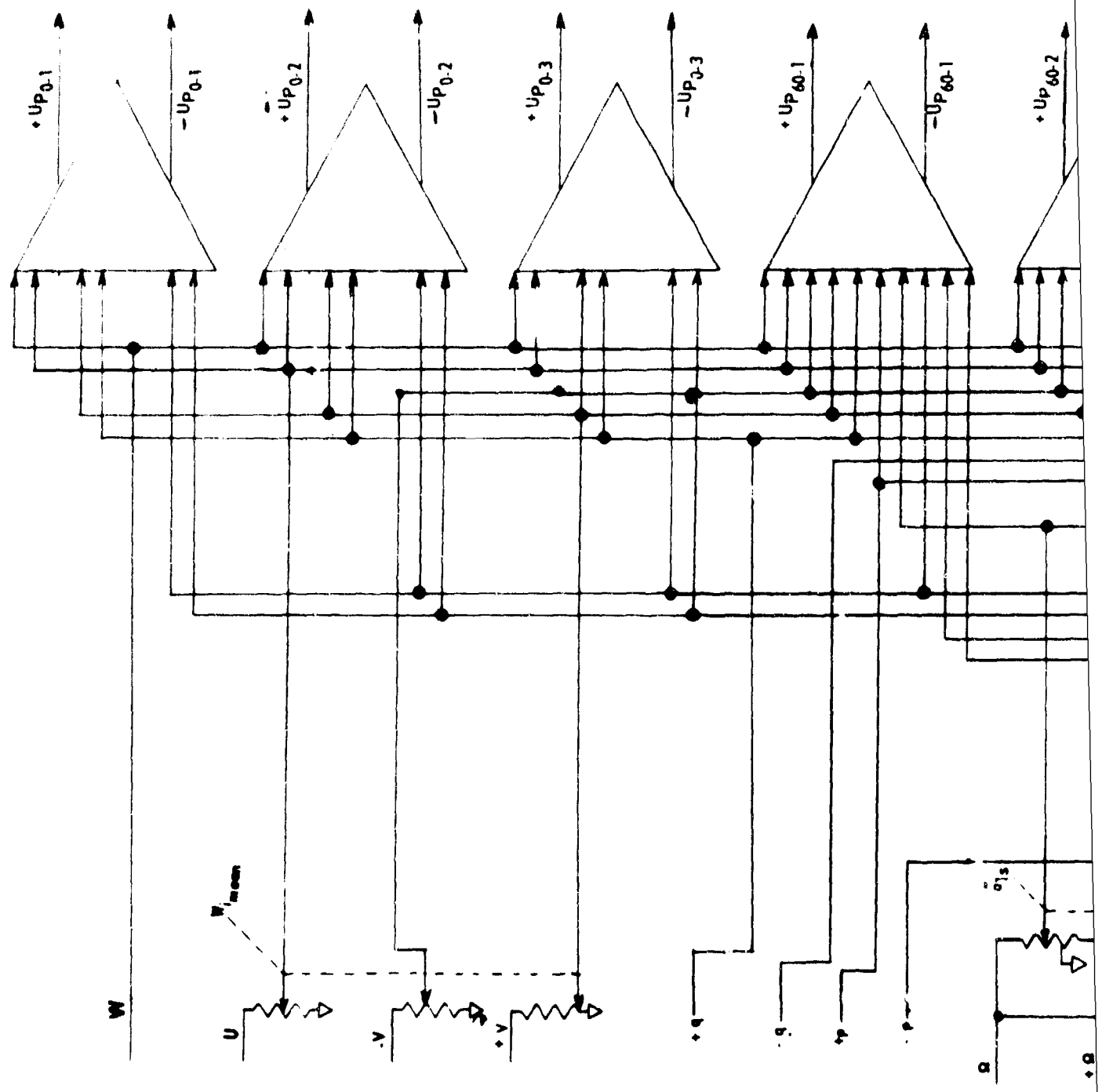

A

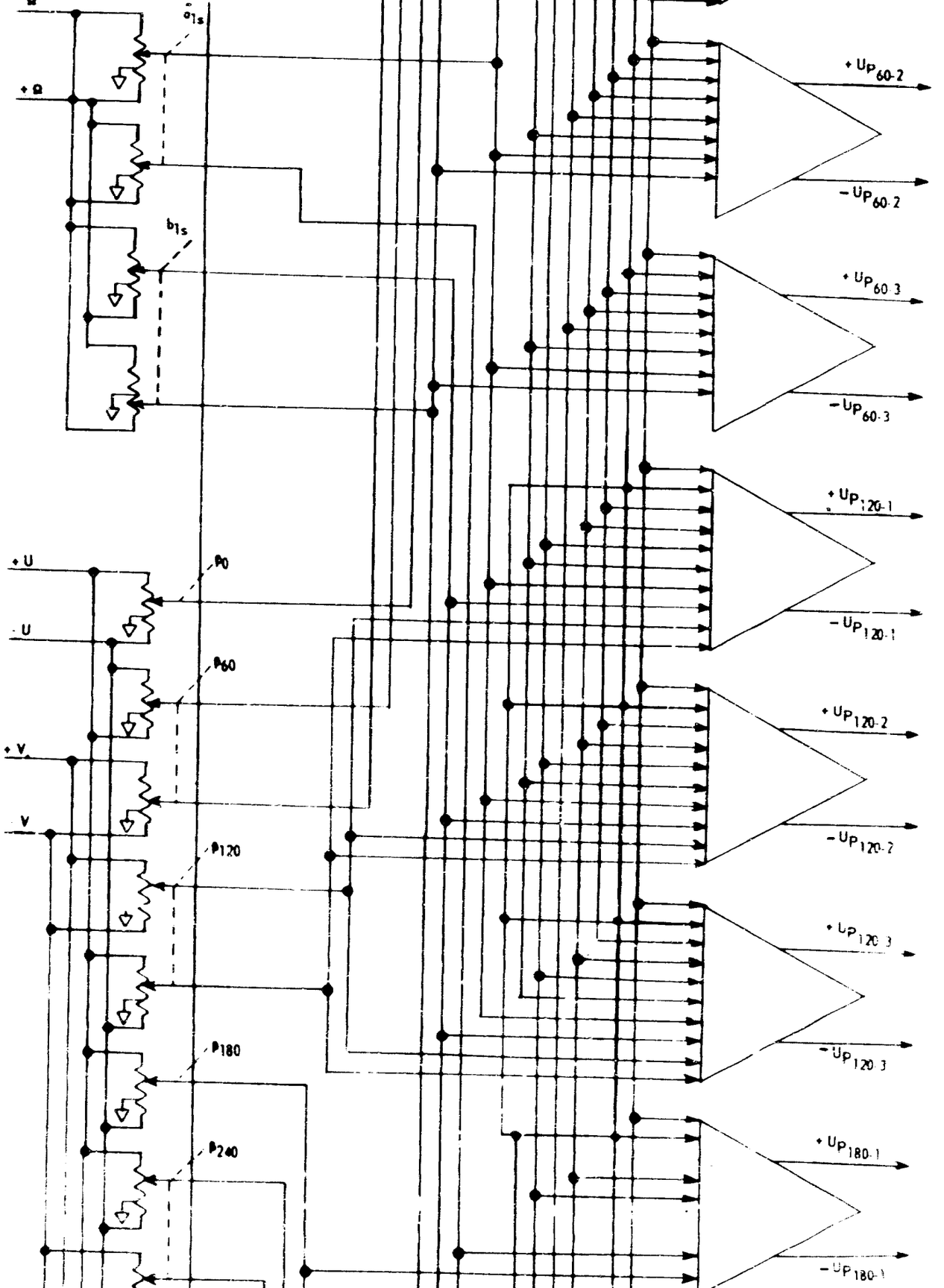
+ a
a_{1s}
b_{1s}
+ U
- U
+ V
- V
P_0
P_{60}
P_{120}
P_{180}
P_{240}
$+U_{P60\text{-}2}$
$-U_{P60\text{-}2}$
$+U_{P60\text{-}3}$
$-U_{P60\text{-}3}$
$+U_{P120\text{-}1}$
$-U_{P120\text{-}1}$
$+U_{P120\text{-}2}$
$-U_{P120\text{-}2}$
$+U_{P120\text{-}3}$
$-U_{P120\text{-}3}$
$+U_{P180\text{-}1}$
$-U_{P180\text{-}1}$

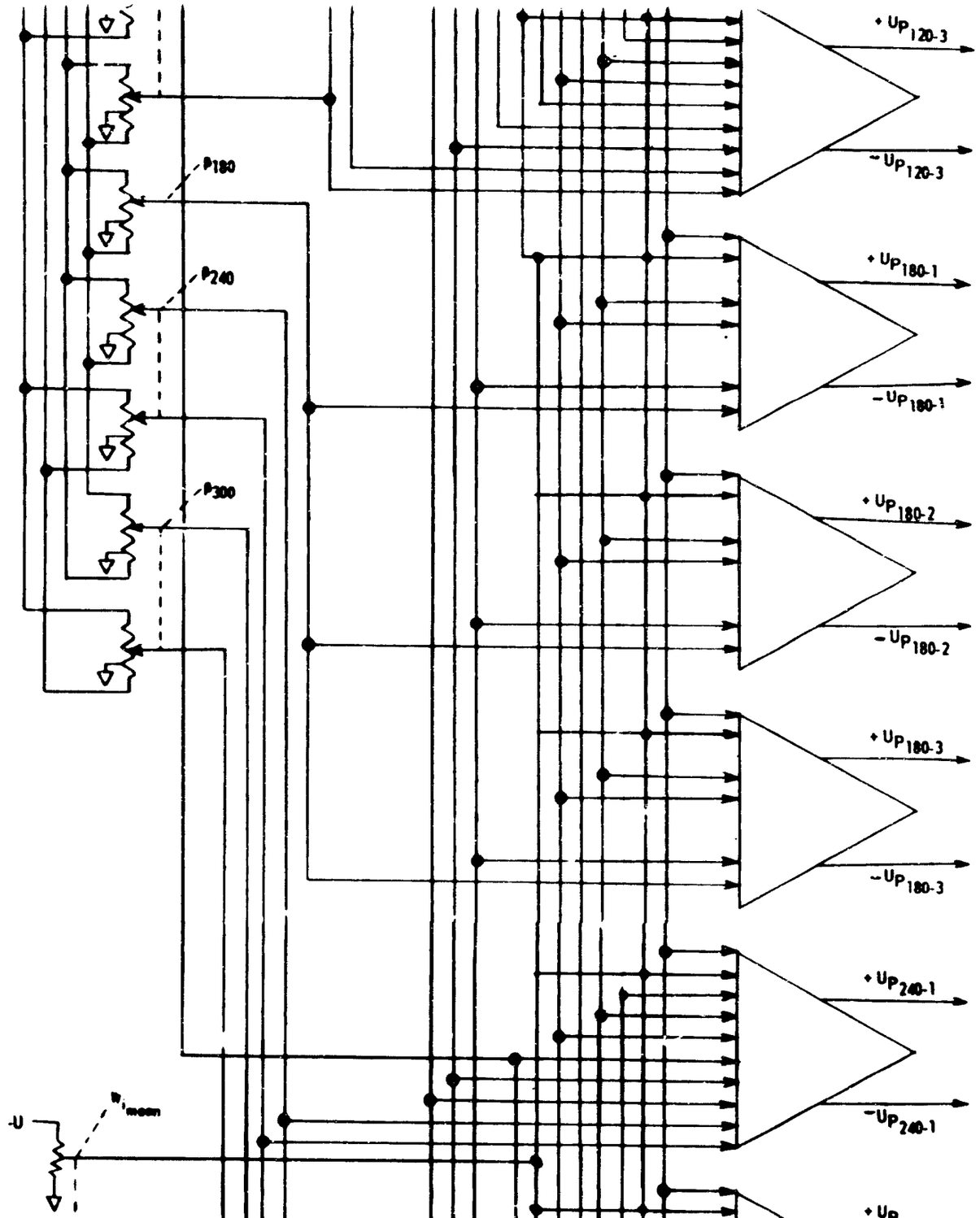
P_{180}
P_{240}
P_{300}
P_{mom}
-U
$+U_{P120-3}$
$-U_{P120-3}$
$+U_{P180-1}$
$-U_{P180-1}$
$+U_{P180-2}$
$-U_{P180-2}$
$+U_{P180-3}$
$-U_{P180-3}$
$+U_{P240-1}$
$-U_{P240-1}$

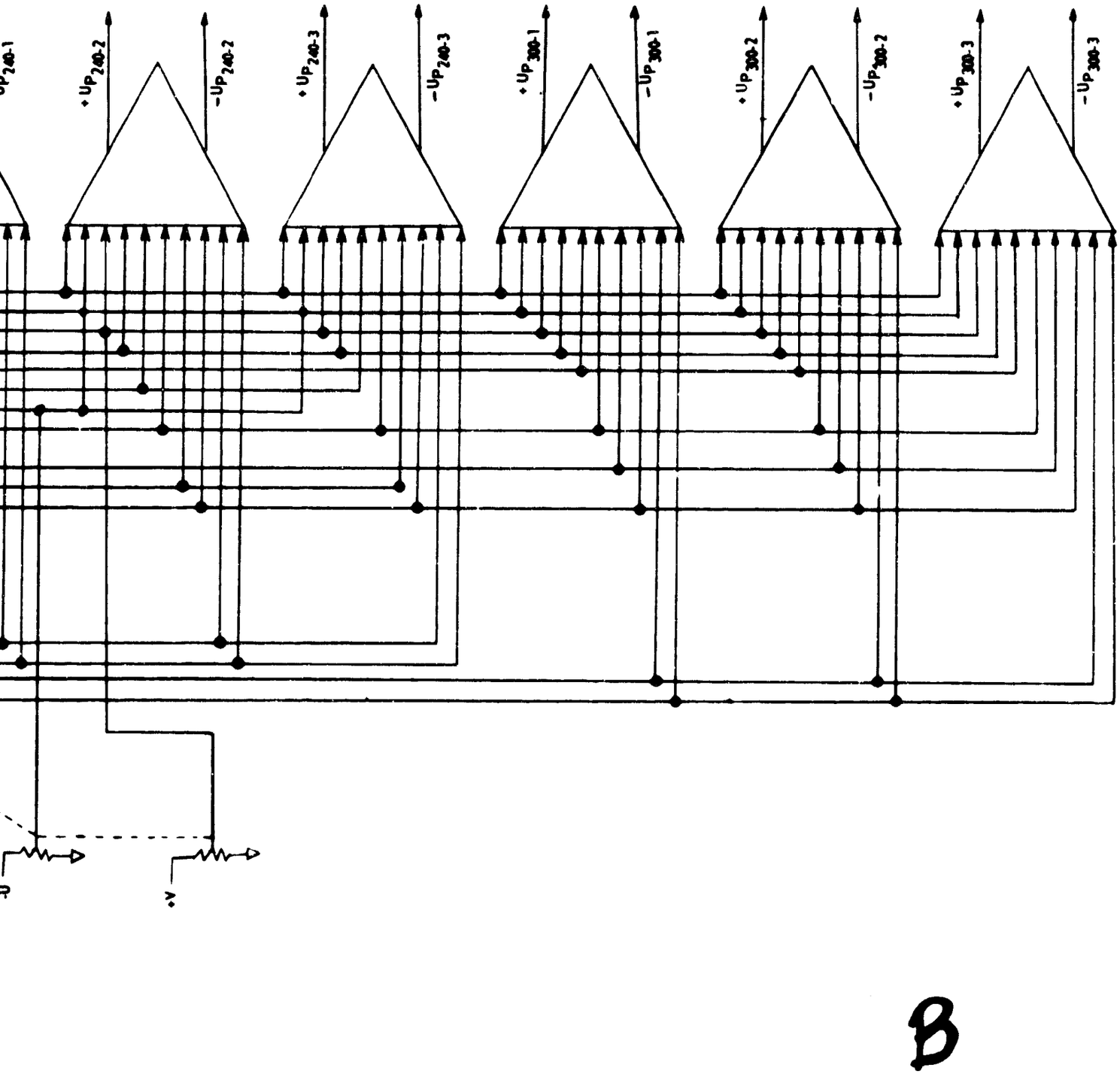

B

Figure 14. Local Vertical Velocity AC Mechanization

(2) Block (2) Tangential Velocity.- The tangential rotor velocity, shown in Figure 15 is a sum of functions of U, V and Ω to obtain the 18 blade element tangential velocities, $U_{T_{\psi-y}}$.

Since succeeding functions are formed by taking functions of $U_{T_{\psi-y}}$, the outputs of this mechanization must be shaft positions. Optimization of this mechanization involves the selection of function generation methods to form the functions of $U_{T_{\psi-y}}$. The present analog state-of-the-art does not furnish any more simple and straightforward method than padded potentiometers. Hence, since servo shafts are required for the potentiometers, the mechanization is equally optimum by either AC or DC methods. Table 10 is the summary of component complexity derived from Figure 15.

	AC		DC	
Component	No.	Wt.	No.	Wt.
Amplifier	18	18	18	36
Servo	18	126	18	126
Complexity		144		162

Table 10. Tangential Velocity

(3) Block (3) Blade Angle of Attack. The eighteen blade element angles of attack, $\alpha_{\psi-y}$, are also required as shaft positions to form functions of angle of attack for later use. Also each $\alpha_{\psi-y}$ is a function of $\frac{U_{P_{\psi-y}}}{U_{T_{\psi-y}}}$. Then the mechanization in Figure 16 follows logically since $U_{T_{\psi-y}}$ exists as a shaft position and it is a simple procedure to divide two functions using potentiometers. Considering the AC mechanization shown in Figure 16 for optimizing purposes it can be seen that the only area that would differ significantly from a DC mechanization would be the requirement of positive and negative functions of δ_θ. Hence the DC mechanization would require three more amplifiers than the AC mechanization. Table 11 reflects component complexity of Figure 16.

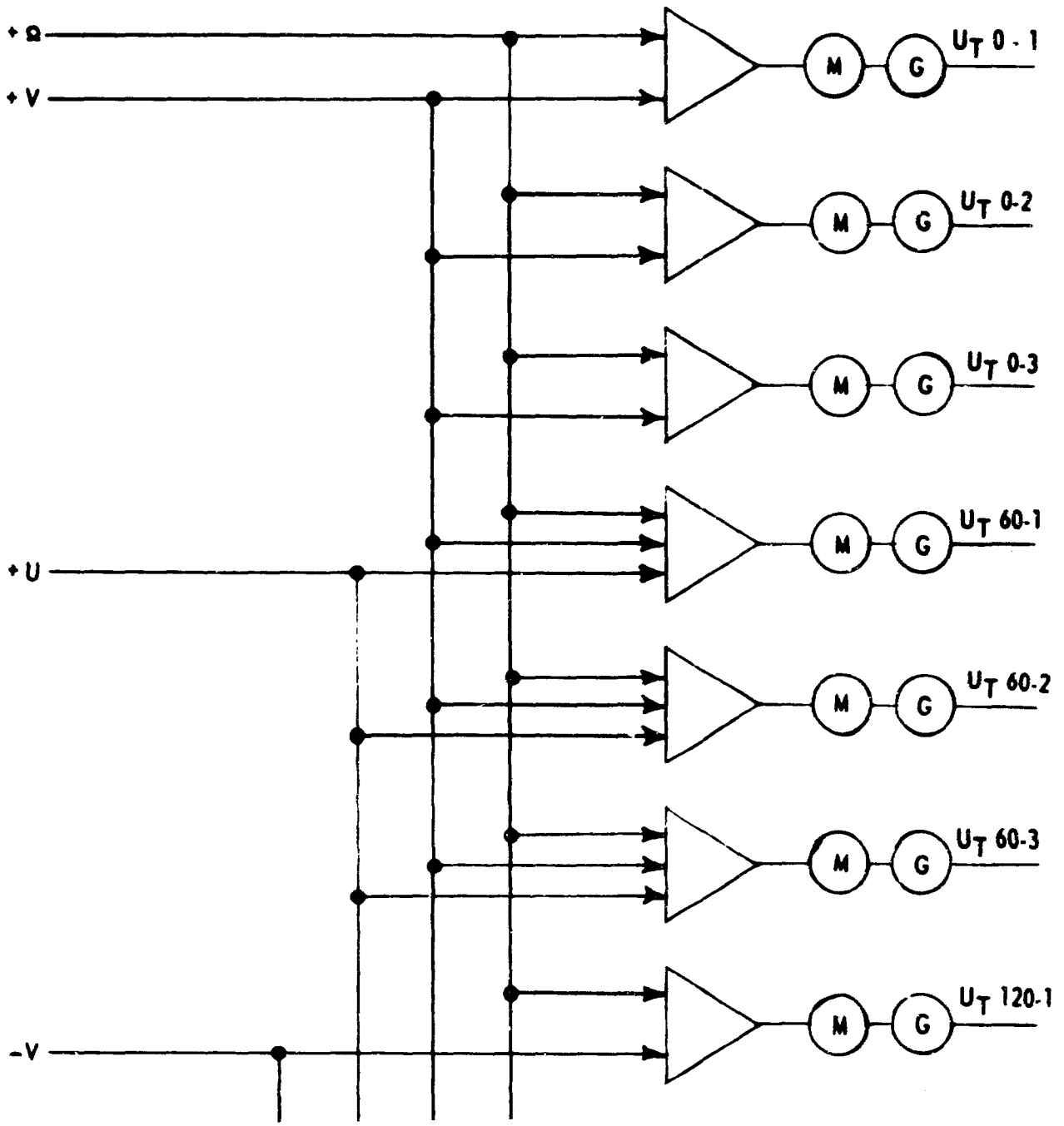

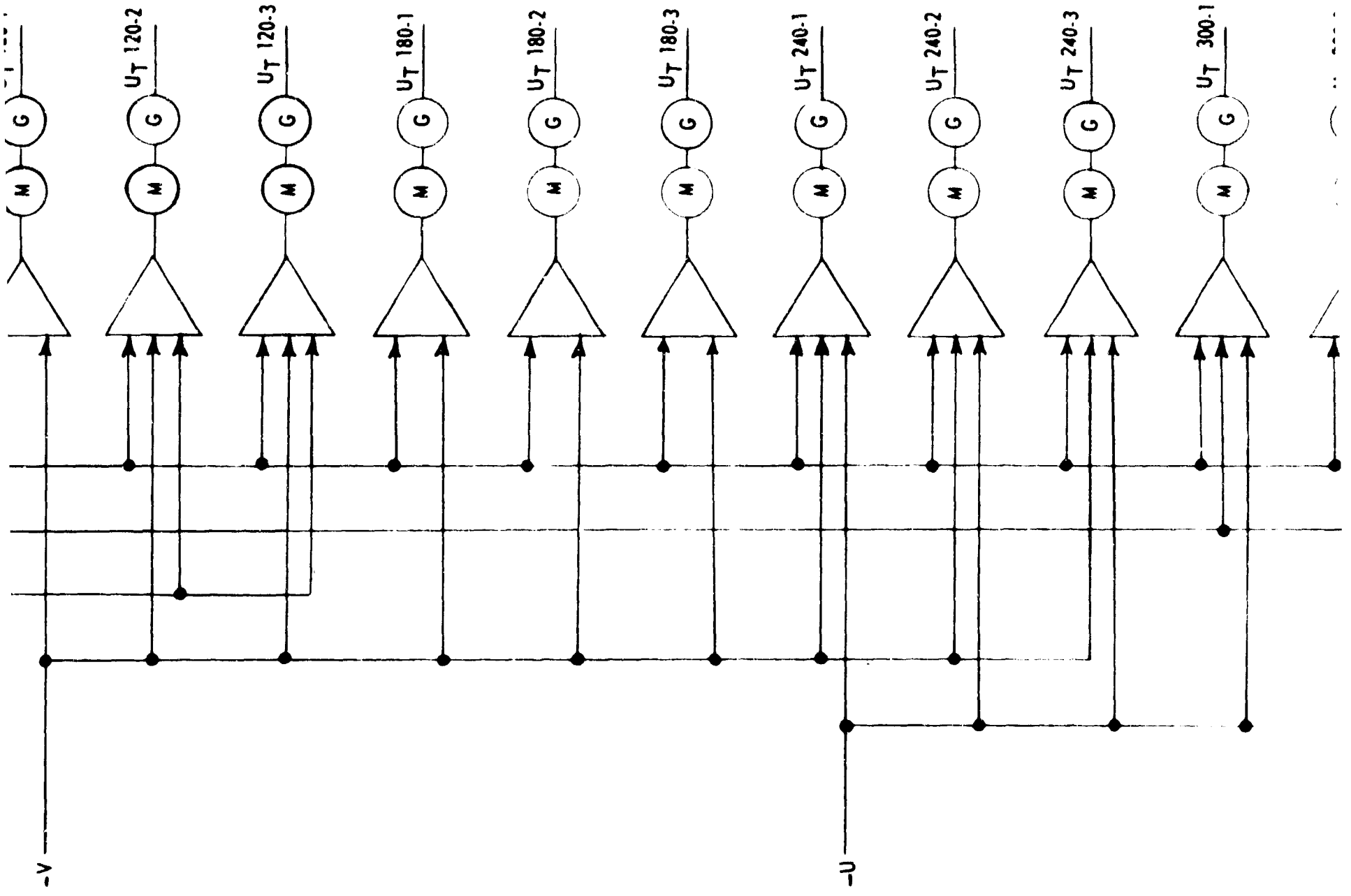

Figure 15. Tangential Velocity AC Mechanization

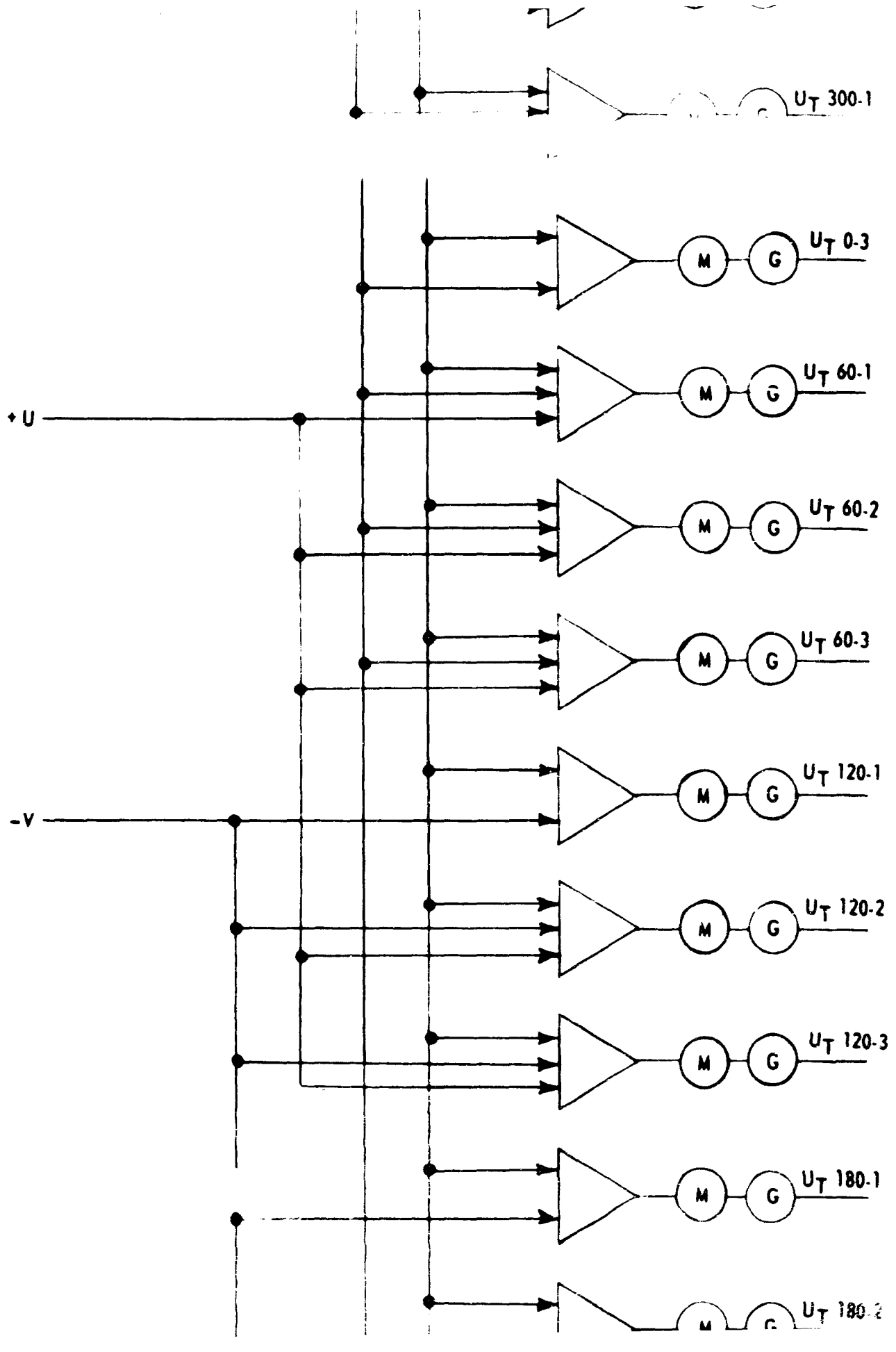
+U
-V
M
G
U_T 300-1
U_T 0-3
U_T 60-1
U_T 60-2
U_T 60-3
U_T 120-1
U_T 120-2
U_T 120-3
U_T 180-1
U_T 180-2

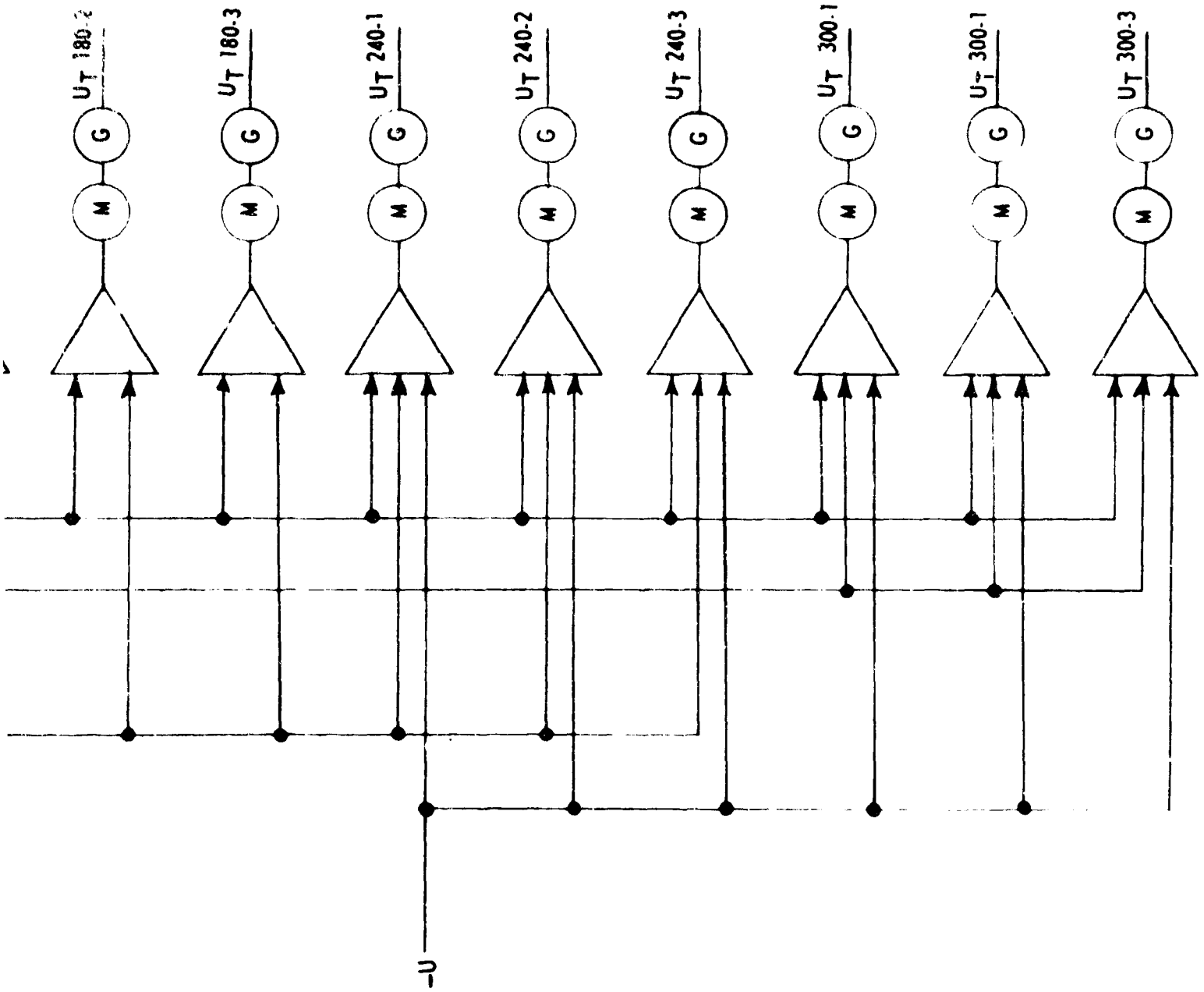

Figure 15. Tangential Velocity AC Mechanization

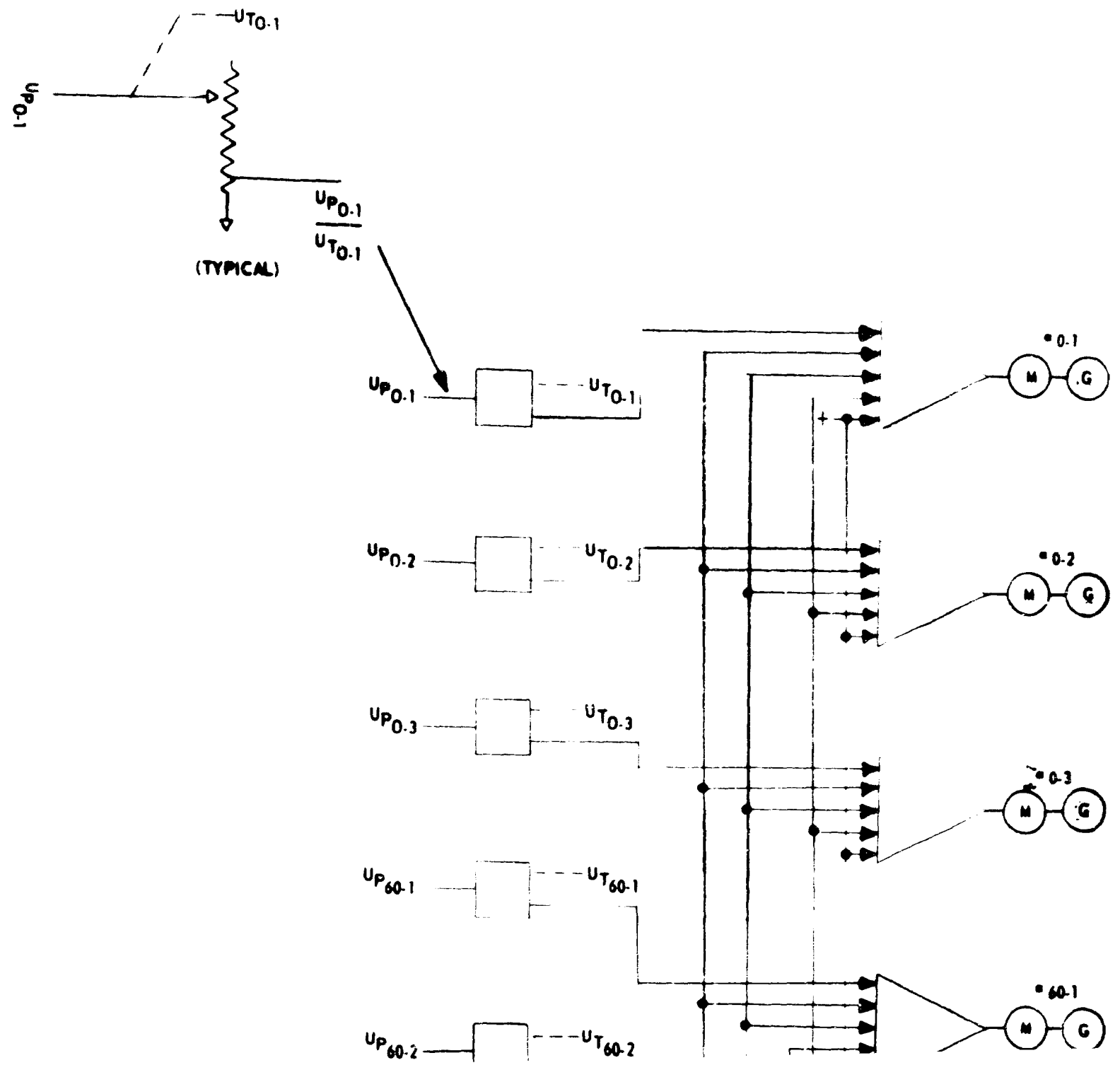
$U_{T0\text{-}1}$
$U_{P0\text{-}1}$
$U_{P0\text{-}1}$
$U_{T0\text{-}1}$
(TYPICAL)
$U_{P0\text{-}1}$
$U_{T0\text{-}1}$
$U_{P0\text{-}2}$
$U_{T0\text{-}2}$
$U_{P0\text{-}3}$
$U_{T0\text{-}3}$
$U_{P60\text{-}1}$
$U_{T60\text{-}1}$
$U_{P60\text{-}2}$
$U_{T60\text{-}2}$
M
G
0-1
0-2
0-3
60-1

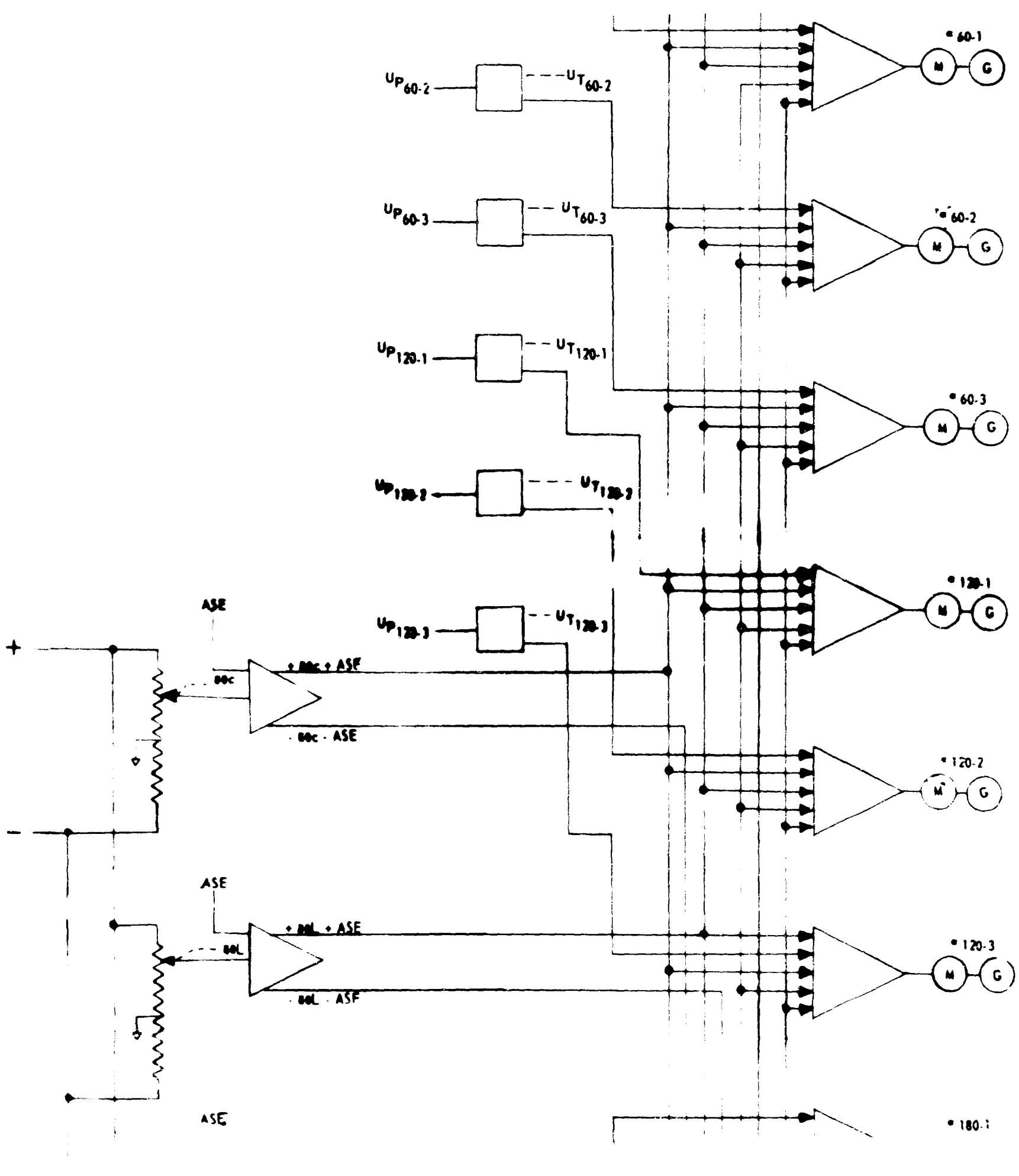
U_{P60-2}
U_{T60-2}
U_{P60-3}
U_{T60-3}
U_{P120-1}
U_{T120-1}
U_{P120-2}
U_{T120-2}
U_{P120-3}
U_{T120-3}
ASE
+
-
60c
+ 60c + ASE
- 60c - ASE
ASE
60L
+ 60L + ASE
- 60L - ASF
ASE
M
G
60-1
60-2
60-3
120-1
120-2
120-3
180-1

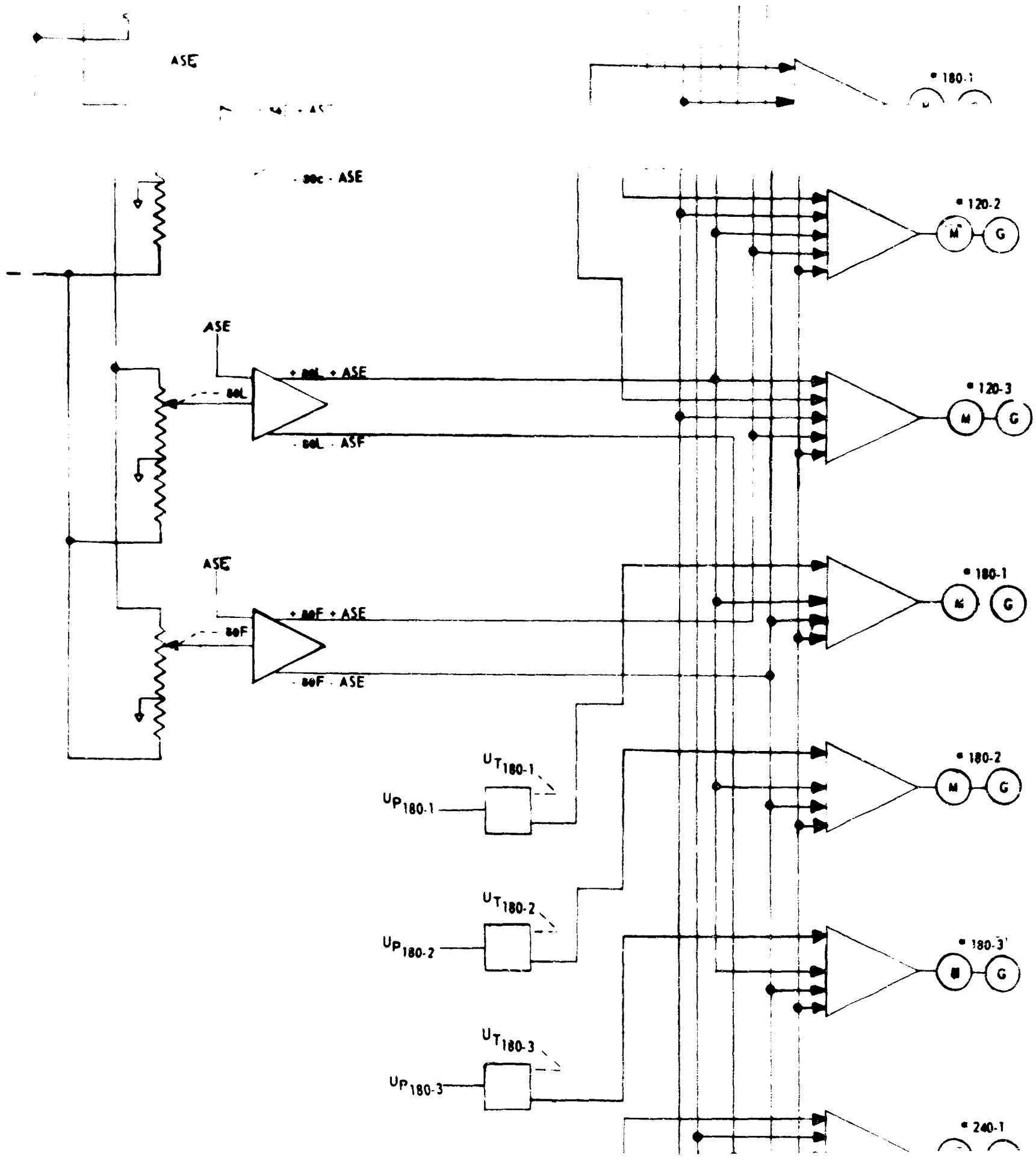
ASE
- 80c - ASE
ASE
+ 80L + ASE
80L
- 80L - ASF
ASE
+ 80F + ASE
80F
- 80F - ASE
U_{T180-1}
U_{P180-1}
U_{T180-2}
U_{P180-2}
U_{T180-3}
U_{P180-3}
* 180-1
* 120-2
* 120-3
* 180-1
* 180-2
* 180-3
* 240-1
M
G

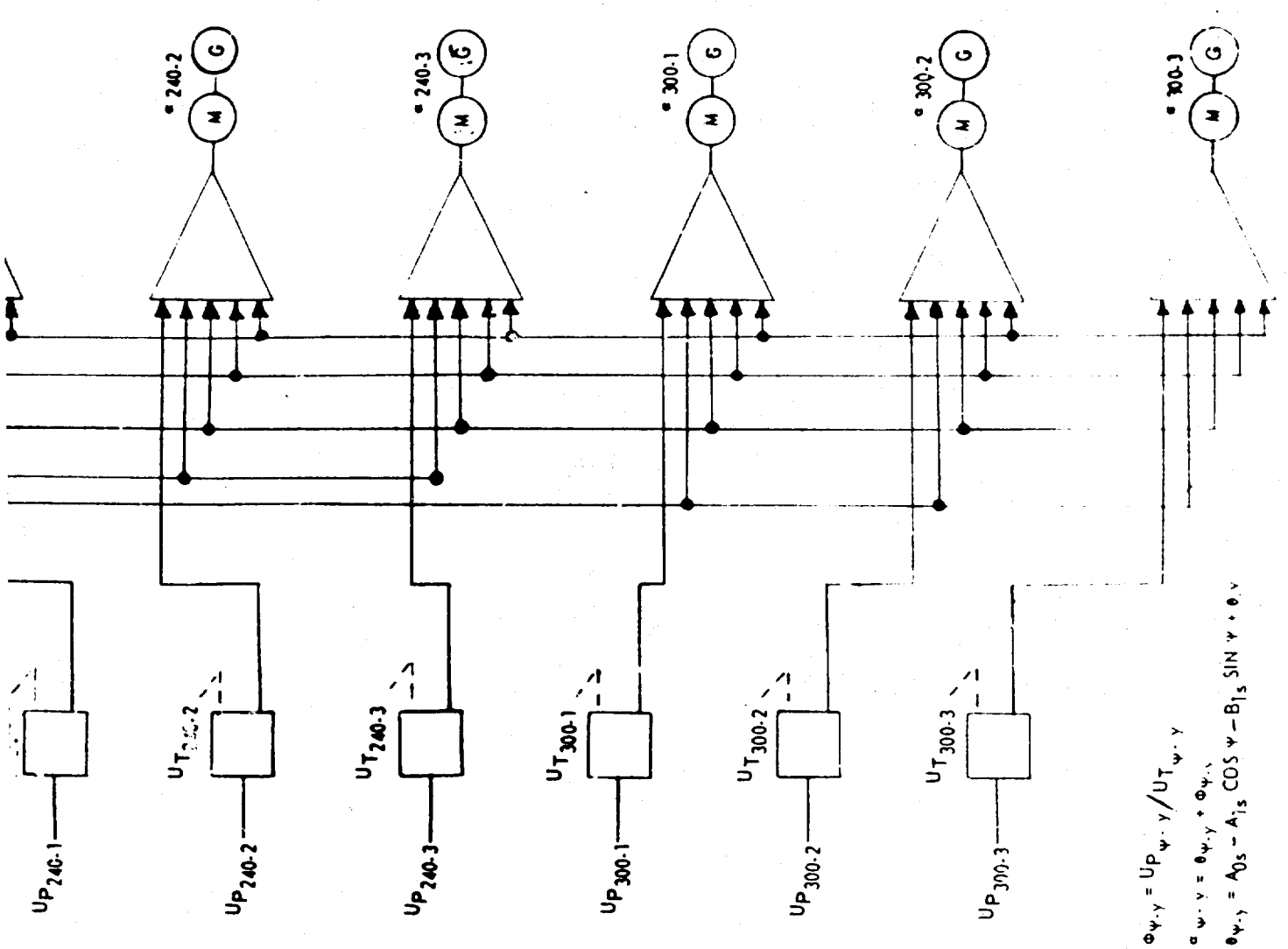

B

Figure 16. Blade Angle of Attack AC Mechanization

	AC		DC	
Component	No.	Wt.	No.	Wt.
Amplifier	21	21	24	48
Servo	18	126	18	126
Pots	21	5 1/4	21	5 1/4
Complexity		152 1/4		179 1/4

Table 11. Blade Angle of Attack

(4) Block (4) Blade Element Flapping Moment and Lift. The blade element flapping moment ($M_{\beta_{\downarrow}}$) and the blade element lift ($L_{\downarrow}$) are formed from the sums of functions of $\alpha_{\downarrow-y}$ and $U_{T_{\downarrow-y}}$ as can be seen in Figure 17. Here again both positive and negative output functions are required which results in the only difference between the AC and DC mechanizations. In this case 12 additional amplifiers are required in the DC mechanization to give both signs of $M_{\beta_{\downarrow}}$ and $L_{\downarrow}$. Table 12 reflects component complexity of Figure 17.

	AC		DC	
Component	No.	Wt.	No.	Wt.
Amplifier	12	12	24	24
Function (f) Generation	36	-	36	-
Complexity		12		24

Table 12. Blade Element Flapping Moment and Lift

(5) Block (5) Blade Element Drag. Figure 18 is the mechanization of the blade element drag computation. This mechanization in itself can be equally optimum in either AC or DC methods. This is evident since the entire mechanization is simply a combination of potentiometer function generators on servo shafts.

(6) Block (6) Blade Element Drag and Main Rotor Torque. The computation of blade element drag and main rotor torque is the same type of summation of potentiometer function generations as in Figure 19. Here again the only difference

2
FRAMES

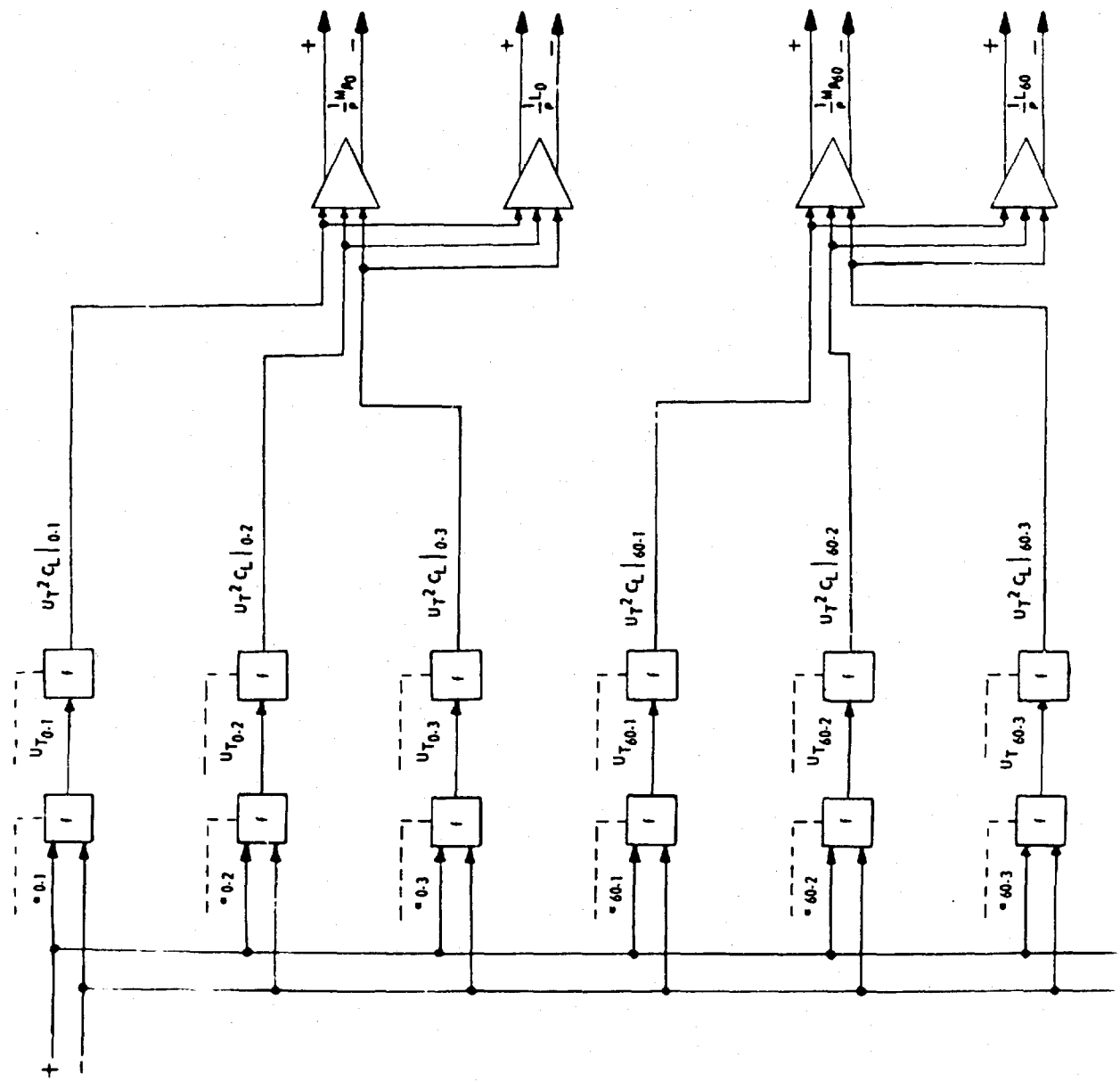
+
−
$\frac{1}{\rho}M_{R0}$
$\frac{1}{\rho}L_0$
$\frac{1}{\rho}M_{R60}$
$\frac{1}{\rho}L_{60}$
$U_T^2 C_L|_{0\cdot1}$
$U_T^2 C_L|_{0\cdot2}$
$U_T^2 C_L|_{0\cdot3}$
$U_T^2 C_L|_{60\cdot1}$
$U_T^2 C_L|_{60\cdot2}$
$U_T^2 C_L|_{60\cdot3}$
$U_{T_{0\cdot1}}$
$U_{T_{0\cdot2}}$
$U_{T_{0\cdot3}}$
$U_{T_{60\cdot1}}$
$U_{T_{60\cdot2}}$
$U_{T_{60\cdot3}}$
•0·1
•0·2
•0·3
•60·1
•60·2
•60·3

A

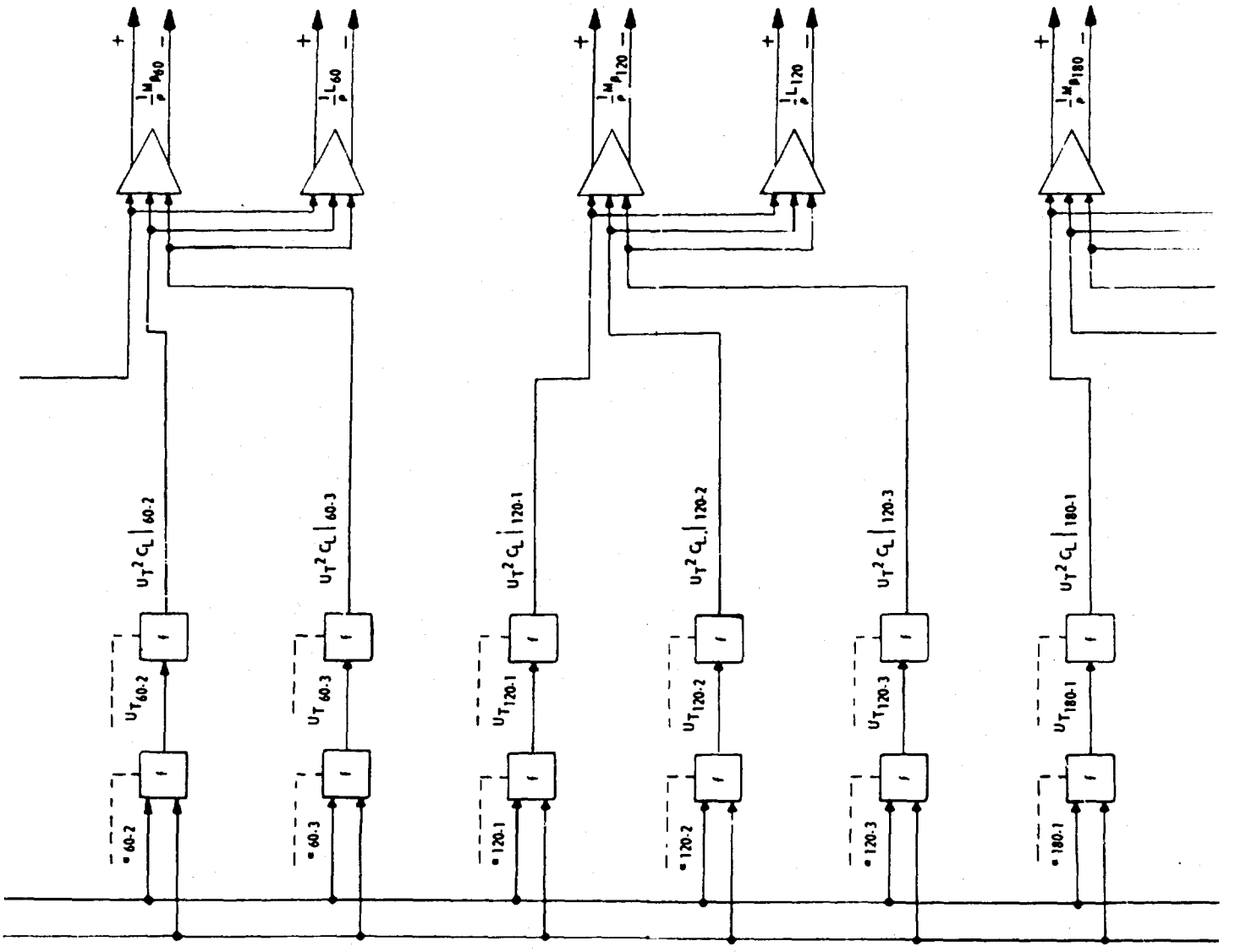
+
−
$\frac{1}{\rho} M_{\beta 60}$
$\frac{1}{\rho} L_{60}$
$\frac{1}{\rho} M_{\beta 120}$
$\frac{1}{\rho} L_{120}$
$\frac{1}{\rho} M_{\beta 180}$
$U_T^2 C_L \mid 60\text{-}2$
$U_T^2 C_L \mid 60\text{-}3$
$U_T^2 C_L \mid 120\text{-}1$
$U_T^2 C_L \mid 120\text{-}2$
$U_T^2 C_L \mid 120\text{-}3$
$U_T^2 C_L \mid 180\text{-}1$
$U_{T_{60\text{-}2}}$
$U_{T_{60\text{-}3}}$
$U_{T_{120\text{-}1}}$
$U_{T_{120\text{-}2}}$
$U_{T_{120\text{-}3}}$
$U_{T_{180\text{-}1}}$
60-2
60-3
120-1
120-2
120-3
180-1

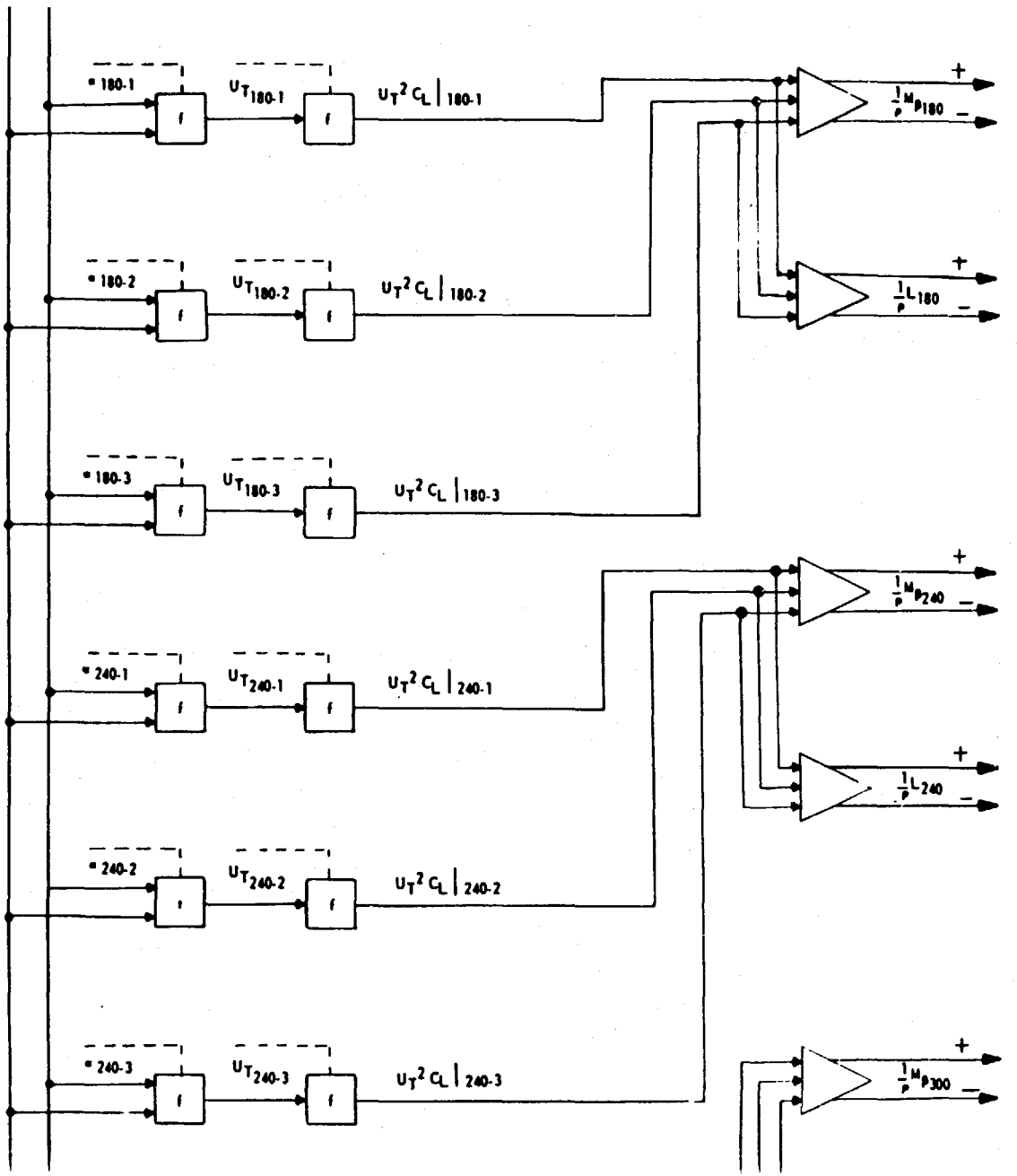
α 180-1
$U_{T_{180\text{-}1}}$
$U_T^2 C_L \mid_{180\text{-}1}$
α 180-2
$U_{T_{180\text{-}2}}$
$U_T^2 C_L \mid_{180\text{-}2}$
α 180-3
$U_{T_{180\text{-}3}}$
$U_T^2 C_L \mid_{180\text{-}3}$
α 240-1
$U_{T_{240\text{-}1}}$
$U_T^2 C_L \mid_{240\text{-}1}$
α 240-2
$U_{T_{240\text{-}2}}$
$U_T^2 C_L \mid_{240\text{-}2}$
α 240-3
$U_{T_{240\text{-}3}}$
$U_T^2 C_L \mid_{240\text{-}3}$
f
+
−
$\frac{1}{\rho} M_{\beta 180}$
$\frac{1}{\rho} L_{180}$
$\frac{1}{\rho} M_{\beta 240}$
$\frac{1}{\rho} L_{240}$
$\frac{1}{\rho} M_{\beta 300}$

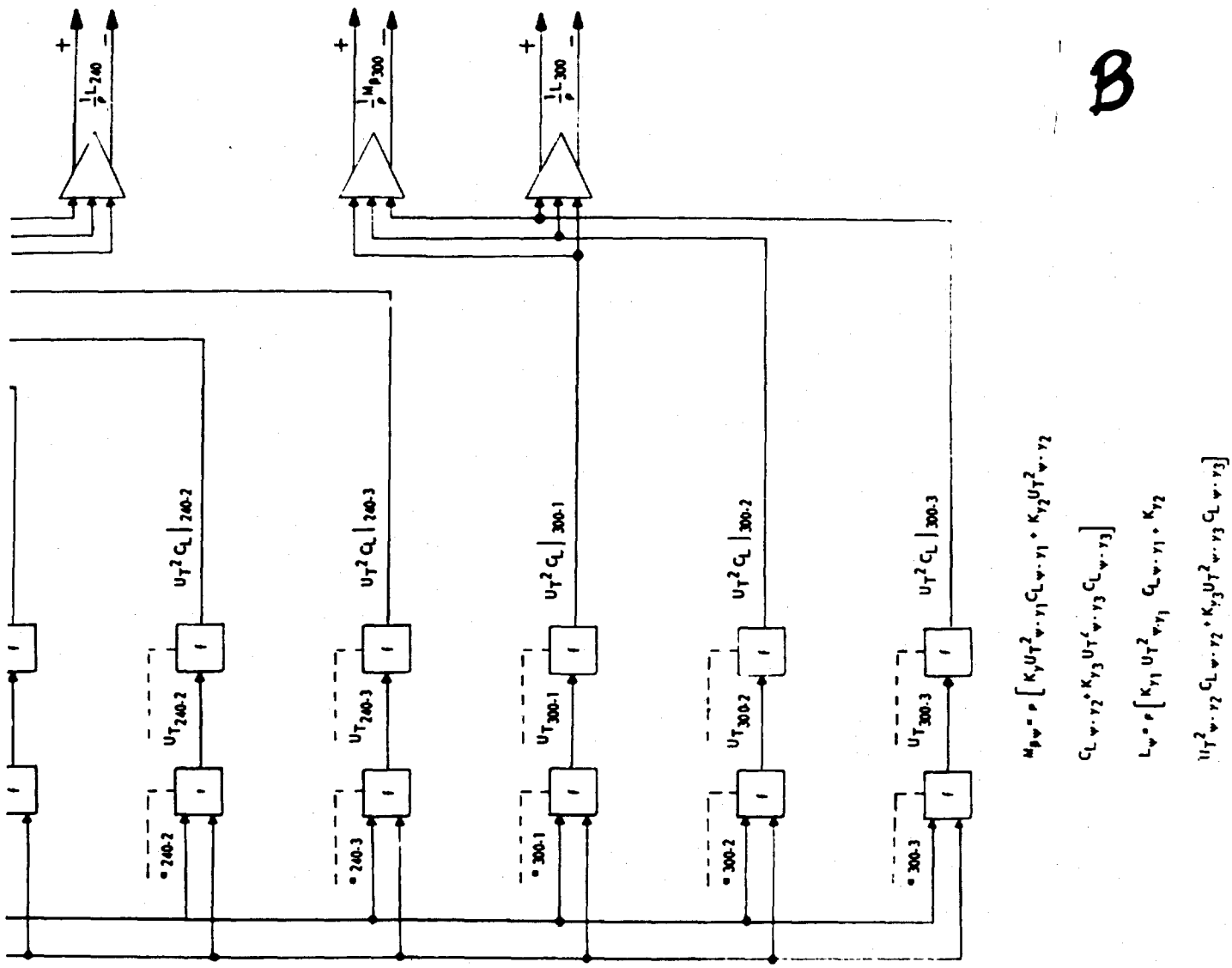

Figure 17. Blade Element Flapping Moment and Lift AC Mechanization

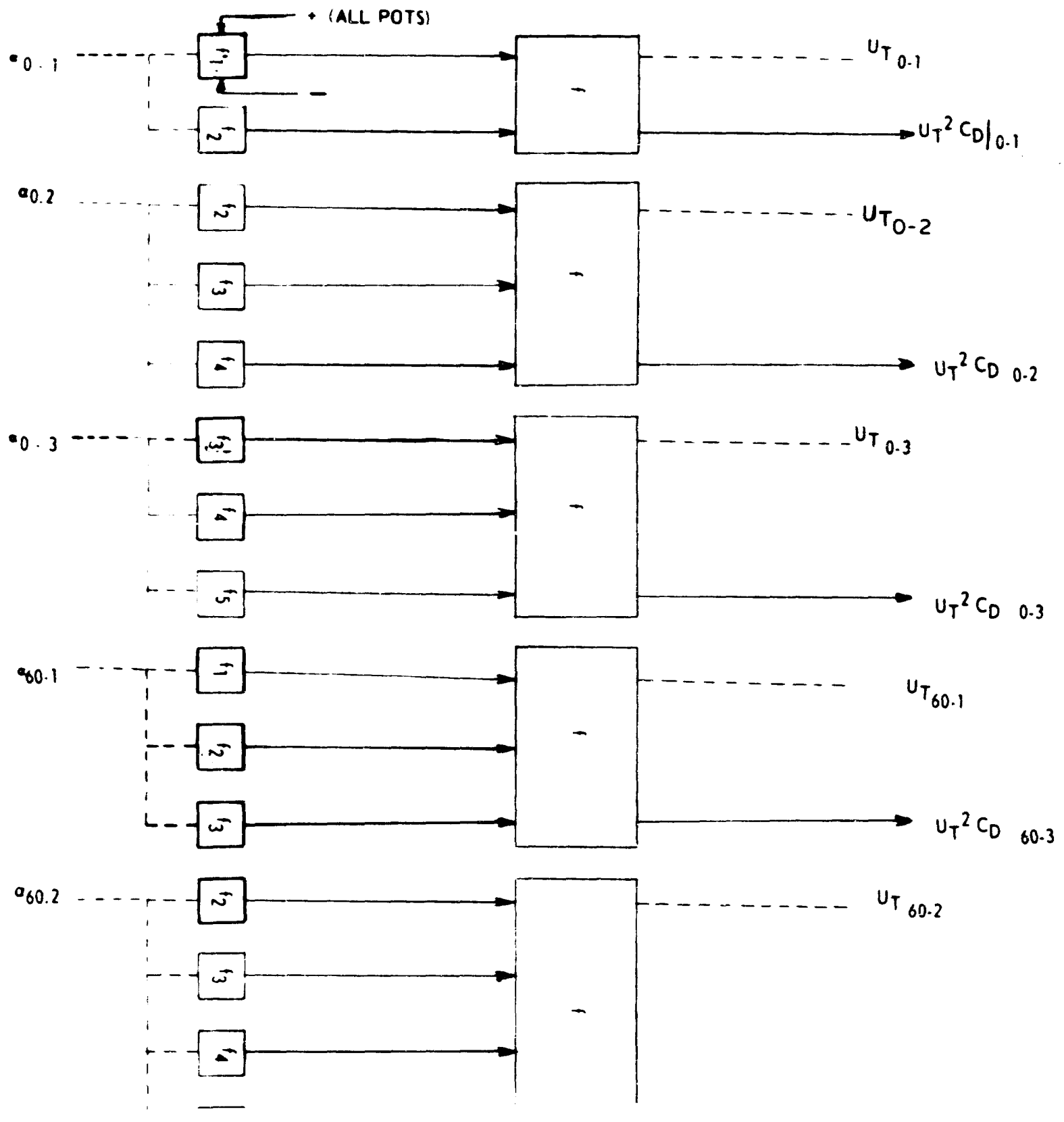
+ (ALL POTS)
α_{0-1}
f_1
f_2
$U_{T\,0-1}$
$U_T^2 C_D|_{0-1}$
$\alpha_{0.2}$
f_2
f_3
f_4
U_{T0-2}
$U_T^2 C_D\ _{0-2}$
α_{0-3}
f_3
f_4
f_5
$U_{T\,0-3}$
$U_T^2 C_D\ _{0-3}$
α_{60-1}
f_1
f_2
f_3
U_{T60-1}
$U_T^2 C_D\ _{60-3}$
$\alpha_{60.2}$
f_2
f_3
f_4
$U_{T\,60-2}$

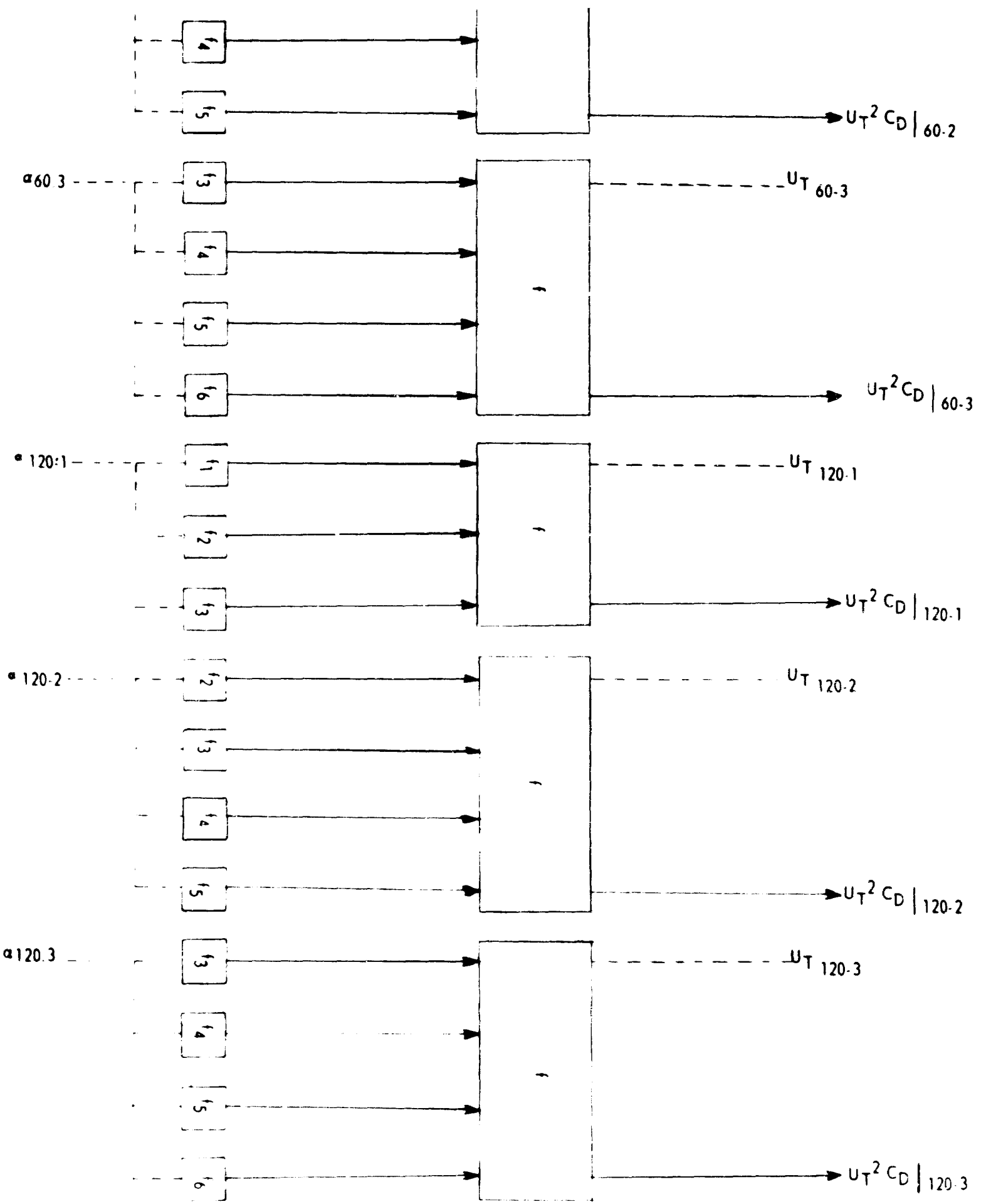
$\alpha_{60\cdot3}$
$\alpha_{120\cdot1}$
$\alpha_{120\cdot2}$
$\alpha_{120\cdot3}$
$U_T{}^2 C_D \mid_{60\cdot2}$
$U_{T\ 60\cdot3}$
$U_T{}^2 C_D \mid_{60\cdot3}$
$U_{T\ 120\cdot1}$
$U_T{}^2 C_D \mid_{120\cdot1}$
$U_{T\ 120\cdot2}$
$U_T{}^2 C_D \mid_{120\cdot2}$
$U_{T\ 120\cdot3}$
$U_T{}^2 C_D \mid_{120\cdot3}$

B

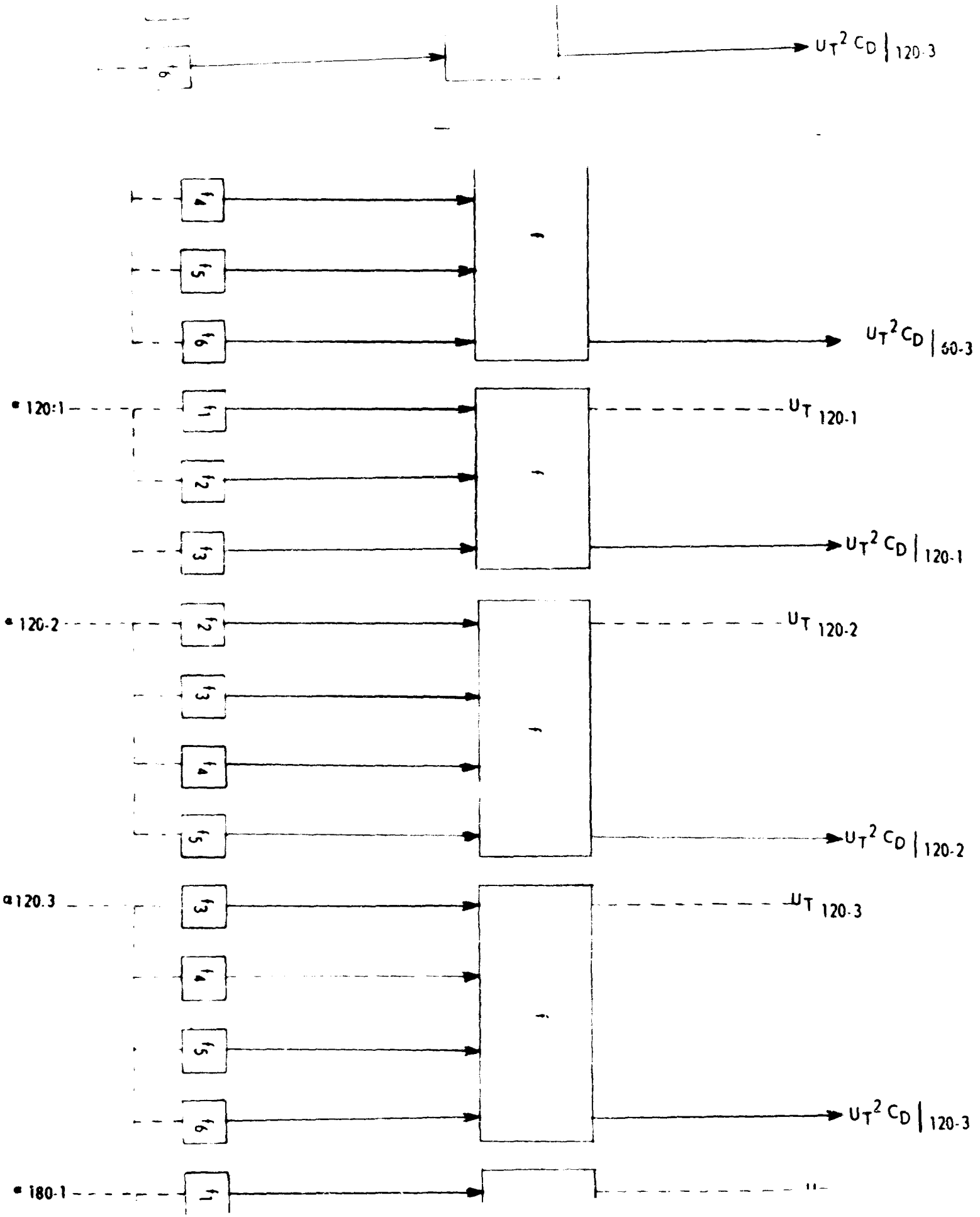
$U_T^2 C_D \mid_{120\text{-}3}$
$U_T^2 C_D \mid_{60\text{-}3}$
• 120:1
U_T 120-1
$U_T^2 C_D \mid_{120\text{-}1}$
• 120-2
U_T 120-2
$U_T^2 C_D \mid_{120\text{-}2}$
• 120-3
U_T 120-3
$U_T^2 C_D \mid_{120\text{-}3}$
• 180-1

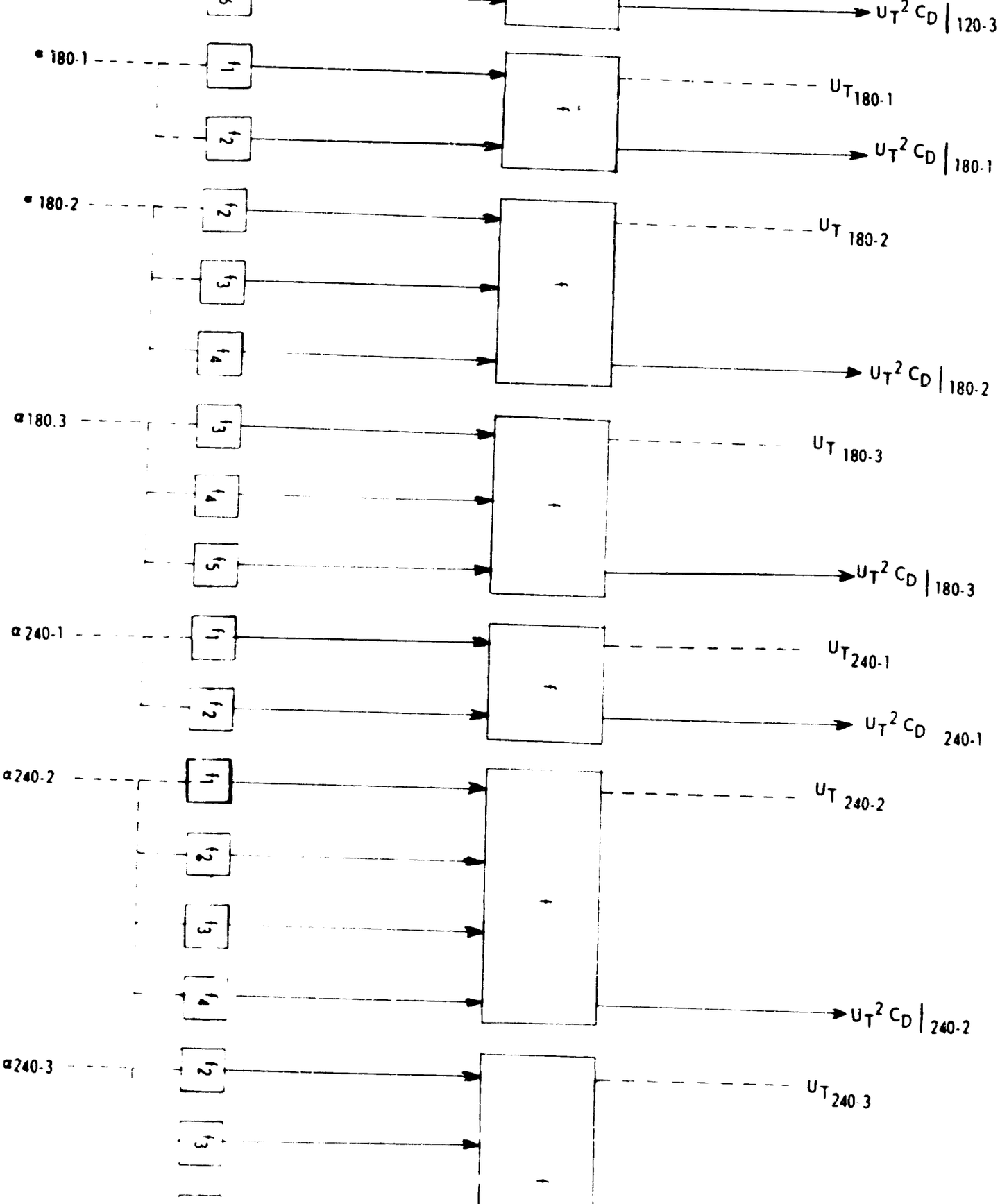
$U_T^2 C_D \mid_{120-3}$
• 180-1
f_1
f_2
$U_{T_{180-1}}$
$U_T^2 C_D \mid_{180-1}$
• 180-2
f_2
f_3
f_4
$U_{T\ 180-2}$
$U_T^2 C_D \mid_{180-2}$
α 180.3
f_3
f_4
f_5
$U_{T\ 180-3}$
$U_T^2 C_D \mid_{180-3}$
α 240-1
f_1
f_2
$U_{T_{240-1}}$
$U_T^2 C_D$ 240-1
α 240-2
f_1
f_2
f_3
f_4
$U_{T\ 240-2}$
$U_T^2 C_D \mid_{240-2}$
α 240-3
f_2
f_3
$U_{T_{240\ 3}}$

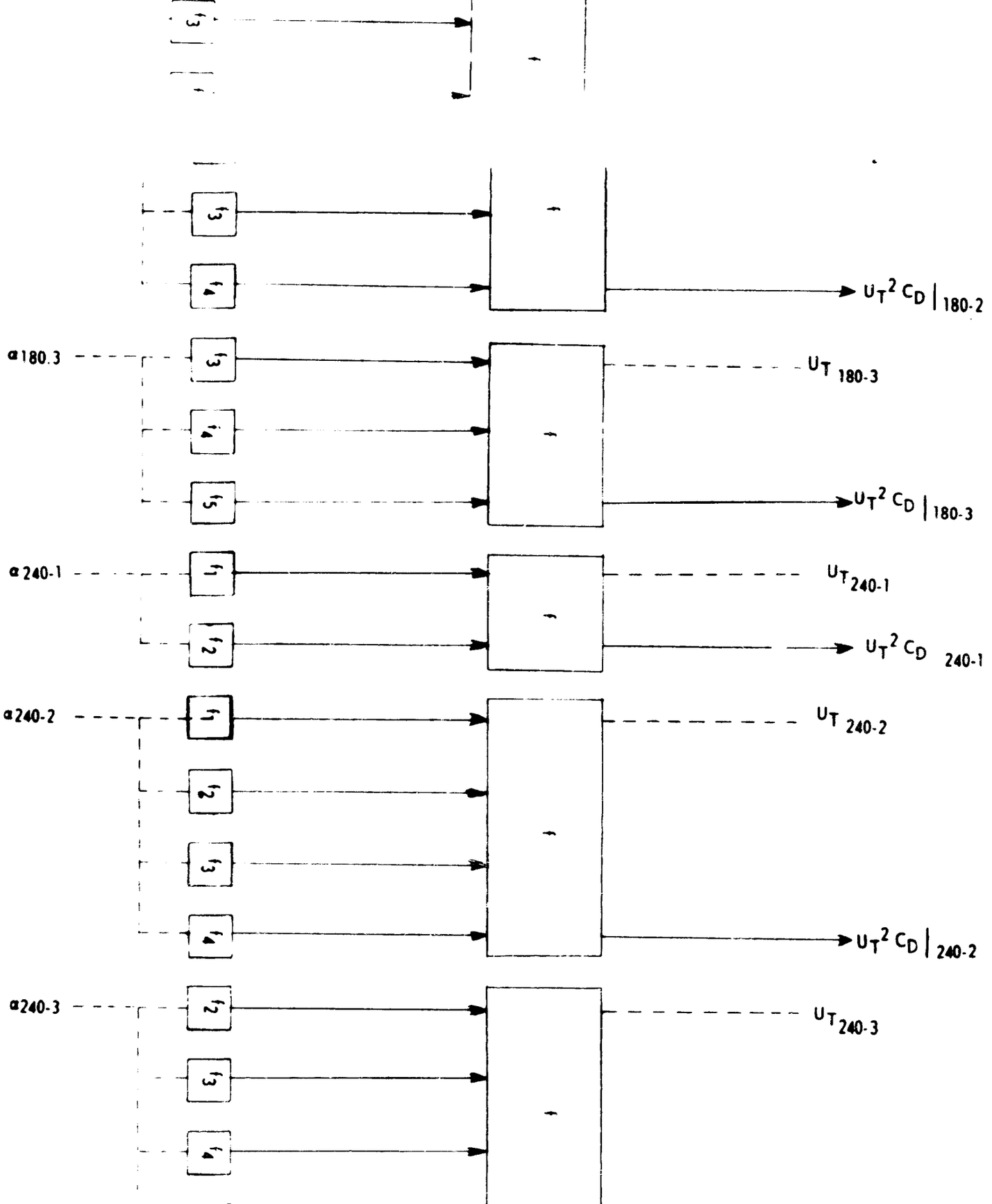
f3
f4
$U_T^2 C_D \mid_{180-2}$
α180.3
f3
f4
f5
$U_{T\ 180-3}$
$U_T^2 C_D \mid_{180-3}$
α240-1
f1
f2
$U_{T_{240-1}}$
$U_T^2 C_{D\ 240-1}$
α240-2
f1
f2
f3
f4
$U_{T\ 240-2}$
$U_T^2 C_D \mid_{240-2}$
α240-3
f2
f3
f4
$U_{T_{240-3}}$

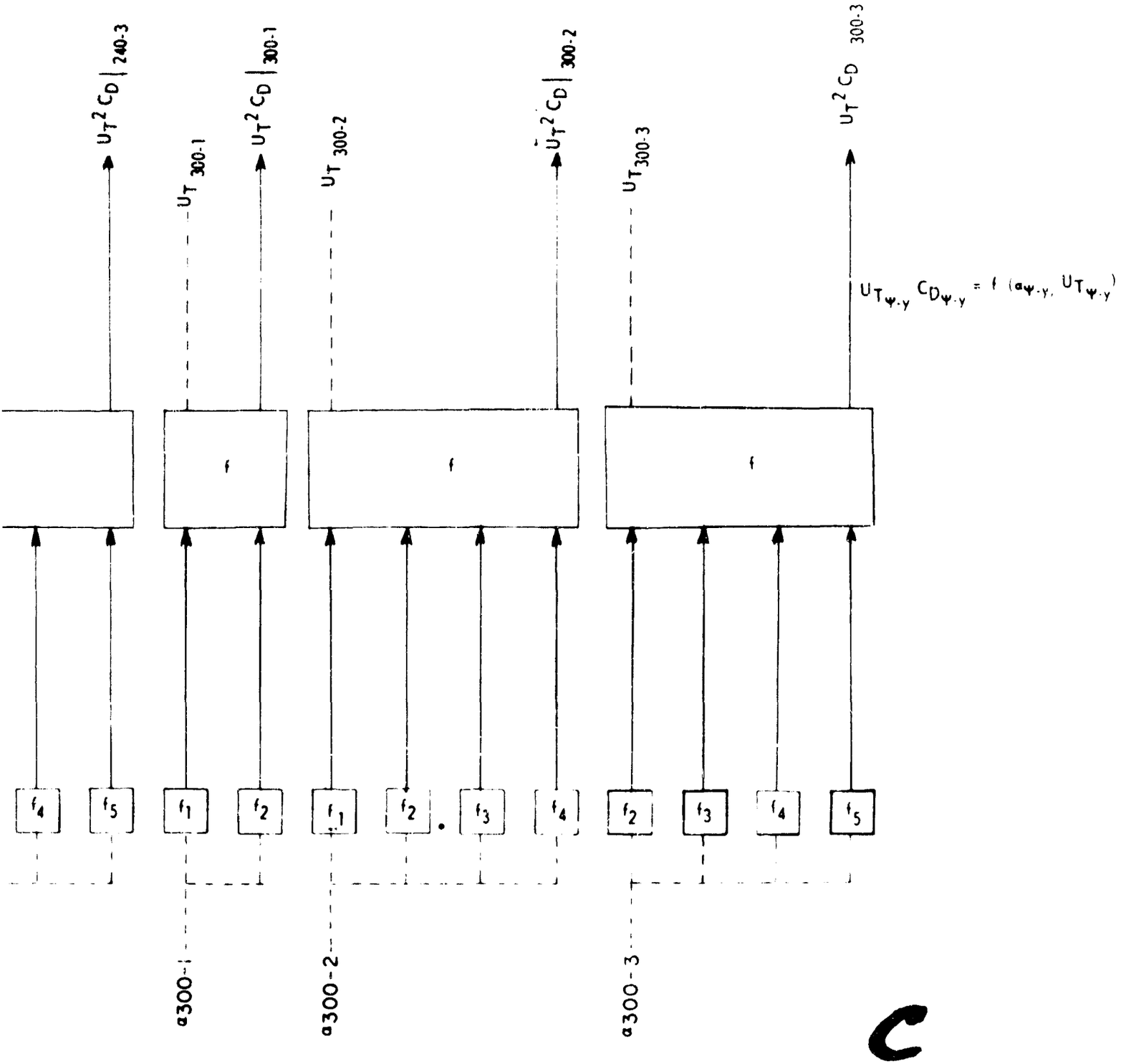

Figure 18 Blade Element Drag AC Mechanization

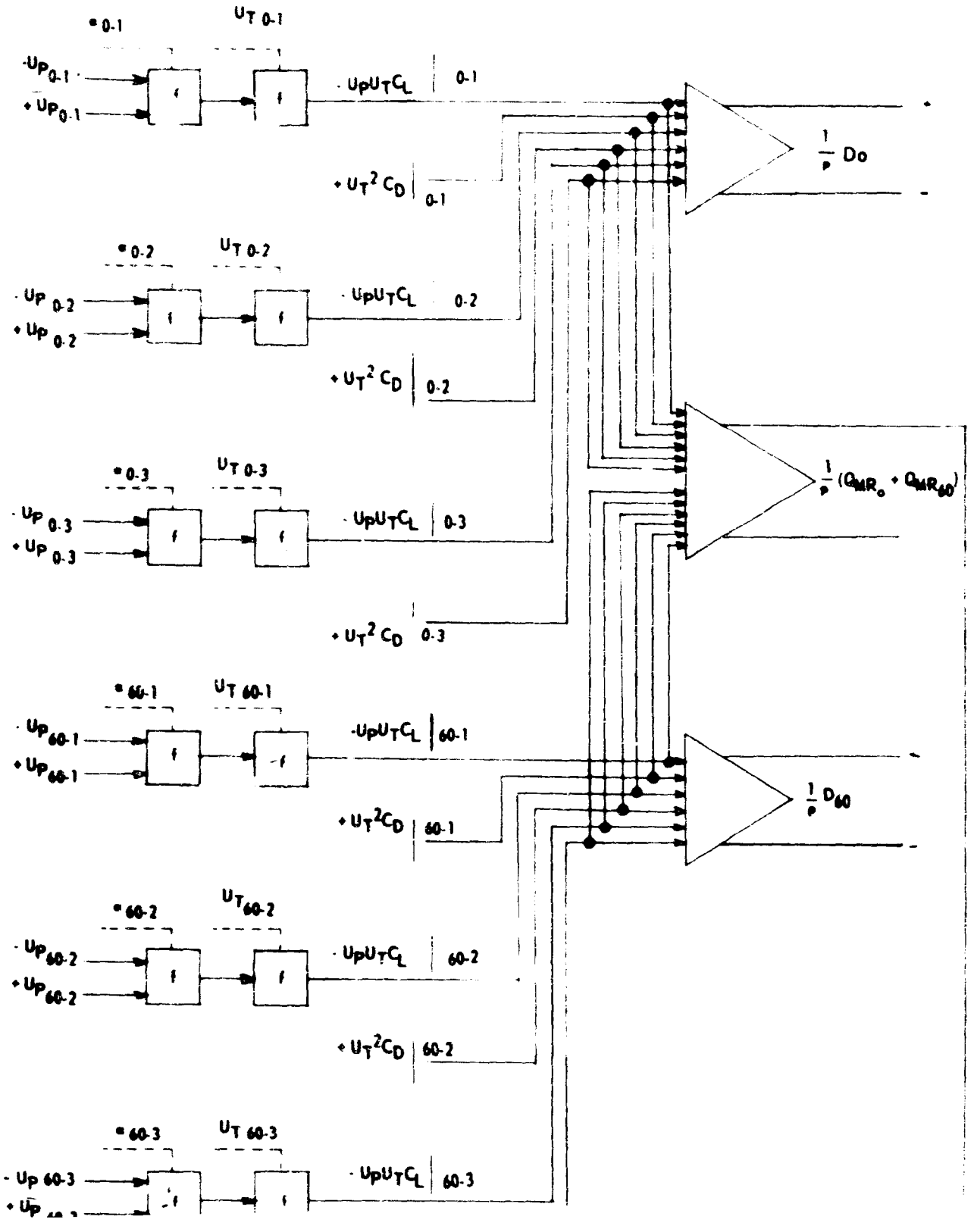
* 0-1
$U_{T\,0-1}$
$-U_{P_{0-1}}$
$+U_{P_{0-1}}$
$-U_P U_T C_L$ | 0-1
$+U_T^2 C_D$ | 0-1
* 0-2
$U_{T\,0-2}$
$-U_{P\,0-2}$
$+U_{P\,0-2}$
$-U_P U_T C_L$ | 0-2
$+U_T^2 C_D$ | 0-2
* 0-3
$U_{T\,0-3}$
$-U_{P\,0-3}$
$+U_{P\,0-3}$
$-U_P U_T C_L$ | 0-3
$+U_T^2 C_D$ | 0-3
* 60-1
$U_{T\,60-1}$
$-U_{P_{60-1}}$
$+U_{P_{60-1}}$
$-U_P U_T C_L$ | 60-1
$+U_T^2 C_D$ | 60-1
* 60-2
$U_{T_{60-2}}$
$-U_{P_{60-2}}$
$+U_{P_{60-2}}$
$-U_P U_T C_L$ | 60-2
$+U_T^2 C_D$ | 60-2
* 60-3
$U_{T\,60-3}$
$-U_{P\,60-3}$
$+U_{P\,60-3}$
$-U_P U_T C_L$ | 60-3
$\frac{1}{p} D_o$
$\frac{1}{p} (Q_{MR_o} + Q_{MR_{60}})$
$\frac{1}{p} D_{60}$

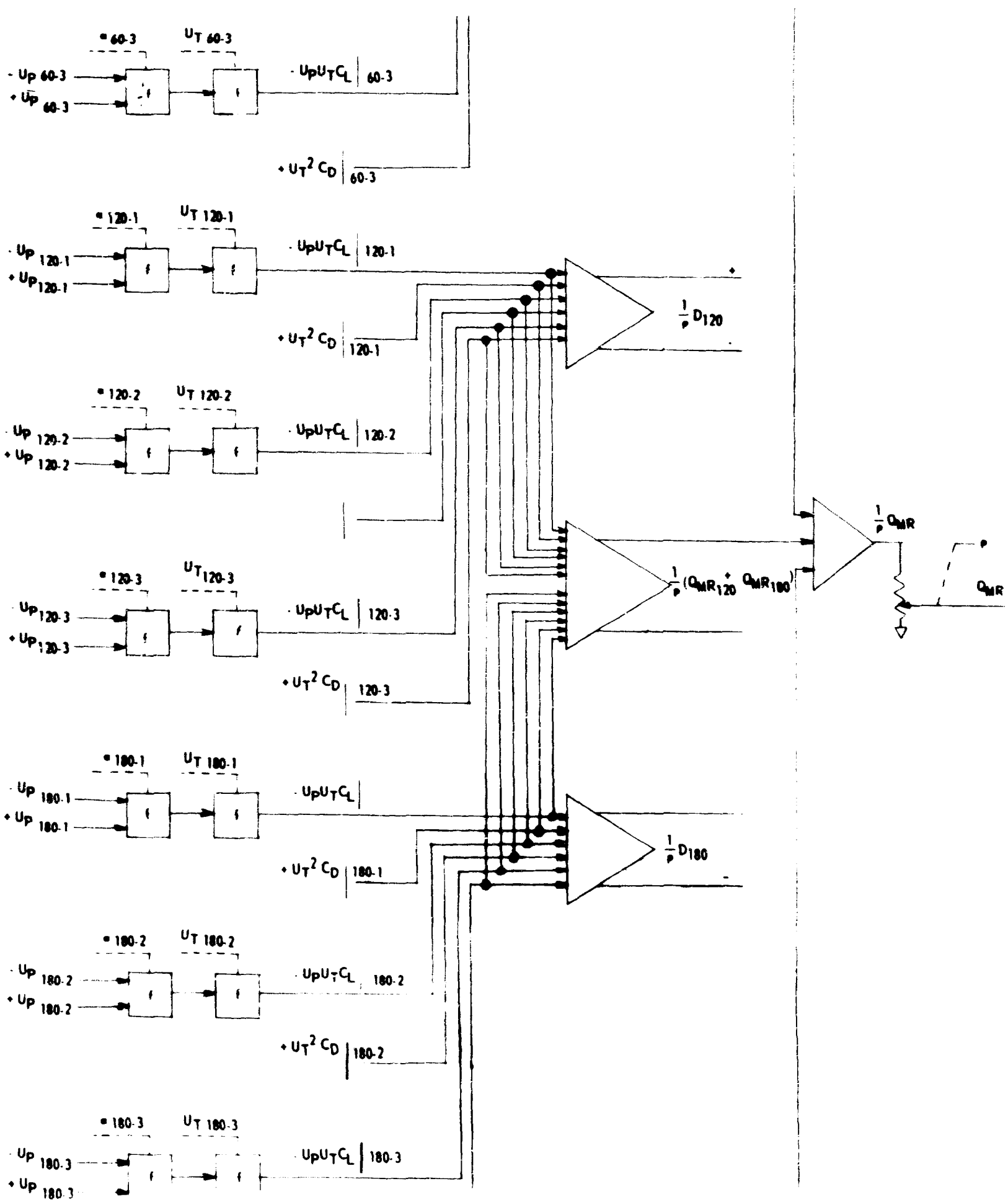
* 60-3
U_T 60-3
$-U_P$ 60-3
$+U_P$ 60-3
$-U_P U_T C_L$ | 60-3
$+U_T^2 C_D$ | 60-3
* 120-1
U_T 120-1
$-U_P$ 120-1
$+U_P$ 120-1
$-U_P U_T C_L$ | 120-1
$+U_T^2 C_D$ | 120-1
* 120-2
U_T 120-2
$-U_P$ 120-2
$+U_P$ 120-2
$-U_P U_T C_L$ | 120-2
* 120-3
U_T 120-3
$-U_P$ 120-3
$+U_P$ 120-3
$-U_P U_T C_L$ | 120-3
$+U_T^2 C_D$ | 120-3
* 180-1
U_T 180-1
$-U_P$ 180-1
$+U_P$ 180-1
$-U_P U_T C_L$
$+U_T^2 C_D$ | 180-1
* 180-2
U_T 180-2
$-U_P$ 180-2
$+U_P$ 180-2
$-U_P U_T C_L$ | 180-2
$+U_T^2 C_D$ | 180-2
* 180-3
U_T 180-3
$-U_P$ 180-3
$+U_P$ 180-3
$-U_P U_T C_L$ | 180-3
$\frac{1}{p} D_{120}$
$\frac{1}{p} (Q_{MR_{120}} + Q_{MR_{180}})$
$\frac{1}{p} D_{180}$
$\frac{1}{p} Q_{MR}$
Q_{MR}

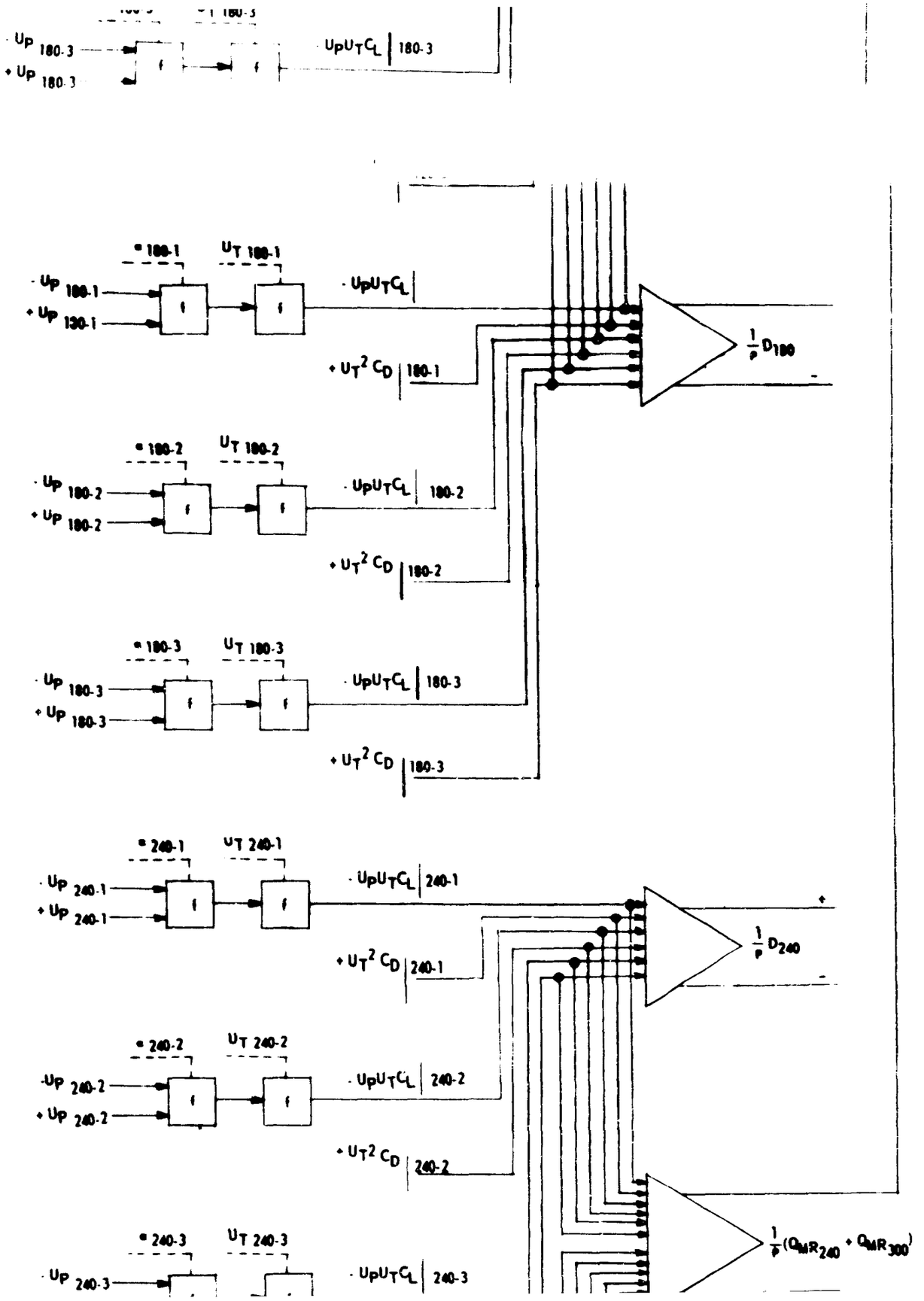
$\cdot U_{P\ 180\text{-}3}$
$+ U_{P\ 180\text{-}3}$
$\cdot U_P U_T C_L \mid 180\text{-}3$
$\cdot U_{P\ 180\text{-}1}$
$+ U_{P\ 180\text{-}1}$
$U_T\ 180\text{-}1$
$\cdot U_P U_T C_L$
$+ U_T^2 C_D \mid 180\text{-}1$
$\frac{1}{p} D_{180}$
$\cdot U_{P\ 180\text{-}2}$
$+ U_{P\ 180\text{-}2}$
$U_T\ 180\text{-}2$
$\cdot U_P U_T C_L \mid 180\text{-}2$
$+ U_T^2 C_D \mid 180\text{-}2$
$\cdot U_{P\ 180\text{-}3}$
$+ U_{P\ 180\text{-}3}$
$U_T\ 180\text{-}3$
$\cdot U_P U_T C_L \mid 180\text{-}3$
$+ U_T^2 C_D \mid 180\text{-}3$
$\cdot U_{P\ 240\text{-}1}$
$+ U_{P\ 240\text{-}1}$
$U_T\ 240\text{-}1$
$\cdot U_P U_T C_L \mid 240\text{-}1$
$+ U_T^2 C_D \mid 240\text{-}1$
$\frac{1}{p} D_{240}$
$\cdot U_{P\ 240\text{-}2}$
$+ U_{P\ 240\text{-}2}$
$U_T\ 240\text{-}2$
$\cdot U_P U_T C_L \mid 240\text{-}2$
$+ U_T^2 C_D \mid 240\text{-}2$
$\cdot U_{P\ 240\text{-}3}$
$U_T\ 240\text{-}3$
$\cdot U_P U_T C_L \mid 240\text{-}3$
$\frac{1}{p}(Q_{MR_{240}} + Q_{MR_{300}})$

$$Q_{MR_\psi} = \rho' \Big[K_{y_1} U_T U_P C_L \big|_{\psi \cdot y1} \cdot K_{y_1} U_T^2 C_D \big|_{\psi \cdot y1}$$

$$+ K_{y2} U_T U_P C_L \big|_{\psi \cdot y2} \cdot K_{y2} U_T^2 C_D \big|_{\psi \cdot y2}$$

$$+ K_{y3} U_T U_P C_L \big|_{\psi \cdot y3} \cdot K_{y3} U_T^2 C_D \big|_{\psi \cdot y3}$$

$$Q_{MR} = \frac{b}{6} \sum_{\psi} Q_{MR_\psi}$$

$$D_\psi = \rho' \Big[K_{y1} U_T^2 C_D \big|_{\psi \cdot y1} \cdot K_{y1} U_T U_P C_L \big|_{\psi \cdot y1} + K_{y2} U_T^2 C_D \big|_{\psi \cdot y2}$$

$$\cdot K_{y2} U_T U_P C_L \big|_{\psi \cdot y1} + K_{y3} U_T^2 C_D \big|_{\psi \cdot y3} \cdot K_{y3} U_T U_P C_L \big|_{\psi \cdot y1} \Big]$$

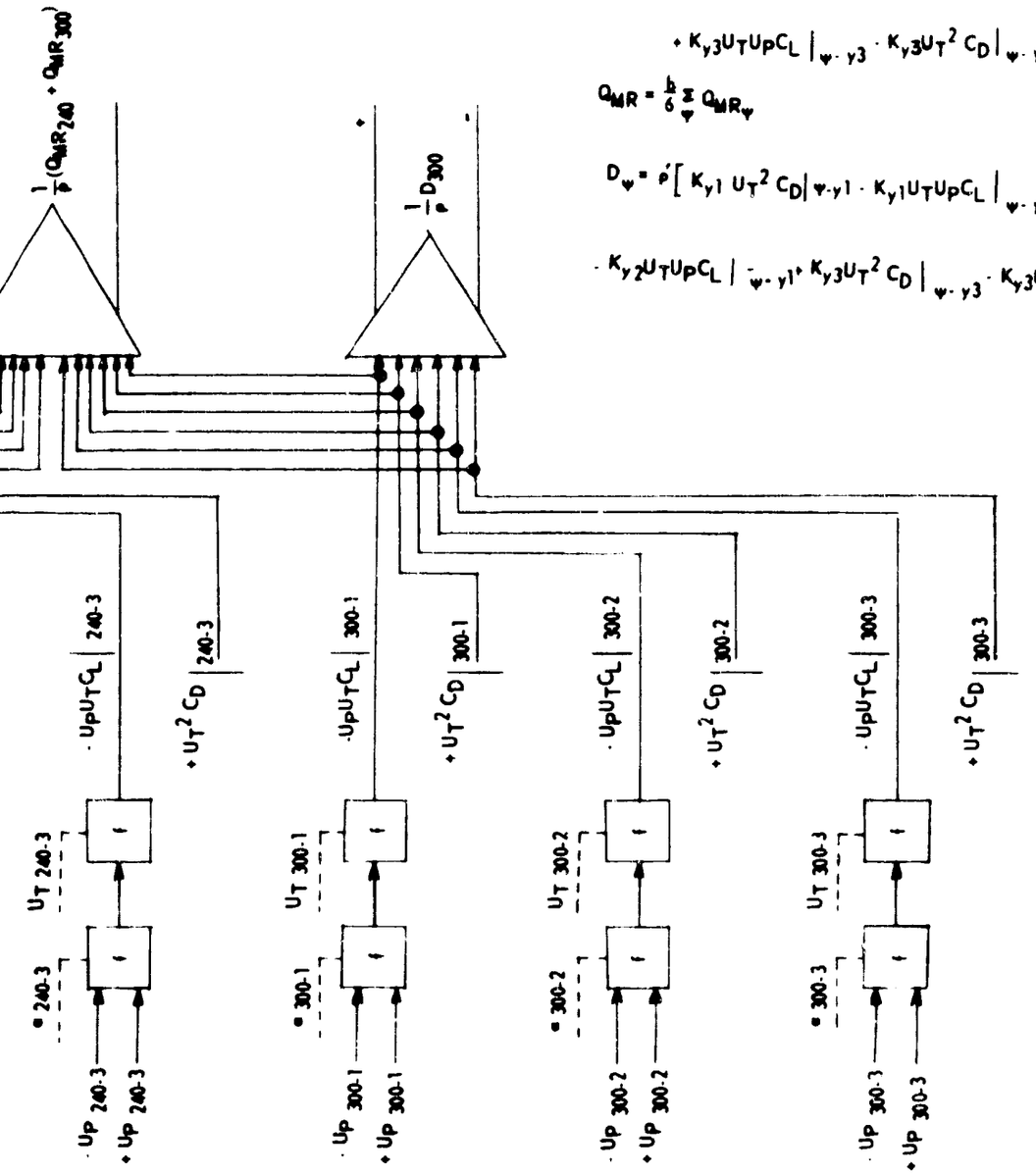

B

Figure 19 Blade Element Drag and Main Rotor Torque AC Mechanization

between AC and DC optimum mechanizations is the number of amplifiers required in the DC mechanization to provide both positive and negative functions. There are 9 amplifiers used in developing blade element drag and main rotor torque in Figure 19. Plus and minus functions are available from each of these 9 amplifiers for the AC mechanization. In order to do the mechanization with DC components, 9 additional amplifiers are necessary for sign purposes. Table 13 reflects the component complexity of Figure 19.

	AC		DC	
Component	No.	Wt.	No.	Wt.
Amplifier	10	10	19	38
Function (f) Generation	36	-	36	-
Complexity		10		38

Table 13. Blade Element Drag and Main Rotor Torque

(7) Block (7) Flap Angle Coefficient and Main Rotor Lift. Figure 20 is the mechanization for flap angle coefficients and main rotor lift. The critical area in the optimization consideration is the requirement of positive and negative a_{os}. DC methods in this mechanization require 1 additional amplifier. Table 14 reflects component complexity of Figure 20.

	AC		DC	
Component	No.	Wt.	No.	Wt.
Amplifier	8	8	9	18
Servo	2	14	2	14
Pots	6	1 1/2	6	1 1/2
Function (f) Generation	2	-	2	-
Complexity		23 1/2		33 1/2

Table 14. Flap Angle Coefficients and Main Rotor Lift

(8) Block (8) Blade Flap Angle. The blade flap angle computation is the difference between flap angle coefficients to form the $\beta_{\downarrow}$ outputs in the form of servo shaft positions. It is seen in Figure 21 that this mechanization would be equivalent in either an AC or a DC mechanization.

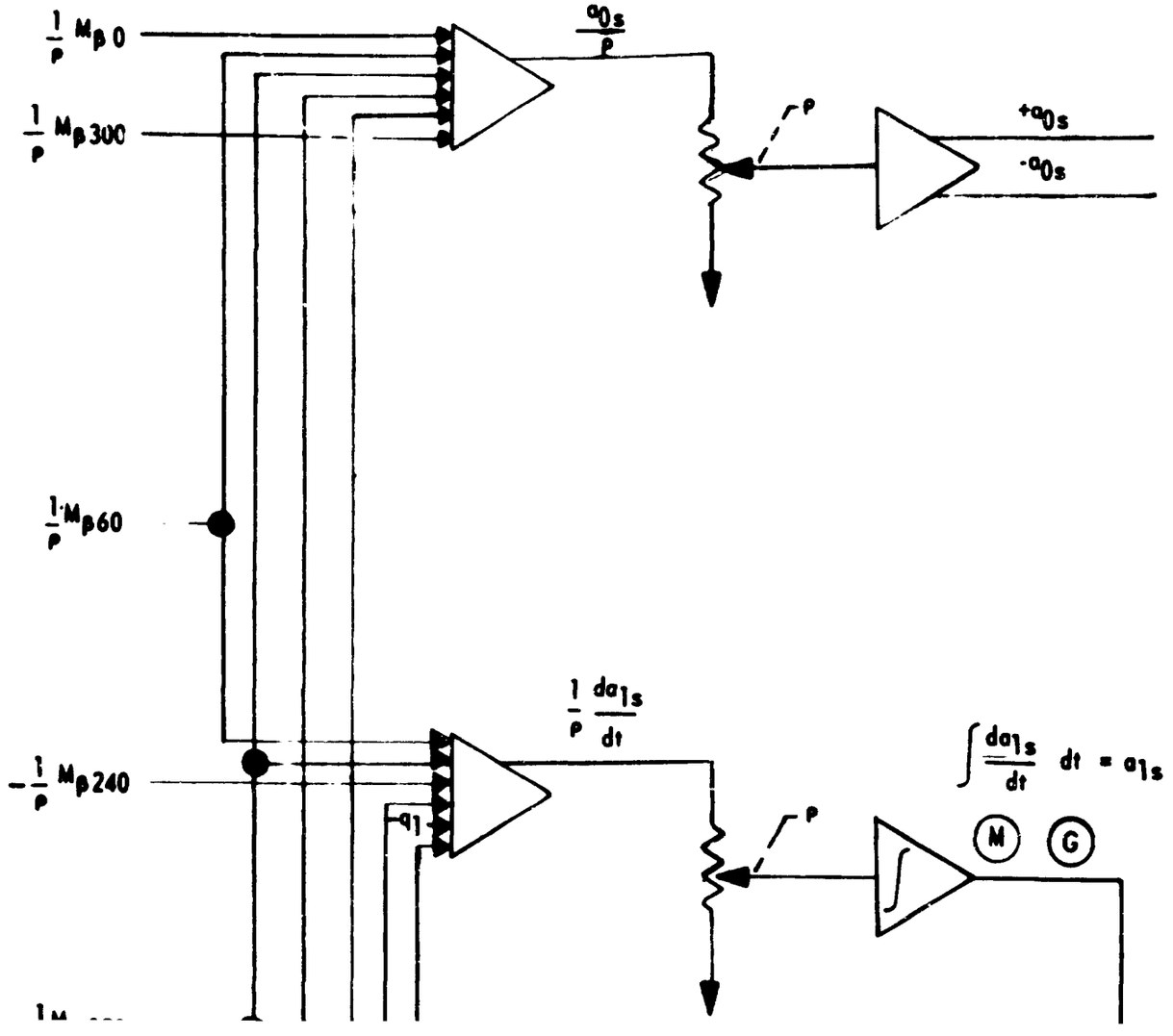
$\frac{1}{p} M_{p0}$
$\frac{1}{p} M_{p300}$
$\frac{1}{p} M_{p60}$
$-\frac{1}{p} M_{p240}$
$\frac{a_{0s}}{p}$
$+a_{0s}$
$-a_{0s}$
$\frac{1}{p} \frac{da_{1s}}{dt}$
$\int \frac{da_{1s}}{dt} dt = a_{1s}$
q_1
M
G
p

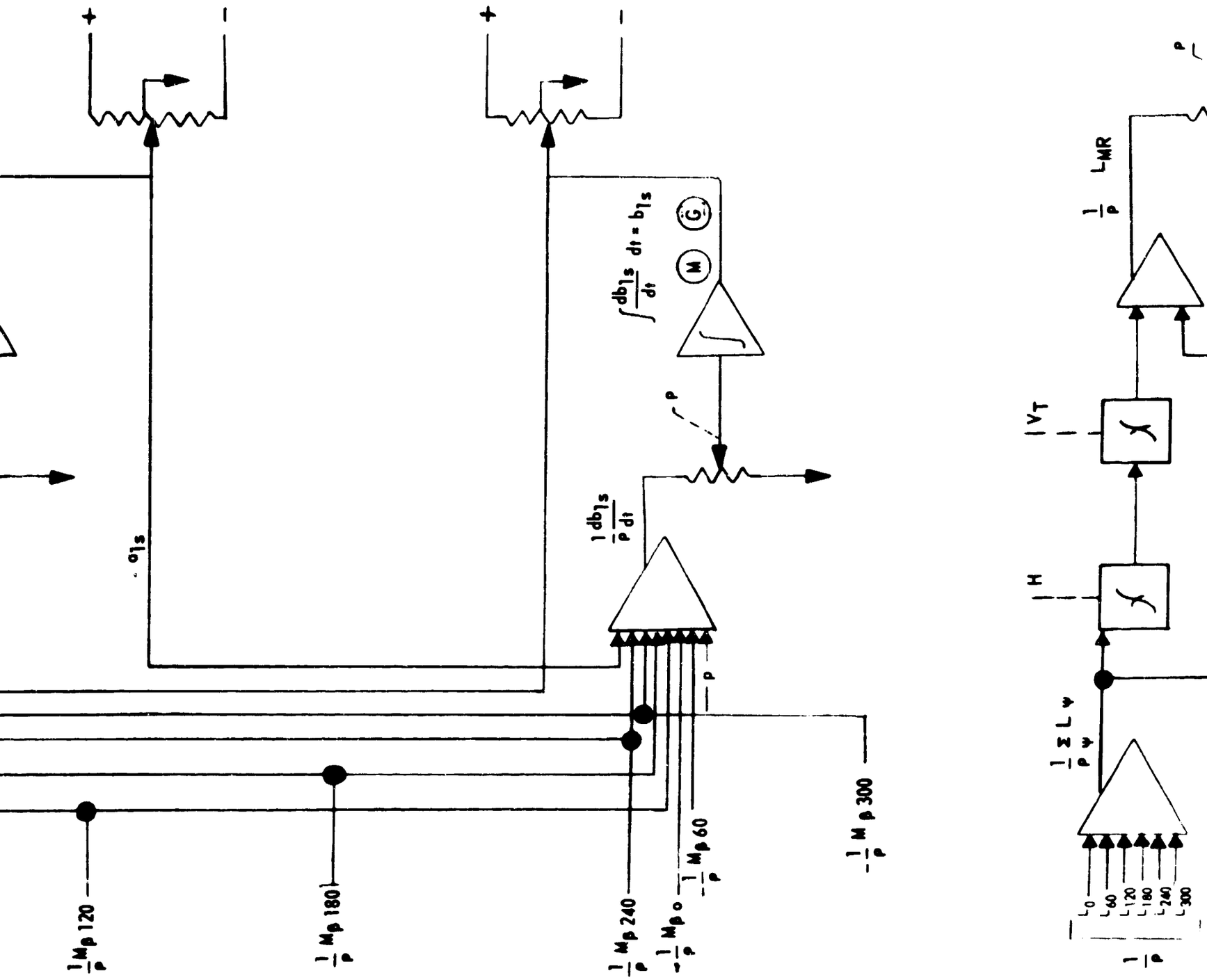

Figure 20. Flap Angle Coefficients and Main

/CEN 120

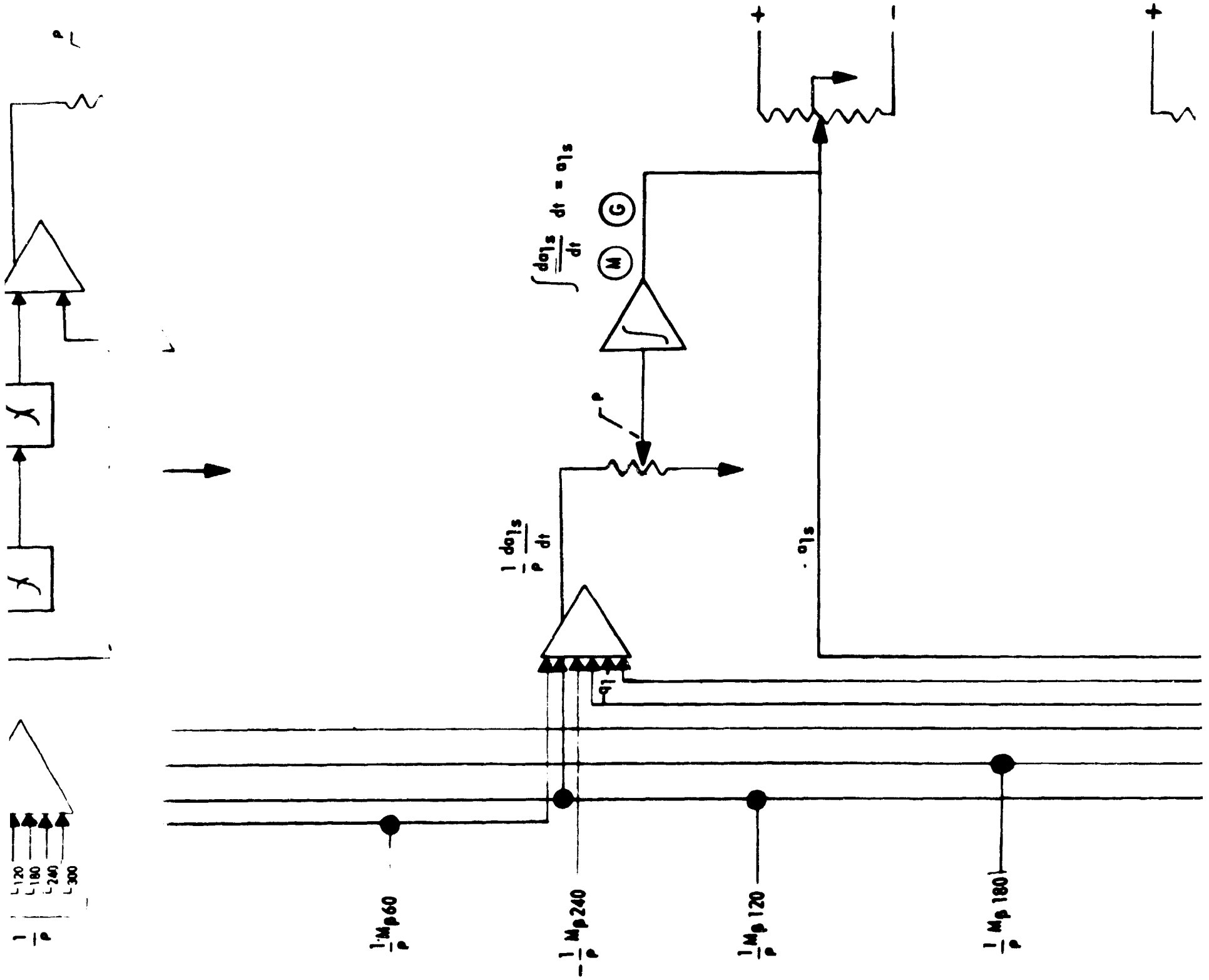

ind Main

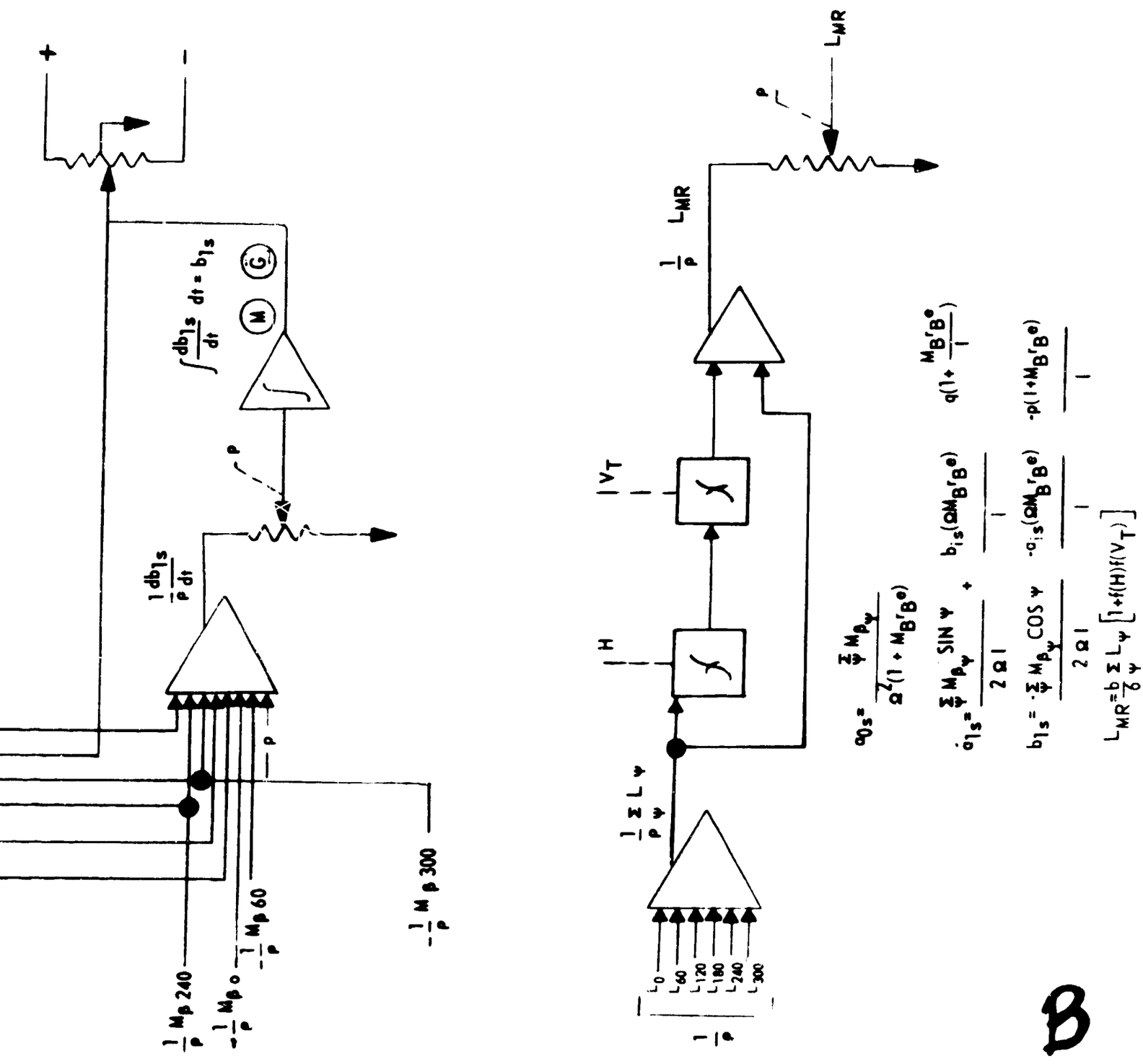

Figure 20. Flap Angle Coefficients and Main Rotor Lift AC Mechanization

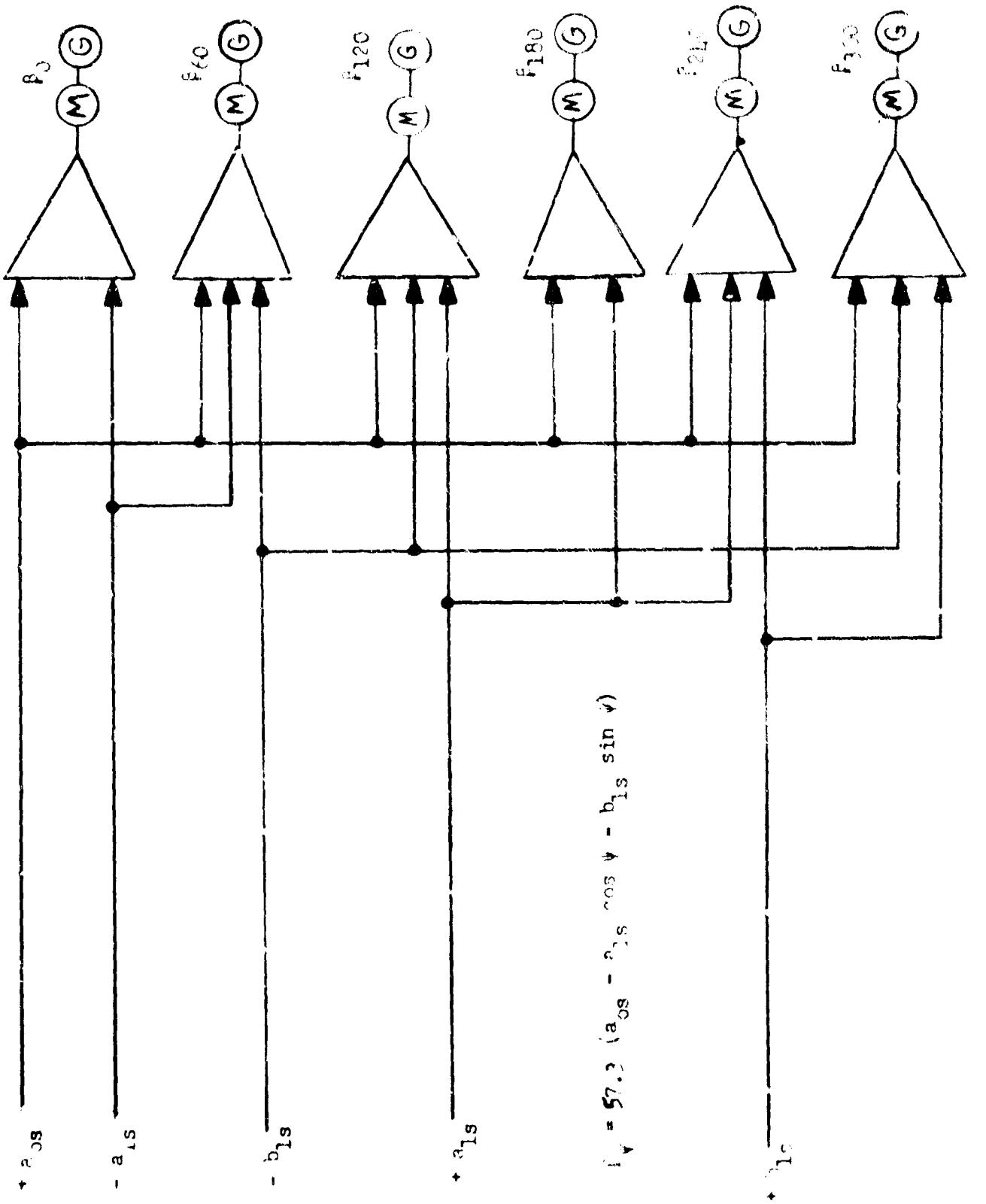

Figure 21. Blade Flap Angle
AC Mechanization

(9) Block (9) Rotor Hub Moments. As seen in Figure 22, the rotor hub moments are functions of the sums of functions of blade element lift ($L_\downarrow$), rotor angular velocity (Ω), flapping angle coefficients (a_{1s}, b_{1s}) and air density (ρ). The mechanization is a simple straightforward summation of functions and does not require a positive and negative output. Consequently, this method would also be equally optimum in either a DC or an AC system. Table 15 reflects component complexity of Figure 22.

	AC		DC	
Component	No.	Wt.	No.	Wt.
Amplifier	4	4	4	8
Pots	6	1 1/2	6	1 1/2
Complexity		5 1/2		9 1/2

Table 15. Rotor Hub Moments

(10) Block (10) Rotor Forces and Angular Velocity. Figure 23 is the mechanization for the rotor forces. There is no area in the mechanization that will cause the AC to differ from the DC mechanization. The integration of the torque summation to obtain rotor angular velocity could be accomplished by an electronic DC integrator, but rotor angular velocity (Ω) is required as a servo shaft position for multiplication (Ω^2). The mechanization as shown in Figure 23 can be done with the same amount of equipment in either a DC or AC system. Table 16 reflects the component complexity of Figure 23.

	AC		DC	
Component	No.	Wt.	No.	Wt.
Amplifier	3	3	3	6
Servo	1	7	1	7
Pots	10	2 1/2	10	2 1/2
Complexity		12 1/2		15 1/2

Table 16. Rotor Forces and Angular Velocity

This completes the rotor aerodynamics. The discussion will continue with Block (5) of Figure 23.

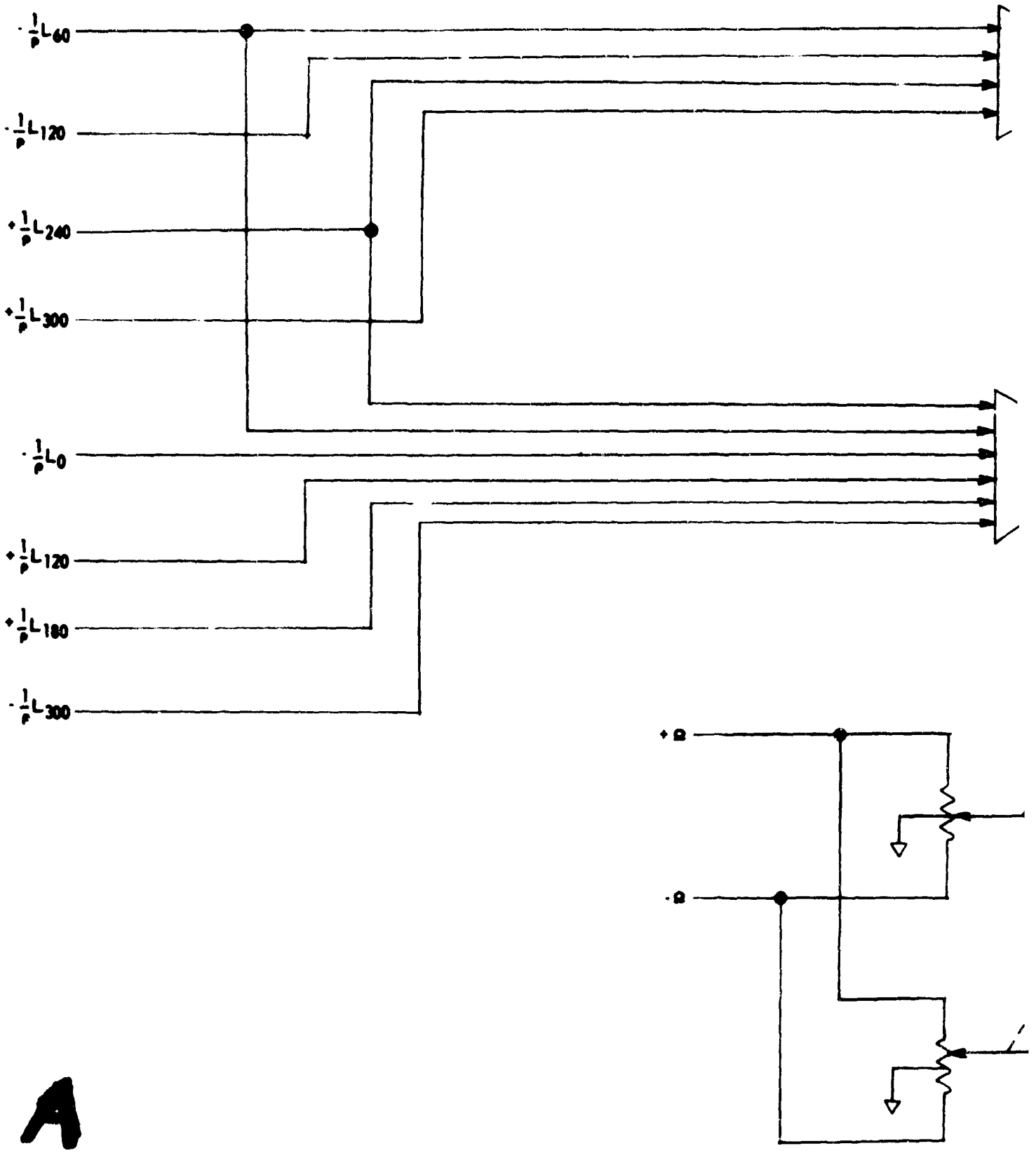
$-\frac{1}{\rho}L_{60}$
$-\frac{1}{\rho}L_{120}$
$+\frac{1}{\rho}L_{240}$
$+\frac{1}{\rho}L_{300}$
$-\frac{1}{\rho}L_{0}$
$+\frac{1}{\rho}L_{120}$
$+\frac{1}{\rho}L_{180}$
$-\frac{1}{\rho}L_{300}$
+Q
-Q

A

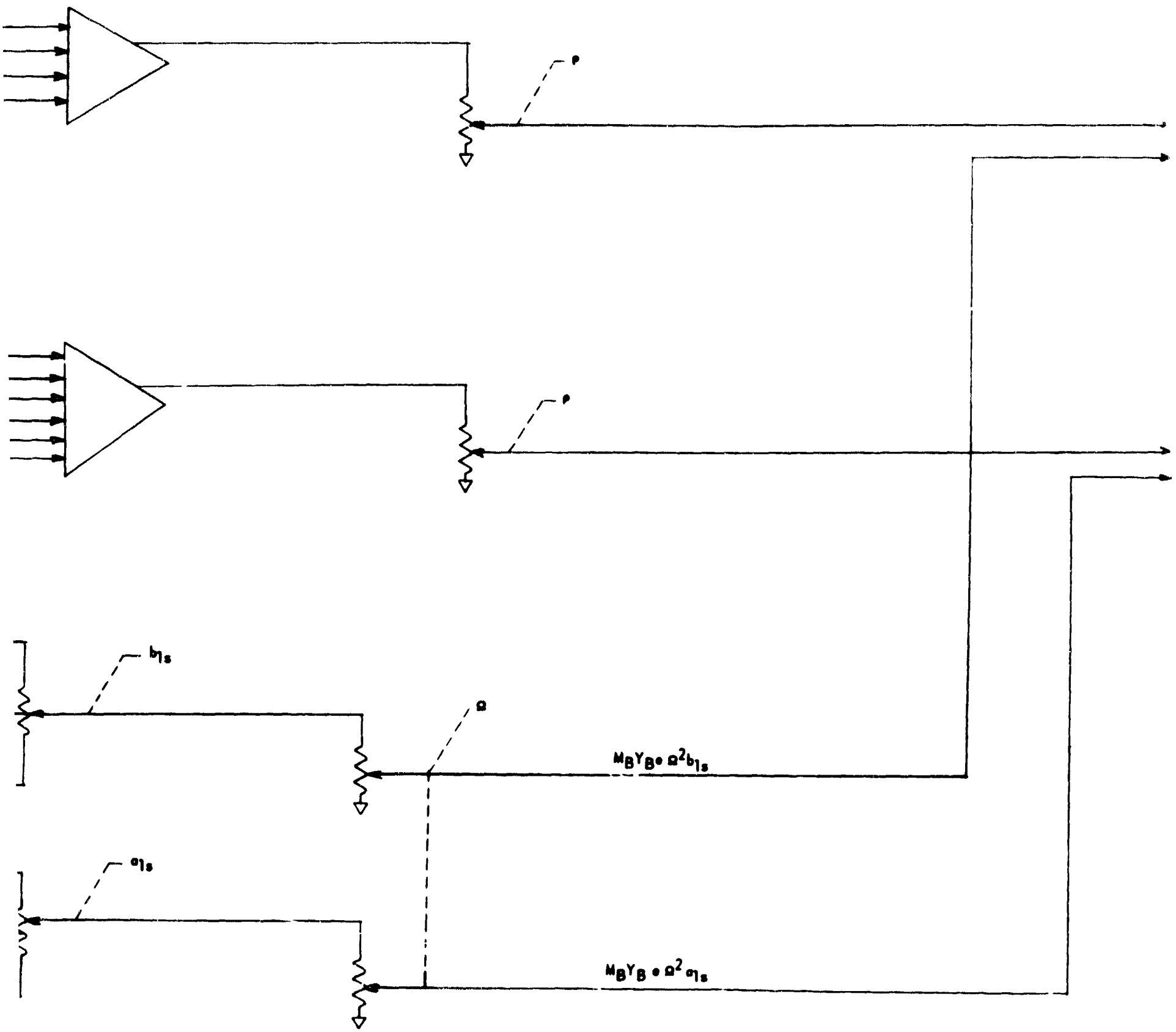

Figure 22. Rotor Hub Moments

DEVCEN

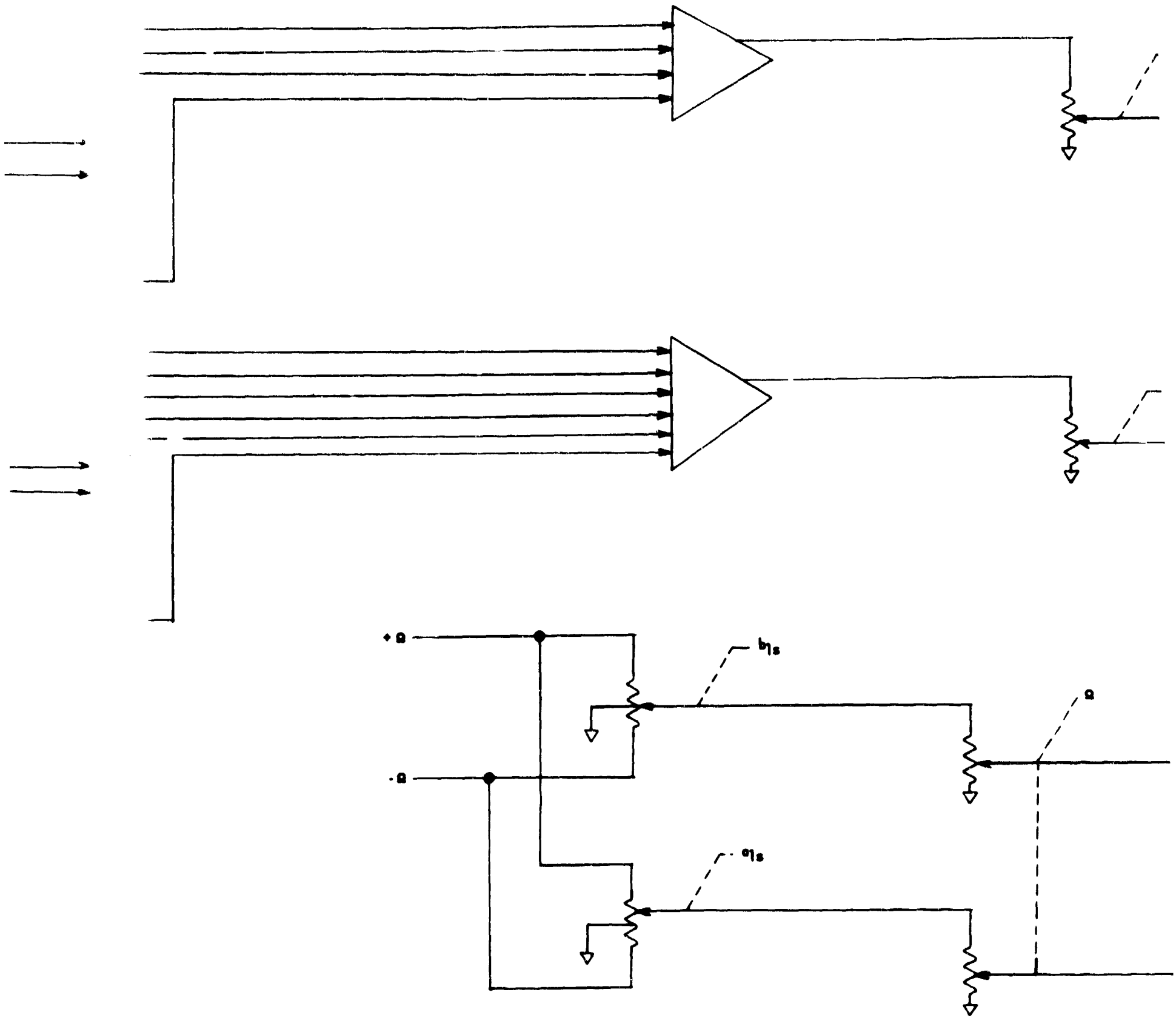

loments

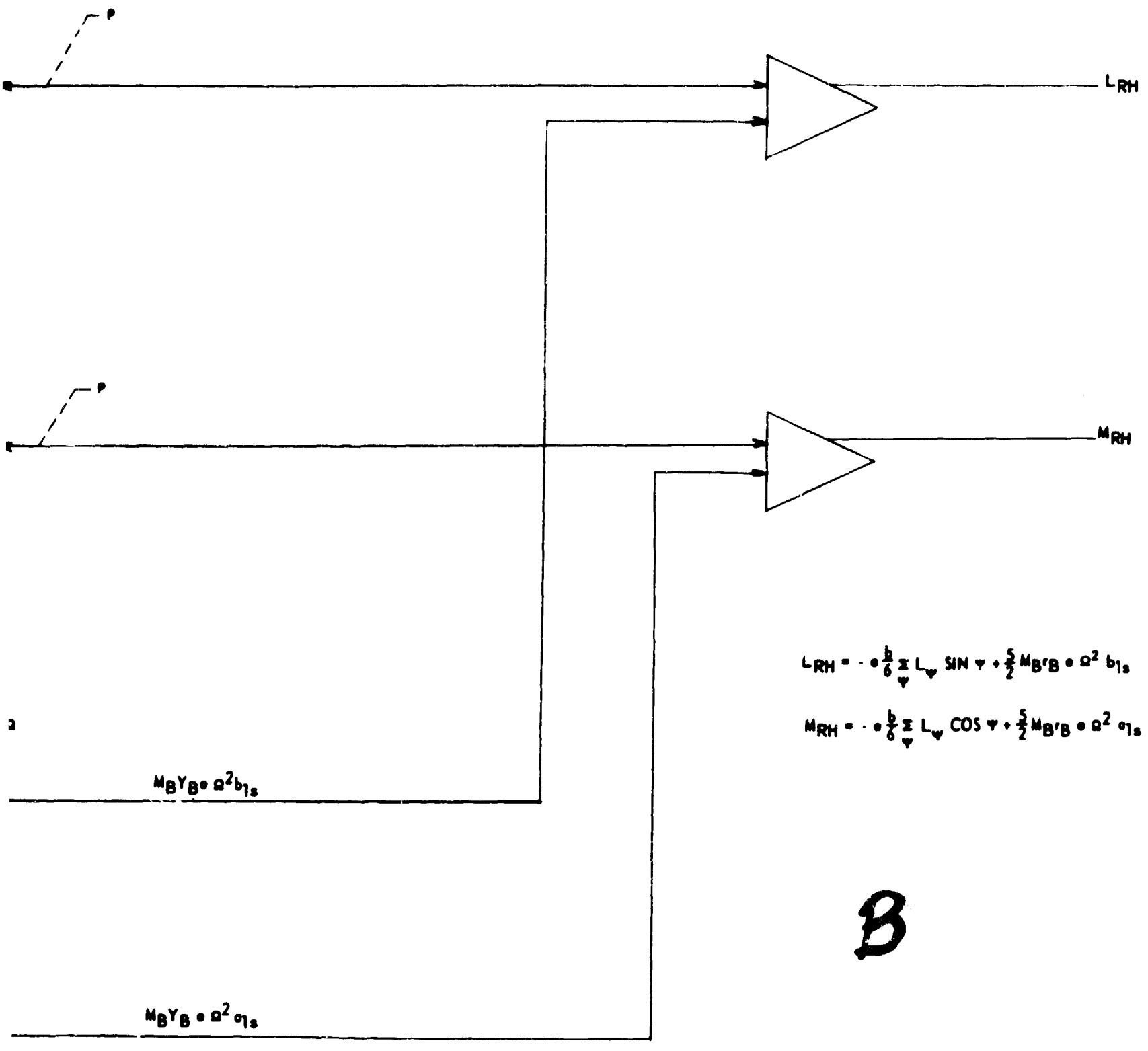

Figure 22. Rotor Hub Moments AC Mechanization

2

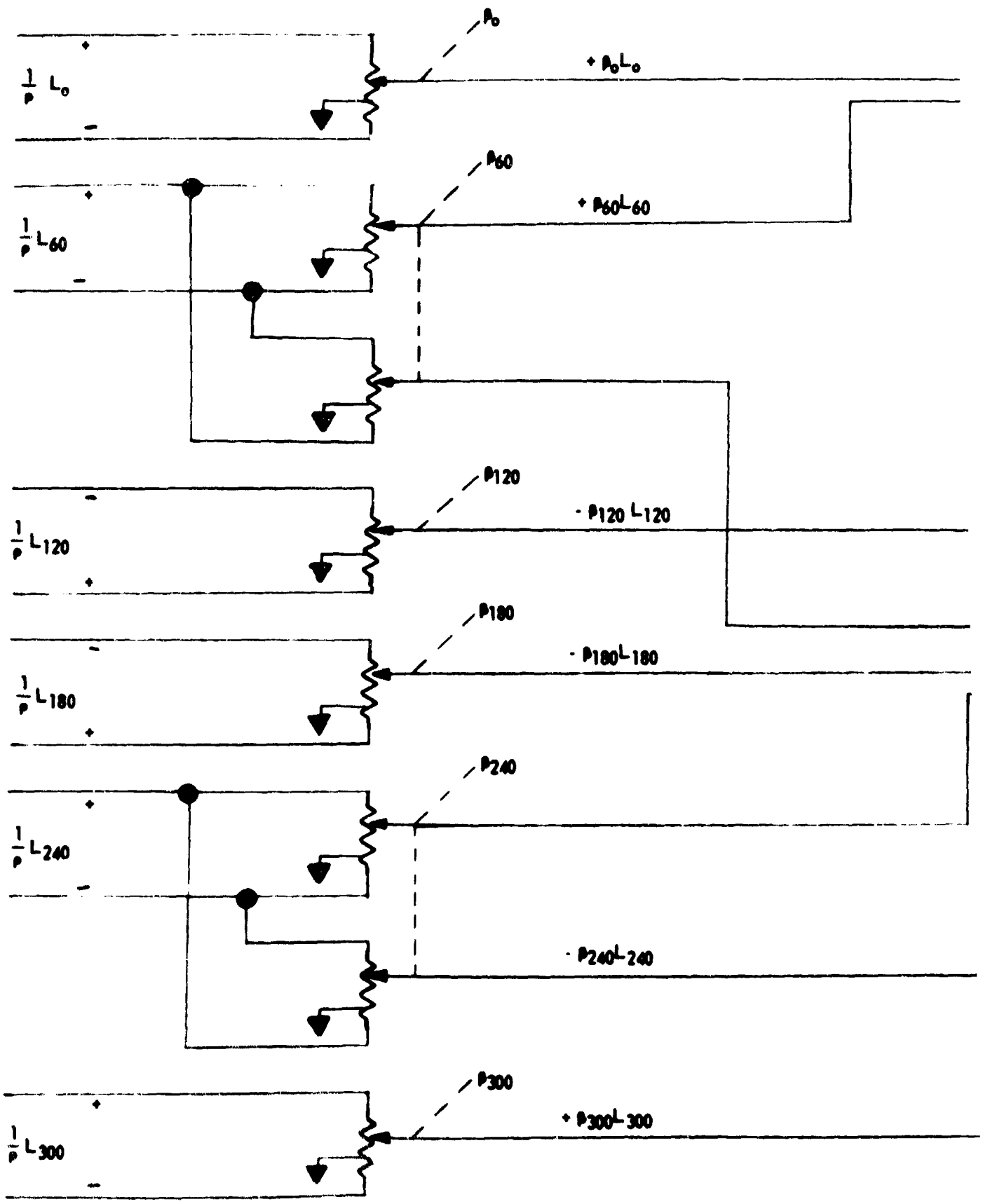
$\frac{1}{\rho} L_0$
P_0
$+ P_0 L_0$
$\frac{1}{\rho} L_{60}$
P_{60}
$+ P_{60} L_{60}$
$\frac{1}{\rho} L_{120}$
P_{120}
$- P_{120} L_{120}$
$\frac{1}{\rho} L_{180}$
P_{180}
$- P_{180} L_{180}$
$\frac{1}{\rho} L_{240}$
P_{240}
$- P_{240} L_{240}$
$\frac{1}{\rho} L_{300}$
P_{300}
$+ P_{300} L_{300}$

A

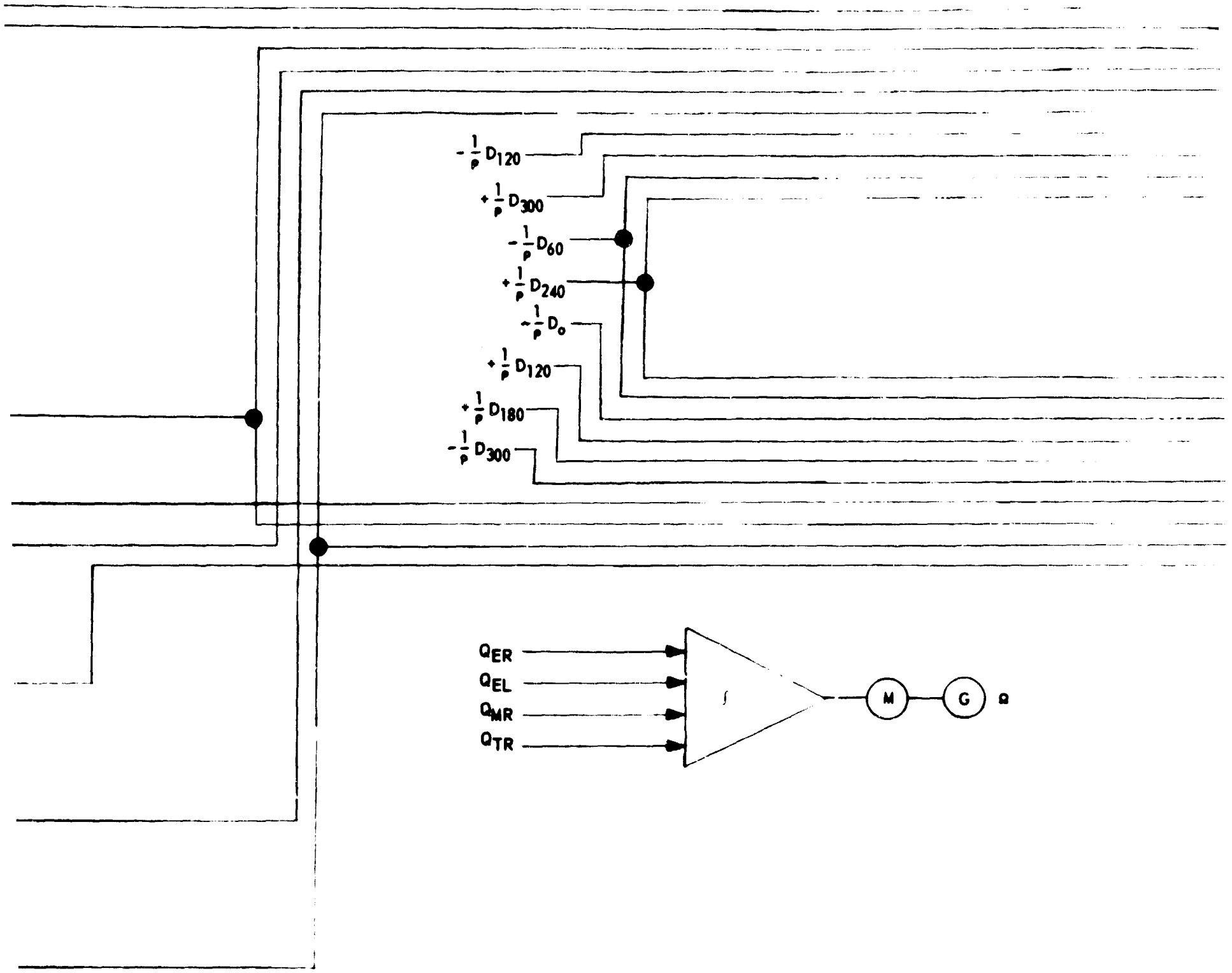
$-\frac{1}{p}D_{120}$
$+\frac{1}{p}D_{300}$
$-\frac{1}{p}D_{60}$
$+\frac{1}{p}D_{240}$
$-\frac{1}{p}D_{o}$
$+\frac{1}{p}D_{120}$
$+\frac{1}{p}D_{180}$
$-\frac{1}{p}D_{300}$
Q_{ER}
Q_{EL}
Q_{MR}
Q_{TR}
M
G
Q

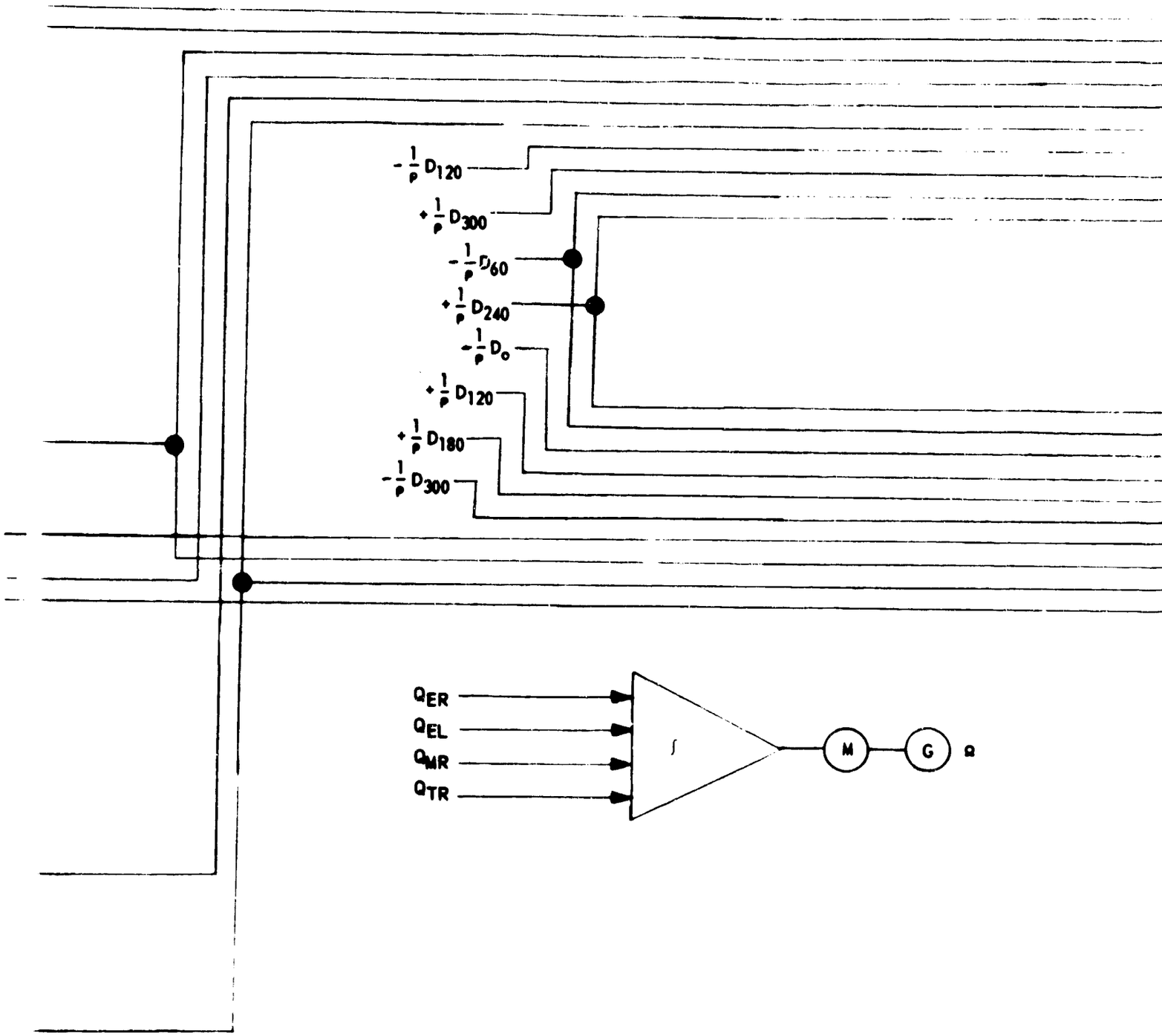
$-\frac{1}{\rho}D_{120}$
$+\frac{1}{\rho}D_{300}$
$-\frac{1}{\rho}D_{60}$
$+\frac{1}{\rho}D_{240}$
$-\frac{1}{\rho}D_{o}$
$+\frac{1}{\rho}D_{120}$
$+\frac{1}{\rho}D_{180}$
$-\frac{1}{\rho}D_{300}$
Q_{ER}
Q_{EL}
Q_{MR}
Q_{TR}
∫
M
G
Ω

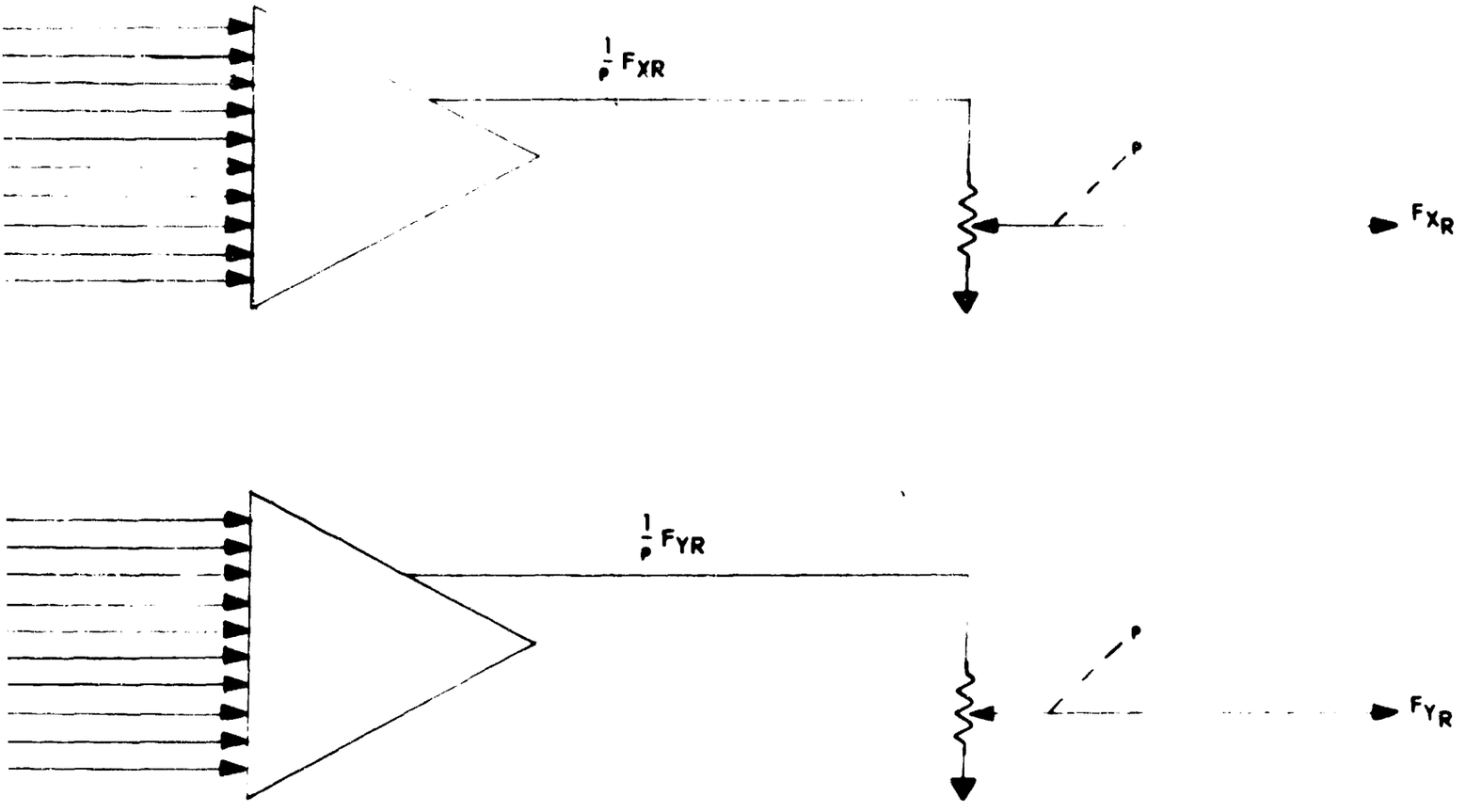

REFER TO EQUATIONS

$$F_{XR} = \frac{b}{\delta} \sum_{\psi} (.0173\, \beta_{\psi} L_{\psi} \cos \psi - D_{\psi} \sin \psi)$$

$$F_{Y_R} = \frac{b}{\delta} \sum_{\psi} (-.0173\, \beta_{\psi} L_{\psi} \sin \psi - D_{\psi} \cos \psi)$$

$$\dot{\alpha} = \frac{Q_{MR} + Q_{TR} + Q_{ER} + Q_{EL} + Q_{RB} - 1700}{10,275}$$

B

Figure 23. Rotor Forces and Angular Velocity AC Mechanization

Block (5) Force Σ. The AC mechanization of Block (5), Figure is shown in Figure 24. Equations 6.21, 6.24 and 6.27 are mechanized to give the force outputs (X_a, Y_a, Z_a). Table 17 reflects the component complexity of Figure 24.

	AC		DC	
Component	No.	Wt.	No.	Wt.
Amplifier	12	12	16	16
Servo				
S-C Pots	4	1	4	1
Complexity		13		17

Table 17. Force Summations

Four extra amplifiers are necessary for DC mechanization so that both signs of a function are available for operation of the sine-cosine potentiometers in Figure 24.

Block (6) Mass, c.g. Block (6) of Figure 9 is mechanized as in Section III.A.

Block (7) Moments and Block (9) Angular Rates. The AC mechanization of Blocks (7) and (9) Figure 9 is shown in Figure 25. Equations 6.30, 6.34 and 6.39 are mechanized to give outputs (L_a, M_a, N_a) and then each moment is integrated after dividing by the appropriate inertia term to give the angular rates (p, q_1, r). The DC mechanisation is essentially the same as the AC mechanisation.

Blocks (8) through (14). These blocks of Figure 9 have been discussed in Section III.A. The correspondence between Figure 9 and Figure 1 is as follows:

Block (8), Figure 9 mechanized by Figure 3.

Block (10), Figure 9 mechanized by Figure 4.

Block (11), Figure 9 mechanized by Figure 5.

Block (12h), Figure 9 mechanized by Figure 7.

Block (13h), Figure 9 mechanized by Figure 7.

Block (14), Figure 9 instructor inputs as noted in Section III.A.

This completes the mechanization of the single rotor helicopter.

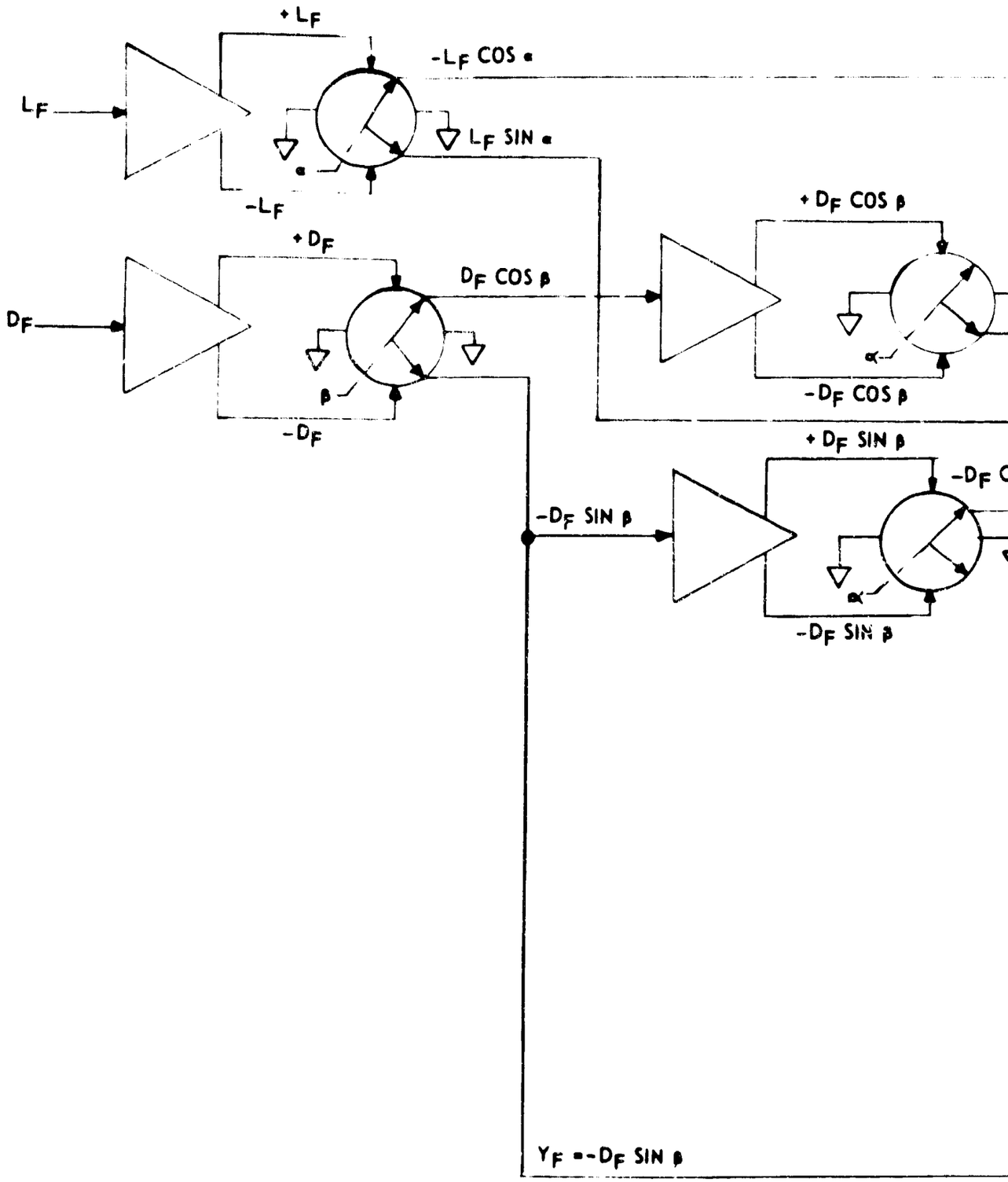
+ L_F
L_F
$-L_F$ COS α
L_F SIN α
α
$-L_F$
+ D_F
D_F
D_F COS β
β
$-D_F$
+ D_F COS β
α
$-D_F$ COS β
+ D_F SIN β
$-D_F$ SIN β
α
$-D_F$ SIN β
Y_F = $-D_F$ SIN β

A

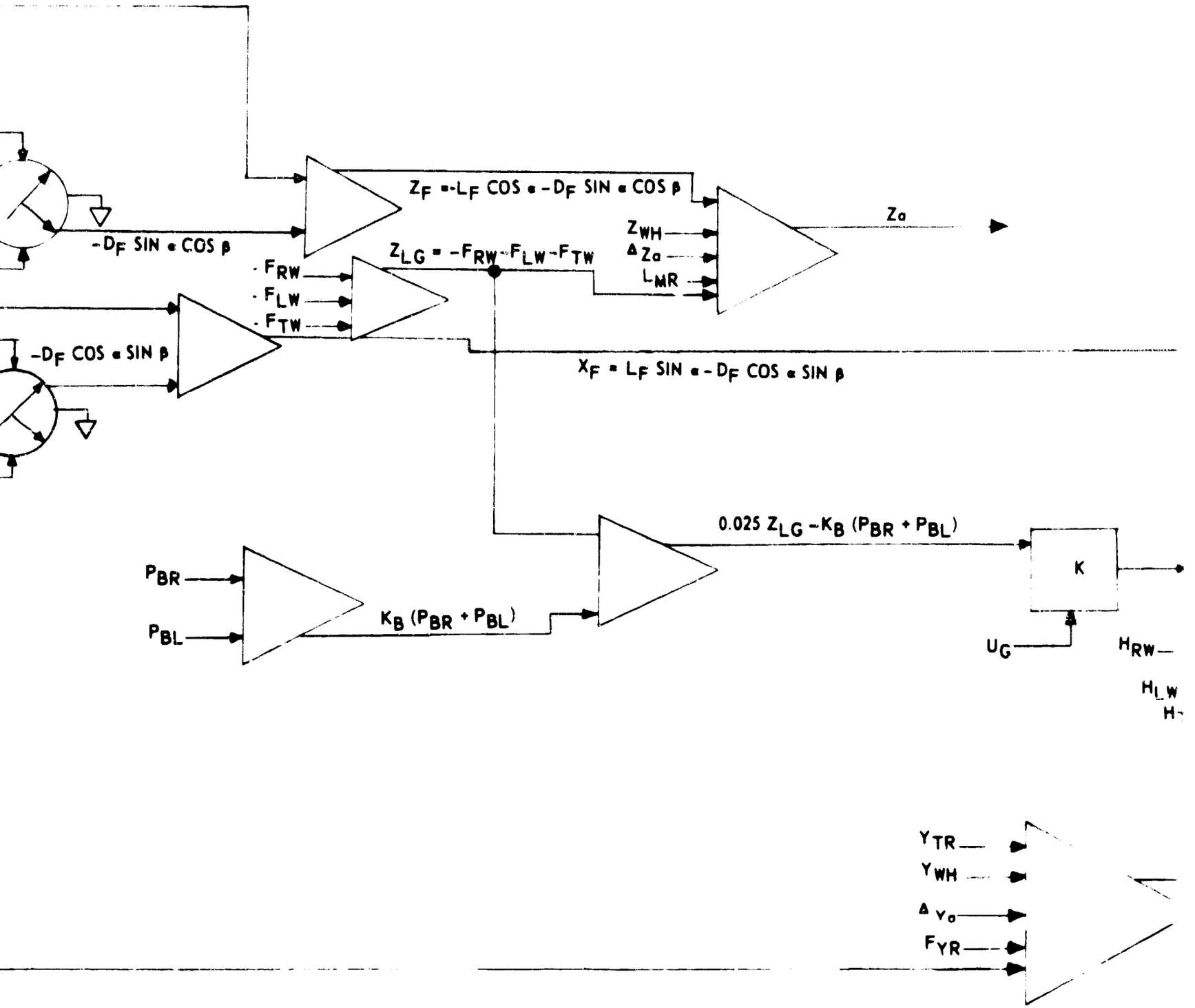
$Z_F = -L_F \cos\alpha - D_F \sin\alpha \cos\beta$
$-D_F \sin\alpha \cos\beta$
$Z_{LG} = -F_{RW} - F_{LW} - F_{TW}$
Z_{WH}
ΔZ_a
L_{MR}
Z_a
F_{RW}
F_{LW}
F_{TW}
$-D_F \cos\alpha \sin\beta$
$X_F = L_F \sin\alpha - D_F \cos\alpha \sin\beta$
$0.025 Z_{LG} - K_B (P_{BR} + P_{BL})$
P_{BR}
P_{BL}
$K_B (P_{BR} + P_{BL})$
K
U_G
H_{RW}
H_{LW}
Y_{TR}
Y_{WH}
ΔY_a
F_{YR}

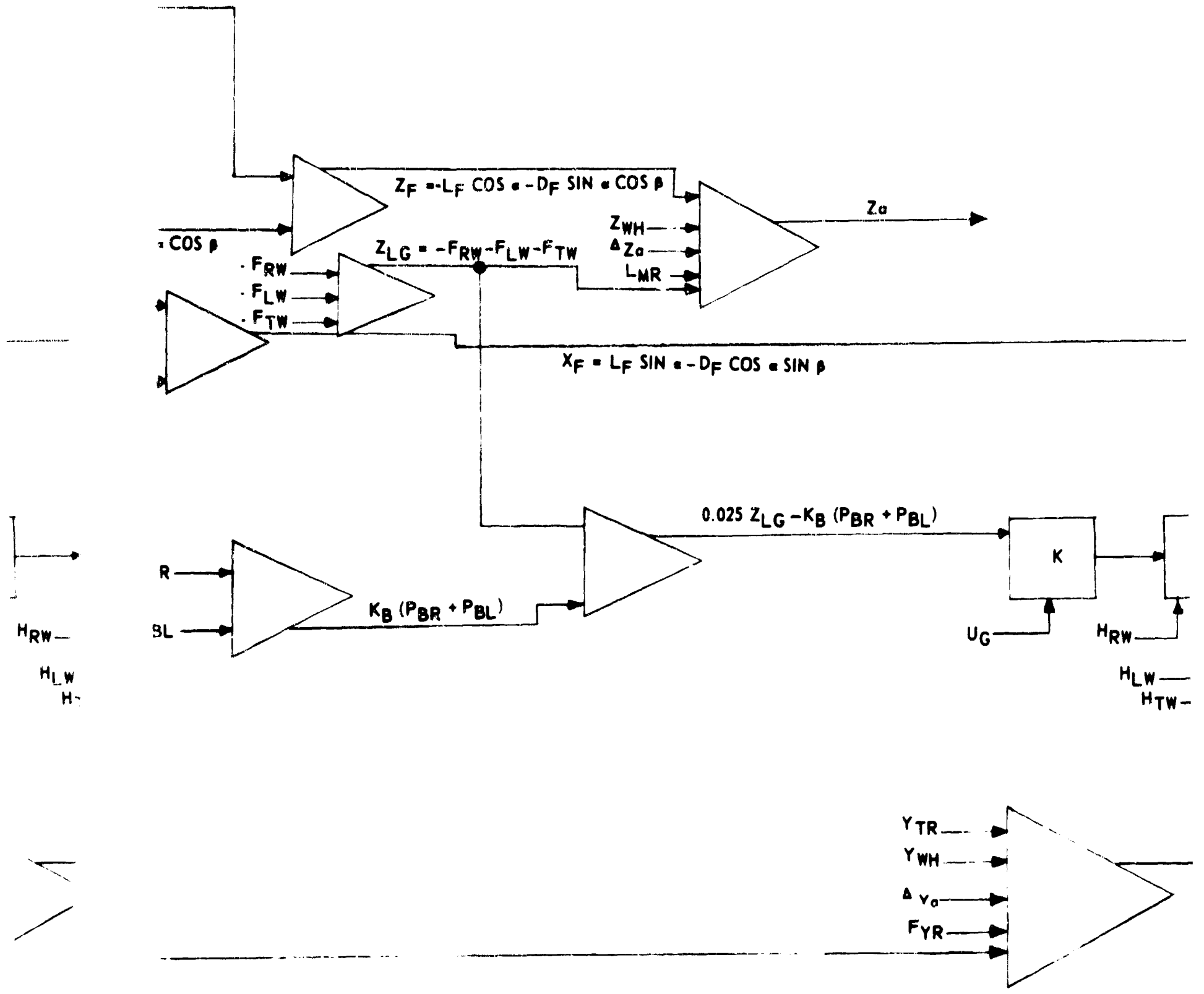
$Z_F = -L_F \cos\alpha - D_F \sin\alpha \cos\beta$
$Z_{LG} = -F_{RW} - F_{LW} - F_{TW}$
$\cos\beta$
F_{RW}
F_{LW}
F_{TW}
Z_{WH}
ΔZ_a
L_{MR}
Z_a
$X_F = L_F \sin\alpha - D_F \cos\alpha \sin\beta$
$0.025\ Z_{LG} - K_B (P_{BR} + P_{BL})$
R
SL
$K_B (P_{BR} + P_{BL})$
K
U_G
H_{RW}
H_{LW}
H_{TW}
Y_{TR}
Y_{WH}
Δy_a
F_{YR}

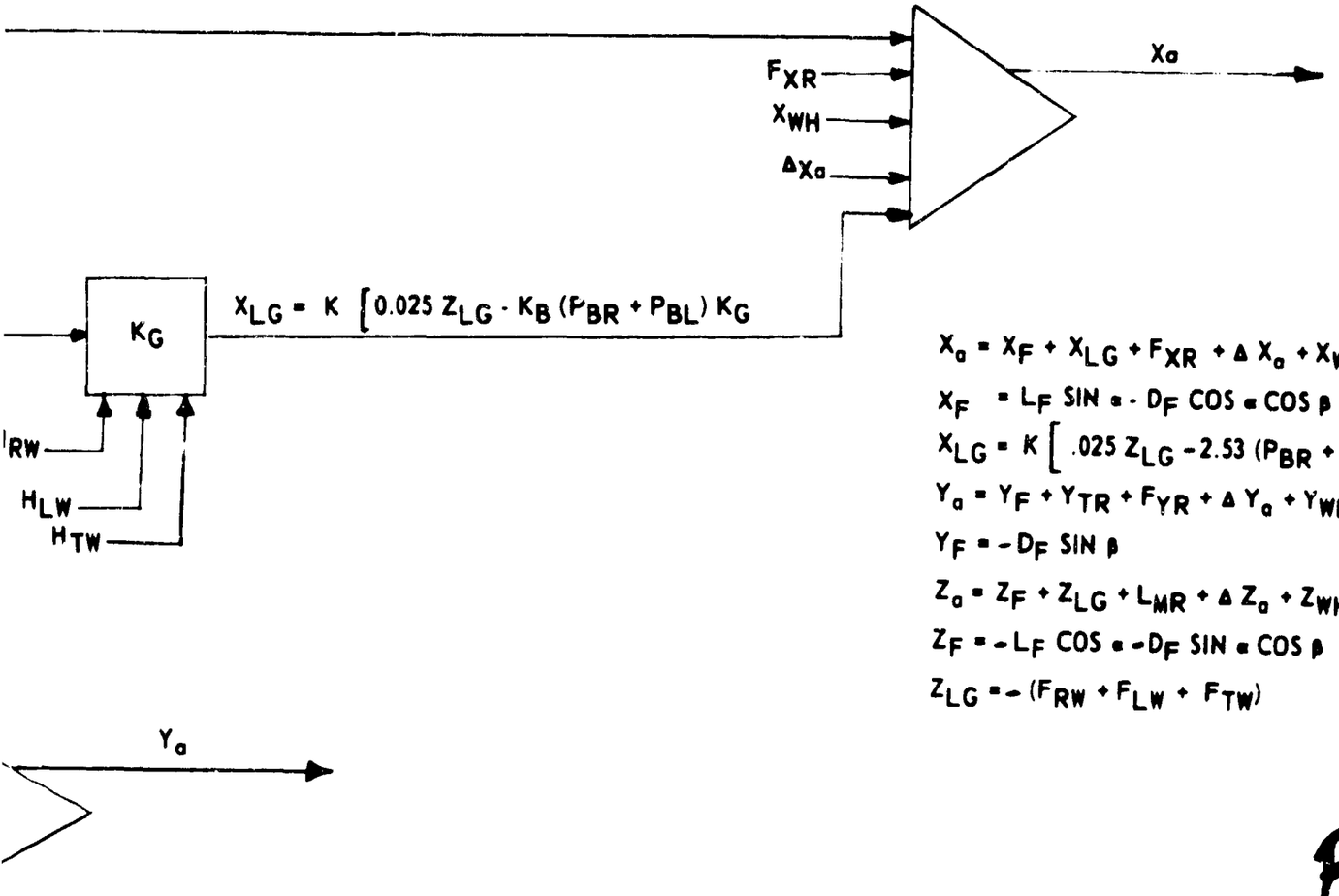

$X_a = X_F + X_{LG} + F_{XR} + \Delta X_a + X_{WH}$

$X_F = L_F \text{ SIN } \alpha - D_F \text{ COS } \alpha \text{ COS } \beta$

$X_{LG} = K \left[.025 Z_{LG} - 2.53 (P_{BR} + P_{BL}) K_G \right]$

$Y_a = Y_F + Y_{TR} + F_{YR} + \Delta Y_a + Y_{WH}$

$Y_F = -D_F \text{ SIN } \beta$

$Z_a = Z_F + Z_{LG} + L_{MR} + \Delta Z_a + Z_{WH}$

$Z_F = -L_F \text{ COS } \alpha - D_F \text{ SIN } \alpha \text{ COS } \beta$

$Z_{LG} = -(F_{RW} + F_{LW} + F_{TW})$

B

Figure 24. Force Summations AC Mechanization

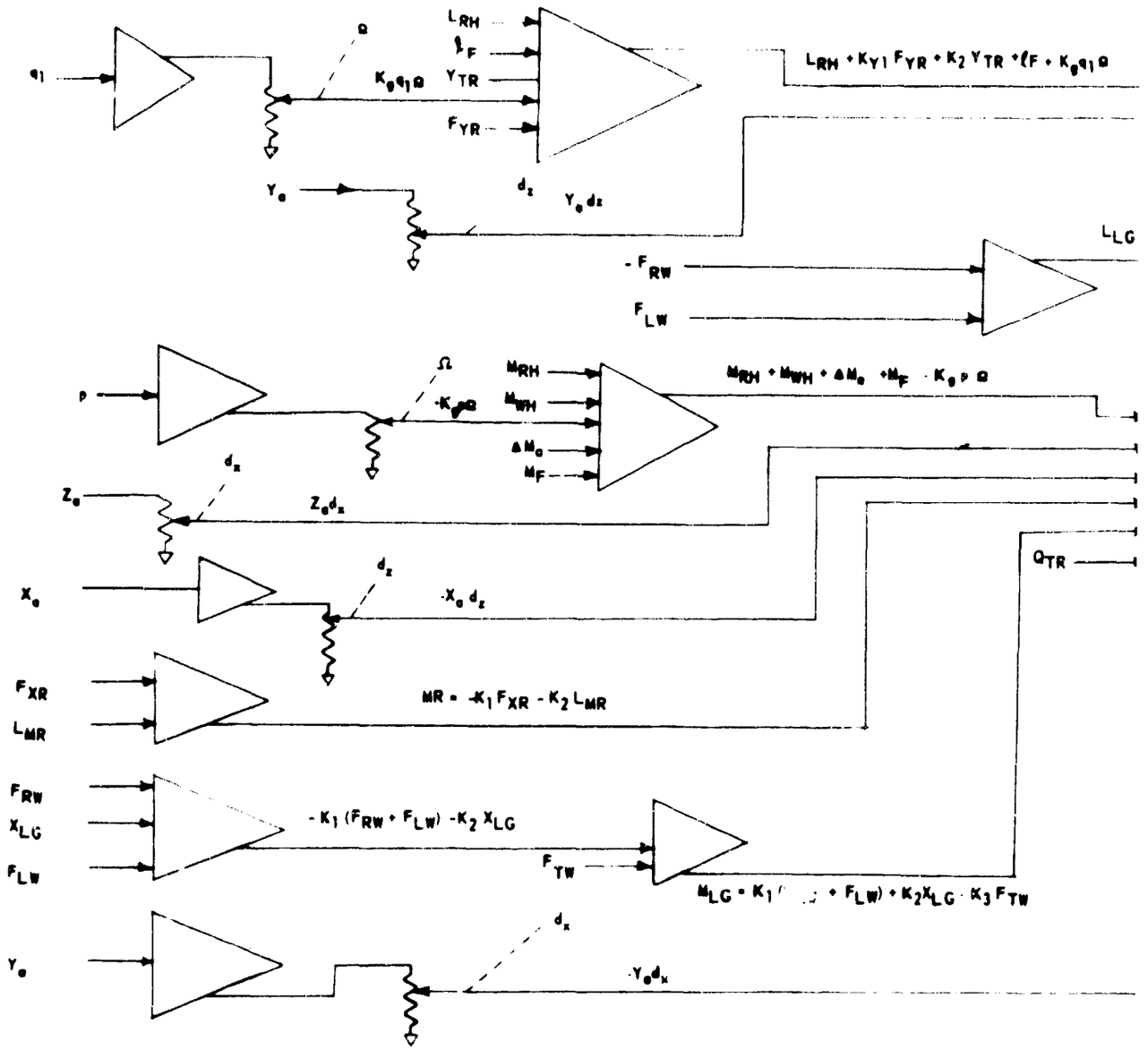
q1
Ω
$K_\theta q_1 \Omega$
L_{RH}
ℓ_F
Y_{TR}
F_{YR}
$L_{RH} + K_{Y1} F_{YR} + K_2 Y_{TR} + \ell_F + K_\theta q_1 \Omega$
Y_θ
d_z
$Y_\theta d_z$
L_{LG}
$-F_{RW}$
F_{LW}
p
$-K_p \Omega$
M_{RH}
M_{WH}
ΔM_α
M_F
$M_{RH} + M_{WH} + \Delta M_\alpha + M_F - K_\theta p \Omega$
Z_θ
$Z_\theta d_x$
Q_{TR}
X_θ
$-X_\theta d_z$
F_{XR}
L_{MR}
$MR = -K_1 F_{XR} - K_2 L_{MR}$
F_{RW}
X_{LG}
F_{LW}
$-K_1 (F_{RW} + F_{LW}) - K_2 X_{LG}$
F_{TW}
$M_{LG} = K_1 (F_{RW} + F_{LW}) + K_2 X_{LG} - K_3 F_{TW}$
Y_θ
d_x
$-Y_\theta d_x$

A

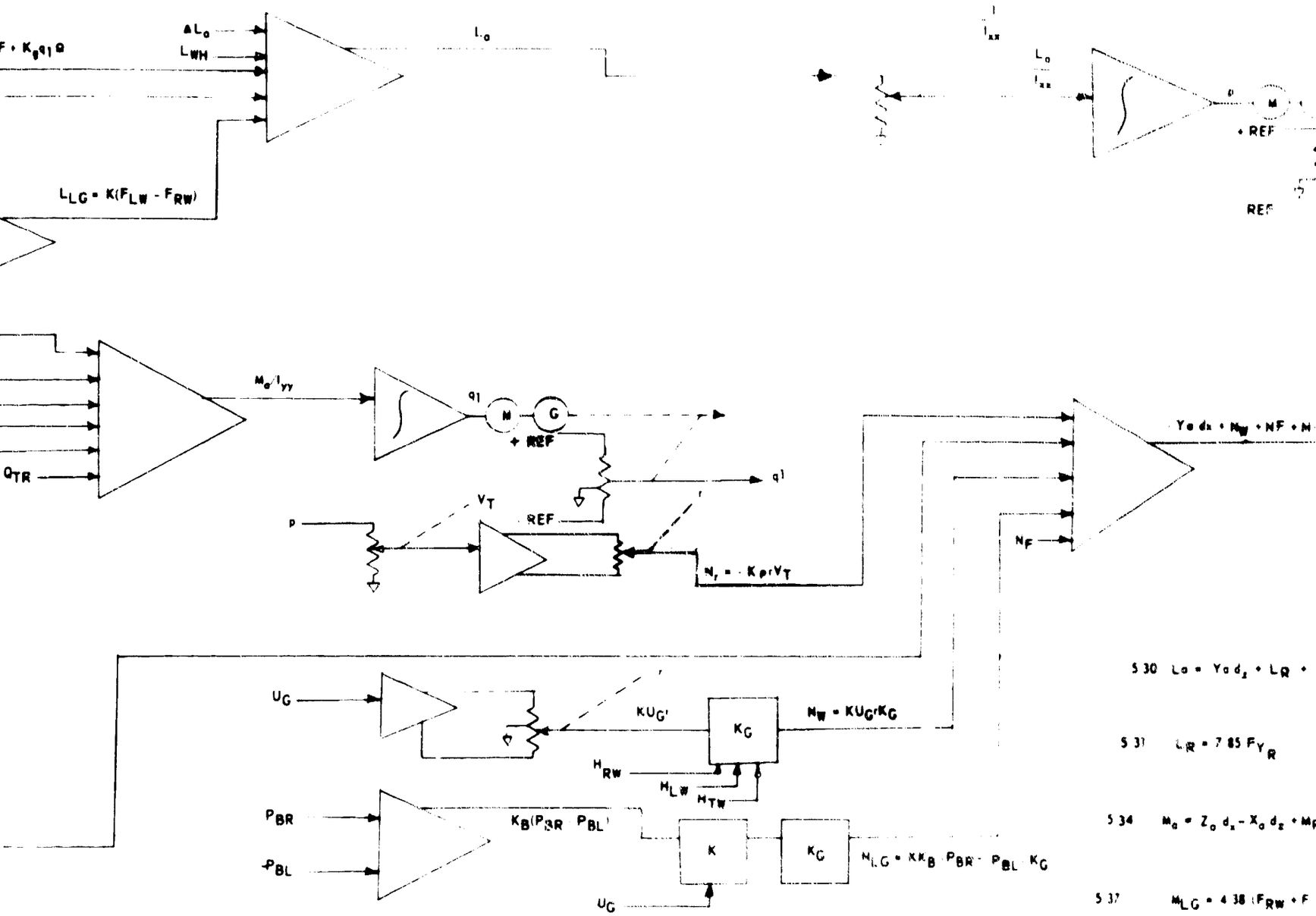

5.30 $L_a = Y_a d_z + L_R +$

5.31 $L_R = 7.85 F_{Y_R}$

5.34 $M_a = Z_a d_x - X_a d_z + M_p$

5.37 $M_{LG} = 4.38 (F_{RW} + F$

5.39 $N_a = Y_a d_x + N_W + N_F$

5.43 $N_{LG} = K\ 16.45 \left[P_B \right.$

5.80 $q_1 = \frac{M_a}{I_{yy}} dt$

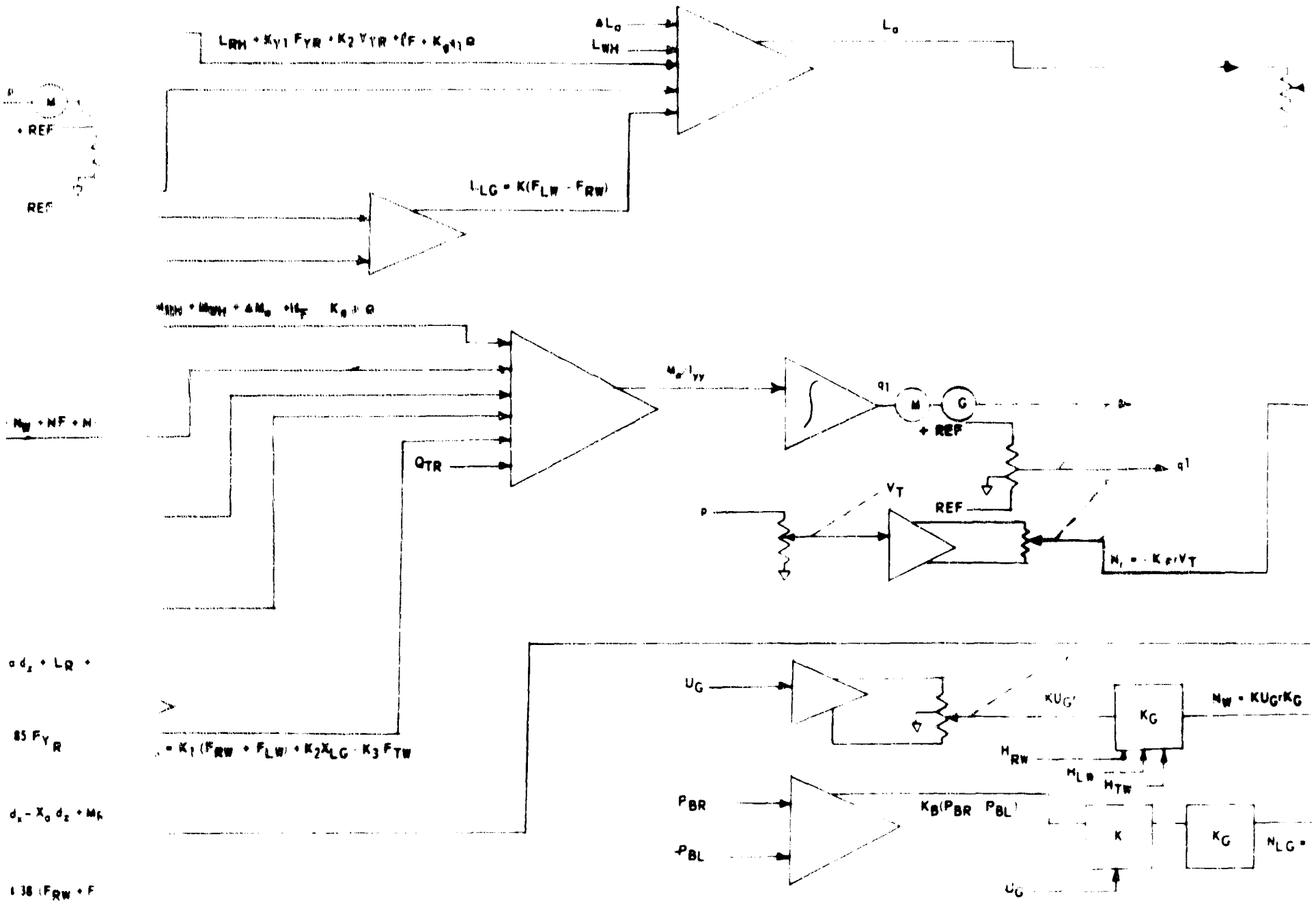
$L_{RH} + K_{Y1} F_{YR} + K_2 \gamma_{TR} + (F + K_{q1} q$
ΔL_a
L_{WH}
L_a
$L_{LG} = K(F_{LW} - F_{RW})$
REF
Q_{TR}
M_a / I_{yy}
q1
+ REF
V_T
REF
$N_1 = - K_{q1} V_T$
U_G
$K U_G$
K_G
$N_W = K U_G K_G$
H_{RW}
H_{LW}
H_{TW}
P_{BR}
P_{BL}
$K_B(P_{BR} - P_{BL})$
K
K_G
$N_{LG} =$
U_G

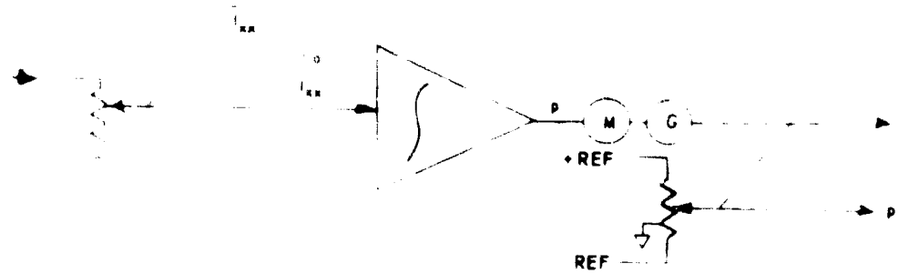

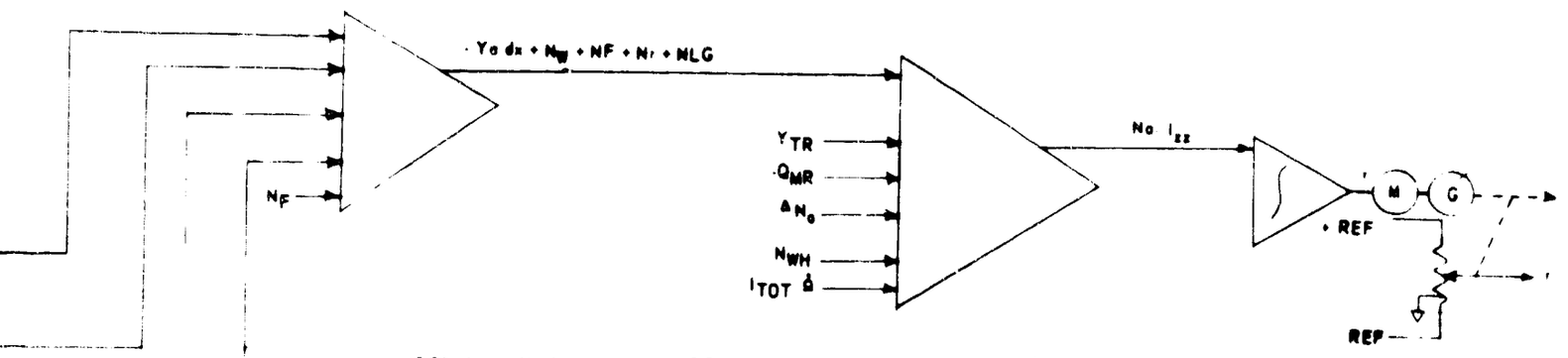

5 30 $L_o = Y_o d_z + L_R + L_{RH} + 2\,74\,Y_{TR} + L_{LG} + \Delta L_o + q_1\,\Omega\,(564\,5) + I_F + L_{WH} - 80.000\,p\,K_W$

5 31 $L_R = 7\,85\,F_{Y_R}$ 5 32 $L_{LG} = 6\,5(F_{LW} \quad F_{RW})$ 5 36 $M_R = -7\,85\,F_{X_R} \quad 073 L_{MR}$

5 34 $M_o = Z_o d_x - X_o d_z + M_R + M_{LG} + M_F + M_{RH} - \frac{Q_{TR}}{6\,1} + \Delta M_o \quad p\,\Omega\,(564\,5) + M_{WH} \quad 56\,000$

5 37 $M_{LG} = 4\,38\,(F_{RW} + F_{LW}) \quad 18\,99\,F_{TW} + 5\,36\,X_{LG}$ 5 40 $N_W = 2200\,U_G / K_G$

5 39 $N_o = Y_o dx + N_W + N_F + N_r \quad 36\,06\,Y_{TR} + N_{LG} \quad Q_{MR} + I_{TOT}\,\Omega + \Delta N_o + N_{RW} + N_{WH}$ 5 42 $N_r = 102\,762\,\frac{r}{V_T}\,q$

5 43 $N_{LG} = K\,16\,45\left[P_{BR} \quad P_{BL} \right] K_G$ 5 79 $p = \int \frac{L_o}{I_{xx}}\,dt$

5 80 $q_1 = \frac{M_o}{I_{yy}}\,dt$ 5 81 $r = \int \frac{N_o}{I_{zz}}\,dt$

B

Figure 25 Moment Summation and Angular Rates AC Mechanization

Summary Single Rotor Helicopter. Figure 1, the general block diagram of the equation solution of the single rotor helicopter, has been developed block by block. Table 18 is a tabulation of the various components (amplifier, servo, potentiometer, sine-cosine potentiometer, and resolver) for the single rotor helicopter. It should be noted that items specified as functions generated in the mechanization have not been included in Table 18 since they are assumed to be potentiometer derived and the same for both AC and DC mechanizations. In order to compare AC and DC systems the weight factors used by Mark E. Connelly in reference 4 are applied to the totals which result in Table 18. The weights resulting from each component are tabulated in Table 19. The summary in Table 19 gives the complexity of the single rotor helicopter for AC and DC systems. The AC system has a complexity of 751-3/4 versus 1106-1/2 for the DC system. This is a marked difference. The difference is primarily due to using a weight factor of two (2) for the DC amplifier and one (1) for the AC amplifier.

	Amplifiers		Servo		Pots		S-C Pots		Resolver	
	AC	DC	AC	DC	AC	DC	AC	DC	AC	DC
Block (1)										
Block (2)										
Block (3)	12	18	6	6	5	5	4		2	
Block (4)	118	167	52	52	73	73		4	2	
Block (5)	12	16			4	4				
Block (6)	3	3	3	3	2	2				
Block (7)(9)	20	20	3	3	12	12				
Block (8)	4	5	3	3	7	7	2	2		
Block (10)	9	15	3	3				6	2	
Block (11)	7	12	3	3			2	4	1	
Block (12)	3	5	1	1	1	1				
Block (13)	6	14	1	1	1		1	6	3	
Block (14)										
TOTAL	194	275	75	75	104	104	9	22	10	

Table 18. Single Rotor Tabulation

	AC		DC	
	No.	Wt.	No.	Wt.
Amplifier	194	194	275	550
Servo	75	525	75	525
Pot	104	26	104	26
S-C Pots	9	1 3/4	22	5 1/2
Resolver	10	5		
Complexity		751 3/4		1106 1/2

Table 19. Single Rotor Summary

Suppose that both AC and DC amplifiers both have weight one (1), then the DC complexity is 831-1/2 which is closer but still larger than the AC complexity. This difference (751-3/4 and 831-1/2) is primarily due to the increased number of DC amplifiers necessary to solve the mechanization problem. Consequently, unless DC amplifiers can be redesigned to be competitive in complexity with AC amplifiers or the choice for a DC system is based on reasons other than component complexity, the AC system is favored.

2. TANDEM ROTOR HELICOPTER. The mechanization of a tandem rotor helicopter simulation equations can be accomplished by again considering Figure 9 which is the block diagram of the single rotor helicopter. The difference in mechanization between single and tandem rotor helicopters is contained in Block (4) Figure 9--the aerodynamic terms. The aerodynamic terms for the single rotor helicopter were considered in three parts--tail rotor aerodynamics, fuselage aerodynamic and main rotor aerodynamics. For the mechanization of the tandem rotor the aerodynamic terms are in two parts--fuselage aerodynamics and rotor aerodynamics. In reference 1 it was shown that the rotor equations of motion of the tandem rotor helicopter could be developed by using a set of equations similar to the single rotor helicopter. The essence of this development in reference 1 is that equations describing the main rotor of the single rotor helicopter are used to describe the forward rotor of the tandem rotor helicopter. Rear rotor effects in the tandem rotor helicopter are mechanized by ratios of the swash plate angles of front and rear rotor. Only the front rotor is simulated. Since this is an overlap tandem rotor helicopter (CH-46A), effects of rotor interference are also mechanized.

In Section VI, equations 6.91 through 6.169 for a tandem rotor helicopter--the CH-46A are presented. These equations are directly analogous to equations 6-1 through 6-90 of the single rotor helicopter. Table 20 is a comparison of single and tandem rotor equations and associated figures used in the single rotor mechanization. Table 20

	Single Rotor Equation Nos.	Mechanized by Figure(s)	Comparable Tandem Rotor Equation Nos.	Mechanized by Figure(s)
Block (1)	N/A	N/A	N/A	N/A
Block (2)	N/A	N/A	N/A	N/A
Block (3)	6.1, 6.2, 6.6 6.82	10	6.91, 6.92, 6.95 6.161	10
Block (4)				
Tail Rotor	6.7 to 6.17, 6.26	11	None	N/A
Fuselage	6.4, 6.5, 6.33, 6.38, 6.41	12	6.94, 6.93, 6.108 6.112, 6.116	12
Aft Rotor	None	N/A	6.107, 6.111, 6.115, 6.126, 6.129, 6.132, 6.134, 6.143, 6.145	26, 27
Rotor	(Main) Rotor		(Front) Rotor	
Block (1)	6.45	14	6.119	14
Block (2)	6.44	15	6.118	15
Block (3)	6.46, 6.47, 6.48	16	6.120, 6.121, 6.122	16
Block (4)	6.49, 6.52	17	6.123, 6.127	17
Block (5)	6.58	18	6.136	18
Block (6)	6.50, 6.51, 6.54	19	6.124, 6.125, 6.130	19
Block (7)	6.53, 6.61, 6.62 6.63	20	6.128, 6.139, 6.140 6.141	20
Block (8)	6.59	21	6.137	21
Block (9)	6.64, 6.65	22	6.142, 6.144	22
Block (10)	6.55, 6.56, 6.83	23	6.131, 6.133, (6.162)	23 28
Block (5)	6.21, 6.22, 6.23 6.24, 6.25, 6.27 6.28, 6.29	24	6.99, 6.100, 6.97 6.101, 6.102 6.103, 6.104, 6.96	24

Table 20. Single Rotor - Tandem Rotor Comparison

	Single Rotor Equation Nos.	Mechanised by Figure(s)	Comparable Tandem Rotor Equation Nos.	Mechanised by Figure(s)
Block (6)	6.90	2	6.169	2
Block (7) and (9)	6.30, 6.31, 6.32 6.34, 6.36, 6.37 6.39, 6.40, 6.42 6.43, 6.79, 6.80 6.81	25	6.105, 6.106, 6.108 6.109, 6.110 6.113, 6.117 6.158, 6.159, 6.160	25
Block (8)	6.67, 6.68, 6.69	3	6.146, 6.147, 6.148	3
Block (10)	6.70, 6.71, 6.72 6.84, 6.85, 6.86	4	6.149, 6.150, 6.151 6.163, 6.164, 6.165	4
Block (11)	6.87, 6.88, 6.89	5	6.166, 6.167, 6.168	5
Block 12h and 13h	6.73, 6.74, 6.75 6.76, 6.77, 6.78	7	6.152, 6.153, 6.154 6.155, 6.156, 6.157	7
Block (14)	N/A	N/A	N/A	N/A

Table 20. Single Rotor - Tandem Rotor Comparison (Cont'd.)

thus enables the identification of figures used in the single rotor mechanization with tandem rotor equations and a consequent count of electronic components. Note that the particular inputs to some of the amplifiers may increase or decrease in the tandem rotor helicopter as compared to the single rotor but the components associated with the figures listed in Table 20 will be the same.

In order to describe the aft rotor, a few additional equations are necessary. The additional equations needed are 6.107, 6.111, 6.115, 6.126, 6.129, 6.132, 6.134, 6.143 and 6.145. Before mechanising these equations, the aft rotor swash plate angles will be mechanised.

The swash plate angles and SAS mechanization considered for the tandem helicopter simulation is an addition to the rotor aerodynamics of the single rotor device. In this mechanisation the swash plate angles are developed in order that aft rotor terms are written as functions of forward rotor terms. Figure 26 is the mechanisation of these functions. The DC mechanisation would require three additional amplifiers by virtue of the requirement of three functions of both polarities. Servo integrators are used to obtain the delta swash plate functions. A DC mechanization using electronic integrators would require follower position servos.

Figure 27 shows the AC mechanisation of the aft rotor equations. There are 12 amplifiers and 4 potentiometers used in the AC mechanisation plus functions not specified as to equipment. The DC mechanisation would require 15 amplifiers and 4 potentiometers plus the functions. The additional amplifiers in the DC mechanisations are due to polarity of functions.

One further area is of interest in the tandem rotor simulation--angular velocity. The mechanisation of the dual rotor angular velocity computation is shown in Figure 28. In comparison to the single rotor angular velocity mechanization, Figure 23, it is seen that Ω is computed essentially the same way as in Figure 23 but there are now two rotor torque terms. One is the torque contributed by the forward rotor. The other term is the torque contributed by the aft rotor.

Table 21 is a summary of the components necessary to mechanise the tandem rotor helicopter <u>in addition</u> to those necessary for the single rotor helicopter less tail rotor as reflected in Figures 26, 27 and 28. The numbers under function generation in Table 21 would actually be mechanized by potentiometers. It is assumed that where functions (f) are used in the mechanization drawings, the mechanisation can be accomplished by the same amount of equipment--AC or DC.

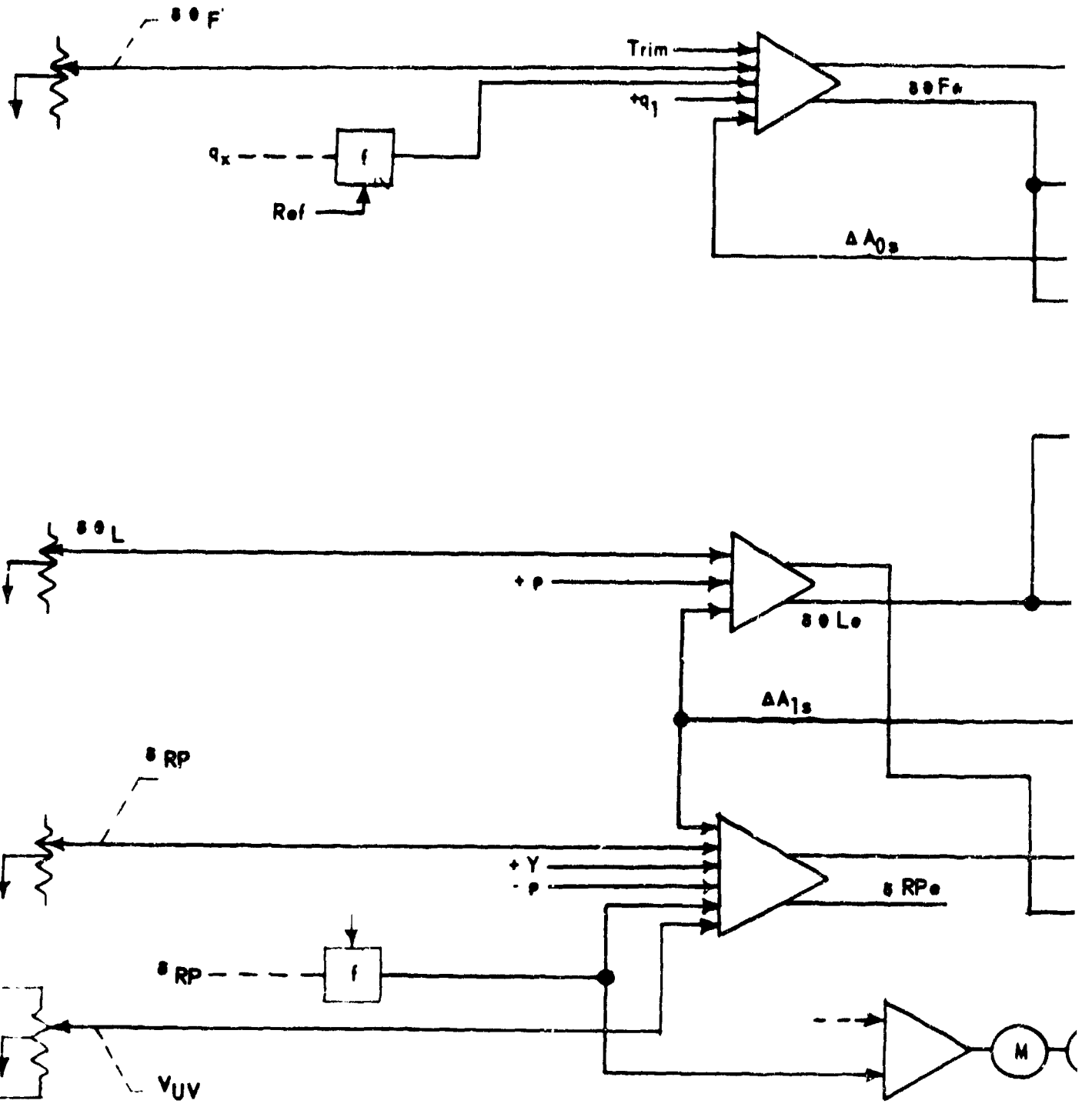
δ F
Trim
+q1
δ Fe
qx
f
Ref
Δ A0s
δ L
+ p
δ Le
Δ A1s
δ RP
+ Y
- P
δ RPe
δ RP
f
+ U
- U
VUV
M

A

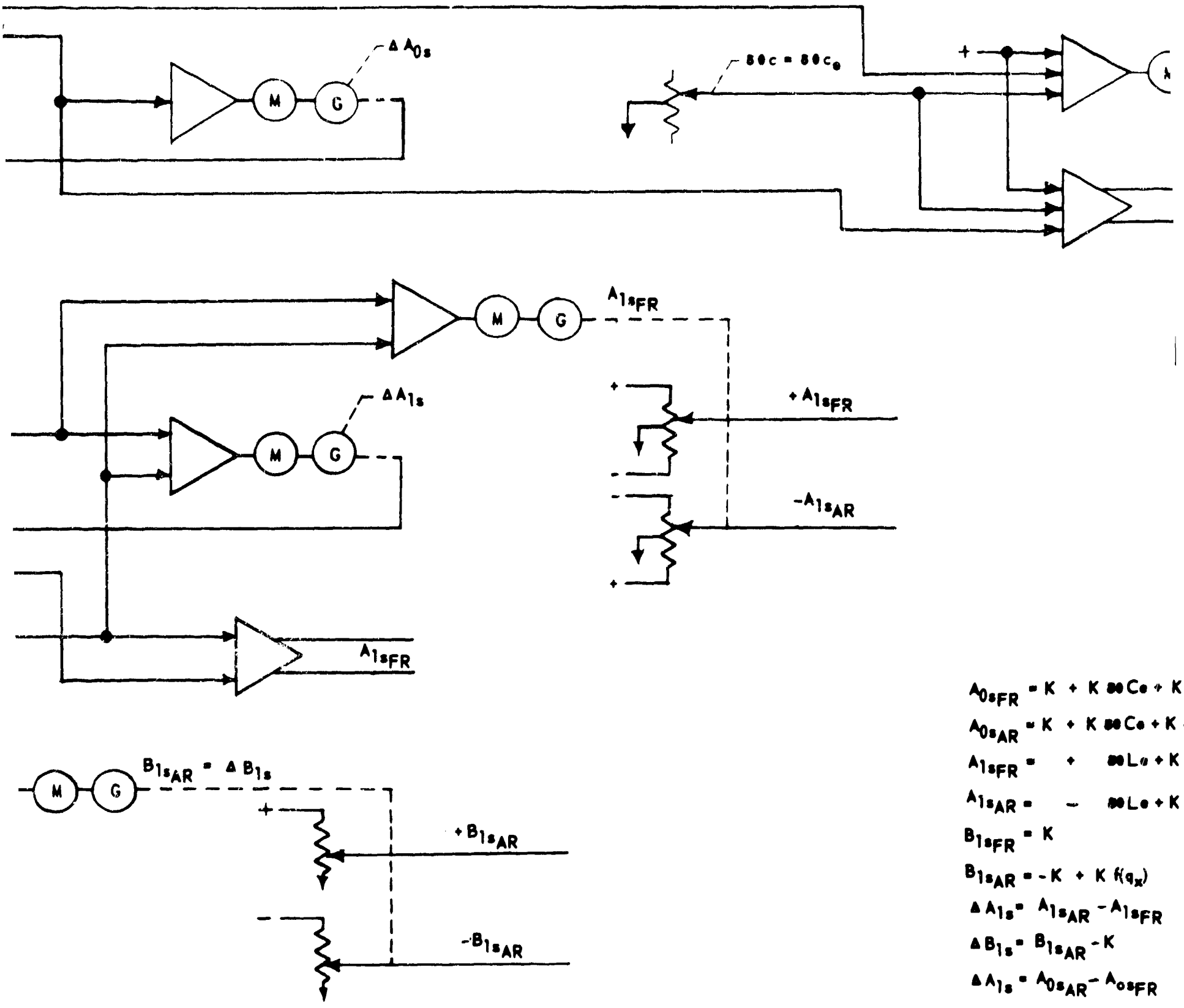

$A_{0s_{FR}} = K + K\,80C_0 + K$

$A_{0s_{AR}} = K + K\,80C_0 + K$

$A_{1s_{FR}} = + \quad 80L_0 + K$

$A_{1s_{AR}} = - \quad 80L_0 + K$

$B_{1s_{FR}} = K$

$B_{1s_{AR}} = -K + K\,f(q_x)$

$\Delta A_{1s} = A_{1s_{AR}} - A_{1s_{FR}}$

$\Delta B_{1s} = B_{1s_{AR}} - K$

$\Delta A_{1s} = A_{0s_{AR}} - A_{os_{FR}}$

Figure 26.

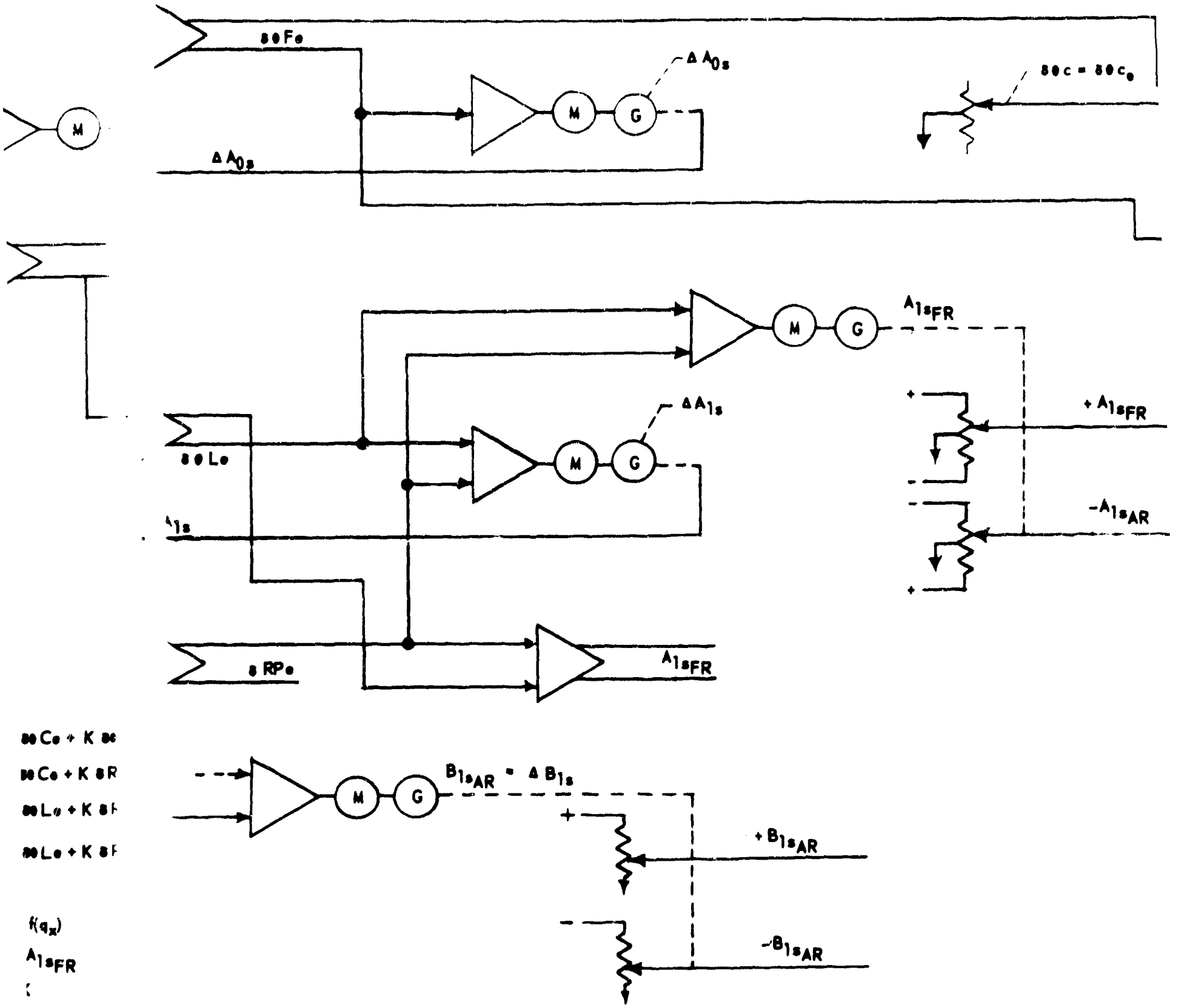

δCo + K δ

δCo + K δR

δLo + K δF

δLo + K δF

f(qx)

A1sFR

A0sFR

ire 26. S

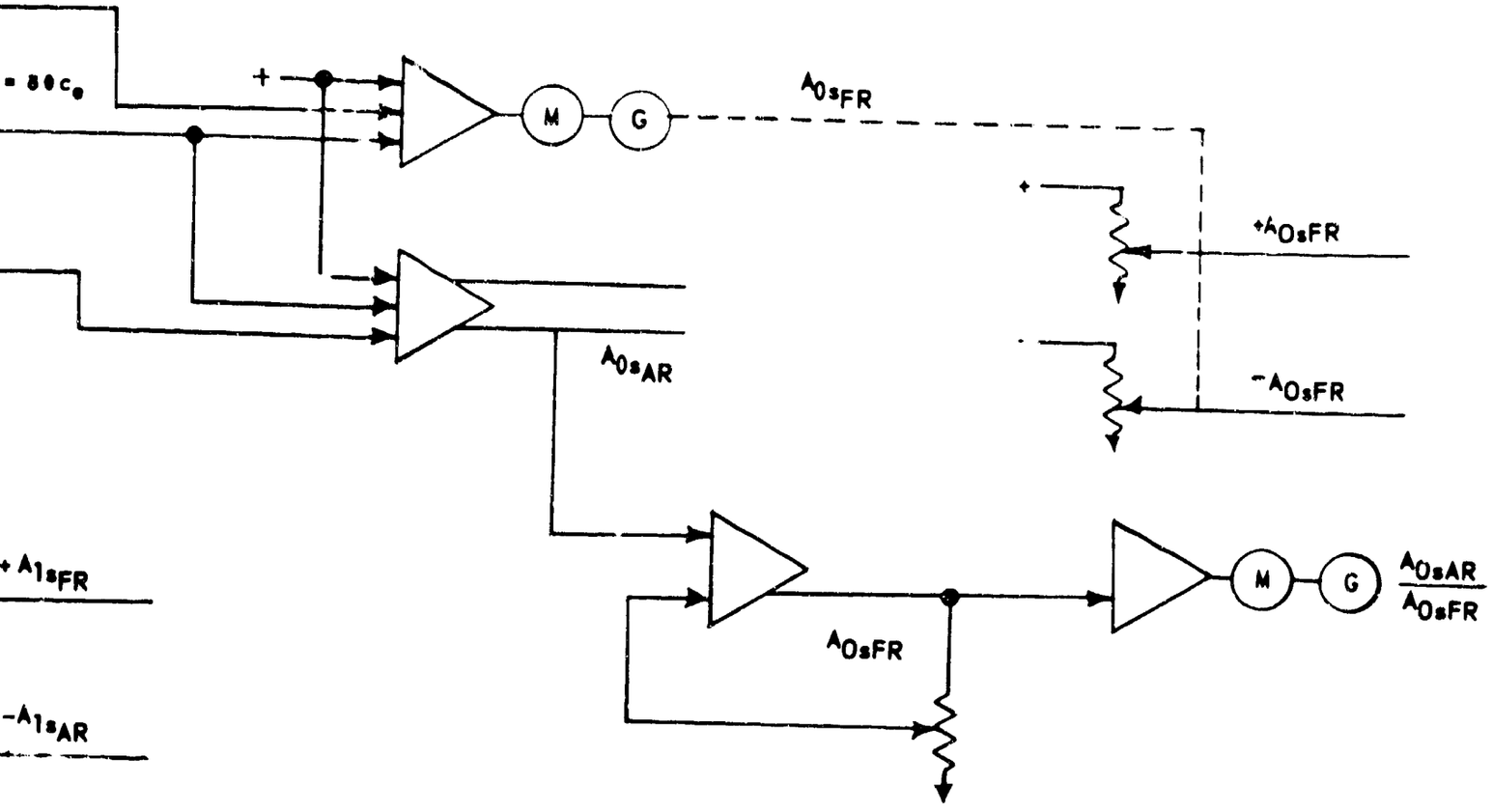

$$A_{0s_{FR}} = K + K\,\theta_0 C_\theta + K\,\theta_0 F_\theta$$

$$A_{0s_{AR}} = K + K\,\theta_0 C_\theta + K\,sRP_\theta$$

$$A_{1s_{FR}} = + \theta_0 L_\theta + K\,sRP_\theta$$

$$A_{1s_{AR}} = - \theta_0 L_\theta + K\,sRP_\theta$$

$$B_{1s_{FR}} = K$$

$$B_{1s_{AR}} = -K + K\,f(q_x)$$

$$\Delta A_{1s} = A_{1s_{AR}} - A_{1s_{FR}}$$

$$\Delta B_{1s} = B_{1s_{AR}} - K$$

$$\Delta A_{1s} = A_{0s_{AR}} - A_{os_{FR}}$$

$$\Delta A_{0s} = K\left[(\theta_0 F + KDCP_{TRIM} + Kf(q_x) + Kq_1 + \Delta A_{0s}\right]$$

$$\Delta A_{1s} = -K\,\theta_0 L_\theta - K\,\theta_0 RP_\theta$$

$$\Delta B_{1s} = K + K\,f(q_x)$$

B

Figure 26. Swash Plate Angles & S.A.S. for Tandem Rotor Helicopter

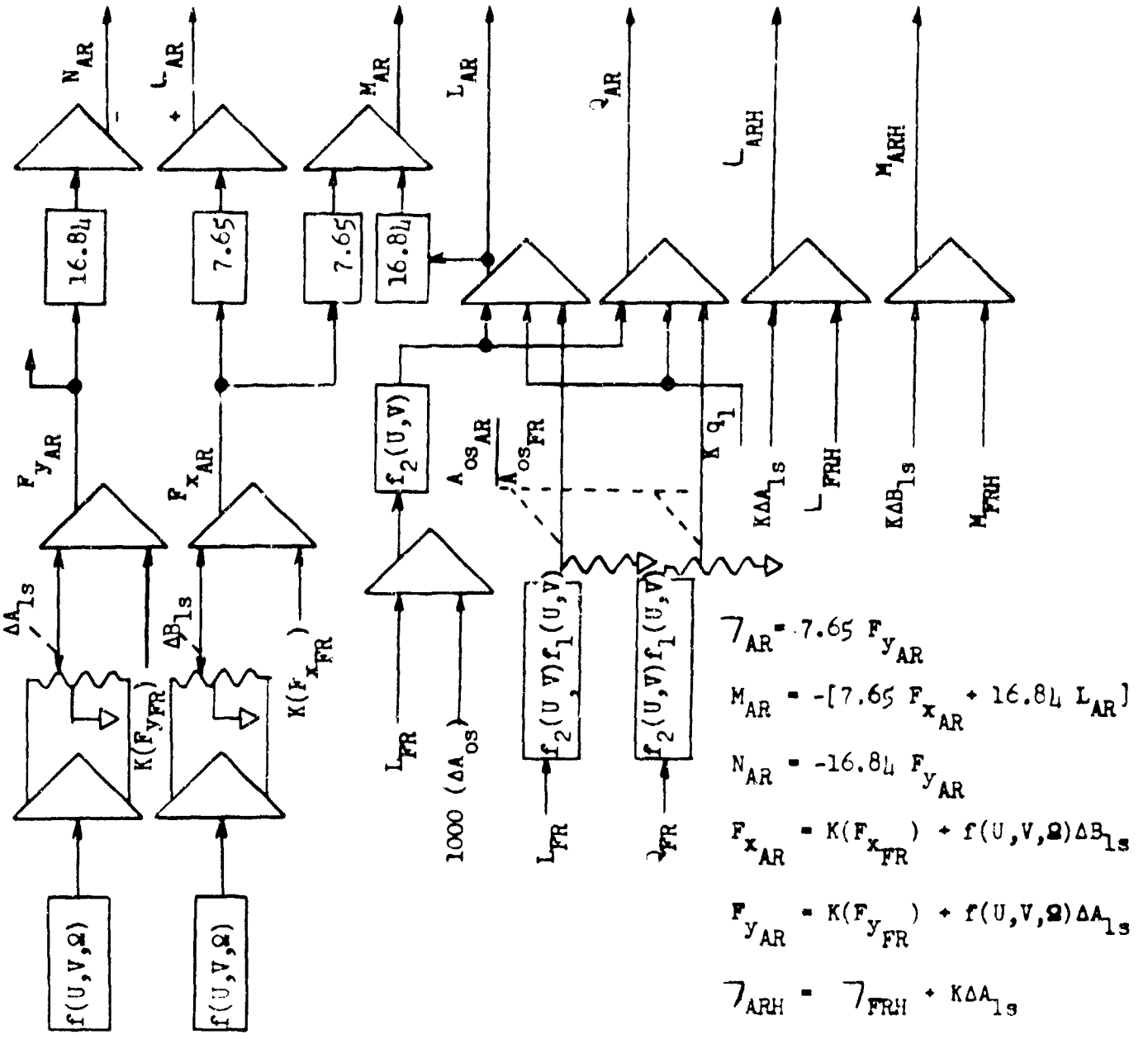

$$Q_{AR} = 7.65\ F_{y_{AR}}$$

$$M_{AR} = -[7.65\ F_{x_{AR}} + 16.84\ L_{AR}]$$

$$N_{AR} = -16.84\ F_{y_{AR}}$$

$$F_{x_{AR}} = K(F_{x_{FR}}) + f(U,V,\Omega)\Delta B_{1s}$$

$$F_{y_{AR}} = K(F_{y_{FR}}) + f(U,V,\Omega)\Delta A_{1s}$$

$$Q_{ARH} = Q_{FRH} + K\Delta A_{1s}$$

$$M_{ARH} = M_{FRH} + K\Delta B_{1s}$$

$$Q_{AR} = \left[f(U,V)\frac{A_{os_{AR}}}{A_{os_{FR}}} Q_{FR}\right]f_1(U,V) + [L_{FR} + 1000\ (\Delta A_{os})]f_2(U,V) + Kq_1$$

$$L_{AR} = \left[f(U,V)\frac{A_{os_{AR}}}{A_{os_{FR}}} L_{FR}\right]f_1(U,V) + [L_{FR} + 1000\ (\Delta A_{os})]f_2(U,V) + Kq_1$$

Figure 27. Aft Rotor Terms, Tandem Rotor Helicopter AC Mechanization

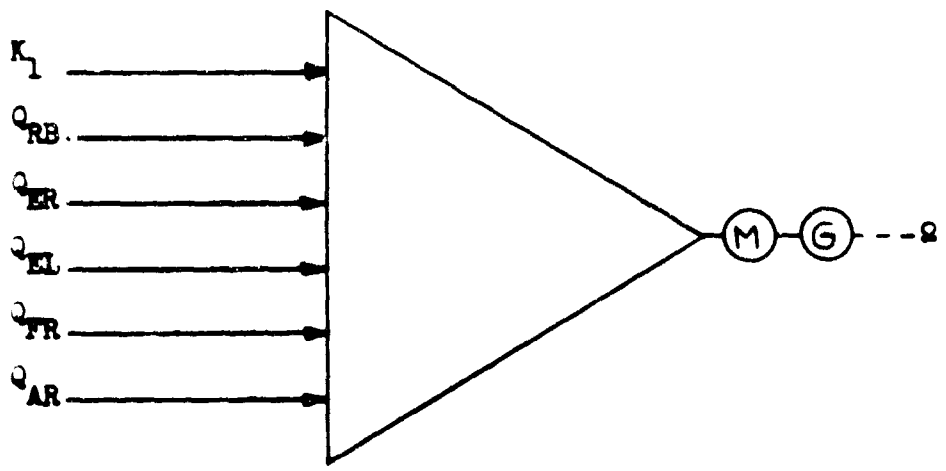

$$\dot{\Omega} = \frac{Q_{FR} + Q_{AR} + Q_{ER} + Q_{EL} + Q_{RB} + K_1}{I_{TOT}}$$

$$I_{TOT} = I_{FR} + I_{AR}$$

Figure 28. Tandem Rotor Angular Velocities
AC Mechanization

	AC		DC	
Component	No.	Wt.	No.	Wt.
Amplifier	25	25	31	62
Servo	5	35	5	35
Pots	16	4	16	4
Function (f) Generation	9	--	9	--
Complexity		64		101

Table 21. Additional Components Tandem Rotor Helicopter

This completes the mechanization of the tandem rotor helicopter.

Summary Tandem Rotor Helicopter. The tandem rotor mechanization has been developed in terms of the single rotor mechanization (Section III.B.). The arguments presented in the single rotor summary (Section III.B.) are equally valid for the tandem rotor helicopter. Table 22 is a summary of tandem rotor component complexity. This table is constructed by taking the component totals of the single rotor helicopter (Table 19) and then subtracting out components due to the mechanization of the tail rotor in the single rotor helicopter (Table 7) and then adding the additional components due to tandem rotor mechanization (Table 21). The AC system for the tandem rotor helicopter has a complexity of 744-3/4 versus 1105-1/2 for the DC system. This is practically the same as the complexity for the single rotor helicopter AC system--751-3/4, DC system--1106-1/2. Consequently, using the same rationale as in Section III.B., the AC system is favored for the tandem rotor helicopter.

C. V/STOL MECHANIZATION

Mechanization for the tilt wing aircraft, the XC-142A, of Ling-Temco-Vought, Hiller, Ryan is considered in this portion of the report. In reference 2 the equations of motion for the tilt-wing were developed and the necessary equations for mechanization of the tilt-wing are reproduced in Section VI. It should be noted that equations of motion were developed for four other V/STOL configurations in reference 2: the tilt-duct represented by the DOAK VZ-4A, the tilt-propeller represented by the Curtiss Wright X-19, the fan-in-wing represented by the General Electric/Ryan XV-5A and the rotating thrust represented by the Hawker Aircraft P.1127. Mechanization of the tilt-duct and tilt-propeller equations of motion would be similar to the tilt-wing mechanization. Mechanization of the fan-in-wing and rotating thrust equations of motion would be similar to mechanizations of ordinary jet aircraft taking into account variations in the thrust components. By accounting for these thrust variations in the equations of motion, existing mechanizations for jet aircraft such as those presented in reference 3 are valid for the fan-in-wing and rotating thrust. The mechanization for the tilt-

		AMPLIFIER				SERVO				POT				S-C POT				RESOLVER				TOTAL WEIGHT	
		AC		DC		AC		DC		AC		DC		AC		DC		AC		DC		AC	DC
		NO	WT	NO	WT	NO	WT	NO	WT	NO	WT	NO	WT	NO	WT	NO	WT	NO	WT	NO	WT	WT	WT
Single Rotor Helicopter (Table 18)		194	194	275	550	75	525	75	525	26	104		26	9	$13\frac{3}{4}$	22	$52\frac{1}{2}$	10	5			$751\frac{3}{4}$	$1106\frac{1}{2}$
Minus Tail Rotor Contributions (Table 7)		-19	-19	-25	-50	-7	-19	-7	-19	-2	-8		-2			-4	-1	-2	-1			-71	-102
Plus Additions From Table 21		26	26	31	62	5	35	5	35	4	19		4									69	101
Tandem Rotor Complexity			201		562		511		511		28		28		$13\frac{3}{4}$		$1\frac{1}{2}$		4			$744\frac{3}{4}$	$1105\frac{1}{2}$

Table 22. Tandem Rotor Summary

wing may not be optimum since the mechanization reflects the equations of motion which could change as data from the manufacturer become available about the particular aircraft. Mechanization of the tilt-wing presented here is based upon the best information available at the time of this report.

References are made to the appropriate tilt-wing equations in Section VI in some of the mechanizations drawings where the equations are lengthy. On other drawings the equations are written explicitly.

1. SIMILARITY OF V/STOL EQUATIONS. Before developing the tilt-wing mechanization in detail consider the similarity of the tilt-duct and tilt-prop equations to the tilt-wing equations and the likeness of the fan-in-wing and rotating thrust equations to existing equations of motion for jet aircraft. In these comparisons which follow only the X-force equations will be compared, the Y-force and Z-force equations contain like similarities.

First consider the tilt-wing, tilt-duct and tilt-prop. X-force equations from Reference 2.

X-Force Equation: Tilt-Wing (XC-142A)

$$m(\dot{U} + W_{q_1} - Vr) + mg \sin\theta \tag{3-1}$$

$$= (C_x)_w Sq_w f(C_{T,S}) + \sum_{n=1}^{4} (T_n \cos i_w - N_n \cos\beta_n \sin i_w)$$

$$- [C_{D_t} \cos(i_t - \alpha_t) + C_{L_t} \sin(i_t - \alpha_t)] Sq(\frac{q_{hs}}{q}) - Sq\, C_{D_o}$$

X-Force Equation: Tilt-Duct (VZ-4A)

$$m(\dot{U} + Wq_1 - Vr) + mg \sin\theta \tag{3-2}$$

$$= (C_x)_w Sq_w + q_E S_v (C_x)_{RC} + K_2 \sum_{j=1}^{2} (\bar{C}_{T_j} \cos i_D - \bar{C}_{N_j} \sin i_D) + T_r$$

$$- [C_{D_t} \cos(i_t - \alpha_t) - C_{L_t} \sin(i_t - \alpha_t)] Sq(\frac{q_{hs}}{q}) - Sq\, C_{D_o}$$

X-Force Equation: Tilt-Prop (X-19)

$$m(\dot{U} + W_{q_1} - Vr) + mg \sin\theta \tag{3-3}$$

$$= (C_x)_{wf} Sq_{wf} + \sum_{n=1}^{4} (T_n \cos i_p - N_n \cos\beta_n \sin i_p) + (C_x)_{wa} Sq_{wa} - Sq\, C_{D_o}$$

Comparing equations (3-2) and (3-3) to (3-1) the only differences are the terms $q_E S_v (C_x)_{RC} + K_2 \sum_{j=1}^{2} (\bar{C}_{T_j} \cos i_D - C_{N_j} \sin i_D) + T_r$ in (3-2) and $(C_x)_{wa} Sq_{wa}$ in (3-3). $q_E S_v (C_x)_{RC}$ and T_r are due to the reaction controls in the tilt duct aircraft. The term $K_2 \sum_{j=1}^{2} (\bar{C}_{T_j} \cos i_D - \bar{C}_{N_j} \sin i_D)$ is thrust expression for the duct fans in coefficient form.

To further illustrate the similarities of the force equations (3-1, 3-2, and 3-3) suppose that the incident angles (i_w, i_p and i_D) are zero. Then there results:

$$m(\dot{U} + Wq_1 - Vr) + mg \sin \theta \tag{3-1a}$$

$$= (C_x)_w Sq_w + \sum_{n=1}^{4} T_n - [C_{D_t} \cos(i_t - \alpha_t) + C_{L_t} \sin(i_t - \alpha_t)] Sq(\frac{q_{hs}}{q}) - Sq\, C_{D_o}$$

$$m(\dot{U} + Wq_1 - Vr) + mg \sin \theta \tag{3-2a}$$

$$= (C_x)_w Sq_w + q_E S_v (C_x)_{RC} + K_2 \sum_{j=1}^{2} \bar{C}_{T_j} + T_r$$

$$- [C_{D_t} \cos (i_t - \alpha_t) + C_{L_t} \sin (i_t - \alpha_t)] Sq(\frac{q_{hs}}{q}) - Sq\, C_{D_o}$$

$$m(\dot{U} + Wq_1 - Vr) + mg \sin \theta \tag{3-3a}$$

$$= (C_x)_{wf} Sq_{wf} + \sum_{n=1}^{4} T_n + (C_x)_{wa} Sq_{wa} - Sq\, C_{D_o}$$

Equations (3-1a), (3-2a) and (3-3a) are very similar. Mechanisation of the tilt-wing equation (3-1) will therefore demonstrate the simulation technique. The Y and Z force equations for the tilt-wing, tilt-duct and tilt-prop have the same degree of likeness as the X-force equations.

Next, let us compare the fan-in-wing and rotating thrust X-force equations from Reference 2 to simulation equations used for jet aircraft.

Fan-In-Wing: X-Force Equation

$$m(\dot{U} + Wq_1 - Vr) = qS[C_x(\alpha, Ma) + C_x(\beta) + C_{x_{\delta F}} \cdot \delta F] \tag{3-4}$$

$$+ T_j \cos \alpha_T + T_F \sin \theta_L - mg \sin \theta$$

Rotating Thrust: X-Force Equation

$$m(\dot{U} + Wq_1 - Vr) = qS[C_{x_U} + C_{x_\alpha} + C_{x_{\delta F}} \cdot \delta F + C_x(\beta)] \quad (3.5)$$

$$+ T \cos(\theta_j + \alpha_T) - mg \sin\theta$$

Ordinary Simulation: X-Force Equation

$$m(\dot{U} + Wq_1 - Vr) = qS[C_x(\alpha, Ma) + C_x(\beta) + C_{x_{\delta F}} \cdot \delta F] \quad (3.6)$$

$$+ T \cos\alpha_T - mg \sin\theta$$

The only difference among equations (3.4), (3.5) and (3.6) is in the thrust terms. Using equation (3.6) as a guide consider (3.4) and (3.5). Equation (3.5) has as a thrust term T cos $(\theta_j + \alpha_T)$. θ_j is the rotation of thrust producers. If the aircraft is in normal flight ($\theta = 0$) and T cos $(\theta_j + \alpha_T)$ = T cos α_T which is the same as equation (3.6).

The thrust term in equation (3.4) is $T_j \cos\alpha_T + T_F \sin\theta_L$. If the fan-in-wing is in normal flight $\theta_L = 0$ and consequently equation (3.4) is the same as equation (3.6). The only added term is $T_F \sin\theta_L$ in equation (3.4) and is of small consequence, though necessary, from the mechanization viewpoint.

Similar arguments can be applied for the Y-force, Z-force and moment equations.

2. TILT-WING MECHANIZATION. Figure 29 is a block diagram for the tilt-wing aircraft similar to Figure 1. Each mechanization drawing refers to the appropriate equations in Section VI. As per the helicopter mechanization, each block in Figure 29 will be considered. A component count will be done in the summary indicating differences in AC and DC mechanization.

Block (1) Pilot Control. Block (1) of Figure 29 contains outputs due to control of the pilot.

Block (2) Engine Simulation. Block (2) of Figure 29 is not simulated.

Block (3) Aero Variables. The AC mechanization of Block (3), Figure 29 is shown in Figure 30 in order to give outputs α_F, β_F, q, ρ and V_B. This mechanization is similar to that shown in Figure 10 for the single rotor helicopter.

2
FRAMES

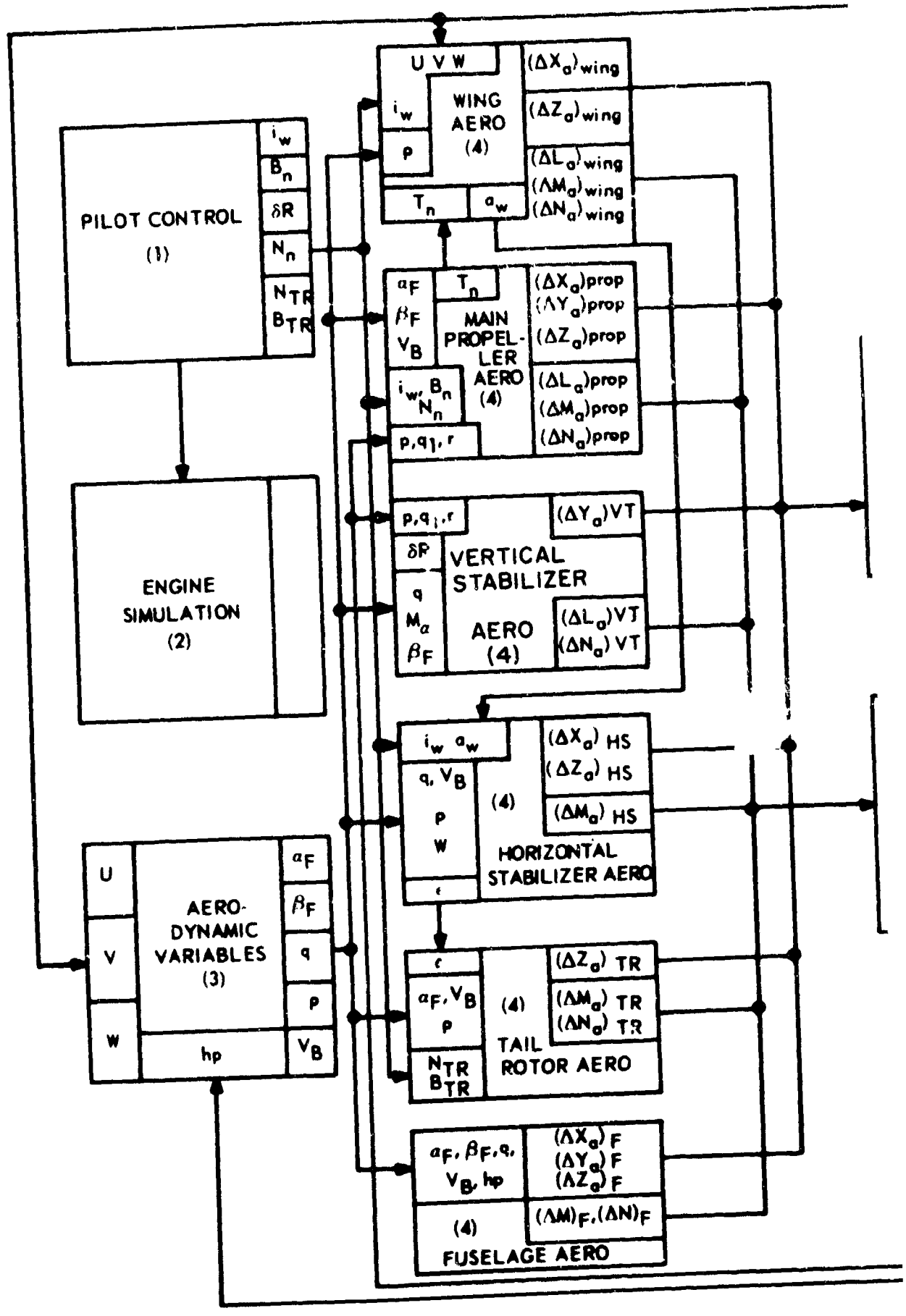
PILOT CONTROL
(1)
i_w
B_n
δR
N_n
N_{TR}
B_{TR}
ENGINE
SIMULATION
(2)
U
V
W
AERO-
DYNAMIC
VARIABLES
(3)
α_F
β_F
q
p
V_B
hp
U V W
i_w
p
WING
AERO
(4)
T_n
a_w
$(\Delta X_a)_{wing}$
$(\Delta Z_a)_{wing}$
$(\Delta L_a)_{wing}$
$(\Delta M_a)_{wing}$
$(\Delta N_a)_{wing}$
α_F
β_F
V_B
T_n
MAIN
PROPEL-
LER
AERO
(4)
i_w, B_n
N_n
p, q, r
$(\Delta X_a)_{prop}$
$(\Delta Y_a)_{prop}$
$(\Delta Z_a)_{prop}$
$(\Delta L_a)_{prop}$
$(\Delta M_a)_{prop}$
$(\Delta N_a)_{prop}$
p, q, r
δR
q
M_α
β_F
VERTICAL
STABILIZER
AERO
(4)
$(\Delta Y_a)VT$
$(\Delta L_a)VT$
$(\Delta N_a)VT$
i_w a_w
q, V_B
p
w
ϵ
(4)
HORIZONTAL
STABILIZER AERO
(ΔX_a) HS
(ΔZ_a) HS
(ΔM_a) HS
ϵ
α_F, V_B
p
N_{TR}
B_{TR}
(4)
TAIL
ROTOR AERO
(ΔZ_a) TR
(ΔM_a) TR
(ΔN_a) TR
$\alpha_F, \beta_F, q,$
V_B, hp
(4)
FUSELAGE AERO
$(\Delta X_a)_F$
$(\Delta Y_a)_F$
$(\Delta Z_a)_F$
$(\Delta M)_F, (\Delta N)_F$

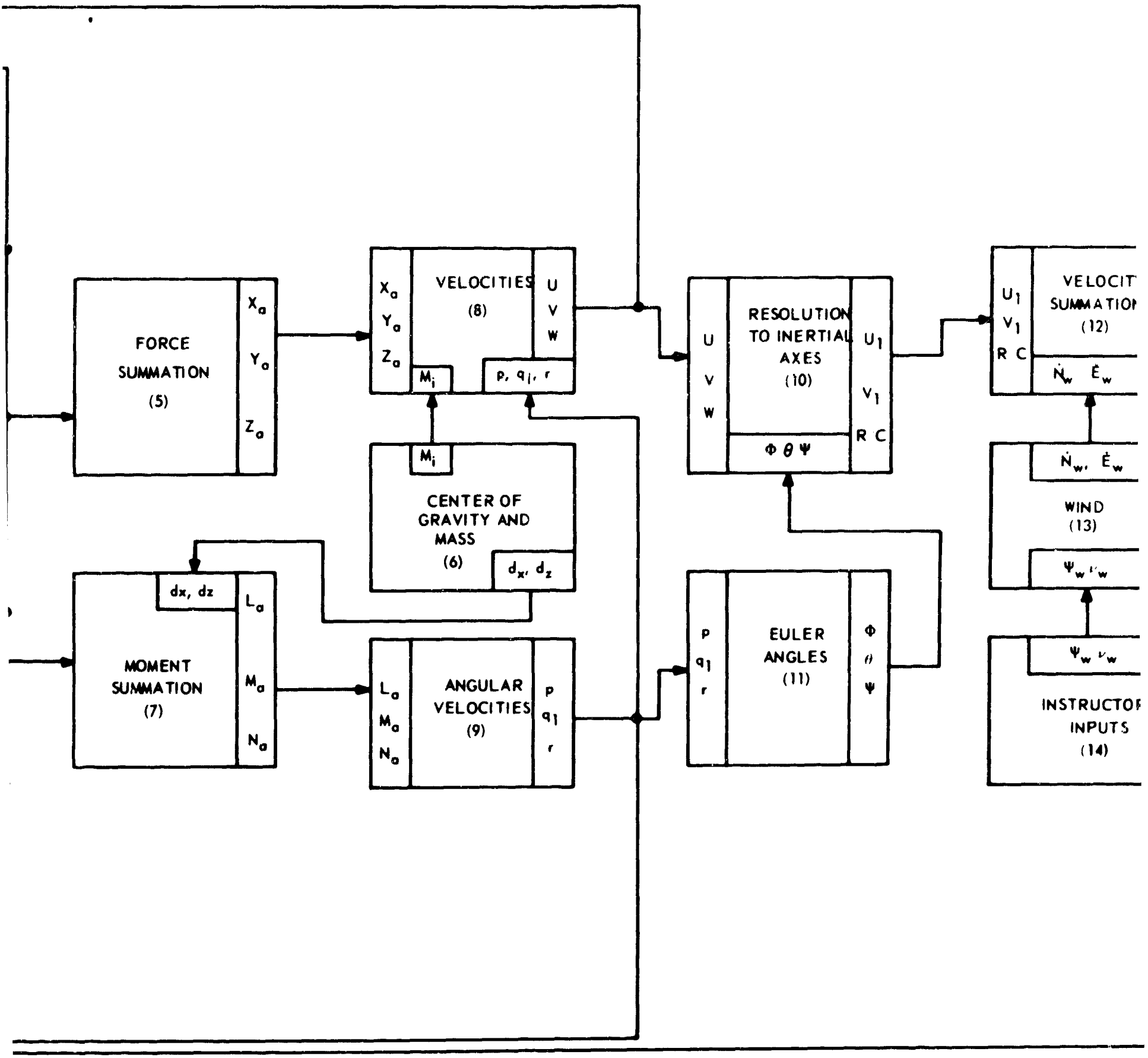

Figure 29. Simplified Block Diagram V STOL (Tilt-Wing) Aircraft

VELOCITY SUMMATION (12)

$\dot{N}_w$ $\dot{E}_w$

$\dot{N}_w$, $\dot{E}_w$

WIND (13)

Ψ_w ν_w

Ψ_w ν_w

STRUCTOR INPUTS (14)

PILOT CONTROL (1)

i_w
B_n
δR
N_n
N_{TR}
B_{TR}

ENGINE SIMULATION (2)

U V W
i_w
p
WING AERO (4)
T_n a_w

$(\Delta X_a)_{wing}$
$(\Delta Z_a)_{wing}$
$(\Delta L_a)_{wing}$
$(\Delta M_a)_{wing}$
$(\Delta N_a)_{wing}$

α_F
β_F
V_B
T_n
MAIN PROPELLER AERO (4)
i_w B_n N_n
p, q, r

$(\Delta X_a)_{prop}$
$(\Delta Y_a)_{prop}$
$(\Delta Z_a)_{prop}$
$(\Delta L_a)_{prop}$
$(\Delta M_a)_{prop}$
$(\Delta N_a)_{prop}$

p, q, r
δR
q
M_α
β_F
VERTICAL STABILIZER AERO (4)

$(\Delta Y_a)VT$
$(\Delta L_a)VT$
$(\Delta N_a)VT$

i_w a_w
q, V_B
p
w
HORIZONTAL STABILIZER AERO (4)
i

(ΔX_a) HS
(ΔZ_a) HS
(ΔM_a) HS

i
α_F, V_B
p
TAIL ROTOR AERO (4)
N_{TR} B_{TR}

(ΔZ_a) TR
(ΔM_a) TR
(ΔN_a) TR

α_F, β_F, q, V_B, hp
FUSELAGE AERO (4)

$(\Delta X_a)_F$
$(\Delta Y_a)_F$
$(\Delta Z_a)_F$
$(\Delta M)_F$, $(\Delta N)_F$

U
V
W
AERO-DYNAMIC VARIABLES (3)
hp

α_F
β_F
q
p
V_B

FORCE SUMMATION (5)

X_a
Y_a
Z_a

dx, dz
MOMENT SUMMATION (7)

L_a
M_a
N_a

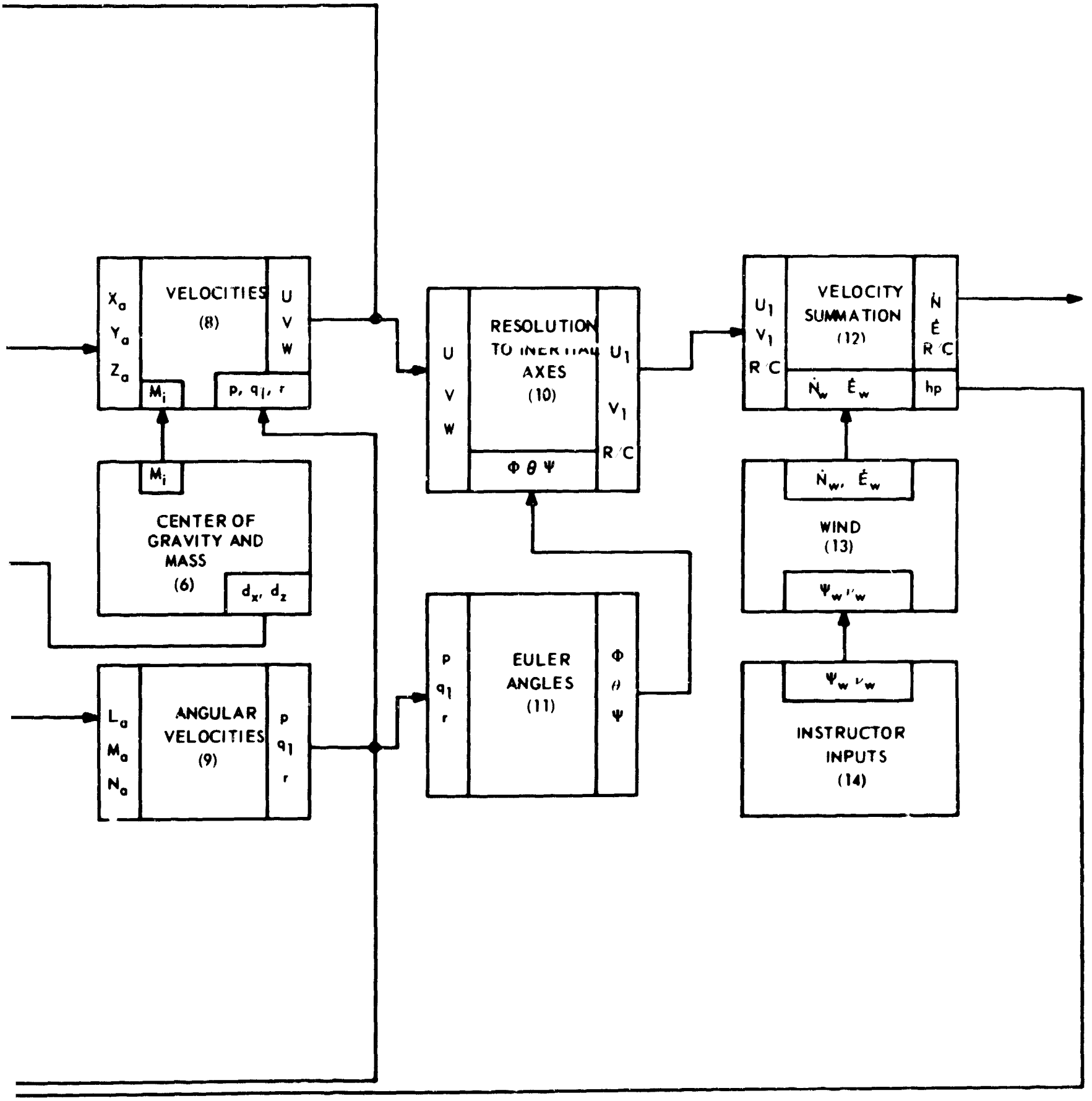

Figure 29. Simplified Block Diagram V STOL (Tilt-Wing) Aircraft

B

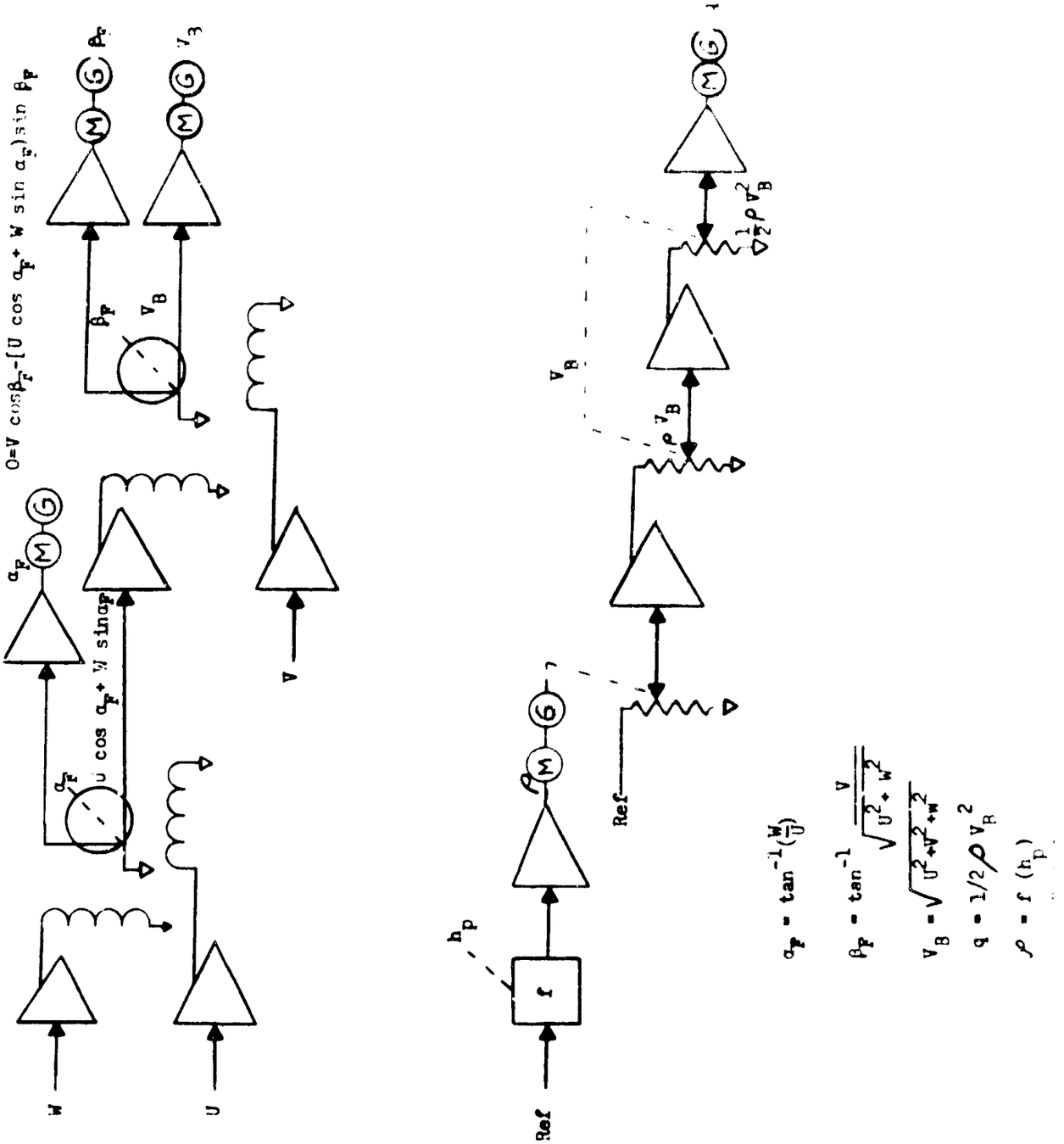

Figure 30. Aerodynamic Variables
AC Mechanization

Block (4) Aero Terms. The AC mechanization of Block (4), Figure 29 is divided into the following six parts:

1. Main Propeller Aerodynamics. Figures 31 through 41 mechanize the equations having to do with propeller aerodynamics. Figure 31 develops velocities associated with each propeller. Figure 32 develops the advance ratio associated with each propeller. Figures 33 and 34 show coefficients used in propeller aerodynamics developed as functions of advance ratio and propeller blade pitch. Figure 35 is the mechanization of each propeller thrust (T_n) and torque (Q_n). Figure 36 is the mechanization of the normal component of thrust (N_n) and propeller moments (Y_n and M_n). Figure 37 resolves M_n and Y_n into appropriate components due to wing tilt (i_w) and orientation of N_n by the angle β_n. Figure 38 is the mechanization of the force components $((\Delta X_a)_p$, $(\Delta Y_a)_p$, $(\Delta Z_a)_p)$due to propeller effects. Finally, Figures 39, 40 and 41 are the mechanization of the respective moment components $((\Delta L_a)_p$, $(\Delta M_a)_p$, $(\Delta N_a)_p)$ due to propeller effects. Equations 6.175 through 6.197 represent propeller aerodynamic effects.

2. Wing Aerodynamics. Figures 42 through 45 mechanize the equations representing wing aerodynamics. Figure 42 shows AC mechanization of wing velocity components, wing angle of attack (α_w), wing sideslip (β_w) and total velocity of the wing (V_w). Figures 43 and 44 show formation of aerodynamics coefficients. Finally, Figure 45 is resulting wing force and moment contributions. Equations 6.198 through 6.221 represent wing aerodynamic effects.

3. Vertical Stabilizer Aerodynamics. Figure 46 shows the AC mechanization of equations 6.222 to 6.227 for the force and moment contributions due to the vertical stabilizer.

4. Horizontal Stabilizer Aerodynamics. Figure 47 shows the AC mechanization of equations 6.228 to 6.233 for the force and moment contributions due to the horizontal stabilizer.

5. Tail Rotor Aerodynamics. Figure 48 shows the AC mechanization of equations 6.234 to 6.246 for the force and moment contributions due to the tail rotor.

6. Fuselage Aerodynamics. Figure 49 shows the AC mechanization of equations 6.247 to 6.251 for the force and moment contributions due to the effects of the fuselage.

Blocks (5) through (14). These blocks of Figure 29 are similar to the same numbered blocks for the single and tandem rotor helicopter.

Block (5), Figure 29 mechanized by Figure 50.

Block (6), Figure 29 mechanized as in Section III.A.

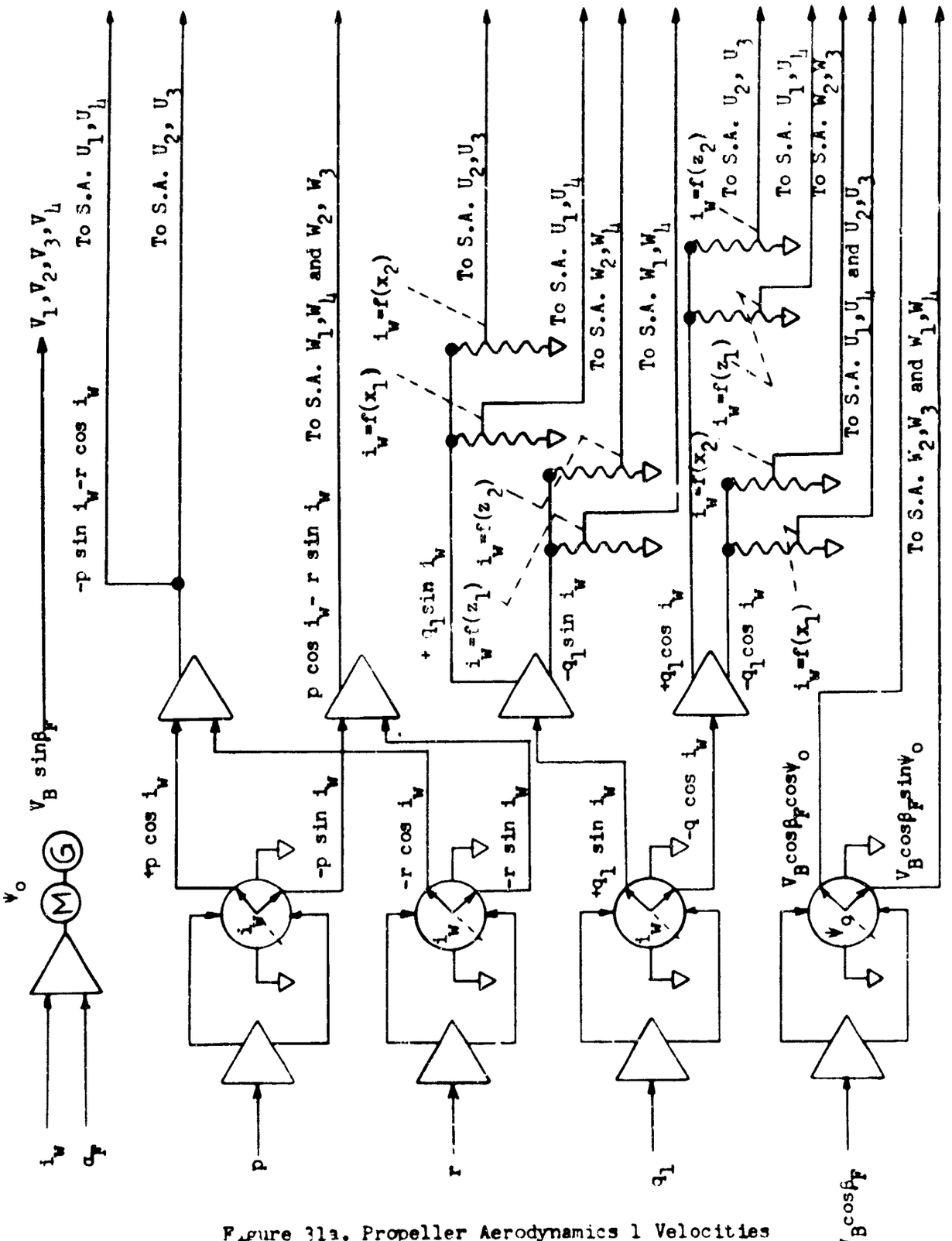

Figure 31a. Propeller Aerodynamics 1 Velocities
AC Mechanization

$$\psi_o = (i_w + \alpha_F)$$

$$U_n = V_B \cos\beta_F \cos\psi_o - y_n(p \sin i_w + r \cos i_w) + x_n q_1 \sin i_w + z_n q_1 \cos i_w$$

$$V_n = V_B \sin\beta_F$$

$$W_n = V_B \cos\beta_F \sin\psi_o + y_n(p \cos i_w - r \sin i_w) - x_n q_1 \cos i_w + z_n q_1 \sin i_w$$

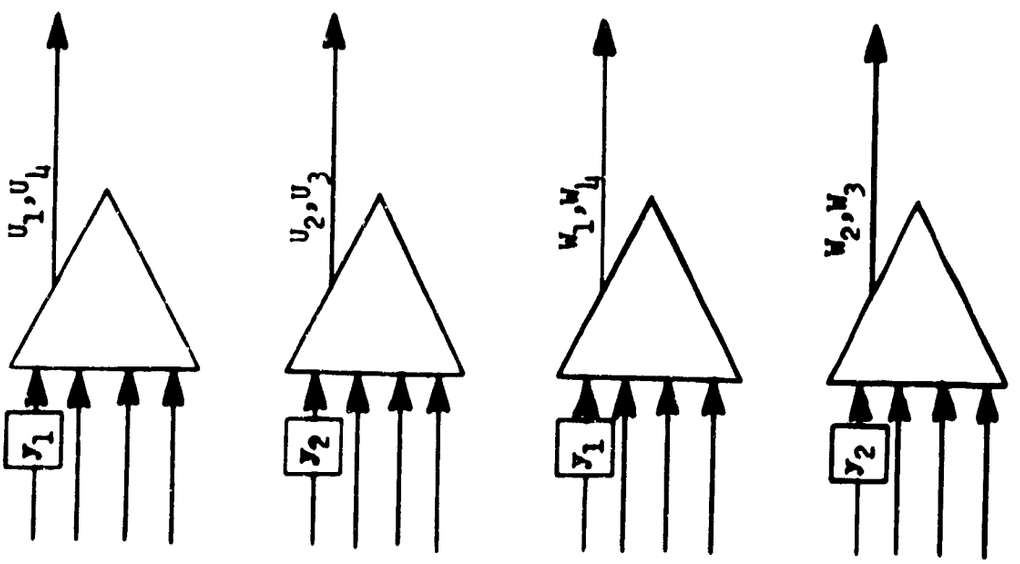

Figure 31b. Propeller Aerodynamics Velocities
AC Mechanization

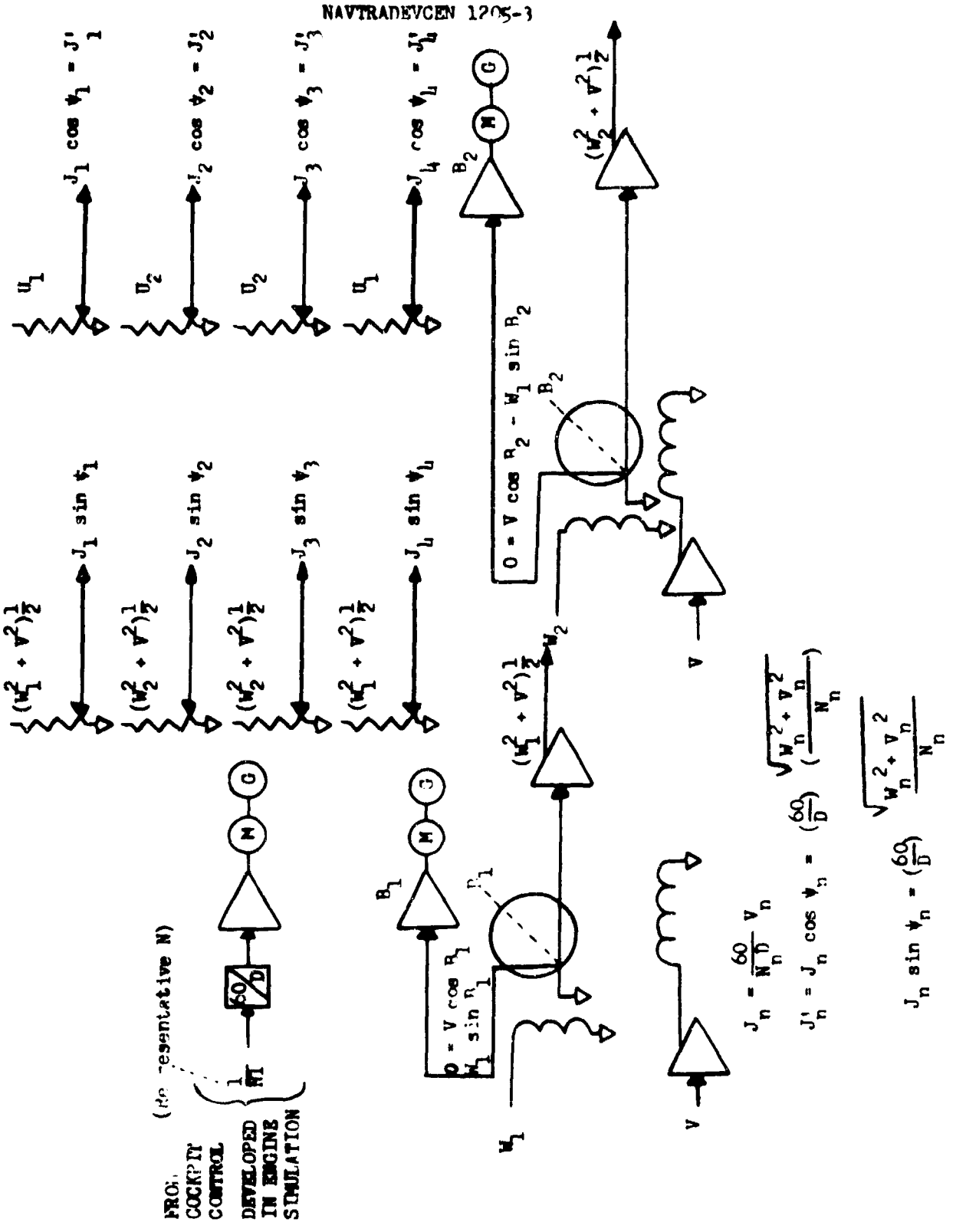

Figure 32. Propeller Aerodynamics Advance Ratio AC Mechanization

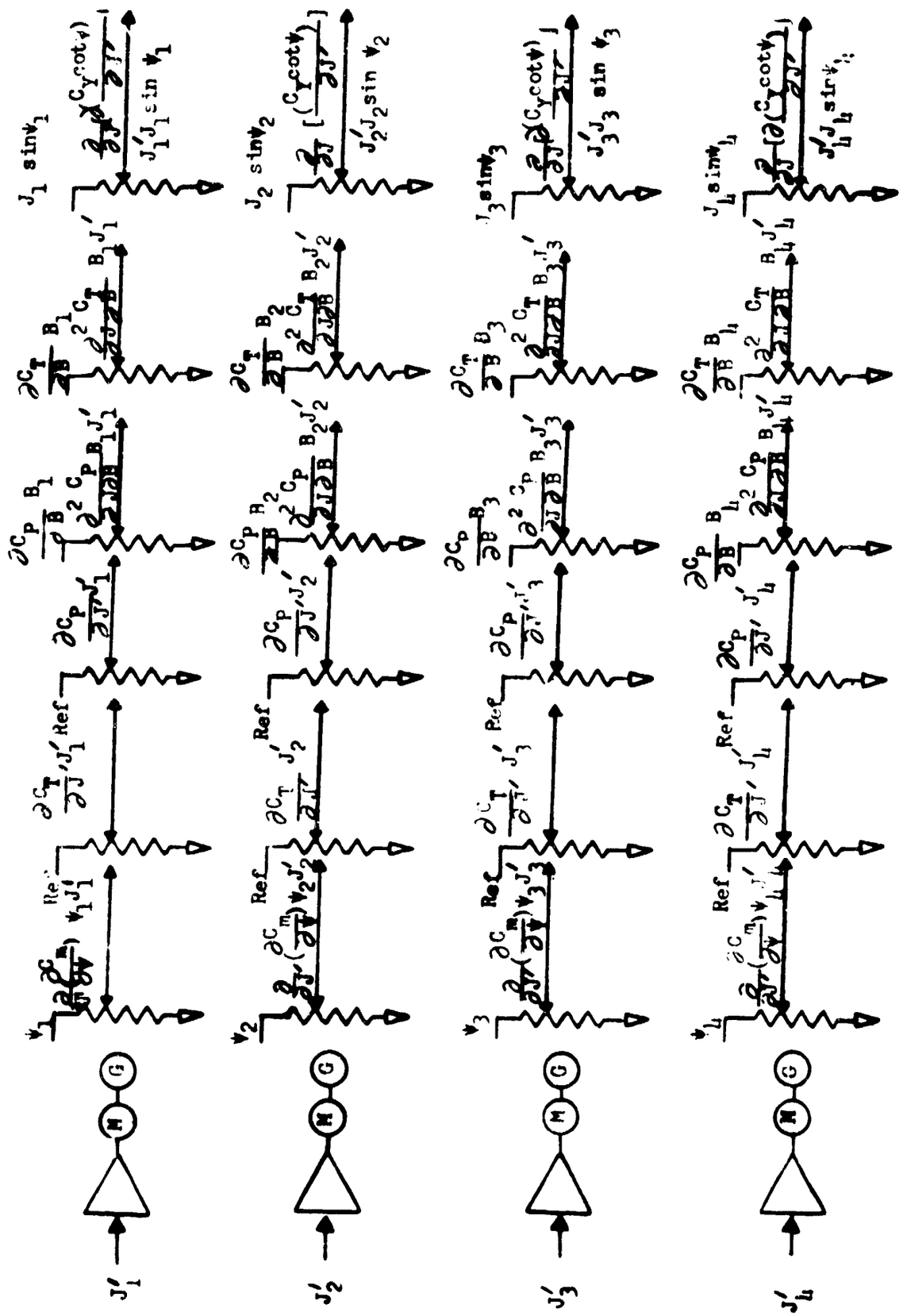

Figure 33. Propeller Aerodynamics Coefficients

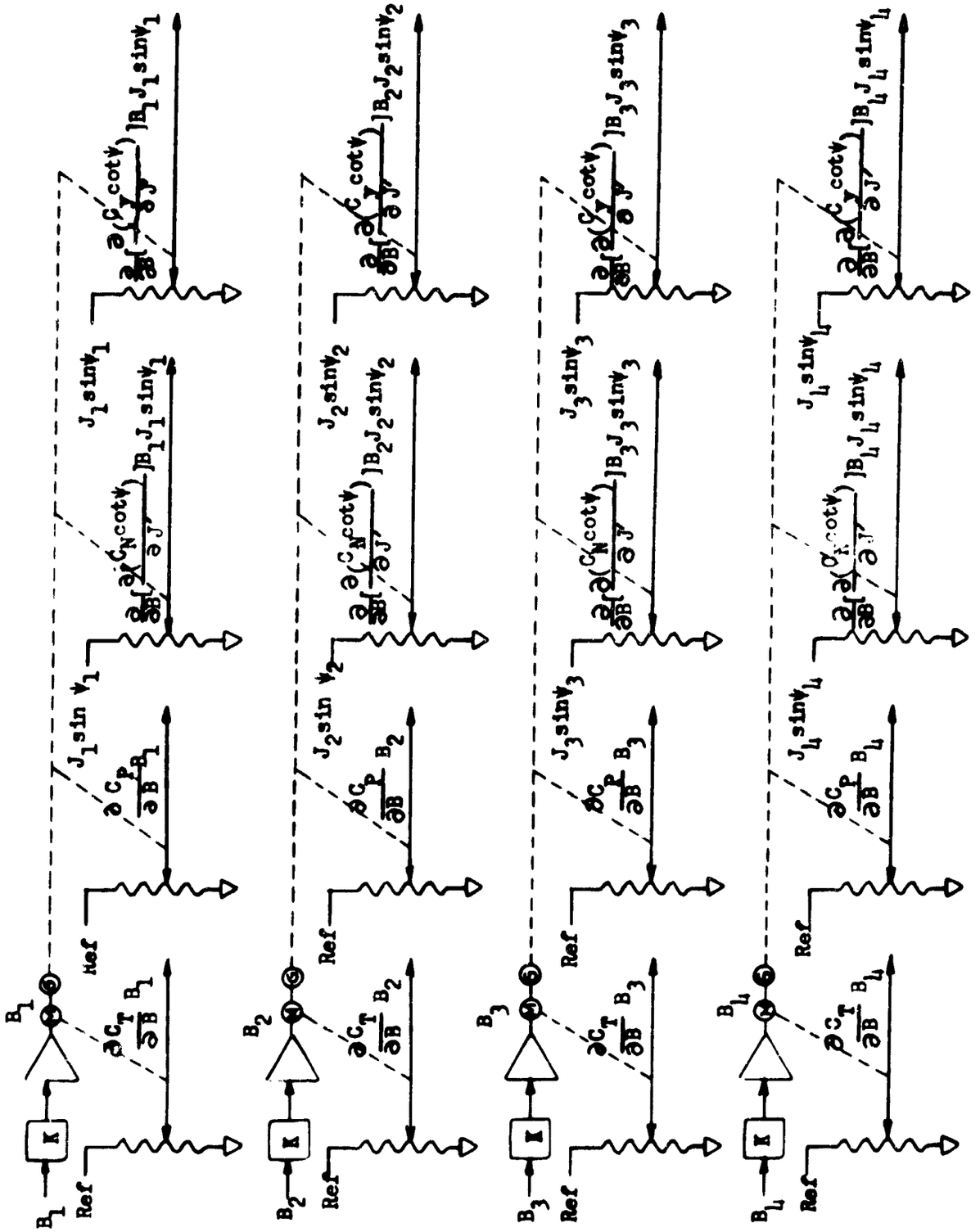

Figure 34. Propeller Aerodynamics Coefficients
AC Mechanization

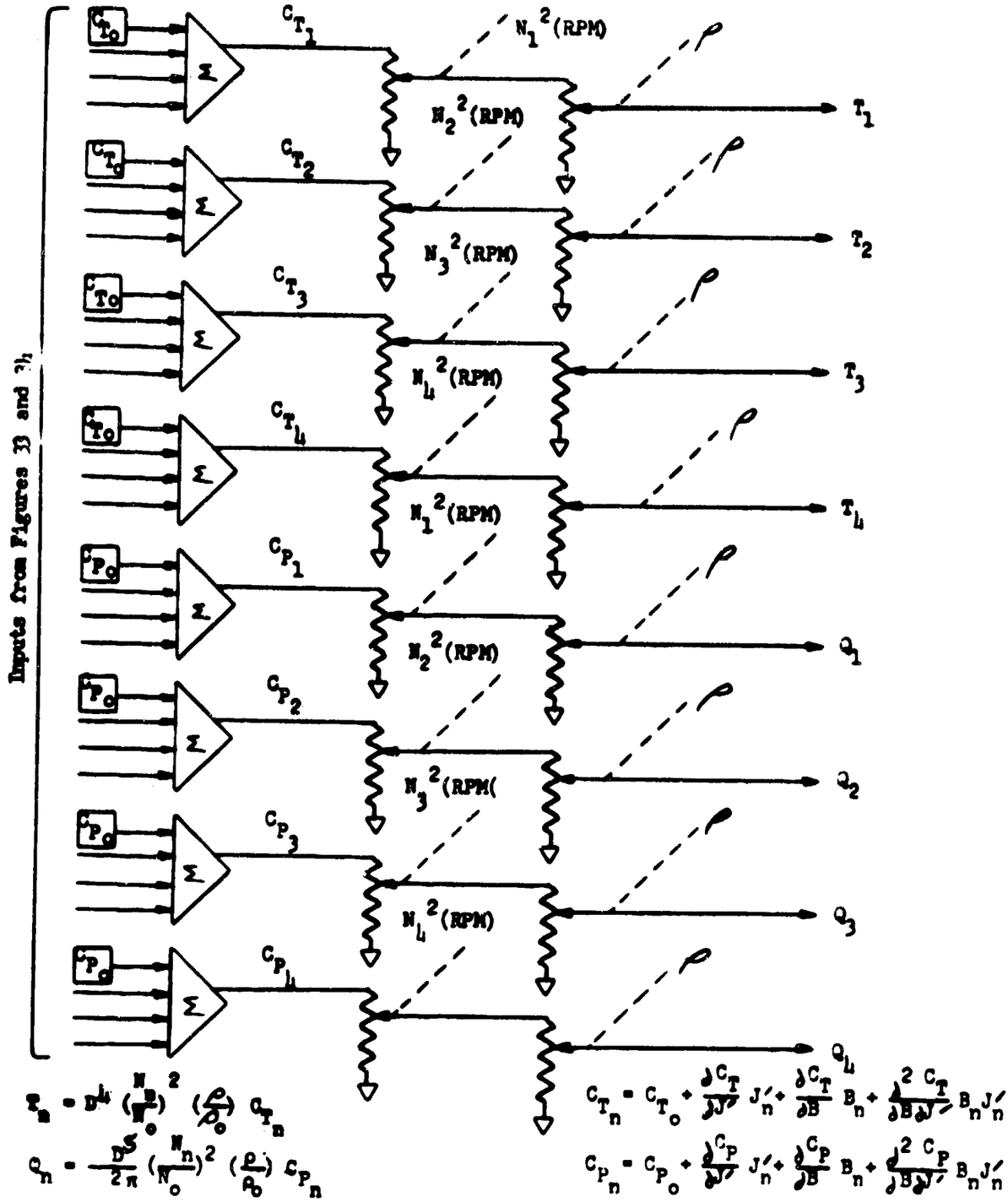

Figure 35. Propeller Aerodynamics
T_n and Q_n AC Mechanization

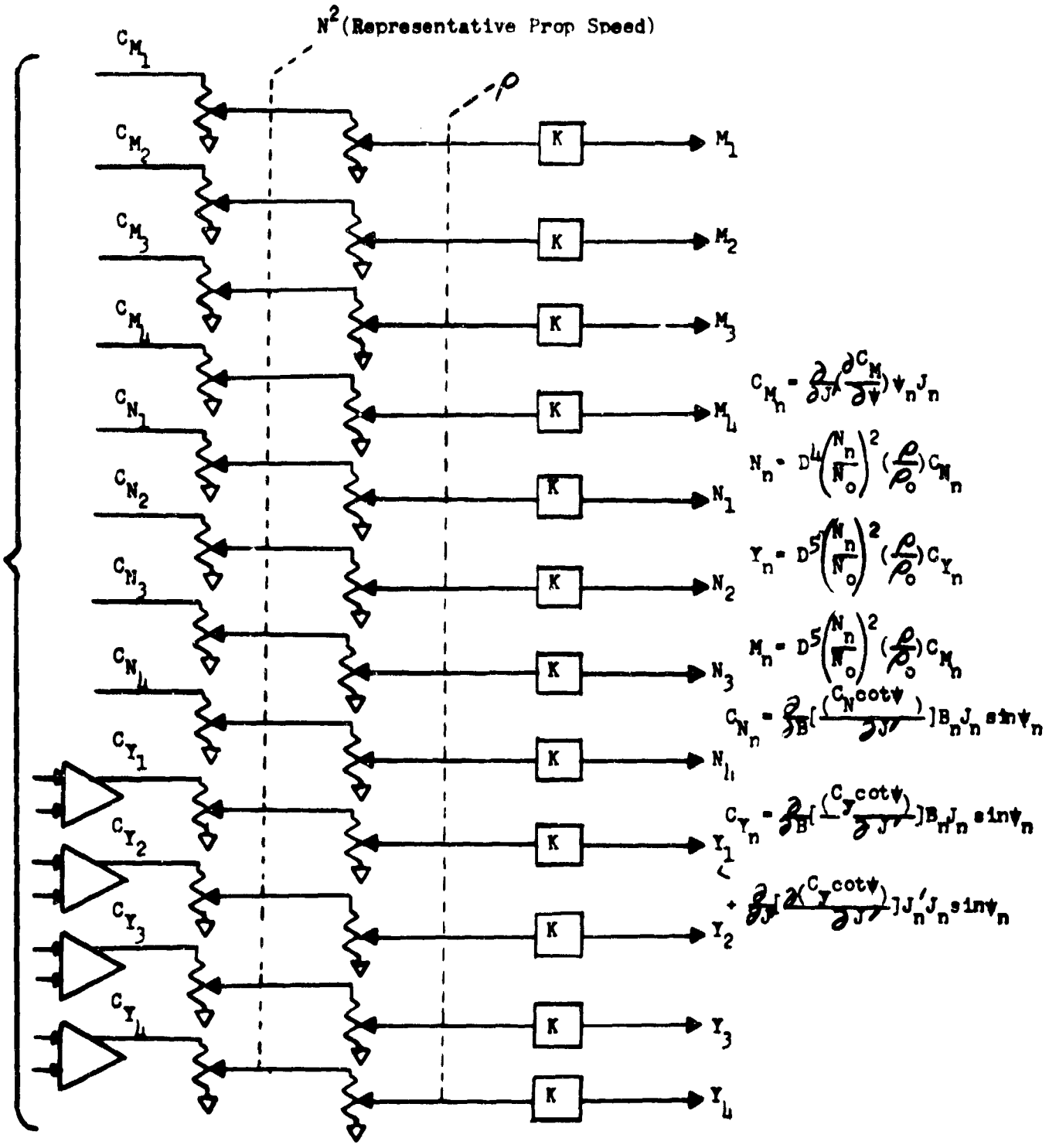

Figure 36. Propeller Aerodynamics M_n, N_n and Y_n AC Mechanisation

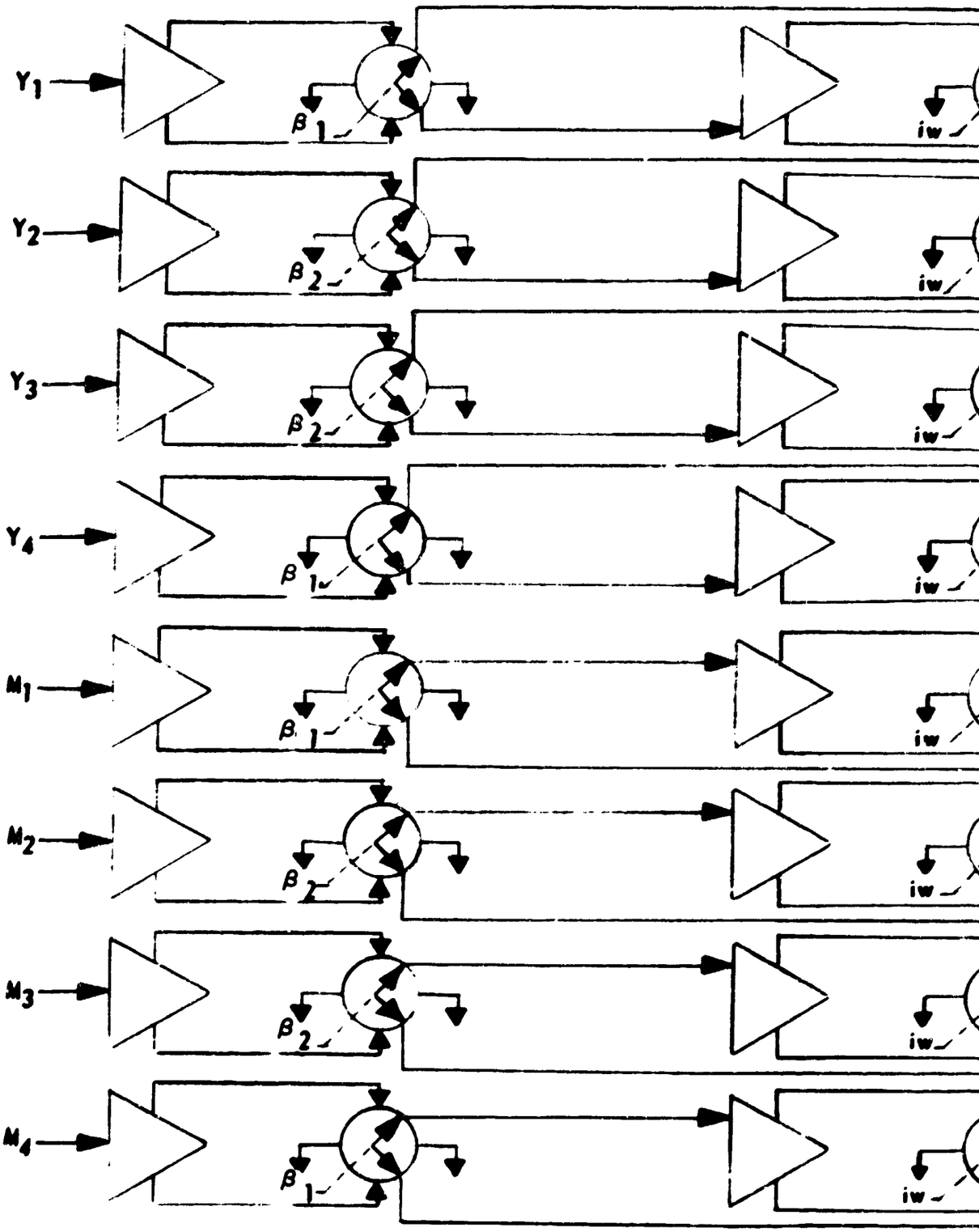

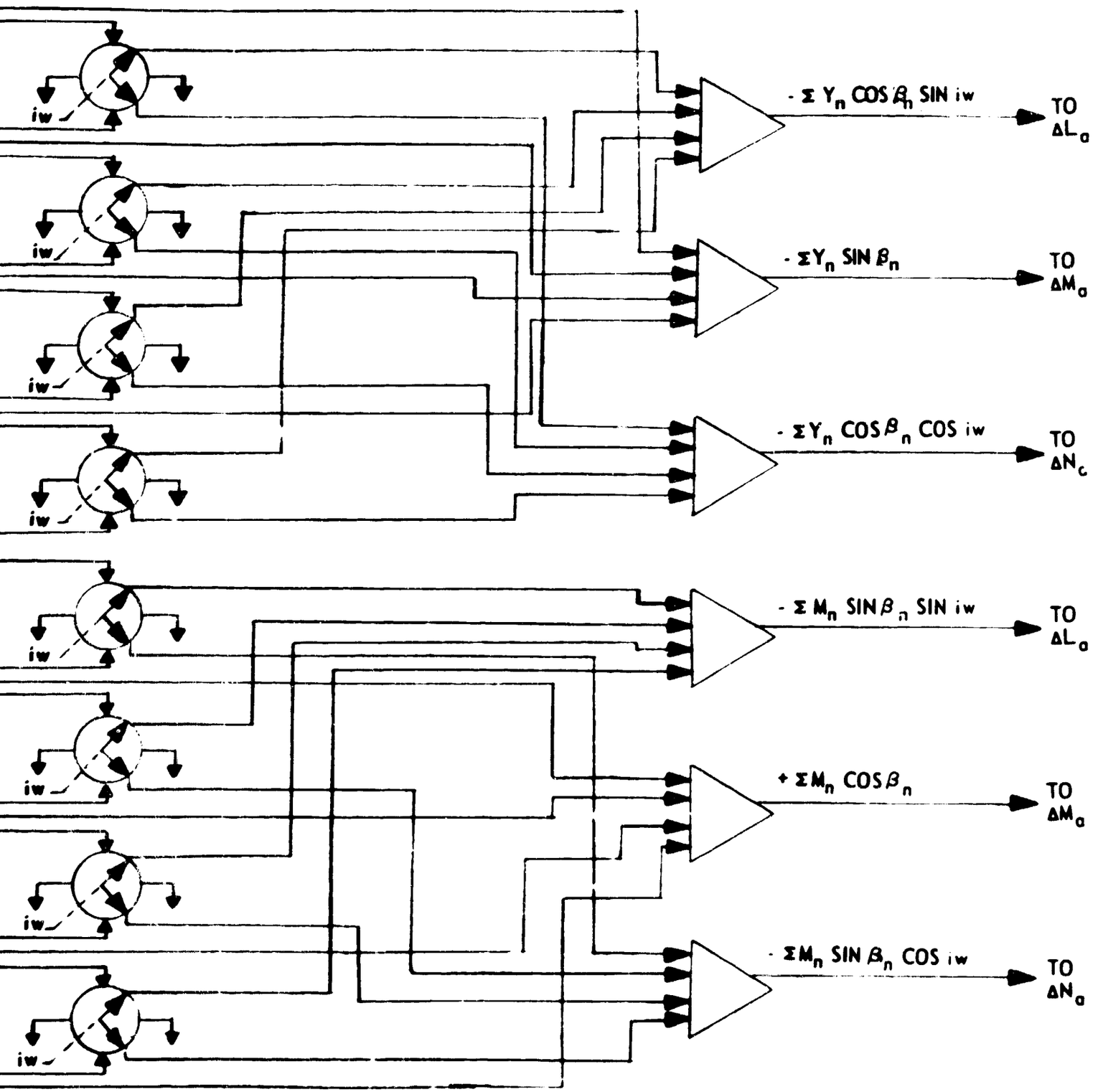

Figure 37. Propeller Aerodynamics Y and M Components AC Mechanization

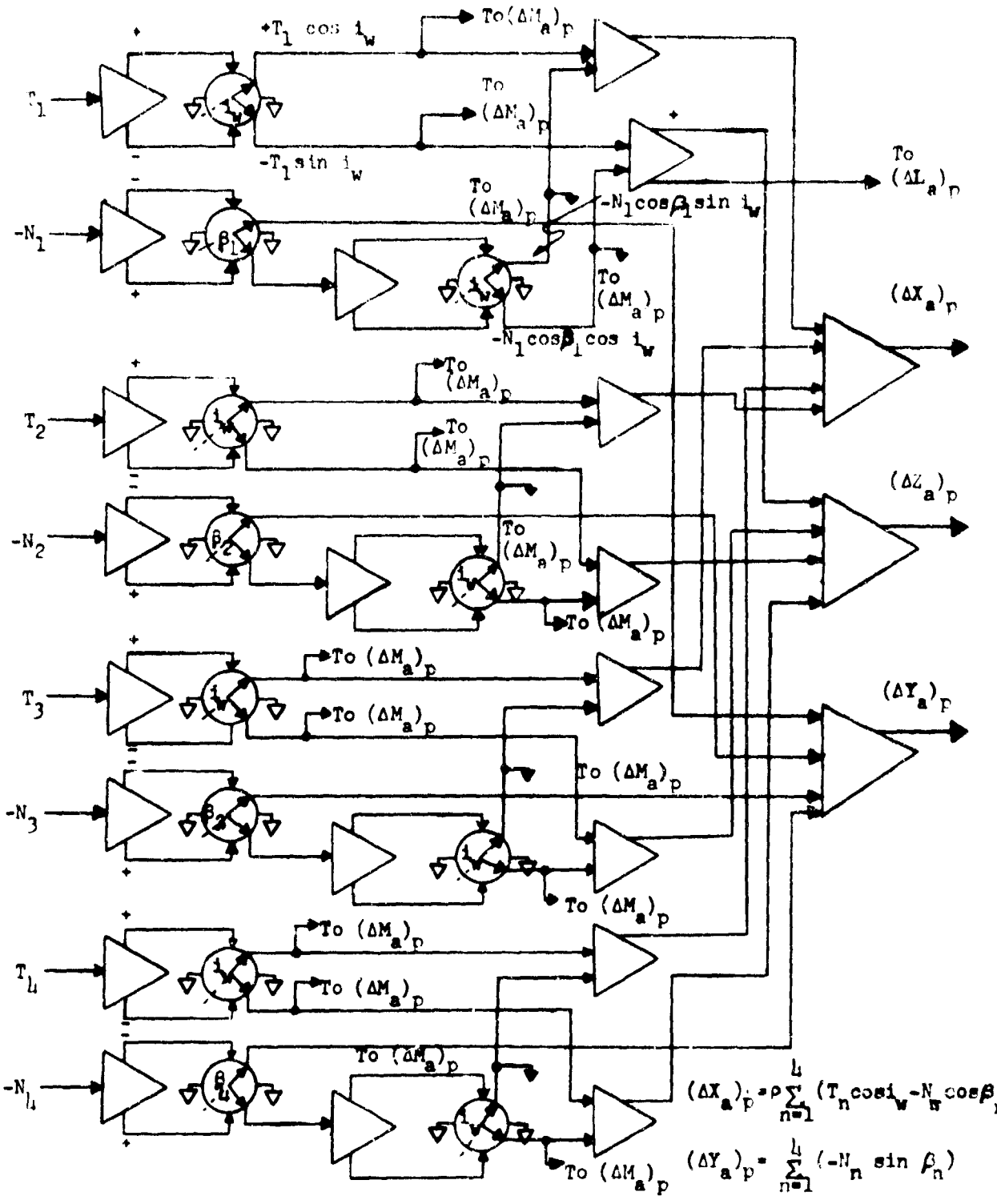

Figure 38. Propeller Aerodynamics Forces AC Mechanization

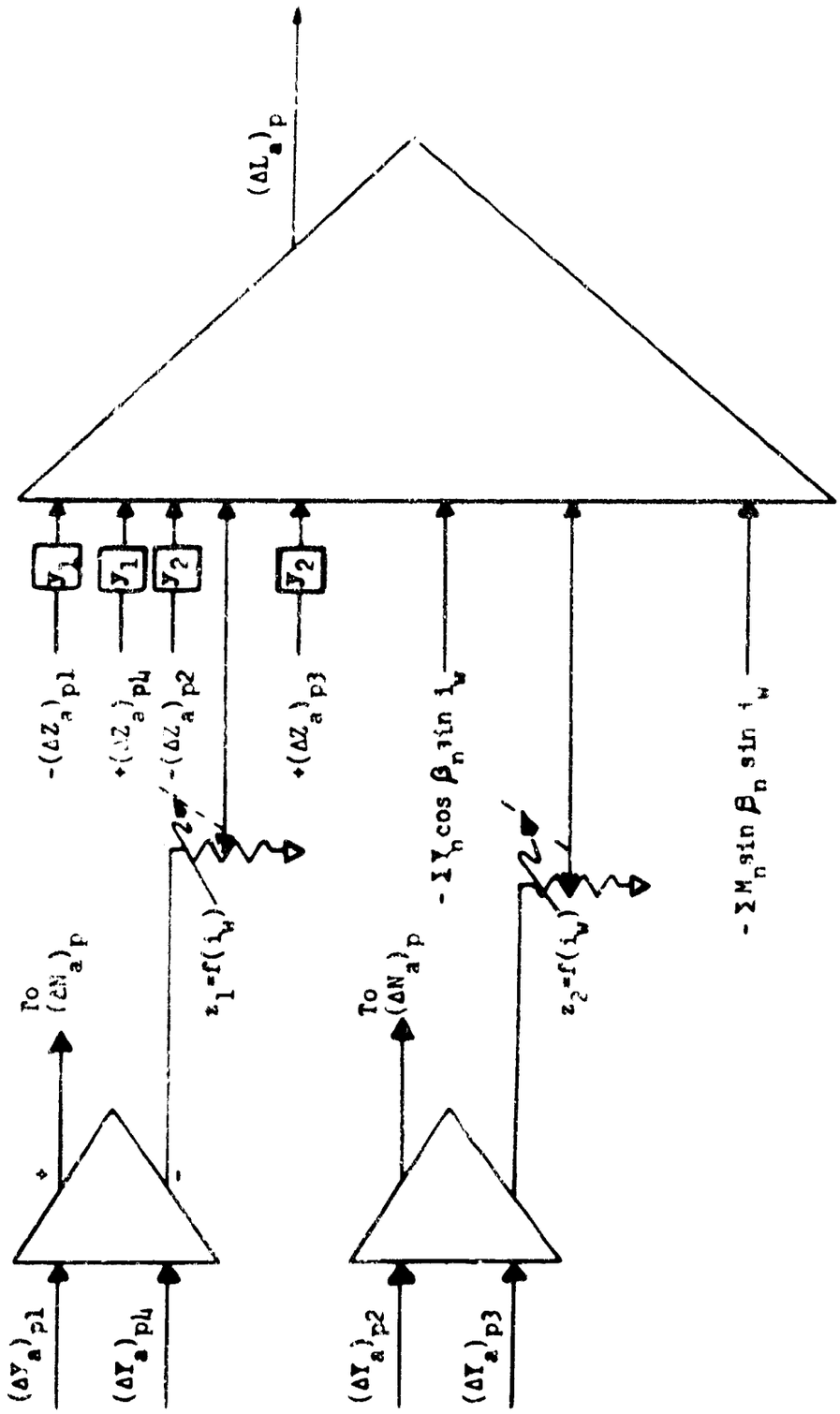

Figure 39. Propeller Aerodynamic Moment $-(\Delta L_a)_p$ AC Mechanization

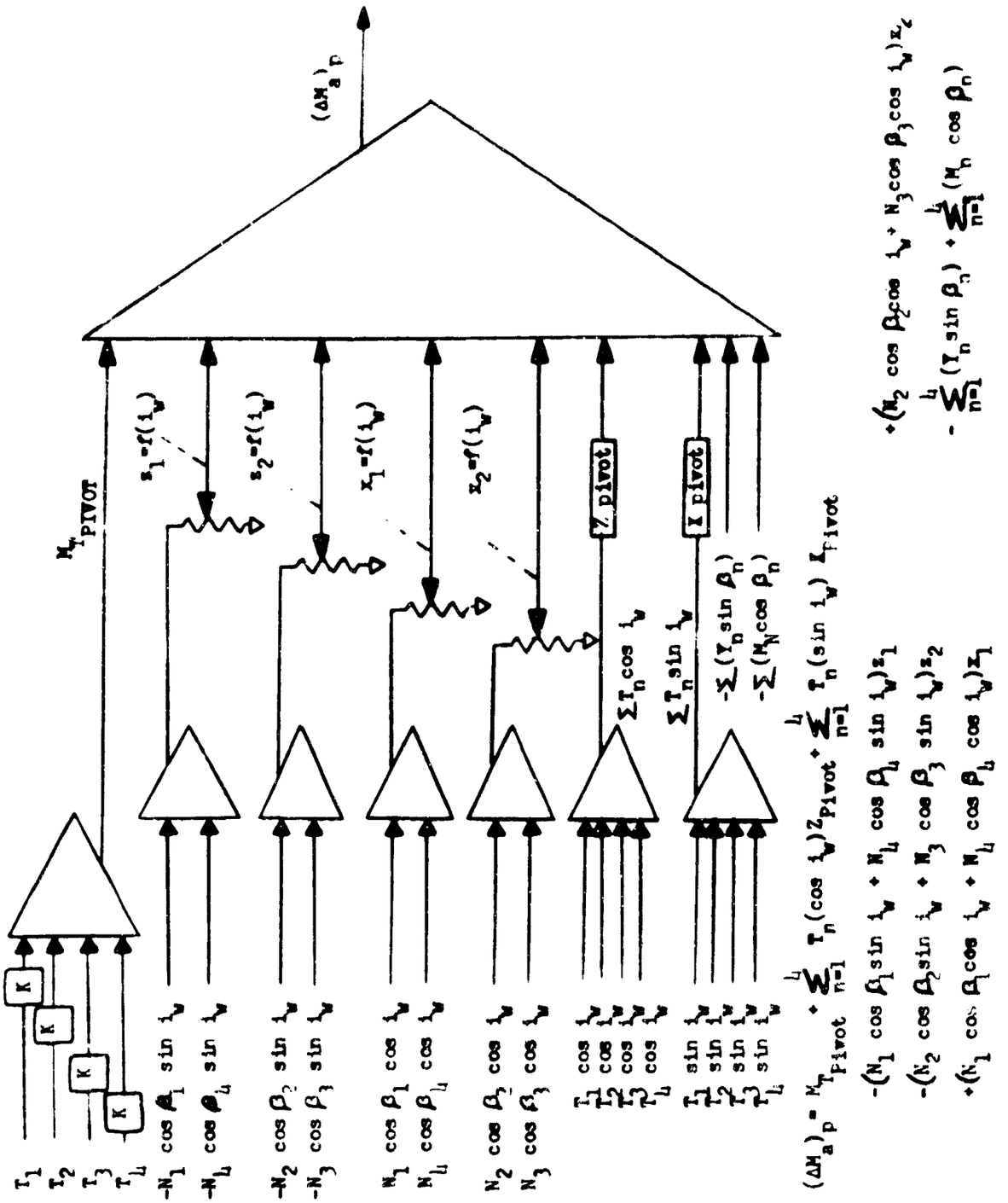

Figure 1.0 Propeller Aerodynamics
Moment - $(\Delta M_a)_p$ AC Mechanization

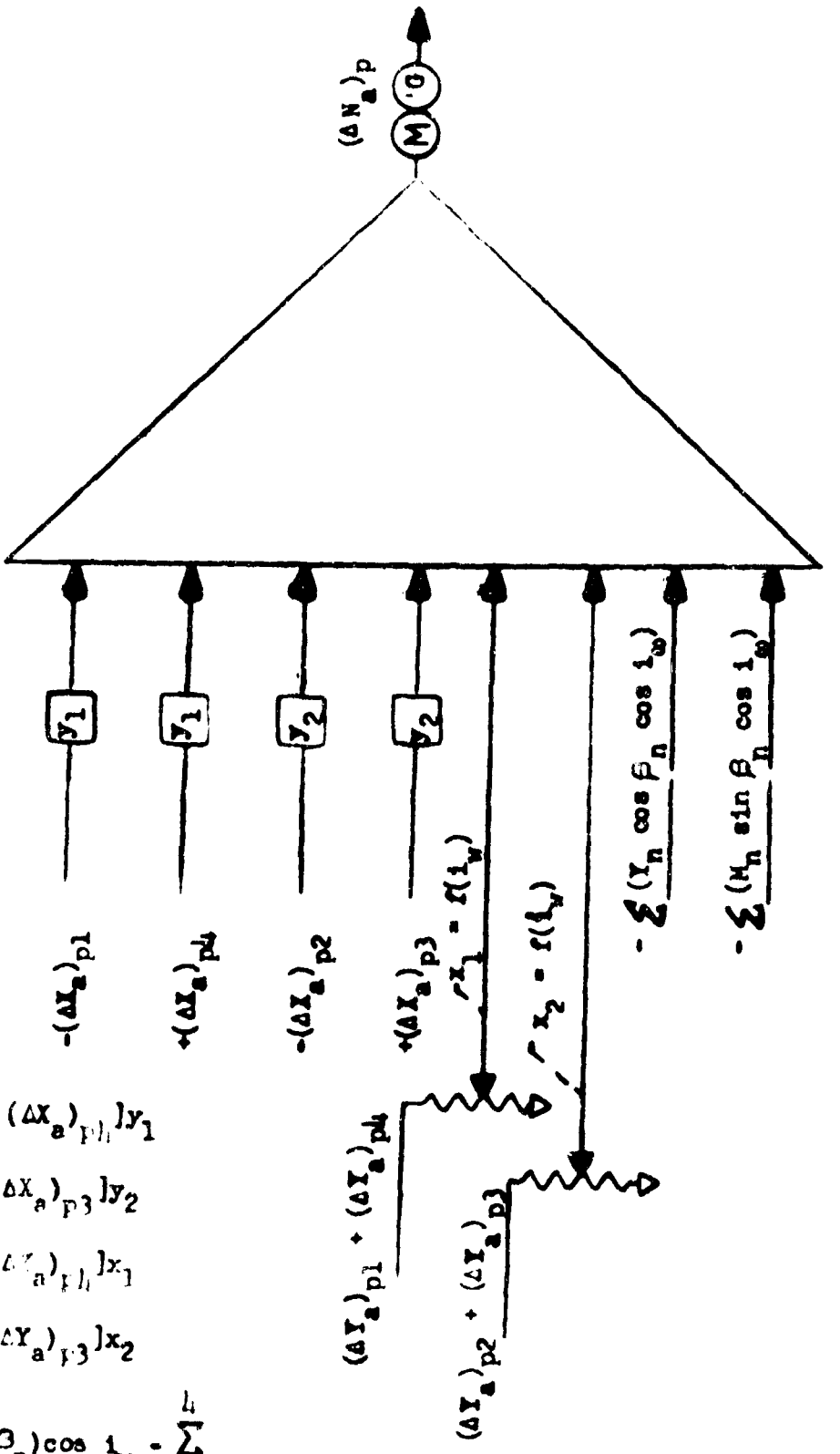

$$(\Delta N_a)_p = -[(\Delta X_a)_{p1} - (\Delta X_a)_{p4}]y_1$$
$$-[(\Delta X_a)_{p2} - (\Delta X_a)_{p3}]y_2$$
$$+[(\Delta Y_a)_{p1} + (\Delta Y_a)_{p4}]x_1$$
$$+[(\Delta Y_a)_{p2} + (\Delta Y_a)_{p3}]x_2$$
$$-\sum_{n=1}^{4}(Y_n \cos\beta_n)\cos i_w - \sum_{n=1}^{4}(N_n \sin\beta_n)\cos i_w$$

Figure 11. Propeller Aerodynamics Moment - $(\Delta N_a)_p$ AC Mechanisation

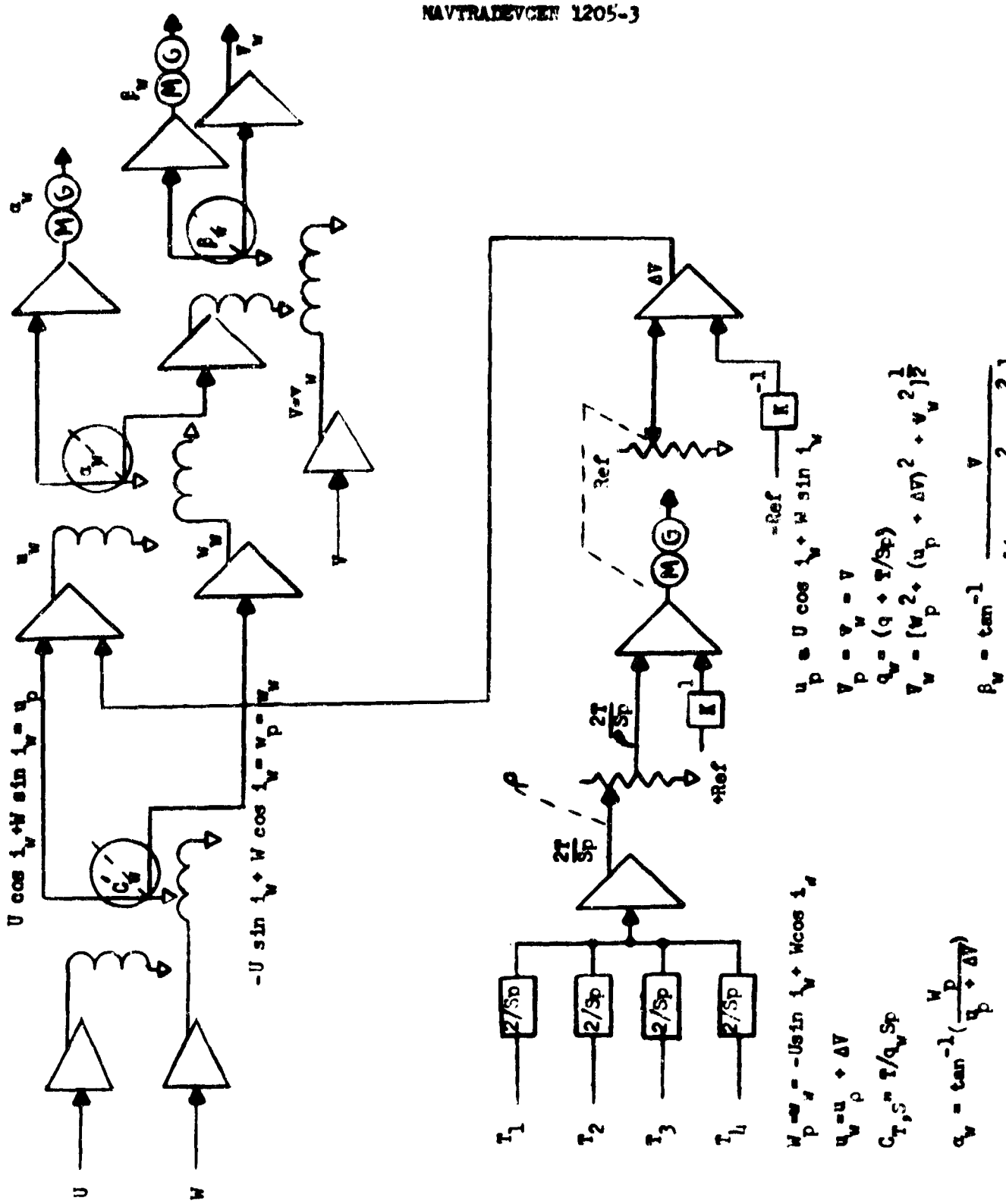

Figure 42. Wing Aerodynamics AC Mechanisation α_w, β_w, V_w

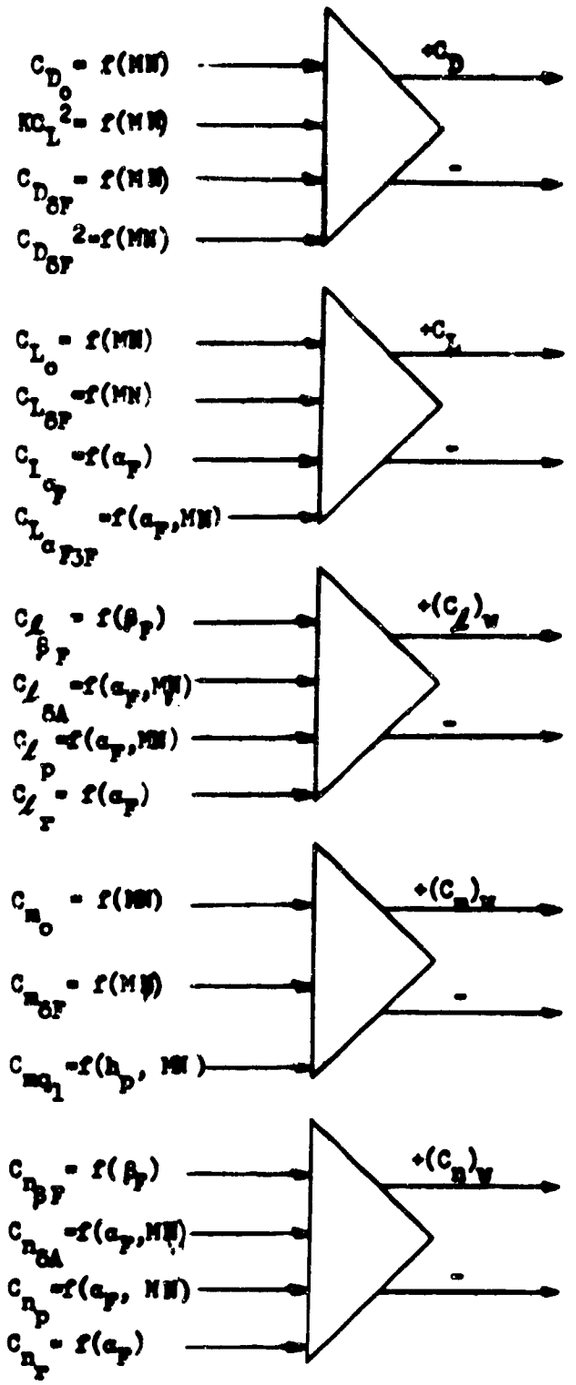

$$C_D = C_{D_o} + KC_L^2 + C_{D_{\delta F}} \cdot \delta F + \frac{\partial^2 C_D}{\partial \delta F^2} \cdot \delta^2 F$$

$$C_L = C_{L_o} + C_{L_{\delta F}} \cdot \delta F + C_{L_{\alpha_F}} \cdot \alpha_W + \frac{\partial C_{L_{\alpha_F}}}{\partial \delta F} \cdot \delta F \cdot \alpha_W$$

$$(C_{\ell_W}) = C_{\ell_{\beta_F}} \cdot \beta_W + C_{\ell_{\delta A}} \cdot \delta A + \frac{b}{2V_W} C_{\ell_p} \cdot P_W + \frac{b}{2V_W} C_{\ell_r} \cdot r_W$$

$$(C_{m_W}) = C_{m_o} + C_{m_{\delta F}} \cdot \delta F + \frac{c}{2V_W} C_{m_{q_1}} \cdot q_1$$

$$(C_{n_W}) = C_{n_{\beta_F}} \cdot \beta_W + C_{n_{\delta A}} \cdot \delta A + \frac{b}{2V_W} C_{n_p} \cdot p_W + \frac{b}{2V_W} C_{n_r} \cdot r_W$$

Figure 43. Wing Aerodynamics Coefficients AC Mechanization

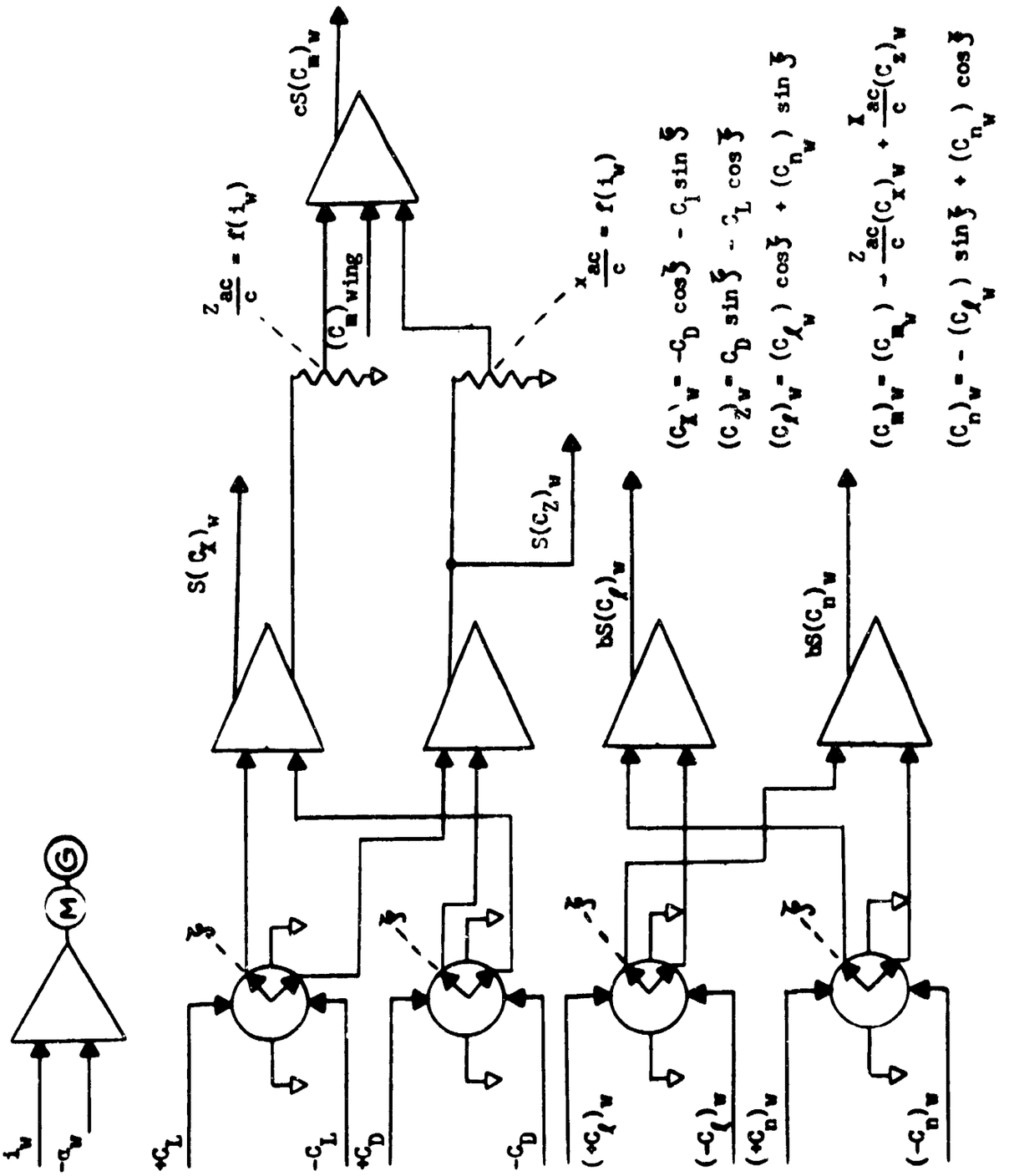

Figure 44. Wing Aerodynamics Coefficients AC Mechanization

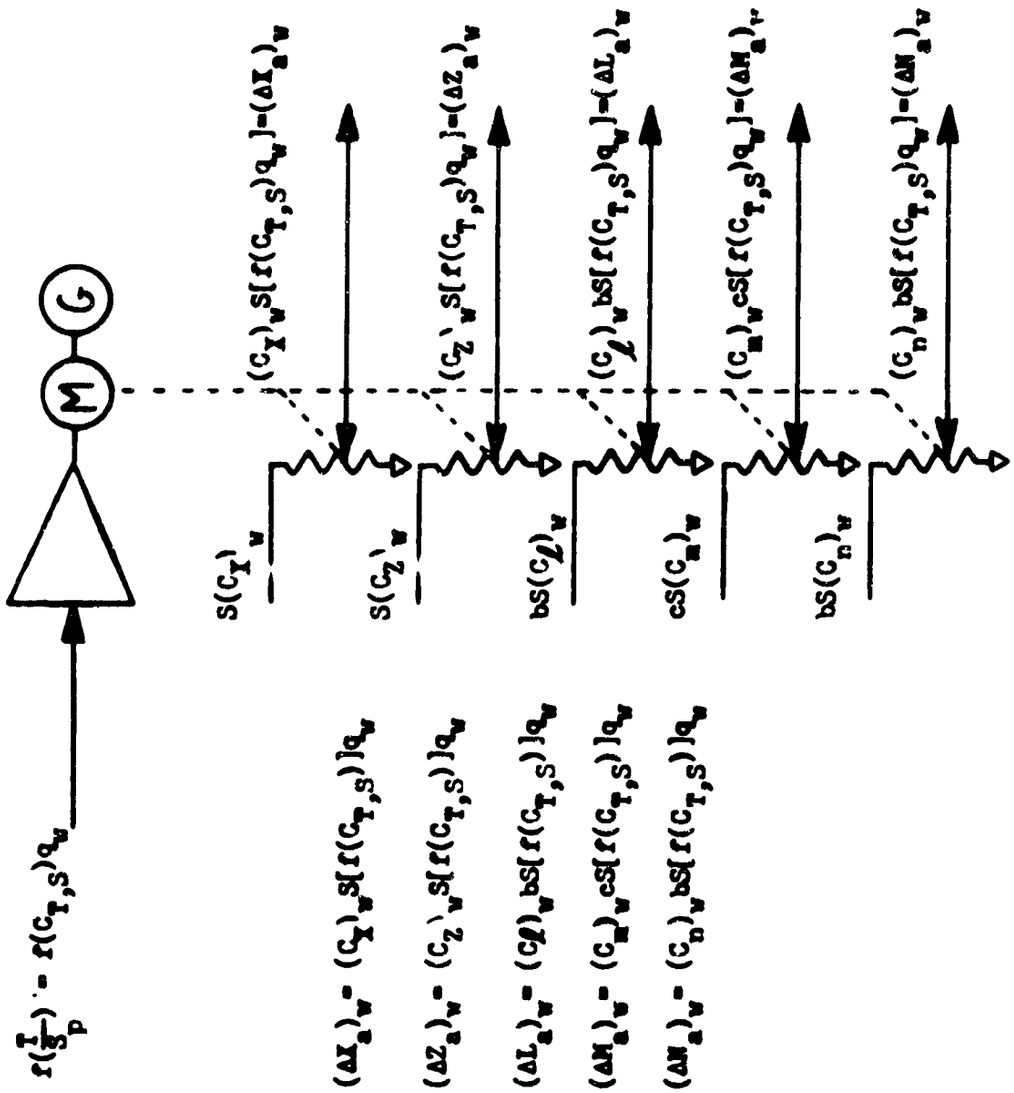

Figure 45. Wing Aerodynamics Forces and Moments AC Mechanization

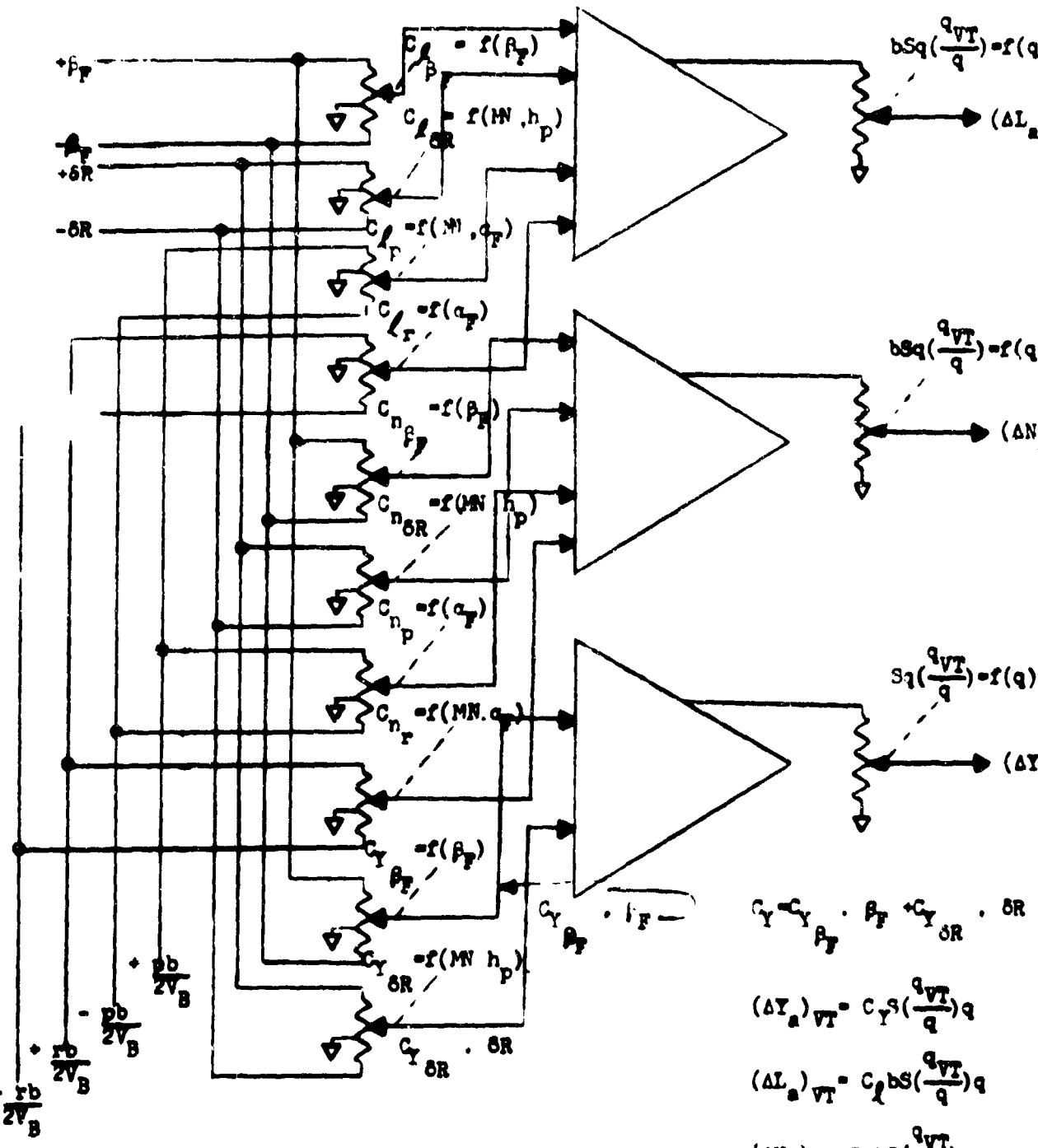

$$C_Y = C_{Y_{\beta_F}} \cdot \beta_F + C_{Y_{\delta R}} \cdot \delta R$$

$$(\Delta Y_a)_{VT} = C_Y S(\frac{q_{VT}}{q})q$$

$$(\Delta L_a)_{VT} = C_l bS(\frac{q_{VT}}{q})q$$

$$(\Delta N_a)_{VT} = C_n bS(\frac{q_{VT}}{q})q$$

$$C_l = C_{l_{\beta_F}} \cdot \beta_F + C_{l_{\delta R}} \cdot \delta R + \frac{b}{2V_B}[C_{l_p} \cdot p + C_{l_r} \cdot r]$$

$$C_n = C_{n_{\beta_F}} \cdot \beta_F + C_{n_{\delta R}} \cdot \delta R + \frac{b}{2V_B}[C_{n_p} \cdot p + C_{n_r} \cdot r]$$

Figure 46 Vertical Stabiliser Aerodynamics Force and Moments AC Mechanisation

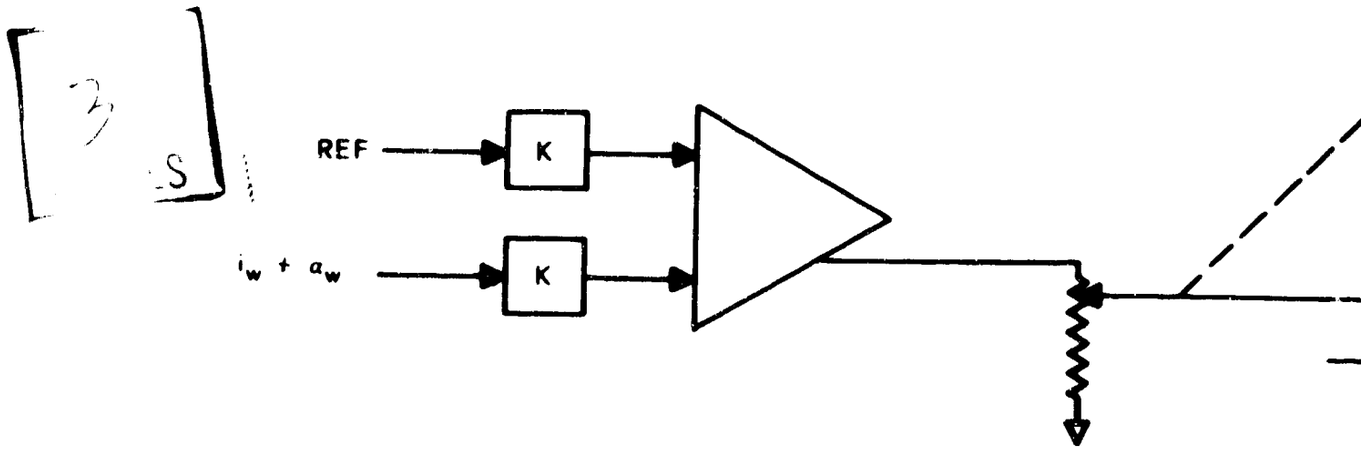

A

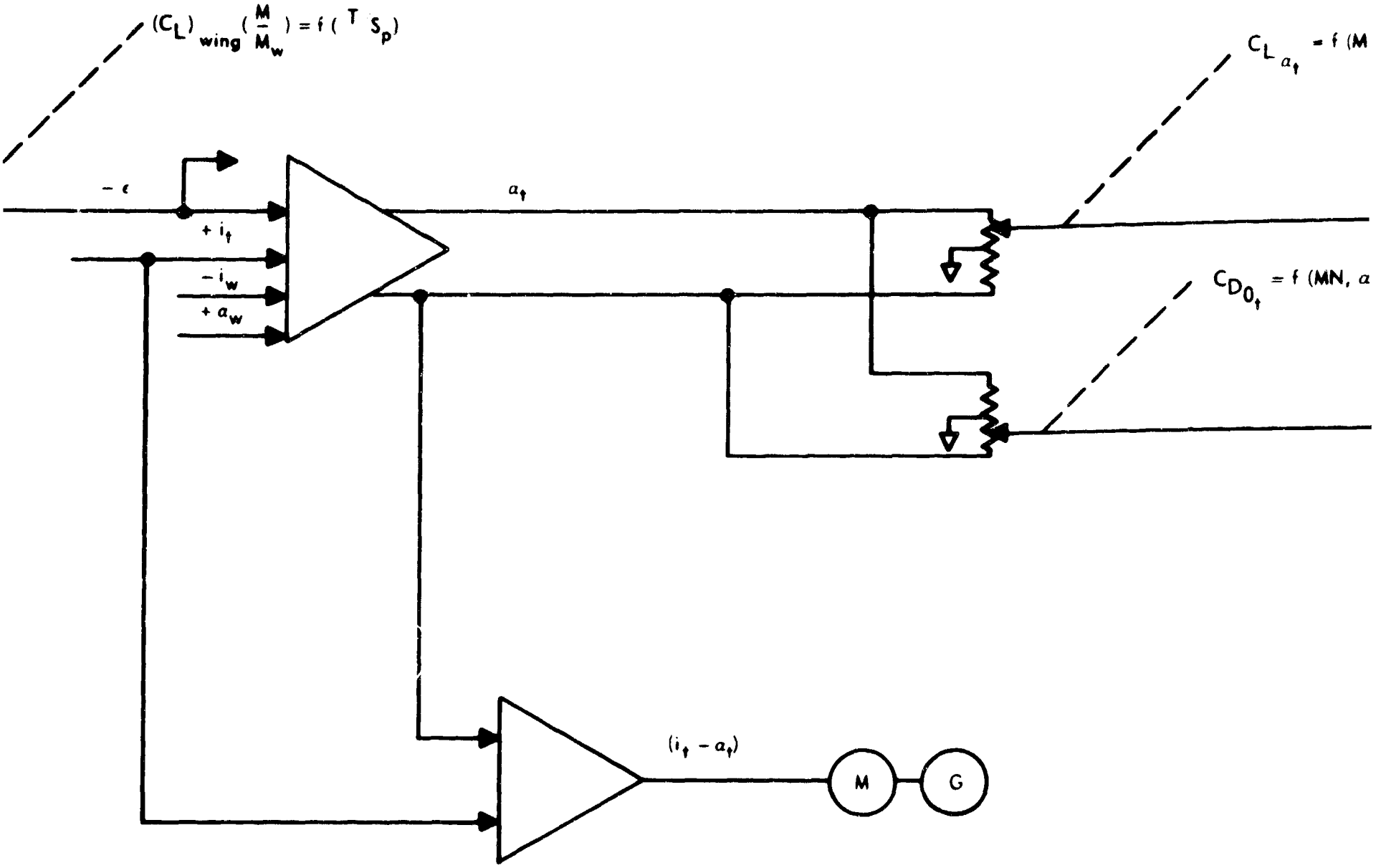

5.228 $-a_t = a_F + i_t - \epsilon$

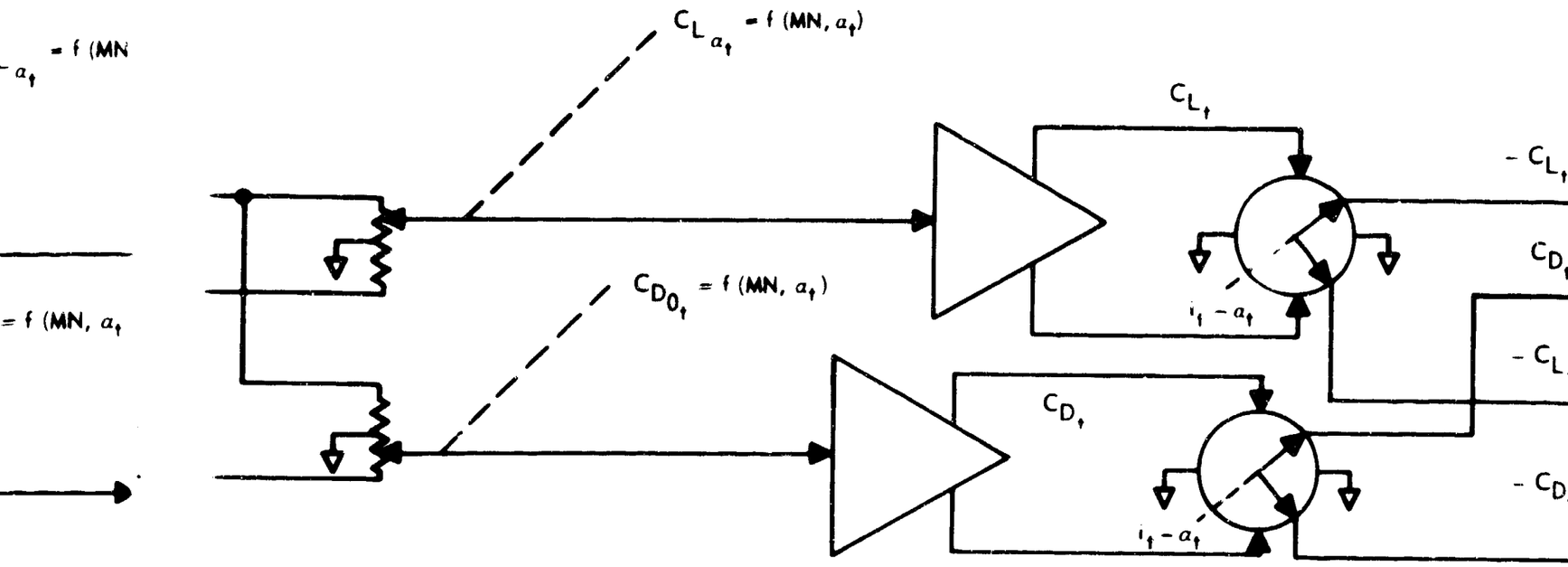
= f (MN
a_t
= f (MN, a_t
$C_{L_{a_t}} = f(MN, a_t)$
$C_{D_{0_t}} = f(MN, a_t)$
C_{L_t}
C_{D_t}
$i_t - a_t$
$i_t - a_t$
- C_{L_t}
- C_L
- C_D


M
G

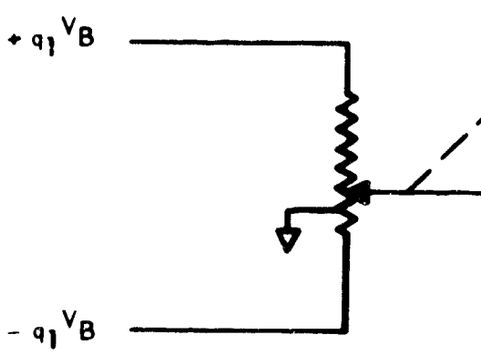
+ $q_1 V_B$
- $q_1 V_B$

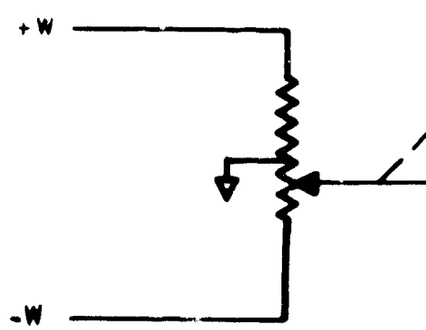
+W
-W

B

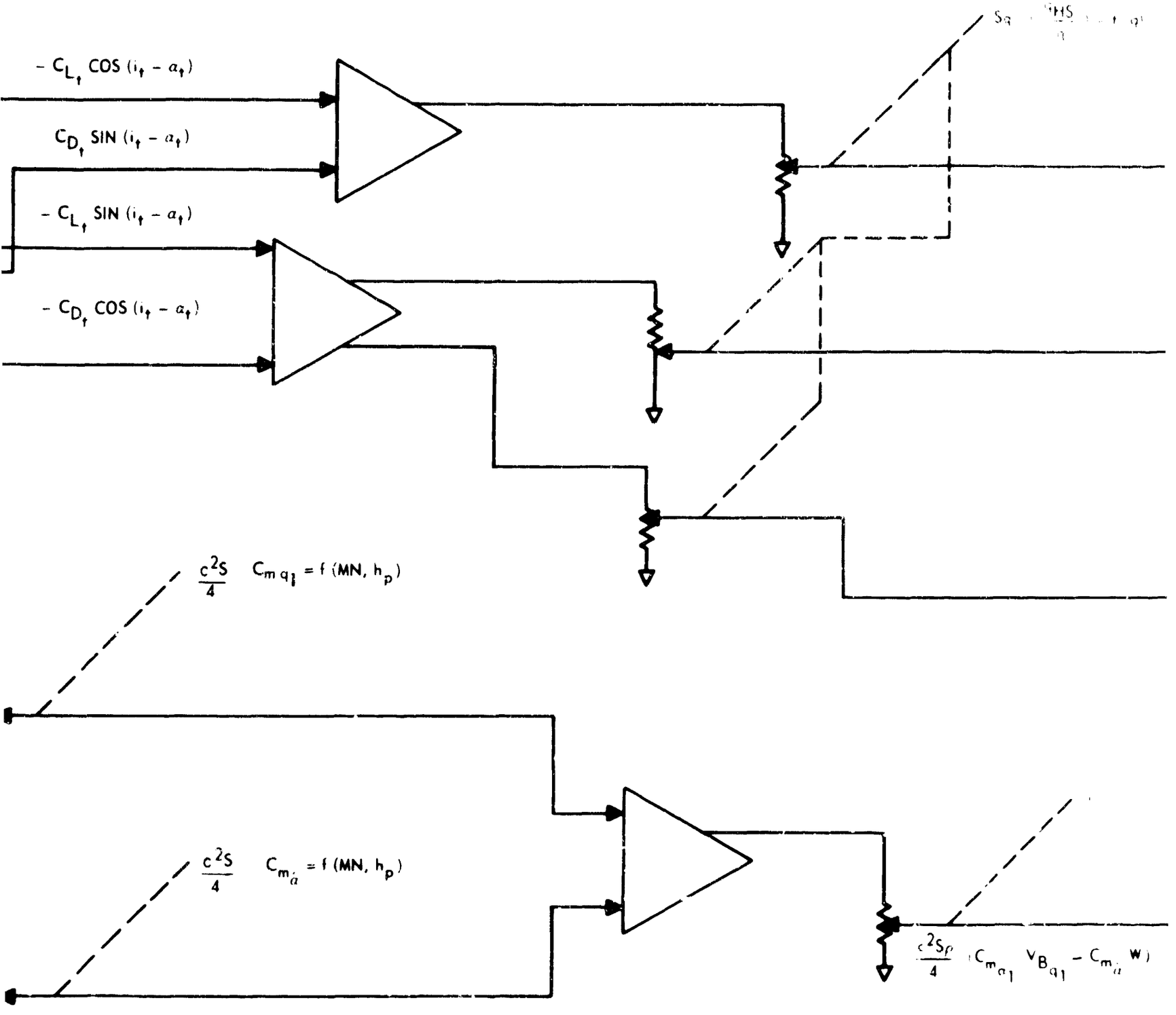
$-C_{L_t} \cos(i_t - \alpha_t)$
$C_{D_t} \sin(i_t - \alpha_t)$
$-C_{L_t} \sin(i_t - \alpha_t)$
$-C_{D_t} \cos(i_t - \alpha_t)$
$\frac{c^2 S}{4} C_{m_{q_1}} = f(MN, h_p)$
$\frac{c^2 S}{4} C_{m_{\dot{\alpha}}} = f(MN, h_p)$
$\frac{c^2 S_p}{4} (C_{m_{q_1}} V_{B_{q_1}} - C_{m_{\dot{\alpha}}} W)$

Figure 47

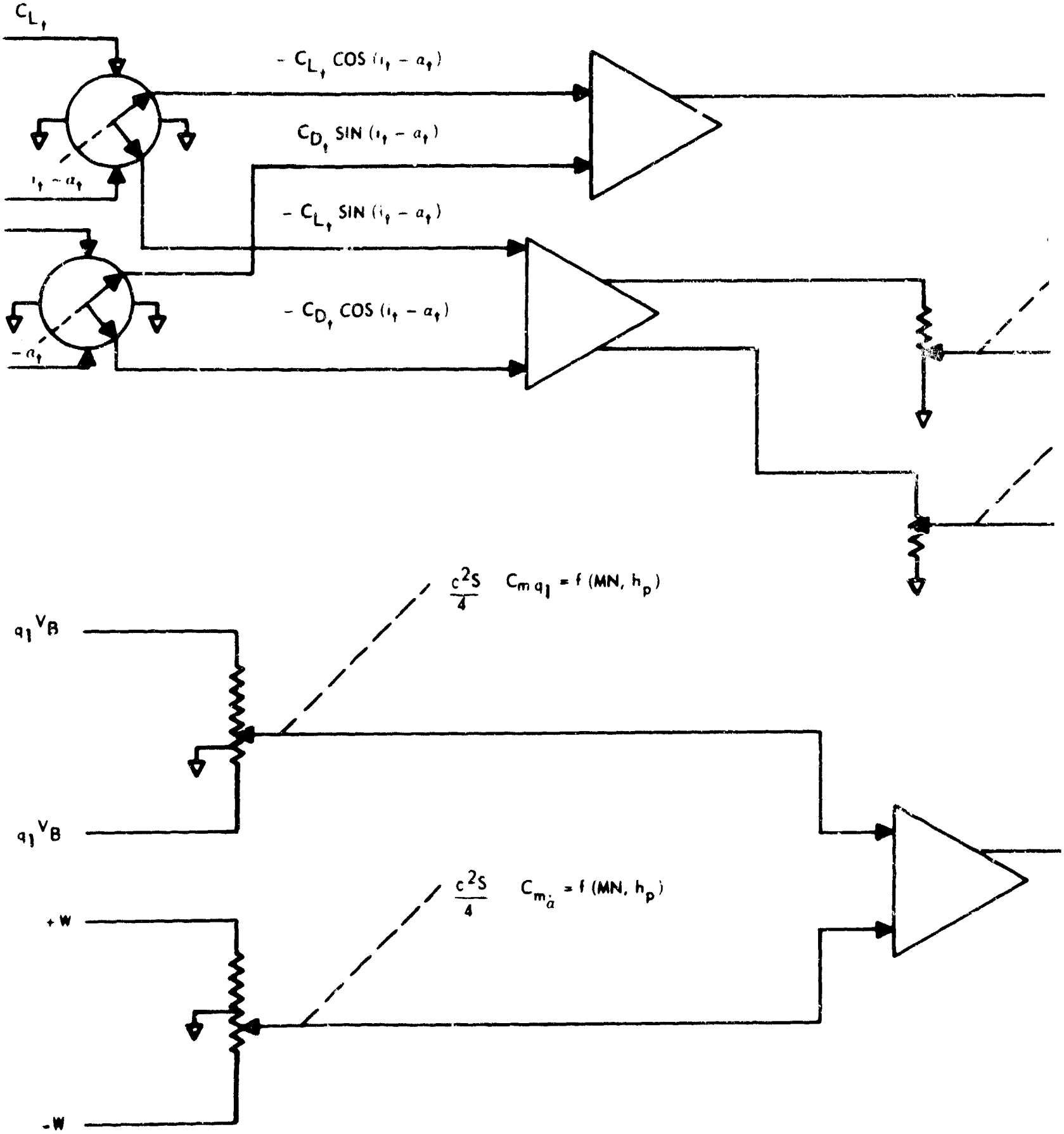
C_{L_t}
$-C_{L_t}\cos(i_t - a_t)$
$C_{D_t}\sin(i_t - a_t)$
$i_t - a_t$
$-C_{L_t}\sin(i_t - a_t)$
$-C_{D_t}\cos(i_t - a_t)$
$-a_t$
$\frac{c^2S}{4}\ C_{m_{q_1}} = f(MN, h_p)$
$q_1 V_B$
$q_1 V_B$
$\frac{c^2S}{4}\ C_{m_{\dot{\alpha}}} = f(MN, h_p)$
+W
-W

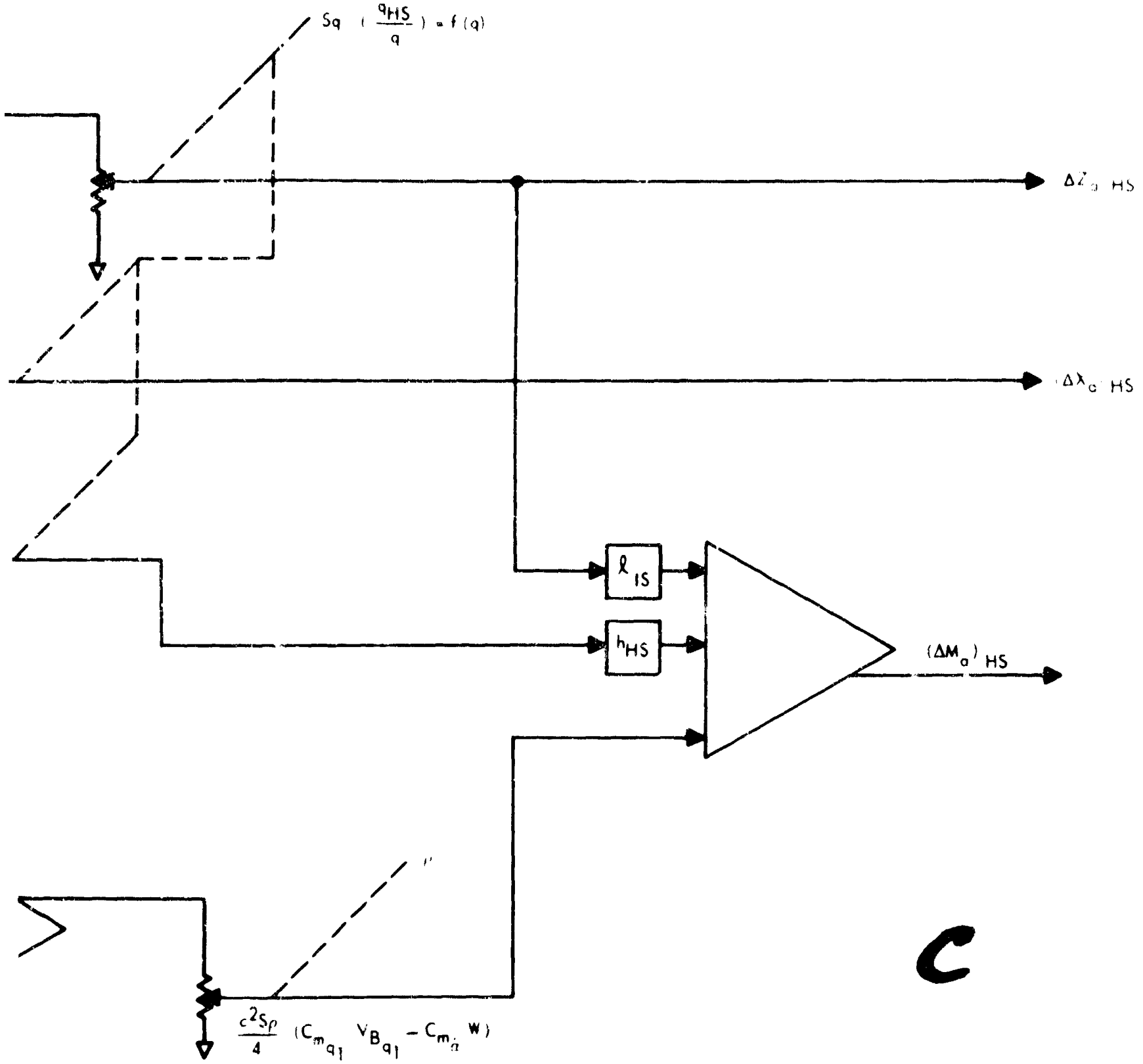

Figure 47. HORIZONTAL STABILIZER AERODYNAMICS FORCES AND MOMENT AC MECHANIZATION

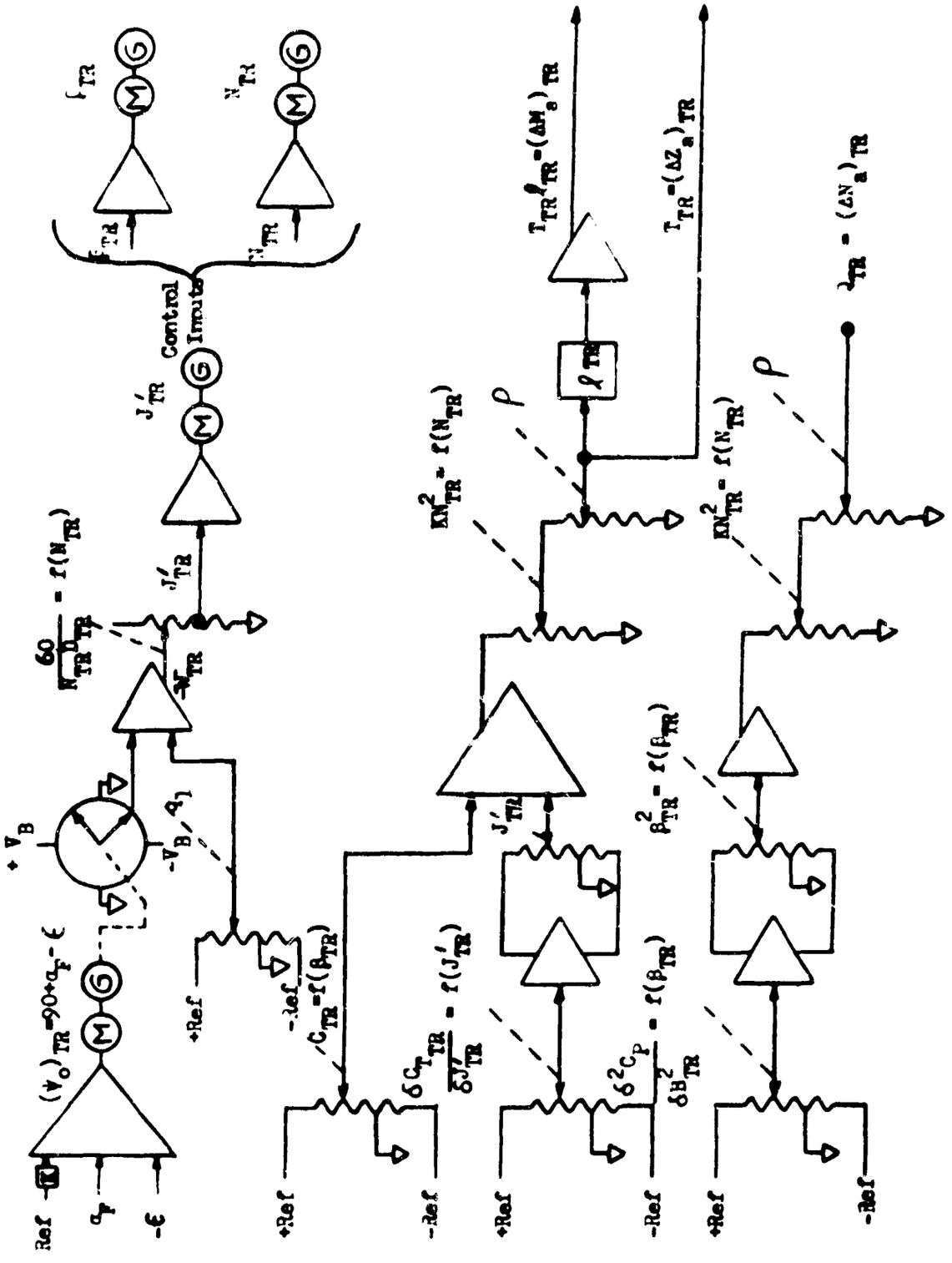

Figure 18. Tail Rotor Aerodynamics Force and Moments (Sheet 1)
AC Mechanization

$$(\Psi_o)_{TR} = 90 + (\alpha_F - \epsilon)$$

$$W_{TR} = V_B \cos (\Psi_o)_{TR} - \ell_{TR}\, q_1$$

$$J'_{TR} = \left(\frac{60}{D_{TR}}\right)\left(\frac{-W_{TR}}{N_{TR}}\right)$$

$$C_{T_{TR}} = C_{T_{TR}}(B_{TR}) + \frac{\partial C_{T_{TR}}}{\partial J'_{TR}}\,(J'_{TR})$$

$$(\Delta Z_a)_{TR} = T_{TR}$$

$$C_{p_{TR}} = \frac{\partial^2 C_p}{\partial B^2_{TR}}\,(B_{TR})^2$$

$$u_{TR} = V_B \sin (\Psi_o)_{TR}$$

$$J_{TR} = \left(\frac{60}{D_{TR}}\right)\frac{V_{TR}}{N_{TR}}$$

1

$$V_{TR} = (u^2_{TR} + w^2_{TR})^{\frac{1}{2}}$$

$$(\Delta N_a)_{TR} = Q_{TR}; (\Delta M_a)_{TR} = T_{TR}\,\ell_{TR}$$

$$T_{TR} = D^4_{TR}\left(\frac{\rho}{\rho_o}\right)\left(\frac{N_{TR}}{N_{o_{TR}}}\right) C_{T_{TR}}$$

$$Q_{TR} = D^5_{TR}\left(\frac{\rho}{\rho_o}\right)\left(\frac{N_{TR}}{N_{o_{TR}}}\right)^2 C_{p_{TR}}$$

Equations for Tail Rotor Aerodynamics Force and Moments
AC Mechanization.

Figure 18. Tail Rotor Aerodynamics Force and Moments (Sheet 2)
AC Mechanization

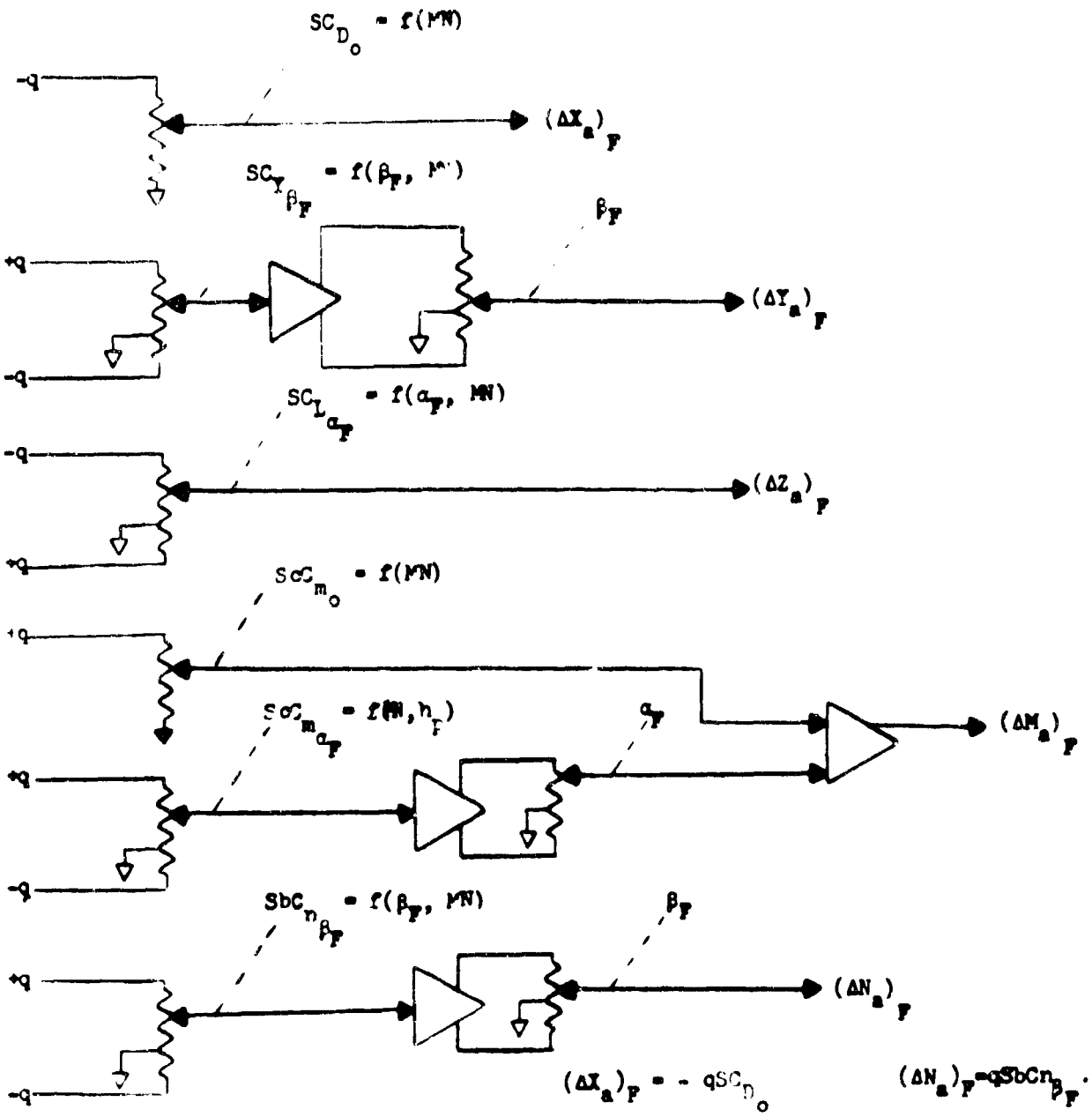

$(\Delta X_a)_F = - qSC_{D_o}$

$(\Delta N_a)_F = qSbCn_{\beta_F} \cdot \beta_F$

$(\Delta Y_a)F = qSC_{Y_{\beta_F}} \cdot \beta_F$

$(\Delta Z_a)_F = qSC_{L_{\alpha_F}} \cdot \alpha_F$

$(\Delta M_a)_F = qSc[Cm_o + C_{m_{\alpha_F}} \cdot \alpha_F]$

Figure 49. Fuselage Aerodynamics
Forces and Moments AC Mechanization

Block (7), Figure 29 mechanised by Figure 50.

Block (8), Figure 29 mechanised by Figure 51.

Block (9), Figure 29 mechanised by Figure 52.

Block (10), Figure 29 mechanised by Figure 4.

Block (11), Figure 29 mechanised by Figure 5.

Block (12), Figure 29 mechanised as in Section III.A.

Block (13), Figure 29 mechanised as in Section III.A.

Block (14), Figure 29--instructor inputs as in Section III.A.

This completes the mechanisation of the tilt-wing aircraft.

Summary Tilt-Wing Aircraft. The mechanisation of the tilt-wing aircraft was accomplished by evaluating the block diagram of the aircraft (Figure 29) block by block just as for the single and tandem-rotor helicopters in accord with Figure 1. As for the helicopters, an evaluation of component complexity is done in order to choose between an AC or DC system of mechanisation. Table 23 is an accounting of the tilt-wing aerodynamics: Block (4) of Figure 29. In Table 23 the various figures that have already been considered are interpreted according to component (amplifier, servo, potentiometer, sine-cosine potentiometer and resolver) count for AC and DC mechanisations. The results of Table 23 are incorporated into Table 24 which is the total tabulation of tilt-wing components just as was done for the single rotor helicopter in Table 18. The tilt-wing summary is shown in Table 25 which corresponds to Tables 19 and 22 for the helicopters.

The complexity of the tilt-wing AC system is 566-1/4 versus 915-1/4 for the DC system. As in the AC and DC system comparisons for the helicopters, this difference in complexity is marked. Again the difference in complexity is primarily due to the greater number of amplifiers needed for the DC mechanization (the need of sign inversions for many functions) and the weight associated with the DC amplifier being greater than of the AC amplifier. Consequently, unless DC amplifiers can be redesigned to give both signs of a function and are competitive in complexity, or the choice for a DC system is based on other factors than components, the AC system is favored.

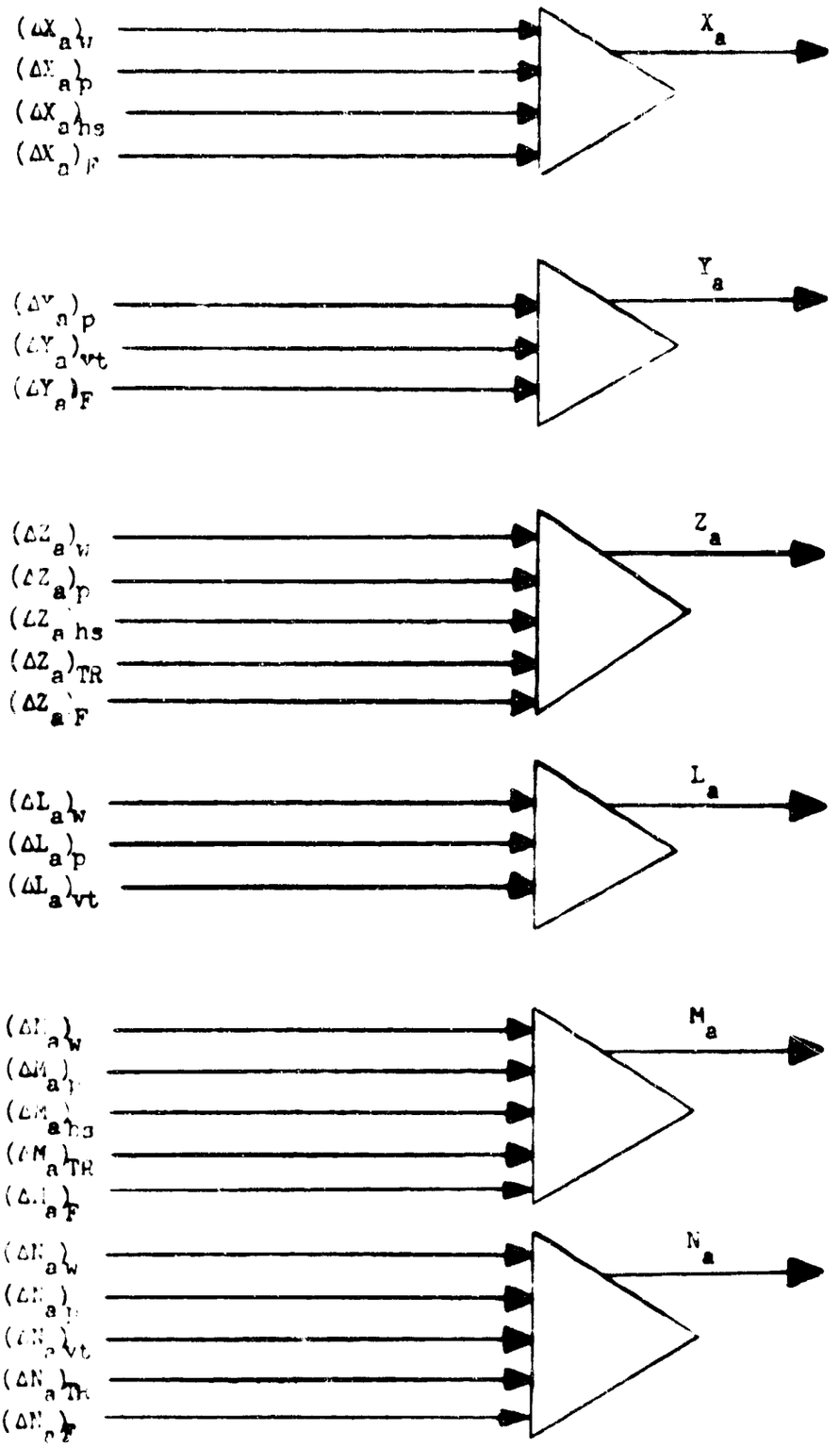

Figure 5Q Force Σ Moment Σ
AC Mechanization

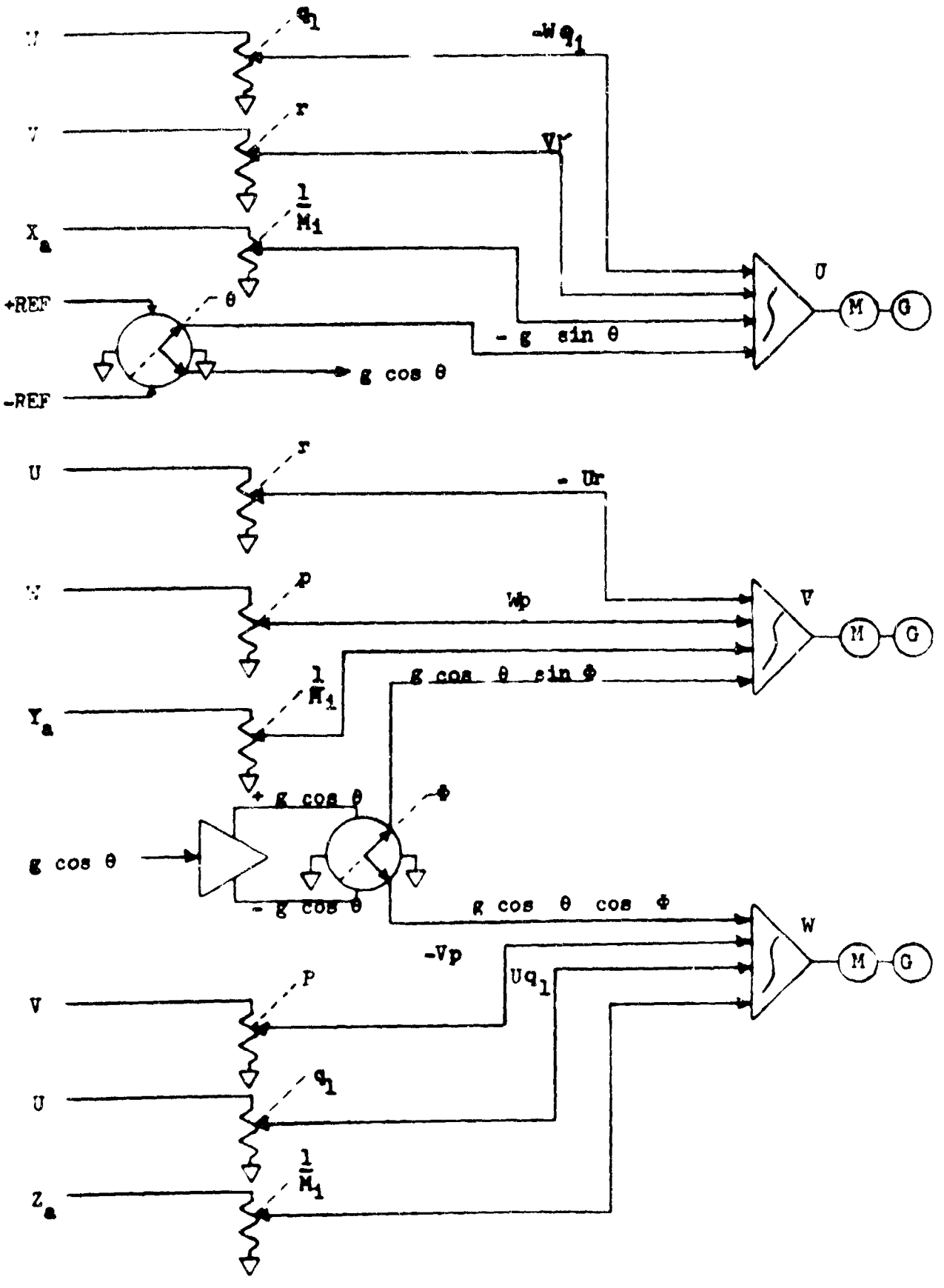

Figure 51. Integration -
Velocities (U, V, W) AC Mechanization

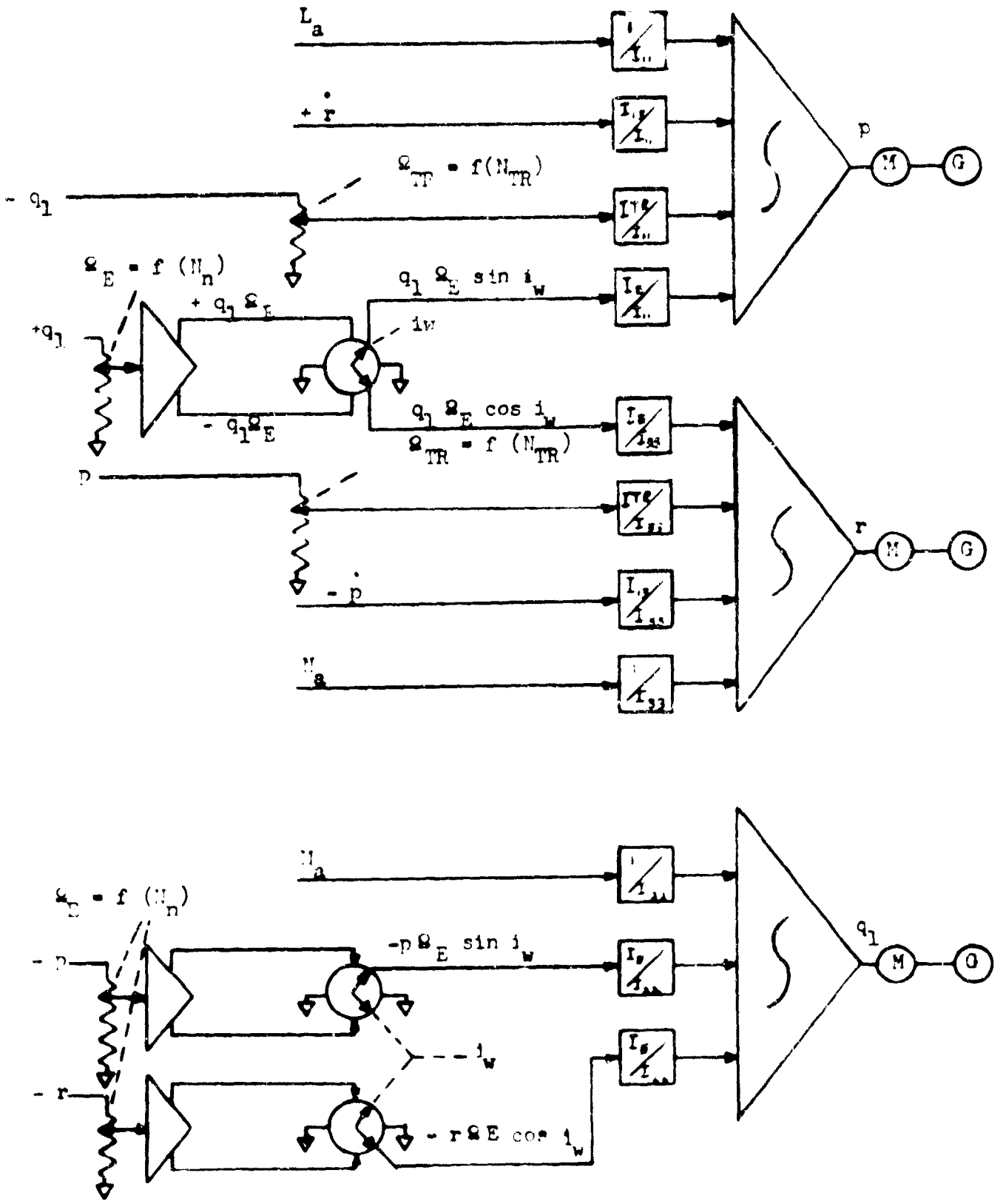

Figure 52. Integration -
Angular Velocities (p, q_1, r) AC Mechanization

Figure	Amplifier		Servo		Pot		S-C Pot		Resolver	
	AC	DC	AC	DC	AC	DC	AC	DC	AC	DC
31	13	19	1	1	8	8	4	4		
32	7	7	3	3	8	8		4	2	
33	4	4	4	4	24	24				
34	4	4	4	4	16	16				
35	8	8			16	16				
36	4	4			24	24				
37	22	38					16	16		
38	23	36					12	12		
39	3	5			2	2				
40	8	8	1	1	4	4				
41	1	1			2	2				
42	12	11	3	3	2	2		6	3	
43	5	10								
44	6	7	1	1	2	2	4	4		
45	1	1	1	1	5	5				
46	3	3			13	13				
47	9	13	1	1	9	9	2	2		
48	10	12	4	4	11	11	1	1		
49	4	7			4	9				

Table 23. Tilt-Wing Aerodynamics Tabulation Block (4)

	Amplifier		Servo		Pot		S-C Pot		Resolver	
	AC	DC	AC	DC	AC	DC	AC	DC	AC	DC
Block (2)										
Block (2)										
Block (3) Figure 30	11	13	5	5	3	3		4		
Block (4) Figure 31 to 49	147	198	23	23	155	155	39	39	5	
Block (5) Figure 50	3	3								
Block (6)	3	3	3	3	2	2				
Block (7) Figure 50	3	3								
Block (8) Figure 51	4	5	3	3	9	9	2	2		
Block (9) Figure 52	6	9	3	3	5	5	3	3		
Block (10)	9	15	3	3				6	1	
Block (11)	7	12	3	3			2	4	1	
Block (12)	2	2								
Block (13)										
Block (14)										
Total	195	263	43	43	174	174	46	58	9	

Table 24. Tilt-Wing Tabulation

	AC		DC	
	No.	Wt.	No.	Wt.
Amplifier	195	195	263	526
Servo	43	301	43	301
Pot	174	43-1/2	174	43-1/2
S-C Pot	46	11-1/2	58	22-2/3
Resolver	9	4-1/2		
Complexity		555-1/2		893-1/6

Table 25. Tilt Wing Summary

SECTION IV

SUMMARY

This report presents a set of guidelines for the selection of the optimum analog mechanization of the V/STOL simulations set forth in reports NAVTRADEVCEN 1205-1 and 1205-2. The guidelines were developed as a series of recommendations by consideration and discussion of certain aspects governing the selection of an optimum computer. These aspects are summarized below and the resultant recommendations briefly stated.

A. AIRCRAFT DATA CONVERSION FOR USE IN THE COMPUTER

Raw aircraft data supplied by the aircraft manufacturer is generally empirical in nature and supplied in the form of smooth curves. The most economical and least complex method of storing and presenting this information to the computer is through the use of tapped or shaped potentiometers driven by servo shafts. Since potentiometers may be used with equal facility in either AC or DC computers, the conversion of data does not influence the choice of computer type one way or the other.

B. SIMPLICITY OF SIMULATION EQUATIONS

To obtain an optimum simulation of a given set of simulation equations it is necessary to simplify the given equations by removal of mathematically insignificant and physically insignificant terms of the equations. This is done to the extent allowed by the required extent of simulation. The equations mechanized in this report were already in the simplified state when taken from Volumes I and II. Since the simplification of the equations is a first step in the simulation process, the optimization obtained by the simplifications would be the same in either an AC or DC computer. Hence, as with data conversion, equation simplification does not influence the choice of computer.

C. COMPUTER FLEXIBILITY

The need for flexibility in the computer used for aircraft simulation is apparent when one considers the usual requirement that the simulator be developed concurrently with the development of the aircraft to be simulated. The aircraft manufacturers are forced to work with a great deal of empirical data and consequently required to redirect design efforts in order to obtain the exact aerodynamic characteristics selected as a design goal. This results in a considerable amount of engineering changes. Since these changes are manifested as changes to the aerodynamic functions stored in tapped potentiometers it is a simple matter to retap the potentiometers in either an AC or a DC computer since both use potentiometers. Consequently, as in paragraph A. above, this aspect does not influence the computer choice.

D. COMPUTATIONAL SEQUENCE

The computational sequence used during the mechanisation of a set of simulation equations is an extremely important optimization technique. It has a direct effect on the accuracy, flexibility and complexity of the computer. However, as in A, B, and C above, it has no direct bearing on the choice of a computer type as AC or DC. Once the choice has been made to use AC or DC carrier computation, the computational sequence can be utilised to arrive at an optimum mechanisation.

E. CHOICE OF CARRIER

The choice of carrier to be used in the simulation computer is the most important aspect to be considered when making the selection of computer type. The simulation problem must be examined to determine the the computer response requirements dictated by the expected signal frequencies. In Section II this was done for the V/STOL simulation first to determine which AC carrier should be used. It was decided that if an AC carrier were to be used it should be 60 cycles. This decision was made since the advantages of accuracy and response of a 400 cycle system are overshadowed by the reduced response requirements of the V/STOL simulation, the relative ease in meeting computer size restrictions in flight simulators, and the maintenance and phase shift problems introduced by 400 cycle carriers. Having narrowed the choice to either a DC or AC system the advantages and disadvantages afforded by the various computational techniques were then discussed.

It was decided that out of the five basic computational techniques of amplification, integration, multiplication, trigonometric resolution and function generation the AC techniques afforded the best applicability to the V/STOL simulation problem in all areas except function generation and multiplication. In these two areas the techniques were found to be equally weighted. Consequently, as far as applicability of techniques is concerned, the choice of computer type is recommended as a 60 cycle AC carrier computer.

F. CHOICE OF SYSTEM

The results of the above discussions in conjunction with the component summaries of Section III indicate clearly the optimum computer to be used on the V/STOL simulation mechanisation is the 60 cycle AC computer. Not only can the mechanisation be done with less components but the cost and computer size are also reduced.

SECTION V

BIBLIOGRAPHY

1. Volume I, Helicopter Analysis Report, NAVTRADEVCEN 1205-1

2. Volume II, V/STOL Analysis Report, NAVTRADEVCEN 1205-2

3. Connelly, Mark E., Simulation of Aircraft, Report 7591-R-1, 15 February 1958

4. Connelly, Mark E., Computers for Aircraft Simulation, Report 7591-R-2, 15 December 1959

5. Northrop Aircraft, Inc., Dynamics of the Airframe, BuAer Report AE-61-111, September 1952

6. Vertol, Technical Aircraft Data for the Design and Fabrication of the Model HRB-1 Helicopter Operational Flight Trainer, Volume 3 of 3 volumes, Report No. 107-M-62.

SECTION VI

NOMENCLATURE AND EQUATIONS

A. HELICOPTER

1. NOMENCLATURE

The following list of symbols is used throughout this report. The list of symbols are arranged in alphabetical order with lower case letters listed first, then capital letters followed by greek letters and symbols of miscellaneous origin.

SYMBOL	DESCRIPTION	UNITS	POSITIVE SENSE
a_{Cw}	Rotor coning angle	radians	Up
a_{1s}	Longitudinal flap angle	radians	Rearward
b_{1s}	Lateral flap angle	radians	Right
d_x	Longitudinal center of gravity	feet	Forward of reference point
d_y	Lateral center of gravity position	feet	Right of reference point
d_z	Normal center of gravity position	feet	Below reference point
g	Gravity constant = 32.2	ft/sec^2	Downward
h_p	Pressure altitude	feet	Upwards
$\dot{h}$	Rate of climb	ft/sec	Upward
q	Incompressible dynamic pressure	lb/ft^2	
q_f	Fuselage dynamic pressure	lb/ft^2	
q_1	Pitching rate	rad/sec	Nose up
$q_{\psi-y}$	Blade element dynamic pressure	lb/ft^2	
r	Turning rate	rad/sec	Nose right
t	Air temperature	degrees C	
Δt	Ground temperature variation from standard (59°F)	degrees F	
y	Distance from blade hinge to blade station	feet	Maximum at tip

SYMBOL	DESCRIPTION	UNITS	POSITIVE SENSE
A_{1s}	Lateral control angle	degrees	Right
A_y	Blade element area	$feet^2$	
B_{1s}	Longitudinal control angle	degrees	Forward
C	Blade chord	feet	
$C_{D_{\Psi-y}}$	Blade element drag coefficient	none	
$C_{L_{\Psi-y}}$	Blade element lift coefficient	none	
$C_{T_{TR}}$	Tail rotor coefficient of thrust		
$C_{Q_{TR}}$	Coefficient of tail rotor torque	non-dimensional	Accelerates rotor
D	Drag	lbs.	Rearward
D_F	Fuselage drag force	lbs.	Rearward
$D_{\Psi-y}$	Blade element drag	lbs.	Rearward
E	East position		
$\dot{E}$	Ground speed, east	ft/sec	
F_{LW}	Force - Left wheel	lbs.	Upward
F_{RW}	Force - Right wheel	lbs.	Upward
F_{TW}	Force - Tail Wheel	lbs.	Upward
F_{X_R}	X Force due to main rotor	lbs.	Forward
F_{Y_R}	Y Force due to main rotor	lbs.	Right
H	Altitude above the field	feet	Upward
H_F	Altitude of field	feet	Upward
H_{LW}	Height left wheel above field	feet	Minus after touchdown
H_{RW}	Height right wheel above field	feet	Minus after touchdown

SYMBOL	DESCRIPTION	UNITS	POSITIVE SENSE
H_{TW}	Height tail wheel above field	feet	Minus after touchdown
I_{TOT}	Moment of inertia of rotor system as seen at main rotor	slug-ft^2	
I_x	Moment of inertia about X axis	slug-ft^2	
I_{xx_B}	Blades moment of inertia about flapping hinge	1710 slug-ft^2	
I_y	Moment of inertia about Y axis	slug-ft^2	
I_z	Moment of inertia about Z axis	slug-ft^2	
L	Lift	lbs.	Upward
L_a	Rolling moment about plane X axis	lb-ft	Right wing down
L_F	Fuselage lift force	lbs.	Upward
L_{MR}	Lift due to main rotor	lbs.	Upward
L_R	Main rotor rolling moment	lb-ft	Pushes right wing down
L_{RH}	Rotor hub rolling moment	lb-ft	Right wing down
L_ψ, L_{MR}	Rotor lift force	lbs.	Up
$L_{\psi-y}$	Blade element lift	lbs.	Upward
M	Pitching moment	lb-ft	Nose up
M_a	Pitching moment about plane Y axis	lb-ft	Nose up
MN	Mach number		
M_B	Blade mass	slugs	
M_F	Fuselage pitching moment	lb-ft	Pushes nose up
M_i	Mass of aircraft	slugs	
M_{LG}	Landing gear pitching moment	lb-ft	Pushes nose up

SYMBOL	DESCRIPTION	UNITS	POSITIVE SENSE
M_R	Effect of main rotor on pitching moment	lb-ft	Pushes nose up
M_{PH}	Rotor hub pitching moment	lb-ft	Nose up
M_{β}	Blade element aerodynamic flapping moment	ft-lbs	Moves blade tip up, increase
N	Engine rotational velocity	RPM	
$\dot{N}$	Ground speed, north	ft/sec	
N_a	Bank moment about plane Z axis	lb-ft	Nose right
N_F	Fuselage yaw moment	lb-ft	Pushes nose right
N_R	Main rotor yaw moment	lb-ft	pushes nose right
N_{TW}	Effect of tail wheel on yaw moment	lb-ft	Pushes nose right
p	Rolling rate	rad/sec	Right wing down
P_{B_L}	Pressure brake, left	$lbs-ft^2$	
P_{B_R}	Pressure Brake, right	$lbs-ft^2$	
P_S	Static pressure at sea level	in. of Hg.	
Q_{EL}	Left engine torque	ft-lbs	Speeds up rotor
Q_{ER}	Right engine torque	ft-lbs	Speeds up rotor
Q_{MR}	Main rotor torque	ft-lbs	Speeds up rotor
Q_{RB}	Rotary brake torque	ft-lbs	Speeds up rotor
Q_{TR}	Tail rotor torque	ft-lbs	Loads engine
$\frac{Q_{TR}}{q}$	Tail rotor turbulence factor	non-dimensional	

SYMBOL	DESCRIPTION	UNITS	POSITIVE SENSE
R	31 ft. Main rotor radius	feet	
R/C	Rate of climb	ft/sec	Upward
U	X axis velocity in air mass	ft/sec	Forward
U_G	Speed in X body axis direction relative to a point on the ground	ft/sec	Forward flight
$U_{P_{TR}}$	Tail rotor normal velocity	ft/sec	Positive to the right
$U_{P_{\psi-y}}$	Blade element relative velocity in air perpendicular to blade span (long) and to U_T	ft/sec	Underside of blade exposed to the wind
$U_{T_{\psi-y}}$	Blade element relative velocity in air perpendicular to blade span (long) axis and to rotor rotation axis	ft/sec	Positive in hover
U_W	Wind speed in X axis	ft/sec	Wind blows on nose
V	Y axis velocity in air mass	ft/sec	to right
V_G	Speed in Y body axis direction relative to a point on the ground	ft/sec	Flight to right
V_T	Fuselage (total) airspeed	ft/sec	Always positive
V_{TR}	Total velocity of tail rotor hub	ft/sec	Always positive
V_W	Wind speed in Y axis	ft/sec	Wind blows on right wing
W	Z axis velocity in air mass	ft/sec	Down
W_F	Fuel flow	lb/hr	Drains tank
W_G	Speed in Z Body axis direction relative to a point on the ground	ft/sec	Descent
W_i	Induced airflow in Z body axis direction	ft/sec	Air blows down
$(W_i)_{mean}$	Mean inflow velocity	ft/sec	Air blows downward
$(W_i)_{\psi-y}$	Local inflow velocity	ft/sec	Air blows down

SYMBOL	DESCRIPTION	UNITS	POSITIVE SENSE
$-W_W$	Wind speed in Z axis	ft/sec	Wind blows down
$\frac{(W_i)}{(W_i)_{mean}}$	Inflow distribution factor = F(y)		
X	Longitudinal force	lbs	Forward
X_a	Total aerodynamic force in fuselage body X direction	lbs	Forward
X_F	Fuselage longitudinal force	lbs	Forward
X_{LG}	Landing gear friction	lbs	Toward nose
Y	Lateral force	lbs	right
Y_a	Total aerodynamic force in fuselage Y direction	lbs	right
Y_B	Distance from flap hinge to blades c.g. = 8.75 ft.	ft.	
Y_F	Fuselage lateral forces	lbs	right
Y_{TR}	Side force due to tail rotor	lbs	Positive to right
Z	Normal force	lbs	Downward
Z_a	Total force in fuselage Z direction	lbs	Downward
Z_F	Fuselage normal force	lbs	Downward
Z_{LG}	Landing gear normal force	lbs	Downward
α	Angle of attack	degrees	Relative Wind from below x axis
α_F	Fuselage angle of attack	degrees	Wind comes from below x axis
α_{TR}	Tail rotor disc plane velocity angle	degrees	Relative wind from below x axis
α_{y-y}	Blade angle of attack	degrees	Wind comes from below blade x-y plane

SYMBOL	DESCRIPTION	UNITS	POSITIVE SENSE
β_F	Sideslip angle	degrees	Relative wind from right
β_B	Ball angle (instrument)	degrees	Ball right
β_{TR}	Tail rotor sideslip angle	degrees	Relative wind from right
β_ψ	Blade flap angle at azimuth	degrees	Blade tip high
$\dot{\beta}_\psi$	Rate of change of blade element flap angle	deg/sec	Blade Tip upward
θ	Pitch angle of fuselage X axis	degrees	Level = 0° Up = 90°
$\dot{\theta}$	Rate of change of Euler angle, θ (Pitch angle)	rad/sec	Nose up
θ_{TR}	Pitch of tail rotor blade at 3/4 point	degrees	Positive when leading edge is deflected toward pylon
ρ	Air density	slugs/ft^3	
Φ	Roll angle of fuselage	degrees	Positive right wing down
$\dot{\Phi}$	Rate of change of Euler Angle, Φ (Roll angle)	rad/sec	Right wing down
$\Phi_{\psi-\gamma}$	Blade element inflow angle	degrees	Wind comes from below the unpitched blade plane
ψ	True heading of fuselage X axis	degrees	North = 0° East = 90°
ψ_w	Wind heading	degrees	Wind blows toward this heading
$\dot{\psi}$	Rate of change of Euler angle ψ (Yaw angle)	rad/sec	Nose right
Ω	Rotor rotational velocity	rad/sec	Counterclockwise from top

SYMBOL	DESCRIPTION	UNITS	POSITIVE SENSE
Λ	Tail rotor solidity/advance ratio parameter	Non-dimensional	
$\mathfrak{L}$	Tail rotor velocity/thrust ratio	non-dimensional	
$\mathcal{L}_{AR}$	Aft rotor rolling moment	lb.-ft.	Roll right
$\mathcal{L}_{FR}$	Front rotor rolling moment	lb.-ft.	Roll right
$\mathcal{L}_{ARH}$	Aft rotor hub rolling moment	lb.-ft.	Roll right
$\mathcal{L}_{FRH}$	Front rotor hub rolling moment	lb.-ft.	Roll right
$\mathcal{L}_{F}$	Fuselage rolling moment	lb.-ft.	Roll right
$\mathcal{L}_{LG}$	Landing Gear rolling moment	lb.-ft.	Roll right
$\overline{\Delta}_{RA}$	Rolling moment due to rough air	lb.-ft.	Roll right
$\mathcal{L}_{f}$	Fuselage rolling moment	lb.-ft.	Roll right

4. HELICOPTER SIMULATION EQUATIONS

a. SINGLE ROTOR DEVICES

(1) FUSELAGE AERODYNAMICS

α_F, β_F, Fuselage Angle of Attack and Sideslip Angle

$$\alpha = 4^\circ + \arctan \frac{W - f\left(W_{i_{mean}}\right) f(W)}{U} \tag{6-1}$$

$$\beta = \arctan \frac{V}{\sqrt{U^2 + \left(W - f\left(W_{i_{mean}}\right) f(W)\right)^2}} \tag{6-2}$$

q_F, Fuselage Dynamic Pressure

$$q = \frac{1}{2} \rho \left[U^2 + V^2 + \left(W - f\left(W_{i_{mean}}\right) f(W)\right)^2 \right] \tag{6-3}$$

D_F, Fuselage Drag

$$D_F = q \left\{ 500 \left[1 - f(\beta_F) + f(\alpha_F) f(\beta_F) \right] + K_1 2.25 \right\} \tag{6-4}$$

K_1 = 0 for no external stores aboard

= 1.0 with external stores aboard

L_F, Fuselage Lift

$$L_F = \left\{ 91.125 \left[.309 + f(\alpha_F) \right] + K_1 5.63 \right\} q \tag{6-5}$$

K_1 = 0 for no external stores aboard

= 1.0 with external stores aboard

Fuselage Airspeed

$$V_T = \sqrt{U^2 + V^2 + \left(W - f\left(W_{i_{mean}}\right) f(W)\right)^2} \tag{6-6}$$

(2) TAIL ROTOR AERODYNAMICS

ρ_{TR}/ρ, Tail Rotor Turbulence Factor

$$\frac{\rho_{TR}}{\rho} = f(\alpha) \tag{6-7}$$

Q_{TR}, Tail Rotor Torque at Main Rotor Shaft

$$Q_{TR} = -\left[C_{Q_{TR}} \rho \pi R_{TR}^2 (\Omega R)_{TR}^2 R_{TR}\right] 6.1 \qquad (6\text{-}8)$$

$$C_{Q_{TR}} = .0084 f\left(C_{T_{TR}}\right)$$

$C_{T_{TR}}$, Tail Rotor Coefficient of Thrust

$$C_{T_{TR}} = A_{32} + B_{32};\ A_{32} = .0480 f(\theta_{TR}) + .0211 f(\theta_{TR}) f(\Lambda) \qquad (6\text{-}10)$$

$U_{P_{TR}}$, Tail Rotor Normal Velocity (Nondimensional)

$$U_{P_{TR}} = \frac{V - 36.06 r + 2.74 p}{30.5 \Omega} \qquad (6\text{-}11)$$

Λ, Tail Rotor Solidity/Advance Ratio Parameter

$$\Lambda = 0.1945 A_{34} + 0.1790 B_{34} \qquad (6\text{-}12)$$

$$A_{34} = f(\Omega) \qquad B_{34} = f(\beta_{TR})$$

α_{TR}, Tail Rotor Disc Plane Velocity Angle

$$\alpha_{TR} = \tan^{-1} \frac{W + 36.06 q_1}{U} \qquad (6\text{-}13)$$

$$0 = U \sin \alpha_{TR} - (W + 36.06 q_1) \cos \alpha_{TR}$$

β_{TR}, Tail Rotor Sideslip Angle

$$\beta_{TR} = \tan^{-1} \frac{V - 36.06 r + 2.74 p}{\sqrt{U^2 + (W + 36.06 q_1)^2}} \qquad (6\text{-}14)$$

$$0 = \sqrt{U^2 + (W + 36.06 q_1)^2} \sin \beta_{TR} - (V - 36.06 r + 2.74 p) \cos \beta_{TR}$$

V_{TR}, Total Velocity of Tail Rotor Hub

$$V_{TR} = \sqrt{U^2 + (V - 36.06r + 2.74p)^2 + (W + 36.06\, q_1)^2} \qquad (6\text{-}15)$$

$\mathcal{Q}$, Tail Rotor Velocity/Thrust Ratio

$$\mathcal{Q} = .0564\, V_{TR}\, f\left(C_{T_{TR}}\right) \qquad (6\text{-}16)$$

θ_{TR}, Pitch of Tail Rotor Blade at 3/4 Point

$$\theta_{TR} = 10.03\, \Delta C' - 4.8 \qquad (6\text{-}17)$$

$$0 \leq \Delta C' \leq 2.293$$

$$\Delta C' = .1076_R + .0676_{\theta C} + 1.77 + \text{ASE Inputs}$$

(3) LANDING GEAR

F_{RW}, Right Wheel Force

$$F_{RW} = -10{,}000\left(H_{RW} + \frac{\dot{h}}{4}\right) \qquad (6\text{-}18)$$

Only when right wheel has touched down. Otherwise zero.

F_{LW}, Left Wheel Force

$$F_{LW} = -10{,}000\left(H_{LW} + \frac{\dot{h}}{4}\right) \qquad (6\text{-}19)$$

Only when left wheel has touched down. Otherwise zero.

F_{TW}, Tail Wheel Force

$$F_{TW} = -2{,}500\left(H_{TW} + \frac{\dot{h}}{4}\right) \qquad (6\text{-}20)$$

Only when tail wheel has touched down. Otherwise zero.

(4) LONGITUDINAL FORCE

X_a, Total Longitudinal Force

$$X_a = X_F + X_{LG} + F_{X_R} + \Delta X_{RA} + X_{WH} \qquad (6\text{-}21)$$

X_F, Fuselage Longitudinal Force

$$X_F = L_F \sin \alpha_F - D_F \cos \epsilon \cos \beta_F \qquad (6\text{-}22)$$

X_{LO}, Landing Gear Force

$$X_{LO} = K \left[.025 Z_{LO} - 2.53 (P_{HR} + P_{HL}) K_0 \right. \qquad (6\text{-}23)$$

$K = +1 \qquad U_0 > 2.25$ fps

$K = 0 \qquad -2.25 < U_0 < 2.25$

$K = -1 \qquad U_0 < -2.25$ fps

(5) SIDE FORCE

Y_a, Total Side Force

$$Y_a = Y_F + Y_{TR} + F_{Y_R} + \Delta Y_{BA} + Y_{WH} \qquad (6\text{-}24)$$

Y_F, Fuselage Side Force

$$Y_F = - D_F \sin \beta_F \qquad (6\text{-}25)$$

Y_{TR}, Side Force Due to Tail Rotor

$$Y_{TR} = C_{T_{TR}} \Omega^2 \, 73{,}085 \qquad (6\text{-}26)$$

(6) DOWN FORCE

Z_a, Total Down Force

$$Z_a = Z_F + Z_{LO} - L_{HR} + \Delta Z_{BA} + Z_{WH} \qquad (6\text{-}27)$$

Z_F, Fuselage Effect

$$Z_F = - L_F \cos \alpha_F - D_F \sin \epsilon \cos \beta_F \qquad (6\text{-}28)$$

Z_{LO}, Landing Gear Force

$$Z_{LO} = - (P_{RW} + P_{LW} + P_{TW}) \qquad (6\text{-}29)$$

(7) ROLLING MOMENTS

Total Rolling Moments

$$L_a = Y_a d_z + L_R + L_{RH} + 2.74 Y_{TR} + L_{LG} + \Delta L_a + q_1 \Omega (564.5) + \ell_F + L_{WH} \quad (6\text{-}30)$$

L_R, Main Rotor Rolling Moments

$$L_R = 7.85 F_{Y_R} \quad (6\text{-}31)$$

L_{LG}, Landing Gear Rolling Moments

$$L_{LG} = 6.5 (F_{LW} - F_{RW}) \quad (6\text{-}32)$$

ℓ_F, Fuselage Effect

$$\ell_F = -574 (f(\beta)) q \qquad U > 0 \quad (6\text{-}33)$$

(8) PITCH MOMENTS

M_a, Total Pitch Moment

$$M_a = Z_a d_x - X_a d_z + M_R + M_{LG} + M_F + M_{RH} - \frac{q_{TR}}{6.1} + \Delta M_a - p\Omega (564.5) + M_{WH} \quad (6\text{-}34)$$

Horizontal Stabiliser

All horizontal stabiliser effects are cancelled due to incorporation into proper fuselage effects.

M_R, Main Rotor Effect

$$M_R = -7.85 F_{X_R} - .073 L_{MR} \quad (6\text{-}36)$$

M_{LG}, Landing Gear Pitch Moments

$$M_{LG} = 4.38 (F_{RW} + F_{LW}) - 18.99 F_{TW} + 5.36 L_{LG} \quad (6\text{-}37)$$

M_F, Fuselage Pitch Moments

$$M_F = \left\{390\ [.058 + f(\alpha)] + K_1\ 23.6\right\}\ q \qquad (6\text{-}38)$$

$K_1 = 0$ for no external stores aboard

$K_1 = 1.0$ with external stores aboard

(9) YAW MOMENTS

N_a, Total Yaw Moments

$$N_a = -Y_a d_x + N_W + N_F + N_r - 36.06\ Y_{TR} + N_{LG} - Q_{MR} + I_{TOT}\dot{\Omega} + N_R + \Delta_{N_a} + N_{WH} \qquad (6\text{-}39)$$

N_W, Wheel Yaw Moment

With either or both main wheels on ground and tail wheel on ground with tail wheel lock off

$$N_W = 2200\ U_G\ r\ K_G \qquad (6\text{-}40)$$

N_F, Fuselage Effects

$$N_F = 4228.8\ q\ f(\beta) \qquad (6\text{-}41)$$

N_r, Turning Moment Due to Turning Rate

$$-N_r = 102{,}762\ \frac{r}{V_T}\ q \qquad (6\text{-}42)$$

N_{LG}, Landing Gear Yaw Moment

$$N_{LG} = K\ 16.45\ [P_{BR} - P_{BL}]\ K_G \qquad (6\text{-}43)$$

(10) BLADE ELEMENT AERODYNAMICS

y, cos ψ, sin ψ Values

In an equation containing y, cos ψ and/or sin ψ, the equation must be computed as many times as necessary to include all combinations. That is 3 times for y alone

6 times for sin ψ and/or cos ψ alone

18 times for both y and sin ψ and/or cos ψ

Stations are distinguished by subscripts ψ-y. Thus, the 18 blade element stations are denoted 0-9.9, 0-21.8, 0-28.1, 60-9.9, 60-21.8, etc.

Tangential Velocity

$$U_{T_{\psi-y}} = (e + y)\Omega + V \cos\psi + U \sin\psi \qquad (6\text{-}44)$$

Vertical Velocity

$$U_{P_{\psi-y}} = W - W_{i_{\psi-y}} - \beta_{\psi}(0.0173) + (1.052 + y)$$

$$(q_1 \cos\psi + p \sin\psi) \qquad (6\text{-}45)$$

$$-\beta_{\psi}(U \cos\psi - V \sin\psi)\ (.0173)$$

$\phi_{\psi-y}$, Inflow Angle

$$\phi_{\psi-y} = \frac{U_{P_{\psi-y}}}{U_{T_{\psi-y}}} \text{ (radians)} \qquad (6\text{-}46)$$

Blade Angle of Attack

$$\alpha_{\psi-y} = \theta_{\psi-y} + \phi_{\psi-y} \qquad (6\text{-}47)$$

$\theta_{\psi-y}$, Pitch Angle, Degrees

$$\theta_{\psi-y} = A_{0s} - A_{1s} \cos\psi - B_{1s} \sin\psi + \theta_1 y \qquad (6\text{-}48)$$

$$A_{0s} = f(\delta_{\theta_C})$$

$$A_{1s} = f(\delta_{\theta_L}, \delta_{\theta_C}, \delta_{\theta_F})$$

$$B_{1s} = f(\delta_{\theta_L}, \delta_{\theta_C}, \delta_{\theta_F}) \qquad \theta_1 = -.258 \text{ deg/ft.}$$

ρ, Density of Atmosphere

$$\rho' = \begin{cases} 0 \text{ when } \Omega < 5 \\ \rho \text{ when } \Omega \geq 5 \end{cases}$$

$M_{\beta_\Downarrow}$, Flapping Moment (Main Rotor)

$$M_{\beta_\Downarrow} = \rho' [78.88\ U^2_{T_{\Downarrow -9.9}}\ C_{L_{\Downarrow -9.9}} + 176.9\ U^2_{T_{\Downarrow -21.8}}\ C_{L_{\Downarrow -21.8}} + 56.50\ U^2_{T_{\Downarrow -28.1}}\ C_{L_{\Downarrow -28.1}}] \quad (6\text{-}49)$$

$Q_{MR_\Downarrow}$, Q_{MR}, Main Rotor Shaft Moment

$$Q_{MR_\Downarrow} = \rho' [(78.54\ U_T\ U_P\ C_L\big|_{\Downarrow -9.9} - 73.02\ U^2_T\ C_D\big|_{\Downarrow -9.9}) + (190.0\ U_T\ U_P\ C_L\big|_{\Downarrow -21.8} - 180.3\ U^2_T\ C_D\big|_{\Downarrow -21.8}) + (60.42\ U_T\ U_P\ C_L\big|_{\Downarrow -28.1} - 106.2\ U^2_T\ C_D\big|_{\Downarrow -28.1})] \quad (6\text{-}50)$$

$$Q_{MR} = 5/6 \sum_{\Downarrow} Q_{MR_\Downarrow} \quad (6\text{-}51)$$

$L_\Downarrow$, L_{MR}, Rotor (Z) Forces

$$L_\Downarrow = \rho [7.733\ U^2_T\ C_L\big|_{\Downarrow -9.9} + 8.395\ U^2_T\ C_L\big|_{\Downarrow -21.8} + 1.969\ U^2_T\ C_L\big|_{\Downarrow -28.1}] \quad (6\text{-}52)$$

$$L_{MR} = 5/6 \left(\sum_{\Downarrow} L_\Downarrow\right) [1 + f(H) \cdot f(V_T)] \quad (6\text{-}53)$$

$D_\Downarrow$, F_{X_R}, Rotor (X) Force

$$D_\Downarrow = \rho [(6.435\ U^2_T\ C_D\big|_{\Downarrow -9.9} - 6.872\ U_T\ U_P\ C_L\big|_{\Downarrow -9.9}) + (9.340\ U^2_T\ C_D\big|_{\Downarrow -21.8} - 8.741\ U_T\ U_P\ C_L\big|_{\Downarrow -21.8}) \quad (6\text{-}54)$$

$$+ (3.38C\ U^2_T\ C_D\Big|_{\psi-28.1} - 2.046\ U_T\ U_P\ C_L\Big|_{\psi-28.1})]$$

$$F_{Y_R} = 5/6 \sum_{\psi} (.0173\beta_\psi\ L_\psi \cos\psi - D_\psi \sin\psi) \qquad (6\text{-}55)$$

F_{Y_R}, Rotor Y Force

$$K_{Y_R} = +\frac{5}{6} \sum_{\psi}^{*} [-D_\psi \cos\psi - .0173\beta_\psi\ L_\psi \sin\psi] \qquad (6\text{-}56)$$

$C_{L_{\psi-y}}$, Coefficient of Lift Function of α

$$C_{L_{\psi-y}} = k_i f(\alpha_{\psi-y}) \qquad i = 1, 2, 3, 4, 5 \qquad (6\text{-}57)$$

$U^2_T\ C_{D_{\psi-y}}$, Drag

$$U^2_{T_{\psi-y}}\ C_{D_{\psi-y}} = f(\alpha_{\psi-y}, U_{T_{\psi-y}}) \qquad (6\text{-}58)$$

β_ψ, Flap Angle

$$\beta_\psi = 57.3\ (a_{0s} - a_{1s} \cos\psi - b_{1s} \sin\psi) \qquad (6\text{-}59)$$

$$\dot{\beta}_\psi = 57.3\,\Omega\ (a_{1s} \sin\psi - b_{1s} \cos\psi) \qquad (6\text{-}5\text{?})$$

a_{0s}, a_{1s}, b_{1s}, Flap Angle Fourier Coefficients

$$a_{0s} = \frac{M\beta_0 + M\beta_{60} + M\beta_{120} + M\beta_{180} + M\beta_{240} + M\beta_{300}}{4{,}768{,}092} \qquad (6\text{-}61)$$

$$a_{1s} = \frac{M\beta_{60} + M\beta_{120} - M\beta_{240} - M\beta_{300}}{248{,}800} + b_{1s}(0.565) - a_1(1.054) \qquad (6\text{-}62)$$

$$b_{1s} = \frac{-(M_{\beta_0} + 0.5M_{\beta_{60}} - 0.5M_{\beta_{120}} - M_{\beta_{180}} - 0.5M_{\beta_{240}} + 0.5M_{\beta_{300}})}{215,460}$$

$$- a_{1s}\,(0.565) - p\,(1.054) \qquad (6\text{-}63)$$

L_{RH}, M_{RH}, Rotor Hub Moments on Fuselage

$$L_{RH} = -\rho \frac{5}{6} \sum_{\psi} L_{\psi} \sin\psi + \frac{5}{2} M_B Y_B \rho \Omega^2 b_{1s} \qquad (6\text{-}64)$$

$$M_{RH} = -\rho \frac{5}{6} \sum_{\psi} L_{\psi} \cos\psi + \frac{5}{2} M_B Y_B \rho \Omega^2 a_{1s} \qquad (6\text{-}65)$$

$(W_i)_{\psi-y}$, Local Inflow Velocity

$$(W_i)_{\psi-y} = (W_i)_{mean} \frac{(W_i)}{(W_i)_{mean}} \left(1 + \frac{X^U}{5300}\cos\psi - \frac{X^V}{5300}\sin\psi\right) \qquad (6\text{-}66)$$

(11) TRANSLATIONAL AND ANGULAR RATES

Body Axis "Ground" Velocities

$$U_0 = \int \left[\frac{X_a}{M_1} - g\sin\theta\right] dt \qquad (6\text{-}67)$$

$$V_0 = \int \left[\frac{Y_a}{M_1} + g\cos\theta\sin\phi - U_0 r\right] dt \qquad (6\text{-}68)$$

$$W_0 = \int \left[\frac{Z_a}{M_1} + g\cos\theta\cos\phi - U_0 q_1\right] dt \qquad (6\text{-}69)$$

$\dot{N}$, $\dot{E}$, $\dot{h}$, Earth Axis Velocities

$$\dot{N} = \cos\psi \left\{U_0\cos\theta + \sin\theta\,(V_0\sin\phi + W_0\cos\phi)\right\} - \sin\psi\,(V_0\cos\phi - W_0\sin\phi) \qquad (6\text{-}70)$$

$$\dot{E} = \sin \Psi \left\{ U_G \cos \theta + \sin \theta \left(V_G \sin \phi + W_G \cos \phi \right) \right\}$$

$$+ \cos \Psi \left(V_G \cos \phi - W_G \sin \phi \right) \qquad (6\text{-}71)$$

$$\dot{h} = U_G \sin \theta - \cos \theta \left(V_G \sin \phi + W_G \cos \phi \right) \qquad (6\text{-}72)$$

Wind Velocity in Body Axes

Wind blows from Ψ_W heading (true) at V_W ft/sec.

No vertical component of wind is considered.

$$-U_W = V_W \cos \theta \cos \left(\Psi - \Psi_W + 180^\circ \right) \qquad (6\text{-}73)$$

$$-V_W = V_W \left\{ \sin \theta \sin \phi \cos \left(\Psi - \Psi_W + 180^\circ \right) \right.$$

$$\left. - \cos \phi \sin \left(\Psi - \Psi_W + 180^\circ \right) \right\} \qquad (6\text{-}74)$$

$$-W_W = V_W \left\{ \sin \theta \cos \phi \cos \left(\Psi - \Psi_W + 180^\circ \right) \right.$$

$$\left. + \sin \phi \sin \left(\Psi - \Psi_W + 180^\circ \right) \right\} \qquad (6\text{-}75)$$

Relative Air Velocity in Body Axes

$$U = U_G + U_W \qquad (6\text{-}76)$$

$$V = V_G + V_W \qquad (6\text{-}77)$$

$$W = W_G + W_W \qquad (6\text{-}78)$$

Fuselage Angular Rates

$$p = \int \frac{L_a}{I_{xx}} \, dt \qquad (6\text{-}79)$$

$$q_1 = \int \frac{M_a}{I_{yy}} \, dt \qquad (6\text{-}80)$$

$$r = \int \frac{N_a}{I_{zz}} \, dt \qquad (6\text{-}81)$$

Mean Inflow Velocity

$$(W_1)'_{mean} = \frac{L_{MR}}{2\rho\pi R^2\sqrt{U^2 + \left[W - f\left(W_{1_{mean}}\right) f(W)\right]^2 + V^2}} \qquad (4-82)$$

Ω, Main Rotor Velocity

$$\dot{\Omega} = \frac{Q_{MR} + Q_{TR} + Q_{ER} + Q_{EL} + Q_{RB} - 1700}{10,275} \qquad (4-83)$$

North and East Positions, Altitude

$$N = \int \dot{N}\, dt \qquad (4-84)$$

$$E = \int \dot{E}\, dt \qquad (4-85)$$

$$h = \int \dot{h}\, dt \qquad (4-86)$$

Heading Angle

$$\dot{\Psi} = (r \cos \Phi + q_1 \sin \Phi) \sec \theta \quad \text{rdns/sec.} \qquad (4-87)$$

$$\Psi = 57.3 \int \dot{\Psi}\, dt \quad \text{degrees}$$

Pitch Angle

$$\dot{\theta} = q_1 \cos \Phi - r \sin \Phi \quad \text{rdns/sec} \qquad (4-88)$$

$$\theta = 57.3 \int \dot{\theta}\, dt \quad \text{degrees}$$

Roll Angle

$$\dot{\Phi} = p + \dot{\Psi} \sin \theta \quad \text{rdns/sec} \qquad (4-89)$$

$$\Phi = 57.3 \int \dot{\Phi}\, dt \quad \text{degrees}$$

(12) MASS AND INERTIA

Center of Gravity Position (Feet)

$$d_x = -.917 + .333\, K_1 + .333\, K_2 - .0086\, M_{f_{fwd}} + .0094\, M_{f_{aft}} \qquad (4-90)$$

$$d_z = 0$$

$$d_y = 0$$

b. TANDEM ROTOR DEVICES

(1) FUSELAGE AERODYNAMICS

α_F, β_F Fuselage Angle of Attack and Sideslip Angles

$$\alpha_F = 9.5^\circ + \tan^{-1}\frac{\left[W - f\left(W_{i_{AV}}\right) f(W)\right]}{U} \tag{6-91}$$

$$\beta_F = \tan^{-1}\left[\frac{V}{\sqrt{U^2 + \left[W - f(W_{i_{AV}})\, f(W)\right]^2}}\right]$$

q_F Fuselage Dynamic Pressure

$$q = \frac{1}{2}\rho\left[V^2_T - 33900\, f(W)\, f\left(W_{i_{AV}}\right) + 21238\, f(W) f\left(W_{i_{AV}}\right)\right] \tag{6-92}$$

L_F, Fuselage Lift

$$L_F = q_y\, f(\beta_F) + q_z\, f(\alpha_F) \tag{6-93}$$

D_F, Fuselage Drag

$$D_F = q_y f(\beta_F) + q_z f(\alpha_F) \tag{6-94}$$

Fuselage Airspeed

$$V_T = \sqrt{U^2 + V^2 + \left[W - f\left(W_{i_{AV}}\right) f(W)\right]^2} \tag{6-95}$$

(2) LANDING GEAR

Z_{LG}

$$Z_{LG} = -[f(H) - K_1\dot{h}]K_H[94000 - 8360\,(.025 + K_{RWB} + K_{LWB})\frac{U_G}{|U_G|}] \tag{6-96}$$

Y_{LG}

$$Y_{LG} = -[f(H) - K_1\dot{h}]K_H[8360 + 94000\,(.025 + K_{RWB} + K_{LWB})\frac{U_G}{|U_G|}] \tag{6-97}$$

η_{LO} Landing Gear Rolling Moment

$$\eta_{LO} = Z_{LO} [K_2 \Phi - K_3 p] \tag{6-98}$$

(3) LONGITUDINAL FORCE

X_a, Total Longitudinal Force

$$X_a = X_F + F_{X_{FR}} + F_{X_{AR}} + \Delta X_{RA} + X_{LO} - .0436 L_{AR} \tag{6-99}$$

X_F, Fuselage Longitudinal Force

$$X_F = - 0.986 D_F - 0.165 L_F \tag{6-100}$$

(4) SIDE FORCE

Y_a, Total Side Force

$$Y_a = Y_F + F_{Y_{FR}} + \Delta Y_{RA} + F_{Y_{AR}} \tag{6-101}$$

Y_F Fuselage Side Force

$$Y_F = - q_y f(\beta_y) \tag{6-102}$$

(5) DOWN FORCE

Z_a, Total Down Force

$$Z_a = Z_F - L_{FR} - L_{AR} + \Delta Z_{RA} + Z_{LO} \tag{6-103}$$

(6) VERTICAL FORCES

Z_F, Fuselage Effect

$$Z_F = 0.165 D_F - 0.986 L_F \tag{6-104}$$

(7) ROLLING MOMENTS

L_a, Total Rolling Moment

$$L_a = + \eta_{AR} + \eta_{FR} + \eta_{FRH} + \eta_{ARH} + \eta_F \tag{6-105}$$

$$- Z_a d_y + \Delta \rceil_{RA} + \rceil_{LO} + .0436\, q_{AR}$$

$\rceil_{FR}, \rceil_{AR}$, Rotor Rolling Moments (6-106)

$$\rceil_{FR} = (8.48)\ (F_{Y_{FR}})$$

$$\rceil_{AR} = (7.65\ (F_{Y_{AR}}) \quad (6\text{-}107)$$

$\rceil_F$, Fuselage Rolling Moment

$$\rceil_F = q\, f(\beta_F) + q[f\ (\alpha_F)\ f(\beta_F)] - K_1 p, \quad (6\text{-}108)$$

K_1 to be determined

(8) PITCH MOMENTS

M_a, Total Pitch Moment

$$M_a = Z_a d_x + M_{FR} + M_{AR} + M_{LO} + \Delta M_{RA} \quad (6\text{-}109)$$

M_{FR}, M_{AR} Rotor Pitching Moments

$$M_{FR} = - 8.48\, F_{X_{FR}} + 16.49\, L_{FR} \quad (6\text{-}110)$$

$$M_{AR} = - [8.377\, F_{X_{AR}} + 16.49\, L_{AR}] \quad (6\text{-}111)$$

(9) YAW MOMENTS

N_a, Total Yaw Moment

$$N_a = - Y_a d_x + N_F - Q_{FR} + Q_{AR} + N_{LO} + \Delta N_{RA} + N_{FR} + N_{AR} \quad (6\text{-}113)$$

N_{FR}, N_{AR} Rotor Yaw Moments

$$N_{FR} = 16.49\ F_{Y_{FR}} \qquad (6\text{-}114)$$

$$N_{AR} = -16.84\ F_{Y_{AR}} \qquad (6\text{-}115)$$

N_F Fuselage Yaw Moments

$$N_F = q\ f(\beta_F) - K_1 r \qquad K_1 \text{ to be determined} \qquad (6\text{-}116)$$

(10) MOMENTS TURNING

N_r, Turning Moment Due to Turning Rate

$$-N_r = K_1 \frac{r}{V_T} q \qquad (6\text{-}117)$$

$$= K_2 \rho V_T$$

(11) BLADE ELEMENT AERODYNAMICS

y, cos Y, sin Y values

In an equation containing y, cos Y and/or sin Y, the equation must be computed as many times as necessary to include all combinations of the forward rotor. That is 3 times for y alone. Six times for sin Y and/or cos Y alone. Eighteen times for both y and sin Y and/or cos Y.

Stations are distinguished by subscripts Y-y. Thus, the 18 blade element stations for each rotor are denoted (0° -y) FR, (60° -y) FR, (0° -y) AR, (60°-y) AR, etc. The subscript FR or AR denotes forward rotor blade station or aft rotor blade station

$U_{T_{Y-y}}$ Tangential Velocity

$$U_{T_{Y-y}} = (e + y)\Omega + V \cos Y + U \sin Y \qquad (6\text{-}118)$$

$U_{P_{(\Psi-y)FR}}$ Local Vertical Velocity

$$U_{P_{\Psi-y}} = W - W_{i_{\Psi-y}} - y\dot{\beta}_{\Psi}(0.0173) + (e + y) \tag{6-119}$$

$$(q_1 \cos \Psi + p \sin \Psi)$$

$$-\beta_{\Psi}(U \cos \Psi - V \sin \Psi)(.0173) - 16.49\, q_1$$

$\Phi_{(\Psi-y)FR}$, $\Phi_{(\Psi-y)AR}$ Inflow Angle

$$\Phi_{\Psi-y} = \frac{U_{P\ \Psi-y}}{U_{T\ \Psi-y}} \quad \text{(RADIAN)} \tag{6-120}$$

$\alpha_{(\Psi-y)}$ Blade Angle of Attack

$$\alpha_{\Psi-y} = \theta_{\Psi-y} + \Phi_{\Psi-y} \tag{6-121}$$

$\theta_{(\Psi-y)FR}$ and $\theta_{(\Psi-y)AR}$ Pitch Angle, Degrees

$$\theta_{\Psi-y} = A_{0s} - A_{1s} \cos \Psi - B_{1s} \sin \Psi - \theta_{1y} \tag{6-122}$$

$M_{\beta_{\Psi}}$, Flapping Moments

$$M_{\beta_{\Psi}} = \rho[52.8\, U^2_{T_{(\Psi-7.3)}} C_{L_{(\Psi-7.3)}} + 132.6\, U_T^2{}_{(\Psi-17)} \tag{6-123}$$

$$C_{L_{(\Psi-17)}} + 23.1\, U_T^2{}_{(\Psi-23.1)}\ C_{L_{(\Psi-23.1)}}]$$

$Q_{\Psi_{FR}}$, C_{FR}, Q_{AR} Rotor Shaft Moments

$$Q_{\Psi_{FR}} = 55\, U_T U_p C_L\Big|_{(\Psi-7.3)FR} - 41\, U_T{}^2 C_D\Big|_{(\Psi-7.3)FR} \tag{6-124}$$

$$+ 70\, U_T U_p C_L\Big|_{(\Psi-17)FR} - 170\, U_T{}^2 C_D\Big|_{(\Psi-17)FR}$$

$$+ 20\ U_T U_P C_L\Big|_{(Y-23.1)FR} - 13\ U_T{}^2 C_D\Big|_{(Y-23.1)FR}]$$

$$\gamma_{FR} = \frac{1}{2} \sum_{\Psi} \gamma_{Y_{FR}} \cdot f(A_{Os_{FR}}) \cdot f(U) \qquad (6\text{-}125)$$

$$\gamma_{AR} = \frac{A_{O_3{}_{AR}}}{A_{Os_{FR}}} \gamma_{FR} \cdot f(V) \cdot f(A_{Os_{FR}}) + f(A_{O_3{}_{FR}})[\gamma_{FR} + 1000(A_{Os_{AR}} - A_{O_3{}_{FR}})] \qquad (6\text{-}126)$$

$L_{Y_{FR}}$, L_{FR}, L_{AR} Rotor (Z) Forces

$$L_{Y_{FR}} = \rho[7.5\ U_T{}^2 C_L\Big|_{(Y-7.3)} + 7.8\ U_T{}^2 C_L\Big|_{(Y-17)} + U_T{}^2 C_L\Big|_{(Y-23.1)}] \qquad (6\text{-}127)$$

$$L_{FR} = \frac{1}{2} \left(\sum_{\Psi} L_{Y_{FR}}\right) [1 + f(H) \cdot f(V_T)]\ 1.10\ f(U) \qquad (6\text{-}128)$$

$$L_{AR} = 1.194\ L_{FR} \cdot \frac{A_{O_3{}_{AR}}}{A_{Os_{FR}}} \cdot f(U) \cdot f(V) \cdot f(A_{Os_{FR}})$$

$$+ f(A_{Os_{FR}})\ [L_{FR} + 1000\ \Delta A_{Os}] + 1000 |\Delta A_{Os}| K_{FRS} + 2000\ q_1 \qquad (6\text{-}129)$$

$K_{FRS} = 1.0$ when $L_{FR} \geq L_{MAX}$

$= 0$ otherwise

$L_{AR} = L'_{AR}$ when $L'_{AR} \leq L_{MAX}$

$= L_{MAX}$ when $L'_{AR} > L_{MAX}$

$L_{MAX} = (6.5 \times 10^6)\rho \cdot f(U)$

$D_{Y_{FR}}$, $F_{X_{FR}}$, $F_{X_{AR}}$ Rotor (X) Forces

$$D_{Y_{FR}} = \rho \Big[(7.43\ U_T^2 C_D\big|_{(\Psi-7.3)} - 7.5\ U_T U_P C_L\big|_{(\Psi-7.3)}) + (4.38\ U_T^2 C_D\big|_{(\Psi-17)FR} - 7.8\ U_T U_P C_L\big|_{(\Psi-17)}) + (6.37\ U_T^2 C_D\big|_{(\Psi-23.1)} - U_T U_P C_L\big|_{(\Psi-23.1)}) \Big] \quad (6\text{-}130)$$

$$F_{X_{FR}} = \frac{1}{2} \sum_{\Psi} (.0173\ \beta_{Y_{FR}} L_{Y_{FR}} \cos\Psi - D_{Y_{FR}} \sin\Psi) \quad (6\text{-}131)$$

$$F_{X_{AR}} = F_{X_{FR}} + 300\ f(U) \cdot f(V) \cdot f(\Omega)\ \Delta B_{1s}$$

$F_{Y_{FR}}$, $F_{Y_{AR}}$ Rotor (Y) Forces

$$F_{Y_{FR}} = \frac{1}{2} \sum_{\Psi} [-D_{Y_{FR}} \cos\Psi - .0173\ \beta_{Y_{FR}} L_{Y_{FR}} \sin\Psi] \quad (6\text{-}133)$$

$$F_{Y_{AR}} = F_{Y_{FR}} + 300\ f(U) \cdot f(V) \cdot f(\Omega)\ \Delta A_{1s} \quad (6\text{-}134)$$

$C_{L_{Y-y}}$. Coefficient of Lift

$$C_{L_{Y-y}} = K_i\ f(\alpha_{Y-y}) \qquad i = 1, 2, 3, 4, 5 \quad (6\text{-}135)$$

$U_T^2 C_{D_{\Psi-Y}}$

$$U_{T_{\Psi-y}}^2 \; C_{D_{(\Psi-y)}} = f(\alpha_{\Psi-y},\ U_{T_{\Psi-y}}) \tag{6-136}$$

β_Y, Flap Angle, FR, $\dot{\beta}_Y$

$$\beta_{Y_{FR}} = 57.3(a_{0s_{FR}} - a_{1s_{FR}} \cos Y - b_{1s_{FR}} \sin Y) \text{ deg.} \tag{6-137}$$

$$\dot{\beta}_{Y_{FR}} = 57.3\Omega(a_{1s_{FR}} \sin Y - b_{1s_{FR}} \cos Y) \text{ deg/sec.} \tag{6-138}$$

a_{0s}, a_{1s}, b_{1s}, Flap Angle Fourier Coefficients

$$a_{0s_{FR}} = \frac{M_{\beta 0_{FR}} + M_{\beta 60_{FR}} + M_{\beta 120_{FR}} + M_{\beta 180_{FR}} + M_{\beta 240_{FR}} + M_{\beta 300_{FR}}}{4,550,253} \tag{6-139}$$

$$\dot{a}_{1s_{FR}} = \frac{M_{\beta 60_{FR}} + M_{\beta 120_{FR}} - M_{\beta 240_{FR}} - M_{\beta 300_{FR}}}{184,807}$$

$$+ b_{1s_{FR}}(.390) - 1.028q_1 \tag{6-140}$$

$$b_{1s_{FR}} = \frac{M\beta_{0_{FR}} + 0.5\, M\beta_{60_{FR}} - 0.5\, M\beta_{120_{FR}} - M\beta_{180_{FR}} - 0.5\, M\beta_{240_{FR}} + 0.5\, M\beta_{300_{FR}}}{160,043}$$

$$- a_{1s_{FR}}(.390) - 1.028\, p \qquad (6\text{-}141)$$

$\underline{\tau_{FRH},\ \tau_{ARH},\ H_{FRH},\ M_{ARH}\ \text{Rotor Hub Moments on Fuselage}}$

$$\tau_{FRH} = -.2125 \sum_{\Psi} (L_{YFR} \sin \Psi) + 41 \Omega^2 b_{1s_{FR}} \qquad (6\text{-}142)$$

$$\tau_{ARH} = \tau_{FRH} + 610\, \Delta A_{1s}\, K \Omega \qquad (6\text{-}143)$$

$$H_{FRH} = -.2125 \sum_{\Psi} I_{YFR} \cos \Psi + 41 \Omega^2 a_{1s_{FR}} \qquad (6\text{-}144)$$

$$M_{ARH} = M_{FRH} + K\, \Delta B_{1s} \qquad (6\text{-}145)$$

$\underline{W_{i_{(\psi-\gamma)}},\ \text{Local Inflow Velocity}}$

$$(W_i)_{(\psi-\gamma)} = (W_i)_{(mean)} \left(\frac{W_{i_\gamma}}{W_{i_{mean_{FR}}}} \right) \left(1 + \frac{V_U}{4690} \cos \psi - \frac{V_V}{4690} \sin \psi \right) \qquad (6\text{-}145a)$$

(12) TRANSLATIONAL AND ANGULAR RATES

$\underline{\text{Body Axes "Ground" Velocities}}$

$$U_0 = \int \left[\frac{X_a}{M_1} - g \sin (\theta - 9.5) \right] dt \qquad (6\text{-}146)$$

$$V_0 = \int \left[\frac{Y_a}{M_1} + g \cos (\theta - 9.5) \sin \Phi - U_0\, r \right] dt \qquad (6\text{-}147)$$

$$W_0 = \int \left[\frac{Z_a}{M_1} + g \cos (\theta - 9.5) \cos \Phi + U_0\, q_1 \right] dt \qquad (6\text{-}148)$$

$\dot{N}$, $\dot{E}$, $\dot{h}$ Earth Axes Velocities

$$\dot{N} = \cos\Psi\,[U_0 \cos(\theta_y - 9.5) + \sin(\theta_y - 9.5)(V_0 \sin\Phi + W_0 \cos\Phi)]$$
$$- \sin\Psi\,(V_0 \cos\Phi - W_0 \sin\Phi) \qquad (6\text{-}149)$$

$$\dot{E} = \sin\Psi\,[U_0 \cos(\theta_y - 9.5) + \sin(\theta_y - 9.5)(V_0 \sin\Phi + W_0 \cos\Phi)]$$
$$+ \cos\Psi\,(V_0 \cos\Phi - W_0 \sin\Phi) \qquad (6\text{-}150)$$

$$\dot{h} = U_0 \sin(\theta_y - 9.5) - \cos(\theta_y - 9.5)(V_0 \sin\Phi + W_0 \cos\Phi) \qquad (6\text{-}151)$$

Wind Velocity in Body Axes

Wind Blows from Ψ_W Heading (True) at V_W ft/sec

No Vertical Component of Wind is Considered

$$-U_W = V_W \cos(\theta_y - 9.5)\cos(\Psi - \Psi_W + 180^\circ) \qquad (6\text{-}152)$$

$$-V_W = V_W\{\sin(\theta_y - 9.5)\sin\Phi\cos(\Psi - \Psi_W + 180^\circ) + \cos\Phi\sin$$
$$(\Psi - \Psi_W + 180^\circ)\} \qquad (6\text{-}153)$$

$$-W_W = V_W\{\sin(\theta_y - 9.5)\cos\Phi\cos(\Psi - \Psi_W + 180^\circ)$$
$$+ \sin\Phi\sin(\Psi - \Psi_W + 180^\circ)\} \qquad (6\text{-}154)$$

Relative Velocity in Air in Body Axes

$$U = U_0 + U_W \qquad (6\text{-}155)$$

$$V = V_0 + V_W \qquad (6\text{-}156)$$

$$W = W_0 + W_W \qquad (6\text{-}157)$$

Fuselage Angular Rates

$$p = \int \frac{\dot{p}}{I_{xx}}\,dt \qquad (6\text{-}158)$$

$$q_1 = \int \frac{M_a}{I_{yy}} dt \qquad (6\text{-}159)$$

$$r = \int \frac{N_a}{I_{zz}} dt \qquad (6\text{-}160)$$

Mean Inflow Velocity

$$w_{i'_{(mean)FR}} = \frac{.00028\ L_{FR}}{\rho V_T} \qquad .00028 = \frac{1}{2\pi R^2} \qquad (6\text{-}161)$$

Ω, Rotor Angular Velocity

$$\dot{\Omega} = \frac{Q_{FR} + Q_{AR} + Q_{ER} + Q_{EL} + Q_{RB} - K_1}{I_{TOT}} \qquad (6\text{-}162)$$

$$I_{TOT} = I_{FR} + I_{AR}$$

North and East Positions, Altitude

$$N = \int \dot{N}\, dt \qquad (6\text{-}163)$$

$$E = \int \dot{E}\, dt \qquad (6\text{-}164)$$

$$h = \int \dot{h}\, dt \qquad (6\text{-}165)$$

Heading Angle

$$\dot{\Psi} = (r \cos\Phi + q_1 \sin\Phi) \sec(\theta_T - 9.5) \quad \text{RDNS/SEC} \qquad (6\text{-}166)$$

$$\Psi = 57.3 \int \dot{\Psi}\, dt \quad \text{DEGREES}$$

Pitch Angle

$$\dot{\theta} = q_1 \cos\Phi - r \sin\Phi \quad \text{RDNS/SEC} \qquad (6\text{-}167)$$

$$\theta = 57.3 \int \dot{\theta}\, dt\ ; \quad \theta_T = \theta + 9.5^\circ \quad \text{DEGREES}$$

Roll Angle

$$\dot{\Phi} = p + \dot{\Psi} \sin(\theta_T - 9.5) \quad \text{RDNS/SEC} \qquad (6\text{-}168)$$

$$\Phi = 57.3 \int \dot{\Phi}\, dt \quad \text{DEGREES}$$

dx, dy, dz, Center of Gravity Position

$$dx = .300 - .00687 \left(M_{f_R} + M_{f_L}\right) + f\,(INST) \qquad (6\text{-}169)$$

$$dy = \left[5.14\, M_{f_R} - 5.14\, M_{f_L}\right] / M_i$$

$$dz = 0$$

V. V/STOL AIRCRAFT (TILT-WING)

1. NOMENCLATURE USED IN XC-142A EQUATIONS

Symbol	Definition
b	Wing Span
c	Mean Aerodynamic Chord
i_t	Incidence Angle Horizontal Stabiliser
i_w	Incidence Angle - Wing
n	Main Propellers n=1, 2, 3, 4 - Top View Left to Right, looking forward
q	Dynamic Pressure - Free Stream
q_{HS}	Dynamic Pressure at Horizontal Stabiliser
q_{VT}	Dynamic Pressure at Vertical Tail
q_w	Dynamic Pressure due to Power on Wing Effects
β_n	Blade Pitch Angle - Main Propeller
$C_{T,S}$	Coefficient of Thrust at Wing Due to Inflow Velocity
D_n	Diameter Main Propeller
D_{TR}	Diameter Tail Rotor
F	Fuselage
HS	Horizontal Stabiliser
I_E	Inertia of Main Propeller Blades and Shaft
I_{TR}	Inertia of Tail Rotor Blades and Shaft
J_n	Advance Ratio Main Propeller

Symbol	Definition
J_{TR}	Advance Ratio Tail Propeller or Rotor
M_n	Main Propeller Moment (Initially Pitching)
N_n	Main Propeller Thrust Component Normal to T_n
N_n	RPM - Main Propeller
N_o	Nominal RPM - Main Propeller
N_{TR}	RPM - Tail Propeller
Q_n	Main Propeller Torque Coefficient
S	Total Area of Wing
S_p	Total Area of Main Propeller Disks
T	Total Thrust of Main Propellers
T_n	Main Propeller Thrust
TR	Tail Propeller or Rotor
T_{TR}	Thrust - Tail Rotor
V_B	Total Velocity in Aircraft Body Axes
VT	Vertical Tail
V_w	Total Velocity in Wind Stability Axes
W	Wing
Y_n	Main Propeller Moment (Initially Turning)
α_F	Angle of Attack - Fuselage
α_{HS}	Angle of Attack - Horisontal Stabiliser
α_w	Angle of Attack - Wing
β_F	Sideslip Angle - Fuselage
β_{TR}	Blade Pitch Angle - Tail Rotor
β_w	Sideslip Angle - Wing
ϵ	Downwash Angle

Symbol	Definition
Ω_e	Angular Velocity Main Propeller
$\dot{\Omega}_e$	Angular Acceleration Main Propeller
I_{TR}	Inertia of tail rotor blades and shaft
Ω_{TR}	Angular velocity tail rotor
$\dot{\Omega}_{TR}$	Angular Acceleration Tail Rotor

2. TILT WING AIRCRAFT SIMULATION EQUATION

a. AERODYNAMIC VARIABLES

$$\alpha_F = \tan^{-1}\left(\frac{W}{U}\right) \tag{6-170}$$

$$\beta_F = \tan^{-1}\left(\frac{V}{\sqrt{U^2 + W^2}}\right) \tag{6-171}$$

$$V_B = \sqrt{U^2 + W^2 + V^2}$$

$$q = 1/2\ \rho V_B^2 \tag{6-173}$$

$$\rho = f(h_F)$$

b. MAIN PROPELLER AERODYNAMICS

$$\psi_o = (i_w + \alpha_F) \tag{6-175}$$

$$u_n = V_B \cos\beta_F \cos\psi_o - y_n(p \sin i_w + r \cos i_w) + x_n q_1 \sin i_w + s_n q_1 \cos i_w \tag{6-176}$$

$$v_n = V_B \sin\beta_F \tag{6-177}$$

$$w_n = V_B \cos\beta_F \sin\psi_o + y_n(p \cos i_w - r \sin i_w) - x_n q_1 \cos i_w + s_n q_1 \sin i_w \tag{6-178}$$

$$J_n = \frac{60}{N_n D} V_n \tag{6-179}$$

$$V_n = \sqrt{u_n^2 + v_n^2 + w_n^2}$$

$$J_n' = J_n \cos \psi_n = \left(\frac{60}{D}\right)\left(\frac{u_n}{N_n}\right) \tag{6-180}$$

$$J_n \sin \psi_n = \left(\frac{60}{D}\right)\left(\frac{\sqrt{w_n^2 + v_n^2}}{N_n}\right) \tag{6-181}$$

$$C_{T_n} = C_{T_o} + \frac{\partial C_T}{\partial J'} J_n' + \frac{\partial^2 C_T}{\partial J'^2} (J_n')^2 + \frac{\partial C_T}{\partial B} B_n + \frac{\partial^2 C_T}{\partial B \partial J'} B_n J_n' \tag{6-182}$$

$$C_{P_n} = C_{P_o} + \frac{\partial C_P}{\partial J'} J_n' + \frac{\partial^2 C_P}{\partial J'^2} (J_n')^2 + \frac{\partial C_P}{\partial B} B_n + \frac{\partial^2 C_P}{\partial B \partial J'} B_n J_n' \tag{6-183}$$

$$C_{N_n} = \frac{\partial}{\partial B}\left[\frac{\partial (C_N \cot \psi)}{\partial J'}\right] B_n J_n \sin \psi_n \tag{6-184}$$

$$C_{Y_n} = \frac{\partial}{\partial B}\left[\frac{\partial (C_Y \cot \psi)}{\partial J'}\right] B_n J_n \sin \psi_n + \frac{\partial}{\partial J'}$$

$$\left[\frac{\partial (C_Y \cot \psi)}{\partial J'}\right] J_n' J_n \sin \psi_n \tag{6-185}$$

$$C_{M_n} = \frac{\partial}{\partial J'}\left(\frac{\partial C_M}{\partial \psi}\right) \psi_n J_n' \tag{6-186}$$

$$T_n = D^4 \left(\frac{N_n}{N_o}\right)^2 \left(\frac{\rho}{\rho_o}\right) C_{T_n} \tag{6-187}$$

$$N_n = D^4 \left(\frac{N_n}{N_o}\right)^2 \left(\frac{\rho}{\rho_o}\right) C_{N_n} \tag{6-188}$$

$$Y_n = D^5 \left(\frac{N_n}{N_o}\right)^2 \left(\frac{\rho}{\rho_o}\right) C_{Y_n} \tag{6-189}$$

$$M_n = D^5 \left(\frac{N_n}{N_o}\right)^2 \left(\frac{\rho}{\rho_o}\right) C_{M_n} \tag{6-190}$$

$$C_n = \frac{D^5}{2^n h}\left(\frac{N_n}{N_o}\right)^2\left(\frac{\rho}{\rho_o}\right)C_{P_n} \qquad (6\text{-}191)$$

$$(\Delta X_a)_p = \sum_{n=1}^{4}(T_n \cos i_w - N_n \cos\beta_n \sin i_w) \qquad (6\text{-}192)$$

$$(\Delta Y_a)_p = \sum_{n=1}^{4}(-N_n \sin\beta_n) \qquad (6\text{-}193)$$

$$(\Delta Z_a)_p = \sum_{n=1}^{4}(-T_n \sin i_w - N_n \cos\beta_n \cos i_w) \qquad (6\text{-}194)$$

$$\begin{aligned}(\Delta L_a)_p = &-[(\Delta Z_a)_{p1} - (\Delta Z_a)_{p4}]\,y_1 - [(\Delta Z_a)_{p2} - (\Delta Z_a)_{p3}]\,y_2 \\ &-[(\Delta Y_a)_{p1} + (\Delta Y_a)_{p4}]\,z_1 - [(\Delta Y_a)_{p2} + (\Delta Y_a)_{p3}]\,z_2 \\ &-\sum_{n=1}^{4}(X_n \cos\beta_n)\sin i_w - \sum_{n=1}^{4}(N_n \sin\beta_n)\sin i_w\end{aligned} \qquad (6\text{-}195)$$

$$\begin{aligned}(\Delta M_a)_p = &M_{T_{Pivot}} + \sum_{n=1}^{4}T_n(\cos i_w)\,s_{Pivot} + \sum_{n=1}^{4}T_n(\sin i_w)\,x_{Pivot} \\ &-(N_1 \cos\beta_1 \sin i_w + N_4 \cos\beta_4 \sin i_w)\,Z_1 \\ &-(N_2 \cos\beta_2 \sin i_w + N_3 \cos\beta_3 \sin i_w)\,Z_2 \\ &+(N_1 \cos\beta_1 \cos i_w + N_4 \cos\beta_4 \cos i_w)\,X_1 \\ &+(N_2 \cos\beta_2 \cos i_w + N_3 \cos\beta_3 \cos i_w)\,X_2 \\ &-\sum_{n=1}^{4}(X_n \sin\beta_n) + \sum_{n=1}^{4}(N_n \cos\beta_n)\end{aligned} \qquad (6\text{-}196)$$

where $M_{T_{Pivot}} = 1.625(T_1 + T_4) + 1.092(T_2 + T_3)$

$$(\Delta N_a)_p = -[(\Delta X_a)_{p1} - (\Delta X_a)_{p4}]y_1 - [(\Delta X_a)_{p2} - (\Delta X_a)_{p3}]y_2$$

$$+[(\Delta Y_a)_{p1} + (\Delta Y_a)_{p4}]x_1 + [(\Delta Y_a)_{p2} + (\Delta Y_a)_{p3}]x_2 \quad (6\text{-}197)$$

$$- \sum_{n=1}^{4} (Y_n \cos\beta_n) \cos i_w - \sum_{n=1}^{4} (M_h \sin\beta_n) \cos i_w$$

c. WING AERODYNAMICS

$$w_p = w_w = -U \sin i_w + W \cos i_w \quad (6\text{-}198)$$

$$u_p = U \cos i_w + W \sin i_w = V_B \quad (6\text{-}199)$$

$$v_w = (u_p + \Delta V) \qquad V = v_w \quad (6\text{-}200)$$

$$\Delta V = u_p + \left(u_p^2 + \frac{2T}{\rho S_p}\right)^{1/2} \quad (6\text{-}201)$$

$$C_{T,S} = T/q_w S_p \quad (6\text{-}202)$$

$$q_w = (q + T/S_p) \quad (6\text{-}203)$$

$$V_w = [w_p^2 + (u_p + \Delta V)^2 + v_w^2]^{1/2} \quad (6\text{-}204)$$

$$\alpha_w = \tan^{-1}\left(\frac{w_p}{u_p + \Delta V}\right) \quad (6\text{-}205)$$

$$\beta_w = \tan^{-1} \frac{V}{[(u_p + \Delta V)^2 + w_p^2]^{1/2}} \quad (6\text{-}206)$$

$$C_D = C_{D_o} + K C_L^2 + C_{D_{\delta F}} \delta F + \frac{\partial^2 C_D}{\partial \delta^2 F} \delta^2 F \quad (6\text{-}207)$$

$$C_L = C_{L_o} + C_{L_{\delta F}} \cdot \delta F + C_{L_{o_F}} \cdot q_w + \frac{\partial C_{L_{\alpha_F}}}{\partial \delta F} \cdot \delta F \cdot \alpha_w \quad (6\text{-}208)$$

$$(C_{\ell_w}) = C_{\ell_{\beta_F}} \cdot \beta_w + C_{\ell_{\delta A}} \cdot \delta A + \frac{b}{2V_w} C_{\ell_p} \cdot p_w + \frac{b}{2V_w} C_{\ell_r} \cdot r_w \quad (6\text{-}209)$$

$$(C_{m_w}) = C_{m_o} + C_{m_{\delta F}} \cdot \delta F + \frac{c}{2V_w} C_{m_{q_1}} \cdot q_1 \quad (6\text{-}210)$$

$$(C_{n_w}) = C_{n_{\beta_F}} \cdot \beta_w + C_{n_{\delta A}} \cdot \delta A + \frac{b}{2V_w} C_{n_p} \cdot p_w + \frac{b}{2V_w} C_{n_r} \cdot r_w \quad (6\text{-}211)$$

In Body Axes

$$(C_X)_w = -C_D \cos \xi - C_L \sin \xi \qquad \xi = i_w - \alpha_w \quad (6\text{-}212)$$

$$(C_Z)_w = C_D \sin \xi - C_L \cos \xi \quad (6\text{-}213)$$

$$(C_\ell)_w = (C_{\ell_w}) \cos \xi + (C_{n_w}) \sin \xi \quad (6\text{-}214)$$

$$(C_m)_w = (C_{m_w}) - \frac{x_{ac}}{c} (C_X)_w + \frac{z_{ac}}{c} (C_Z)_w \quad (6\text{-}215)$$

$$(C_n)_w = -(C_{\ell_w}) \sin \xi + (C_{n_w}) \cos \xi \quad (6\text{-}216)$$

$$(\Delta X_a)_w = (C_X)_w S [f(C_{T,S})] q_w \quad (6\text{-}217)$$

$$(\Delta Z_a)_w = (C_Z)_w S [f(C_{T,S})] q_w \quad (6\text{-}218)$$

$$(\Delta L_a)_w = (C_\ell)_w b S [f(C_{T,S})] q_w \quad (6\text{-}219)$$

$$(\Delta M_a)_w = (C_m)_w c S [f(C_{T,S})] q_w \quad (6\text{-}220)$$

$$(\Delta N_a)_w = (C_n)_w b S [f(C_{T,S})] q_w \quad (6\text{-}221)$$

d. VERTICAL STABILIZER AERODYNAMICS

$$C_Y = C_{Y_{\beta_F}} \cdot \beta_F + C_{Y_{\delta R}} \cdot \delta R \quad (6\text{-}222)$$

$$C_{\ell} = C_{\ell_{\beta_F}} \cdot \beta_F + C_{\ell_{\delta R}} \cdot \delta R + \frac{b}{2V_B} [C_{\ell_p} \cdot p + C_{\ell_r} \cdot r] \quad (6\text{-}223)$$

$$C_n = C_{n_{\beta_F}} \cdot \beta_F + C_{n_{\delta R}} \cdot \delta R + \frac{b}{2V_B} [C_{n_p} \cdot p + C_{n_r} \cdot r] \quad (6\text{-}224)$$

$$(\Delta X_a)_{vt} = C_T S (\frac{q_{vt}}{q}) q \quad (6\text{-}225)$$

$$(\Delta L_a)_{vt} = C_{\ell} bS (\frac{q_{vt}}{q}) q \quad (6\text{-}226)$$

$$(\Delta N_a)_{vt} = C_n bS (\frac{q_{vt}}{q}) q \quad (6\text{-}227)$$

e. HORIZONTAL STABILIZER AERODYNAMICS

$$\alpha_t = \alpha_F + i_t - \epsilon \quad (6\text{-}228)$$

$$C_{L_t} = C_{L_{\alpha_t}} \cdot \alpha_t \quad (6\text{-}229)$$

$$C_{D_t} = C_{D_{o_t}} + K_t (C_{L_t})^2 \quad (6\text{-}230)$$

$$(\Delta X_a)_{HS} = - [C_{D_t} \cos (i_t - \alpha_t) + C_{L_t} \sin (i_t - \alpha_t)] S (\frac{q_{HS}}{q}) q \quad (6\text{-}231)$$

$$(\Delta Z_a)_{HS} = [+ C_{D_t} \sin (i_t - \alpha_t) - C_{L_t} \cos (i_t - \alpha_t)] S (\frac{q_{HS}}{q}) q \quad (6\text{-}232)$$

$$(\Delta M_a)_{HS} = -(\Delta X_a)_{HS} \cdot h_{HS} + (\Delta Z_a)_{HS} \cdot \ell_{HS} + \frac{c^2 S \rho}{4} [C_{m_{q_1}} \cdot q_1 V_B + C_{m_{\dot{\alpha}}} \cdot \dot{w}] \quad (6\text{-}233)$$

f. TAIL ROTOR AERODYNAMICS

$$(\Psi_o)_{TR} = 90 + (\alpha_F - \epsilon) \quad (6\text{-}234)$$

$$u_{TR} = V_B \sin (\Psi_o)_{TR} \quad (6\text{-}235)$$

$$w_{TR} = V_B \cos(\phi_o)_{TR} - \ell_{TR} q_1 \tag{6-236}$$

$$J_{TR} = \left(\frac{60}{D_{TR}}\right) \frac{V_{TR}}{N_{TR}} \tag{6-237}$$

$$J'_{TR} = \left(\frac{60}{D_{TR}}\right) \left(\frac{-w_{TR}}{N_{TR}}\right) \tag{6-238}$$

$$V_{TR} = \left(u_{TR}^2 + w_{TR}^2\right)^{1/2} \tag{6-239}$$

$$C_{T_{TR}} = C_{T_{TR}}(B_{TR}) + \frac{\partial C_{T_{TR}}}{\partial J'_{TR}}(J'_{TR}) \tag{6-240}$$

$$C_{P_{TR}} = \frac{\partial^2 C_P}{\partial B_{TR}^2}(B_{TR})^2 \tag{6-241}$$

$$T_{TR} = D_{TR}^4 \left(\frac{\rho}{\rho_o}\right) \left(\frac{N_{TR}}{N_{o_{TR}}}\right)^2 C_{T_{TR}} \tag{6-242}$$

$$Q_{TR} = D_{TR}^5 \left(\frac{\rho}{\rho_o}\right) \left(\frac{N_{TR}}{N_{o_{TR}}}\right)^2 C_{P_{TR}} \tag{6-243}$$

$$(\Delta Z_a)_{TR} = T_{TR} \tag{6-244}$$

$$(\Delta M_a)_{TR} = T_{TR} \ell_{TR} \tag{6-245}$$

$$(\Delta N_a)_{TR} = Q_{TR} \tag{6-246}$$

g. FUSELAGE AERODYNAMICS

$$(\Delta X_a)_F = -q S C_{D_o} \tag{6-247}$$

$$(\Delta Y_a)_F = q S C_{Y_{\beta_F}} \cdot \beta_F \tag{6-248}$$

$$(\Delta Z_a)_F = -q\,S\,C_{L_{\alpha_F}} \cdot \alpha_F \tag{6-249}$$

$$(\Delta M_a)_F = qSc[C_{m_o} + C_{m_{\alpha_F}} \cdot \alpha_F] \tag{6-250}$$

$$(\Delta N_a)_F = q\,Sb\,C_{n_{\beta_F}} \cdot \beta_F \tag{6-251}$$

C_{D_o}, $C_{L_{\alpha_F}}$, C_{m_o} and $C_{n_{\beta_F}}$ also have effects in the wing aerodynamics.

h. TILT WING AIRCRAFT FORCE AND MOMENT EQUATIONS

(1) X Force Equation

$$C_{X_W}S[f(C_{T,S})]q_w + \sum_{n=1}^{4}(T_n \cos i_w - N_n \cos\beta_n \sin i_w)$$

$$-[C_{D_t}\cos(i_t - \alpha_t) + C_{L_t}\sin(i_t - \alpha_t)]\,Sq(\frac{q_{HS}}{q}) - SqC_{D_o}$$

$$= m(\dot{U} + Wq_1 - Vr) + mg\sin\theta$$

(2) Y Force Equation

$$\sum_{n=1}^{4}(-N_n \sin\beta_n) + C_Y\,Sq(\frac{q_{wt}}{q}) + SqC_{Y_{\beta_F}} \cdot \beta_F$$

$$= m(\dot{V} + Ur - Wp) - mg\cos\theta\sin\phi$$

(3) Z Force Equation

$$C_{Z_W}S[f(C_{T,S})]q_w + \sum_{n=1}^{4}(-T_n \sin i_w - N_n \cos\beta_n \cos i_w)$$

$$+[C_{D_t}\sin(i_t - \alpha_t) + C_{L_t}\cos(i_t - \alpha_t)]Sq(\frac{q_{HS}}{q}) + T_{TR} - SqC_{L_{\alpha_F}} \cdot \alpha_F$$

$$= m(\dot{W} + Vp - Uq_1) - mg\cos\theta\cos\phi$$

(4) Roll Equation

$$C_{\ell_w} bS[f(C_{T,S})]\, q_w$$

$$+[(+T_1 \sin i_w + N_1 \cos\beta_1 \cos i_w) - (+T_4 \sin i_w + N_4 \cos\beta_4 \cos i_w)]y_1$$

$$+[(+T_2 \sin i_w + N_2 \cos\beta_2 \cos i_w) - (+T_3 \sin i_w + N_3 \cos\beta_3 \cos i_w)]y_2$$

$$+(+N_1 \sin\beta_1 + N_4 \sin\beta_4)\, z_1 + (+N_2 \sin\beta_2 + N_3 \sin\beta_3)\, z_2$$

$$-\sum_{n=1}^{4} (Y_n \cos\beta_n) \sin i_w - \sum_{n=1}^{4} (M_n \sin\beta_n) \sin i_w + C_{\ell} b\, Sq(\frac{q_{vt}}{q})$$

$$= I_{11}\dot{p} + I_{13}(\dot{r} + pq_1) + (I_{33} - I_{22})\, q_1 r + (I_E \dot{\Omega}_E) \cos i_w$$

$$- q_1(I_E \Omega_E) \sin i_w + q_1 I_{TR} \Omega_{TR}$$

(5) Pitch Equation

$$C_{m_w} cS[f(C_{T,S})]\, q_w$$

$$+ M_{T_{Pivot}} + \sum_{1}^{4} T_n(\cos i_w)\, z_{pivot} + \sum_{1}^{4} T_n(\sin i_w)\, x_{pivot}$$

$$-(N_1 \cos\beta_1 \sin i_w + N_4 \cos\beta_4 \sin i_w)\, z_1$$

$$-(N_2 \cos\beta_2 \sin i_w + N_3 \cos\beta_3 \sin i_w)\, z_2$$

$$+(N_1 \cos\beta_1 \cos i_w + N_4 \cos\beta_4 \cos i_w)\, x_1$$

$$+(N_2 \cos\beta_2 \cos i_w + N_3 \cos\beta_3 \cos i_w)x_2 - \sum_{n=1}^{4} (Y_n \sin\beta_n)$$

$$+ \sum_{n=1}^{4} (M_n \cos\beta_n)$$

$$+[C_{D_t} \cos(i_t - \alpha_t) + C_{L_t} \sin(i_t - \alpha_t)]\, Sq(\frac{q_{HS}}{q})\, h_{HS}$$

$$+[C_{D_t} \sin(i_t - \alpha_t) - C_{L_t} \cos(i_t - \alpha_t)]\, Sq(\frac{q_{HS}}{q})\, l_{HS}$$

$$+ \frac{\rho^2 S \ell}{4} [C_{m_{q_1}} \cdot q_1 X_B + C_{m_{\dot{\alpha}}} \cdot \dot{\alpha}] + T_{TR} \ell_{TR} + qSc(C_{m_o} + C_{m_{\alpha_F}} \cdot \alpha_F)$$

$$= I_{22}\dot{q} - \cancel{I_{13}(r^2 - p^2)} + \cancel{(I_{33} - I_{11}) pr}$$

$$+ p(I_E \Omega_E) \sin i_w + r(I_E \Omega_E) \cos i_w$$

(6) Yaw Equation

$$C_{n_w} bS[f(C_{T,S}) q_w$$

$$-[(T_1 \cos i_w - N_1 \cos \beta_1 \sin i_w) - (T_4 \cos i_w - N_4 \cos \beta_4 \sin i_w)] y_1$$

$$-[(T_2 \cos i_w - N_2 \cos \beta_2 \sin i_w) - (T_3 \cos i_w - N_3 \cos \beta_3 \sin i_w)] y_2$$

$$-(+N_1 \sin \beta_1 + N_4 \sin \beta_4) x_1 - (+N_2 \sin \beta_2 + N_3 \sin \beta_3) x_2$$

$$- \sum_{n=1}^{4} (T_n \cos \beta_n) \cos i_w - \sum_{n=1}^{4} (N_n \sin \beta_n) \cos i_w$$

$$+ C_{n_\beta} b \cancel{\beta q}\left(\frac{q_{vt}}{q}\right) + q S b C_{n_{\beta_F}} \cdot \beta_F + Q_{TR}$$

$$= I_{33}\dot{r} + I_{13}(\dot{p} - \cancel{Q_I r}) + \cancel{(I_{22} - I_{11}) pq_1}$$

$$\cancel{- (I_E \dot{\Omega}_E) \sin i_w} - q_1 (I_E \Omega_E) \cos i_w - p I_{TR} \Omega_{TR}$$

No simplifications have been made on the right side of these six equations. Terms ignored in mechanisation are those with diagonal line through them. External stores, rough air, or landing gear conditions are not developed in these equations.

NOTE: In equations 6-217 to 6-221 and equations 1, 3-6 of the preceding force and moment equations, $[f(C_{T,S}) \cdot q_w]$ is a dynamic pressure term due to propeller slipstream. $C_{T,S}$ is the coefficient of thrust due to the induced wing velocity ΔV, contributed by the propeller slipstream, giving an increased lift effect. With engines off, $[f(C_{T,S}) \cdot q_w] \cong 1.00$ and equations 6-217 to 6-221 become force and moment equations as would be expected for jet aircraft. $C_{T,S}$ is a $f(V_B)$ and dependent on wing tilt and wing flap angles.